

Fundamentals of Electronics 2

Fundamentals of Electronics 2

*Continuous-time
Signals and Systems*

Pierre Muret

ISTE

WILEY

First published 2018 in Great Britain and the United States by ISTE Ltd and John Wiley & Sons, Inc.

Apart from any fair dealing for the purposes of research or private study, or criticism or review, as permitted under the Copyright, Designs and Patents Act 1988, this publication may only be reproduced, stored or transmitted, in any form or by any means, with the prior permission in writing of the publishers, or in the case of reprographic reproduction in accordance with the terms and licenses issued by the CLA. Enquiries concerning reproduction outside these terms should be sent to the publishers at the undermentioned address:

ISTE Ltd
27-37 St George's Road
London SW19 4EU
UK

www.iste.co.uk

John Wiley & Sons, Inc.
111 River Street
Hoboken, NJ 07030
USA

www.wiley.com

© ISTE Ltd 2018

The rights of Pierre Muret to be identified as the author of this work have been asserted by him in accordance with the Copyright, Designs and Patents Act 1988.

Library of Congress Control Number: 2017961003

British Library Cataloguing-in-Publication Data
A CIP record for this book is available from the British Library
ISBN 978-1-78630-182-6

Contents

Preface	ix
Introduction	xiii
Chapter 1. Continuous-time Systems: General Properties, Feedback, Stability, Oscillators	1
1.1. Representation of continuous time signals	2
1.1.1. Sinusoidal signals.	2
1.1.2. Periodic signals	4
1.1.3. Non-periodic real signals and Fourier transforms	5
1.2. Representations of linear and stationary systems and circuits built with localized elements	8
1.2.1. Representation using ordinary differential equation	8
1.2.2. Periodic permanent conditions and harmonic conditions.	10
1.2.3. Unilateral Laplace transform of causal systems and study of the various regimes.	12
1.3. Negative feedback.	25
1.3.1. Inversion of a transfer function.	26
1.3.2. Linearization of a nonlinear system	27
1.3.3. Gain-bandwidth product for first-order low-pass systems	28
1.3.4. Simultaneous negative and positive feedback	29
1.4. Study of system stability	30
1.4.1. Time response: pole mapping.	31
1.4.2. Nyquist criterion in general case	33
1.4.3. Stability of looped systems assumed stable in open loop: Nyquist and Bode criteria	35
1.4.4. Stability of linear and nonlinear networks of any order, analyzed from state variables.	37

1.5. State space form	40
1.6. Oscillators and unstable systems	42
1.6.1. Sinusoidal oscillators.	42
1.6.2. Relaxation oscillators using a nonlinear dipole and other resonant circuit oscillators	49
1.6.3. General case of systems comprising a nonlinear dipole and study of oscillation in phase space.	52
1.7. Exercises	66
1.7.1. Response and stability of an operational amplifier not compensated until unity gain and loaded by a capacitor	66
1.7.2. Active filters built with operational amplifiers.	69
1.7.3. Study of a looped system and its stability: sample and hold circuit.	72
1.7.4. Study of a Colpitts oscillator built with a JFET	78
1.7.5. Study of a system in state-space form	80

**Chapter 2. Continuous-time Linear Systems: Quadripoles,
Filtering and Filter Synthesis** 85

2.1. Quadripoles or two-port networks	85
2.1.1. Quadripoles deduced from dynamic circuits	86
2.1.2. Quadripoles and transfer matrices	87
2.1.3. Modification of the parameters of the quadripoles using negative feedback	89
2.1.4. Passive quadripoles.	91
2.1.5. Dipole impedances and admittances; iterative impedance	92
2.1.6. Scattering matrix (or s-matrix) and transfer matrix	102
2.1.7. Powers in quadripoles and matching	107
2.1.8. Image-impedances and image-matching	118
2.1.9. Representation of quadripoles by block diagrams.	124
2.2. Analog filters.	126
2.2.1. Definition and impulse response	126
2.2.2. Properties of real, causal and stable filters	131
2.3. Synthesis of analog active filters using operational amplifiers.	146
2.3.1. Cascading second-order cell filters	146
2.3.2. Multiple feedback loop cell	148
2.4. Non-dissipative filters synthesis methods	150
2.4.1. Synthesis based on effective parameters	151
2.4.2. Synthesis based on image parameters	166
2.4.3. Filter sensitivity and Orchard's argument	195
2.5. Exercises	196

2.5.1. Impedance matching by means of passive two-port networks; application to class B push–pull power RF amplifier with MOS transistors	196
2.5.2. Passive low-pass filtering of an ideal voltage source by a two-port network built with an LC ladder (single-ended ladder filter)	204
2.5.3. Dual-ended passive filter, synthesized by the image-impedance method	211
2.5.4. Lattice filter	214
Appendix	223
Bibliography	233
Index	235

Preface

Today, we can consider electronics to be a subject derived from both the theoretical advances achieved during the 20th Century in areas comprising the modeling and conception of components, circuits, signals and systems, together with the tremendous development attained in integrated circuit technology. However, such development led to something of a knowledge diaspora that this work will attempt to contravene by collecting both the general principles at the center of all electronic systems and components, together with the synthesis and analysis methods required to describe and understand these components and subcomponents. The work is divided into three volumes. Each volume follows one guiding principle from which various concepts flow. Accordingly, Volume 1 addresses the physics of semiconductor components and the consequences thereof, that is, the relations between component properties and electrical models. Volume 2 addresses continuous time systems, initially adopting a general approach in Chapter 1, followed by a review of the highly involved subject of quadripoles in Chapter 2. Volume 3 is devoted to discrete-time and/or quantized level systems. The former, also known as sampled systems, which can either be analog or digital, are studied in Chapter 1, while the latter, conversion systems, we address in Chapter 2. The chapter headings are indicated in the following general outline.

Each chapter is paired with exercises and detailed corrections, with two objectives. First, these exercises help illustrate the general principles addressed in the course, proposing new application layouts and showing how theory can be implemented to assess their properties. Second, the exercises act as extensions of the course, illustrating circuits that may have been described briefly, but whose properties have not been studied in detail. The

first volume should be accessible to students with a scientific literacy corresponding to the first 2 years of university education, allowing them to acquire the level of understanding required for the third year of their electronics degree. The level of comprehension required for the following two volumes is that of students on a master's degree program or enrolled in engineering school.

In summary, electronics, as presented in this book, is an engineering science that concerns the modeling of components and systems from their physical properties to their established function, allowing for the transformation of electrical signals and information processing. Here, the various items are summarized along with their properties to help readers follow the broader direction of their organization and thereby avoid fragmentation and overlap. The representation of signals is treated in a balanced manner, which means that the spectral aspect is given its proper place; to do otherwise would have been outmoded and against the grain of modern electronics, since now a wide range of problems are initially addressed according to criteria concerning frequency response, bandwidth and signal spectrum modification. This should by no means overshadow the application of electrokinetic laws, which remains a necessary first step since electronics remains fundamentally concerned with electric circuits. Concepts related to radio-frequency circuits are not given special treatment here, but can be found in several chapters. Since the summary of logical circuits involves digital electronics and industrial computing, the part treated here is limited to logical functions that may be useful in binary numbers computing and elementary sequencing. The author hopes that this work contributes to a broad foundation for the analysis, modeling and synthesis of most active and passive circuits in electronics, giving readers a good start to begin the development and simulation of integrated circuits.

Outline

1) Volume 1: Electronic Components and Elementary Functions [MUR 17].

i) Diodes and Applications

ii) Bipolar Transistors and Applications

iii) Field Effect Transistor and Applications

iv) Amplifiers, Comparators and Other Analog Circuits

2) Volume 2: Continuous-time Signals and Systems.

i) Continuous-time Stationary Systems: General Properties, Feedback, Stability, Oscillators

ii) Continuous-time Linear and Stationary Systems: Two-port Networks, Filtering and Analog Filter Synthesis

3) Volume 3: Discrete-time Signals and Systems and Conversion Systems [MUR 18].

i) Discrete-time Signals: Sampling, Filtering and Phase Control, Frequency control circuits

ii) Quantized Level Systems: Digital-to-analog and Analog-to-digital Conversions

Pierre MURET
November 2017

Introduction

This volume is dedicated to the study of linear and stationary systems in which time is considered as a continuous variable, as well as certain extensions in the case of nonlinear systems. It is mainly centered on single-input and single-output systems but a method capable of generalizing studies to linear or nonlinear multi-input and multi-output systems is also addressed. Generally, in order to highlight the properties of these systems, one must necessarily rely on the analysis of electrical signals that either characterize their response to an excitation signal or their natural (or proper) response. The former output signal is dependent on the input signal and is called forced response, whereas their natural response is independent of the excitation signal placed on their input. Therefore, it is essential to begin with the representations of signals by forming a close correlation between the time domain and the frequency domain, which are connected by the Fourier transform or decomposition into Fourier series. It is then natural to customize the study to the case of stationary systems, for which the forced response is invariant under time translation of the signal applied on input, and which, in addition, follow the principle of causality. The unilateral Laplace transform then proves to be useful and it leads us to the notion of transfer function or transmittance, together with the Fourier transform in the case of finite energy signals. The properties of these two types of transforms and their application to the case of electronic systems are covered in the first part of Chapter 1 while the consequences of causality are addressed in Chapter 2.

The second part of Chapter 1 is dedicated to the study of feedback and its applications, and then to the different methods for studying the stability of the systems, or to means able to control their instability, as is the case for

oscillators. A system is stable if, after a finite life span excitation, it finally returns to its previous idle state, namely without any variation of electrical quantities, and it is unstable otherwise. In the early stages of electronics, feedback was paramount and it led to much progress and the development of a multitude of applications, which are reviewed here. The mathematical tools constituted by the time–frequency transforms mentioned earlier or representations in the complex plane are then used to address problems of system stability, including the case of those that incorporate a feedback loop, known as looped systems. The extension to state variables and state representation, which is based on the decomposition of the response of a system into a set of first-order differential equations, is then addressed. The previous concepts finally make it possible to detail the different ways for analyzing oscillators' operation, which initially can be considered as linear systems at the limit of stability, but which in practice are always subject to a limitation of the amplitude that requires nonlinearity to be taken into account. The transition from predictable operation to a chaotic regime is presented in the case of a model system.

In Chapter 2, the properties of stable electronic systems are particularized to the case of networks and specially quadripoles. The different representations of networks in the form of quadripoles are discussed, as well as all notions of impedance or admittance deriving therefrom. Some are measurable, thus experimentally feasible, while others are fictional, such as image impedances, but open a highly fruitful scope of application, which is the subject of the last section of this chapter. The concepts of matching, whether power or impedance matching, are detailed, as well as their consequences and rules to apply in practice in order to optimize the operation of electronic assemblies and to best take advantage of the components that are included.

The last part of Chapter 2 is devoted to stable systems that can be analyzed as analog filters, namely satisfying the principle of causality, of which the general consequences are presented. There are either circuits incorporating one or more active devices such as operational amplifiers or passive circuits, limited here to non-dissipative cases. The synthesis of these analog filters is thorough, and can be used to determine the value of all the components of a filter based on imposed criteria, most often a template in the frequency domain. Two topics are presented; on the one hand for active filters and on the other hand for non-dissipative passive filters. In the second case, the method using effective parameters is an exact method, but not

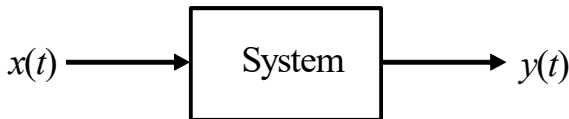
covering all the applications, while the method of image parameters is suitable to most requirements, with a deviation from the template that can be minimized. The ways to make adjustments and all circuits necessary for the practical implementation of the filters are detailed. Examples are given for each important case, based on the transfer functions calculated by means of software programs (here, MATLAB). The different possible choices for the computational functions are presented in relation to the criteria to be verified. In the case of the synthesis based on image parameters, formulas allowing the calculation of all elements are demonstrated. Although the case of systems with distributed (or scattered) elements, essential when the wavelength becomes comparable to the dimensions of the circuit, is not explicitly addressed, the description of the quadripoles using s -parameters, as detailed in Chapter 2, easily adapts.

Continuous-time Systems: General Properties, Feedback, Stability, Oscillators

The linear and stationary systems that concern us here deliver output signal $y(t)$ when input signal $x(t)$ is applied to them, solution to a *real* and linear ordinary differential equation, where t represents the time variable:

$$a_n \frac{d^n y}{dt^n} + a_{n-1} \frac{d^{n-1} y}{dt^{n-1}} + \dots + a_1 \frac{dy}{dt} + a_0 y = b_m \frac{d^m x}{dt^m} + b_{m-1} \frac{d^{m-1} x}{dt^{m-1}} + \dots + b_1 \frac{dx}{dt} + b_0 x$$

which can also be seen as a linear application:



Function $\exp(\alpha t)$, with *real or complex* α , is of special importance since it is the specific function of the system's differential equation, which means that if $x(t) = \exp(\alpha t)$, the output signal is also proportional to $\exp(\alpha t)$. It is this fundamental property that warrants the approaches discussed in the following sections 1.1 and 1.2. Another method, based on the state-space form, also applicable to nonlinear systems, is presented in sections 1.4.5 and 1.5.

1.1. Representation of continuous time signals

These signals are real electrical quantities and thus measurable functions of time variable t , which itself is a continuous variable. They are also referred to as analog signals. An additional representation is formed by the frequency spectrum.

1.1.1. Sinusoidal signals

In general, any real sinusoidal signal of angular frequency ω_1 and constant frequency f_1 ($\omega_1 = 2\pi f_1$) is written as $y(t) = A \cos(\omega_1 t + \varphi_1)$, once a time and phase origin has been selected. But in complex numbers, this can also be written as:

$$y(t) = A \frac{\exp[j(\omega_1 t + \varphi_1)] + \exp[-j(\omega_1 t + \varphi_1)]}{2}$$

Both exponential terms with imaginary exponent appear with the same A coefficient and are always complex conjugates, two conditions that are required if $y(t)$ is real. The two vectors corresponding to images on the complex plane rotate in opposite directions; thus, frequency $-f_1$ is consistently found at the same time as frequency f_1 .

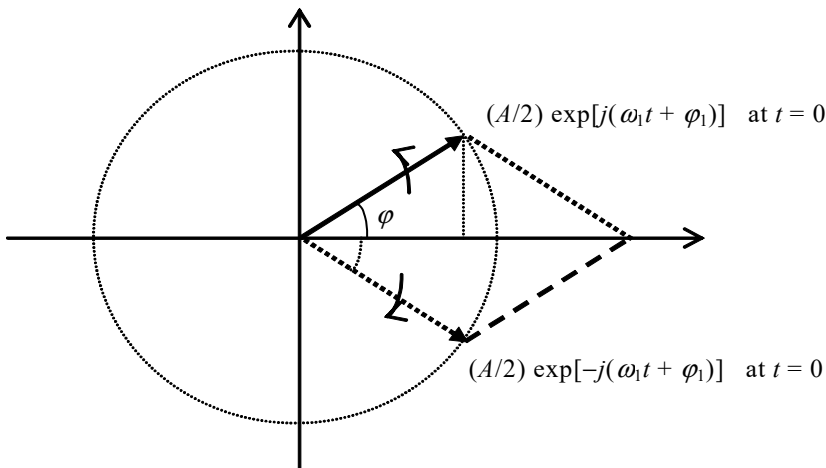


Figure 1.1. Representation of a sinusoidal signal on the complex plane

The spectral or frequency representation is thus formed simply by two lines of amplitude $A/2$ at frequencies f_1 and $-f_1$, and phase lines φ_1 and $-\varphi_1$ at these same frequencies.

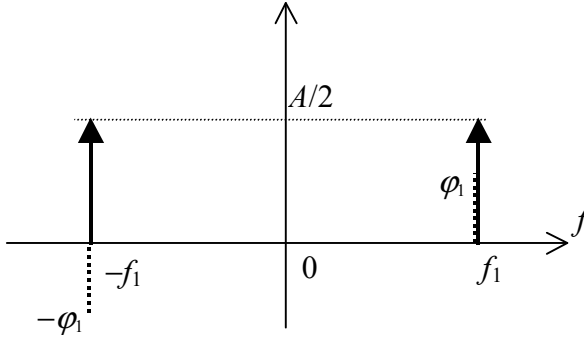


Figure 1.2. Spectrum of a sinusoidal signal (amplitude solid line, phase dotted)

Indeed, sinusoidal signals of the same frequency form a two-dimensional vector space for which a basis is provided by $\exp[j\omega_1 t]$ and $\exp[-j\omega_1 t]$ ($\cos[\omega_1 t]$ and $\sin[\omega_1 t]$ form another basis). Thus, we can write:

$$y(t) = c_1 \exp[j2\pi f_1 t] + c_{-1} \exp[-j2\pi f_1 t]$$

with

$$c_1 = \frac{A}{2} \exp(j\varphi_1)$$

and

$$c_{-1} = \frac{A}{2} \exp(-j\varphi_1)$$

where c_1 and c_{-1} are complex conjugates.

However, here only the first of these terms will be considered, with the second provided by complex conjugates. This leads to rotating vector or Fresnel representation: concerning the instantaneous values, only $A \exp[j(\omega_1 t + \varphi_1)]$ is used in the complex plane (or rather $\frac{A}{\sqrt{2}} \exp[j(\omega_1 t + \varphi_1)]$) if these values are considered to be root mean square (rms) quantities for

power calculations). Again, $y(t)$ is found in the first case by projection on the real axis, that is, by taking the real part of symbolic representation to within a coefficient of 2.

1.1.2. Periodic signals

From sinusoidal signals, the case of periodic signals $y_T(t)$ with period T equal to $1/f_1$ can be generalized by performing the development as a Fourier series. Periodic signals of period T also constitute a vector space but of dimension $2N$ if signal reconstitution requires N sinusoidal signals of harmonic frequencies $f_1, 2f_1, 3f_1, 4f_1, \dots, Nf_1$. The series' convergence to $y_T(t)$ is made certain if N approaches infinity:

$$y_T(t) = \lim_{N \rightarrow \infty} \sum_{n=-N}^N c_n \exp\left[j \frac{2\pi n t}{T}\right]$$

where the coefficients are calculated by Fourier series decomposition:

$$c_n = \frac{1}{T} \int_{t_0}^{t_0+T} y_T(t) \exp\left[-j \frac{2\pi n t}{T}\right] dt$$

Since $y_T(t)$ is real, c_n and c_{-n} are complex conjugates (same module and opposite phase). Hence, the even and odd symmetries respectively for module spectrum $|c_n|$ and for that of argument $\text{Arg}\{c_n\}$.

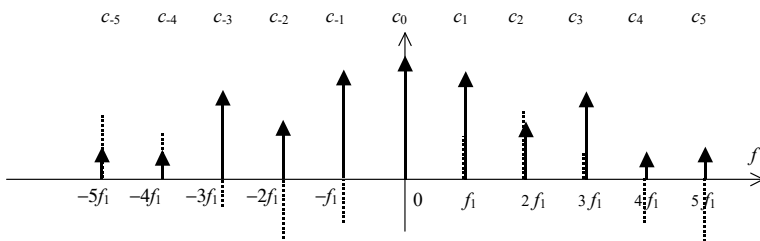


Figure 1.3. Spectrum of a periodic signal of repetition frequency f_1 (modules in bold and arguments in dotted lines)

By merging the conjugated terms, the real series can be written as:

$$y_T(t) = c_0 + \lim_{N \rightarrow \infty} 2 \sum_{n=1}^N |c_n| \cos \left[\frac{2\pi n t}{T} + \phi_n \right] \text{ where } \phi_n = \text{Arg}\{c_n\}$$

1.1.2.1. Power of a periodic signal

Power (average energy over time) is calculated by Parseval's rule, which shows that this energy is independent of time or frequency representation (to within the factor R or $1/R$) and is obtained by a scalar product of the signal by itself:

$$S = \frac{1}{T} \int_{t_0}^{t_0+T} [y_T(t)]^2 dt = \sum_{n=-\infty}^{\infty} |c_n|^2$$

No $c_n c_{n'}$ term with $n \neq n'$ appears since the basis of the vector space is orthogonal (scalar products of all basis vectors are zero unless $n = n'$). It should be noted that $|c_n|^2 = c_n \overline{c_n}$ and in the frequent event where power is calculated from a complex voltage U or a current I , using $\sum_{n=-\infty}^{\infty} U_n \overline{U_n}$ or alternatively $\sum_{n=-\infty}^{\infty} I_n \overline{I_n}$ if U_n and I_n represent, respectively, the $u(t)$ and $i(t)$ complex Fourier series decomposition coefficients.

1.1.3. Non-periodic real signals and Fourier transforms

If the signals are non-periodic, it can be assumed that the period T of the signals approach infinity on condition that $\lim_{T \rightarrow \infty} T c_n$ is convergent (the signals have to approach zero for $t \rightarrow \pm\infty$), replacing discrete variable n/T by continuous variable f (frequency) and thus defining the Fourier transform of $y(t)$ by : $\lim_{T \rightarrow \infty} T c_n = \int_{-T}^T y(t) \exp[-j2\pi ft] dt$ thus:

$$\text{FT}[y(t)] =$$

$$Y(f) = \int_{-\infty}^{\infty} y(t) \exp[-j2\pi ft] dt = \int_{-\infty}^{\infty} y(t) \cos[j2\pi ft] dt - j \int_{-\infty}^{\infty} y(t) \sin[j2\pi ft] dt$$

The symmetry properties are the same as for c_n since $y(t)$ is assumed to be a real function:

$$Y(-f) = \overline{Y(f)}$$

By changing variable t to $-t$, only the sine term changes sign thus providing:

$$\text{FT}[y(-t)] = \overline{Y(f)}$$

Obtaining $y(t)$ by means of the reverse FT calculated from the Fourier series by approaching the limit $y(t) = \lim_{T \rightarrow \infty} \sum_{n=-\infty}^{\infty} Tc_n \exp\left[j\frac{2\pi nt}{T}\right] \frac{1}{T}$ by replacing $\lim_{T \rightarrow \infty} Tc_n$ by $Y(f)$, n/T by f , $1/T$ by df and the total by an integral:

$$\text{FT}^{-1}[Y(f)] = y(t) = \int_{-\infty}^{\infty} Y(f) \exp[j2\pi ft] df$$

Other properties of the FT are as follows:

– The FT and the reverse transform are linear applications:

$$\text{If } y(t) = ay_1(t) + by_2(t) \quad \text{FT}[y(t)] = a\text{FT}[y_1(t)] + b\text{FT}[y_2(t)]$$

$$\text{If } Y(f) = \alpha Y_1(f) + \beta Y_2(f) \quad \text{FT}[Y(f)] = \alpha\text{FT}[Y_1(f)] + \beta\text{FT}[Y_2(f)]$$

– Derivation and integration of $y(t)$:

$$\begin{aligned} \text{If } Y(f) &= \text{FT}[y(t)], \quad \text{FT}\left[\frac{dy}{dt}\right] = j\omega Y(f) = j2\pi f Y(f) \quad \text{and} \quad \text{FT}\left[\int y(t) dt\right] \\ &= \frac{Y(f)}{j\omega} = \frac{Y(f)}{j2\pi f} \quad (\text{integration by parts of the definition where } y(t) \text{ is replaced} \\ &\text{by } dy/dt). \end{aligned}$$

– Delay theorem:

$$\text{If } Y(f) = \text{FT}[y(t)], \quad \text{FT}[y(t - t_0)] = \exp(-j2\pi ft_0) Y(f)$$

The phase alone is modified (phase delay if $t_0 > 0$ is a time delay) and not the transform modulus.

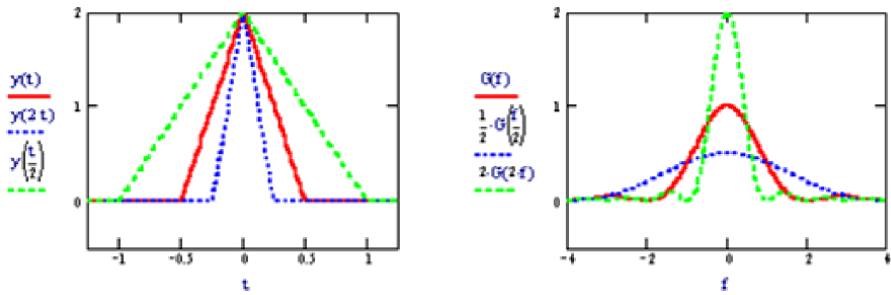


Figure 1.4. Triangular signals (left) and their spectrum (FT) (right). For a color version of this figure, see www.iste.co.uk/muret/electronics2.zip

– Similarity and dilatation/contraction of time/frequency scales:

If $Y(f) = \text{FT}[y(t)]$, $\text{FT}[y(\alpha t)] = \frac{1}{|\alpha|} Y\left(\frac{f}{\alpha}\right)$ (obtained by changing variable $t' = \alpha t$ in the definition, α real), as illustrated in Figure 1.4.

– Ordinary product of two functions and convolution product

If $Y(f) = \text{FT}[y(t)]$ and $X(f) = \text{FT}[x(t)]$, $Z(f) = \text{FT}[y(t) x(t)] = \int_{-\infty}^{\infty} Y(f - \nu) X(\nu) d\nu = \int_{-\infty}^{\infty} Y(\nu) X(f - \nu) d\nu$

and $\text{FT}^{-1}[Y(f) X(f)] = \int_{-\infty}^{\infty} y(t - \tau) x(\tau) d\tau = \int_{-\infty}^{\infty} y(\tau) x(t - \tau) d\tau$ or alternatively

$$\text{FT}\left[\int_{-\infty}^{\infty} y(t - \tau) x(\tau) d\tau\right] = \text{FT}\left[\int_{-\infty}^{\infty} y(\tau) x(t - \tau) d\tau\right] = Y(f) X(f)$$

– Wiener–Kinchine and Parseval theorems:

$\text{FT}^{-1}\left[|Y(f)|^2\right] = \text{FT}^{-1}\left[Y(f)\overline{Y(f)}\right] = \int_{-\infty}^{\infty} y(\tau) y(-t + \tau) d\tau = \int_{-\infty}^{\infty} y(t) y(t - \tau) dt$, the autocorrelation function of $y(t)$ (after reversing the names of variables t and τ) or rather $\text{FT}\left[\int_{-\infty}^{\infty} y(t) y(t - \tau) dt\right] = |Y(f)|^2$.

The autocorrelation function $C_{yy}(\tau) = \int_{-\infty}^{\infty} y(t)y(t-\tau)dt$ measures the degree of resemblance between the function and delayed function. Unlike the convolution product, the integration variable operates with the same sign in both factors under the integral symbol.

FT $\left[\int_{-\infty}^{\infty} y(t)y(t-\tau)dt \right] = |Y(f)|^2$ is the Wiener–Kinchine theorem stating that

the FT of the autocorrelation function of $y(t)$ is equal to the squared modulus of the FT of $y(t)$. This autocorrelation function may be calculated not only for known (or determined) signals but also for random signals such as noise defined only by a density of probability.

FT⁻¹ $\left[|Y(f)|^2 \right] = \int_{-\infty}^{\infty} |Y(f)|^2 \exp(j2\pi f \tau)df = \int_{-\infty}^{\infty} y(t)y(t-\tau)dt$ is rewritten

simply for $\tau = 0$:

$$\int_{-\infty}^{\infty} |Y(f)|^2 df = \int_{-\infty}^{\infty} [y(t)]^2 dt$$

This is the Parseval theorem that allows us to perform the energy calculation (clearly visible in the second member to within R or $1/R$ coefficient if y is, respectively, a current or a voltage) both in the time domain from $y(t)$ and in the frequency domain from $Y(f)$. Thus, we can proceed to $\int_{-\infty}^{\infty} |Y(f)|^2 df$, which is an energy with $|Y(f)|^2$ a spectral energy density in J/Hz; $|Y(f)|$ a spectral density of current or voltage within R or $1/R$ factor in A/Hz^{1/2} or in V/Hz^{1/2}.

1.2. Representations of linear and stationary systems and circuits built with localized elements

1.2.1. Representation using ordinary differential equation

Electric or electronic circuits built with localized elements are those featuring elements in which instantaneous currents (and voltages) are the same irrespective of the location considered in a conductor. Accordingly, it can be assumed that the wavelength of these currents, voltages and

associated fields is very large relative to the dimensions of these circuits (approximation applicable up to approximately 1 GHz, corresponding to a vacuum wavelength of 30 cm). Furthermore, the only operational elements here are the sources of current and voltage, together with the linear passive elements: resistance, capacitance, self-inductance and mutual inductance. In electronics, this generally results from an approximation of linearization, which is applicable over a voltage or current range that must be defined.

The result of these two hypotheses is that these systems are also stationary, which is to say that their response is unchanging irrespective of the instant chosen as the time origin, and that they can be described mathematically by one or several linear ordinary differential equations.

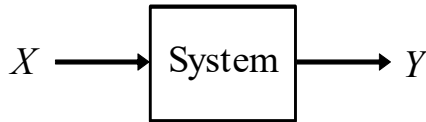
The laws for linear electrical circuits (although this also applies in mechanical engineering for forces or torques, velocities and movements) are those of electrokinetics, valid for resistances ($u = Ri$), capacitances ($i = C \frac{du}{dt}$) and inductances ($u = L \frac{di}{dt}$) (where coefficients R , C and L are assumed to be constant if the system is linear), loop law and node law (system of linear equation) (see the Appendix in Volume 1 [MUR 17]). Any system in which value $y(t)$ depends on circuit elements and on an excitation $x(t)$ can thus be described by one (or several) ordinary differential equations of the form:

$$a_n \frac{d^n y}{dt^n} + a_{n-1} \frac{d^{n-1} y}{dt^{n-1}} + \dots + a_1 \frac{dy}{dt} + a_0 y = b_m \frac{d^m x}{dt^m} + b_{m-1} \frac{d^{m-1} x}{dt^{m-1}} + \dots + b_1 \frac{dx}{dt} + b_0 x$$

All of these linear equations can also be constructed by means of the superposition theorem. Solutions are always given by the total of the equation's general solution without the second member and a special solution to the whole equation, the first corresponding to the system's free regime and the second to the regime forced by $x(t)$.

If the system is *stable*, the equation's solution without the second member corresponds to a transient response that ceases after a certain duration. This does not persist while the forced regime will continue. One may assume that the forced regime has begun at $t \rightarrow -\infty$ since the system is stationary so its responses are independent of the time origin. Under permanent conditions, if $x(t) = \exp(\alpha t)$, $y(t)$ is also proportional to $\exp(\alpha t)$. As shown previously, real signals that can be expressed as linear

combinations of complex exponentials (as is the case for sinusoidal signals) also verify this fundamental property. This allows for a transformation from the time domain to the frequency domain, or alternatively, from real signals to the complex plane, while simultaneously defining transmittance, which draws out the proportionality relation between the complex representation of input and output signals. These complex representations will be indicated in the following with capital letters in the frequency domain or in the complex plane.



The systems' responses for various signals are studied in section 1.2.2.

1.2.2. Periodic permanent conditions and harmonic conditions

In permanent sinusoidal conditions at frequency $\omega_1 = 2\pi f_1$, $x(t) = X_0 \cos(2\pi f_1 t)$ if $x(t)$ is chosen as the phase origin, and $y(t) = Y_0 \cos(2\pi f_1 t + \varphi_1)$. These signals can be rewritten as $x(t) = X_0 \frac{\exp[j2\pi f_1 t] + \exp[-j2\pi f_1 t]}{2}$ and $y(t) = Y_0 \frac{\exp[j(2\pi f_1 t + \varphi_1)] + \exp[-j(2\pi f_1 t + \varphi_1)]}{2}$, which duplicate each term of the differential equation, on the one hand, into a term factor of $\exp(j2\pi f_1 t)$, with frequency f_1 , and, on the other hand, into a term factor of $\exp(-j2\pi f_1 t)$, the complex conjugate, with frequency $-f_1$. Since this equation has to be verified irrespective of instant t , the only solution is that the two equations, one written with $\exp(j2\pi f_1 t)$ as a common factor, and the other with $\exp(-j2\pi f_1 t)$ as a common factor, be verified separately. As a consequence, the member to member total will also be the same.

We can manage the first set of terms by writing $Y(f_1) = Y_0 \exp(j\varphi_1)$ and $X(f_1) = X_0$, and by simplifying both members by $\exp(j2\pi f_1 t)$ after the derivations have been performed. The result reads:

$$\begin{aligned}
 & [a_n (j2\pi f_1)^n + a_{n-1} (j2\pi f_1)^{n-1} + \dots + a_1 (j2\pi f_1) + a_0] Y(f_1) \\
 & = [b_m (j2\pi f_1)^m + b_{m-1} (j2\pi f_1)^{m-1} + \dots + b_1 (j2\pi f_1) + b_0] X(f_1)
 \end{aligned}$$

We also obtain a similar equation in which f_1 has been replaced by $-f_1$. Variable t has disappeared.

Signals $Y(f_1) = Y_0 \exp(j\varphi_1)$ and $X(f_1) = X_0$ are typically complex numbers expressed from a modulus and an argument. These are representations of only half of the amplitude spectrum of real sinusoidal signals; they are known as “symbolic signals” or cissoidal representations, or complex exponentials.

It should be noted that the equation above is verified at each frequency f_1 with coefficients of $Y(f_1)$ in the first member and $X(f_1)$ in the second member, which differs at each frequency since they are polynomials of variable f_1 .

1.2.2.1. Symbolic (complex) notation of signals, impedances and admittances and power calculation in sinusoidal conditions

In sinusoidal conditions, the use of values $Y(f_1)$ and $X(f_1)$ whose modulus is equal to the rms value of $y(t)$ and $x(t)$ is preferred, that is $Y_0/\sqrt{2}$ and $X_0/\sqrt{2}$, respectively. The ratios of current $I = Y(f_1)$ and voltage $V = X(f_1)$ are then complex impedances or admittances.

The active power $P = \frac{1}{T} \int_{t_0}^{t_0+T} y(t)x(t)dt = \frac{Y_0}{\sqrt{2}} \frac{X_0}{\sqrt{2}} \cos \varphi_1$ is then obtained by:

$$P = \operatorname{Re}(I\bar{V}) = \operatorname{Re}(\bar{I}V) = \frac{1}{2}(I\bar{V} + \bar{I}V)$$

If the conditions are periodic but non-sinusoidal, a Fourier series decomposition of the signals lets us process this equation as many times as there are useful harmonics in the signals, at frequencies $f_1, f_2 = 2f_1, f_3 = 3f_1, \dots$ to deduce $Y(f_1), Y(f_2), Y(f_3), \dots$ as a function of $X(f_1), X(f_2), X(f_3), \dots$. We can then recompose the total signal $y(t)$ accounting for the signal’s decomposition coefficients $x(t)$.

If the signal is not periodic but has an FT, the transform of the differential equation must be verified for each frequency f belonging to the infinite set of real numbers.

In all cases (periodic sinusoidal conditions or with calculable FT), that can be grouped under the term harmonic conditions, this equation establishes the equality of the coordinates of the two vectors representing signals in the time domain after projection on a basis of exponential functions $\exp(j2\pi f t)$ in the first member and in the second member.

Indeed, by taking the FT of both members of the whole differential equation, where $X(f) = \text{TF}[x(t)]$ and $Y(f) = \text{TF}[y(t)]$, we obtain:

$$\begin{aligned} & [a_n (j2\pi f)^n + a_{n-1} (j2\pi f)^{n-1} + \dots + a_1 (j2\pi f) + a_0] Y(f) \\ & = [b_m (j2\pi f)^m + b_{m-1} (j2\pi f)^{m-1} + \dots + b_1 (j2\pi f) + b_0] X(f) \end{aligned}$$

Thus, by writing $H(f) = Y(f)/X(f)$, the ratio of FTs of both quantities present in the system (or with $\omega = 2\pi f$):

$$H(f) = \frac{Y(f)}{X(f)} = \frac{b_m (j2\pi f)^m + b_{m-1} (j2\pi f)^{m-1} + \dots + b_1 (j2\pi f) + b_0}{a_n (j2\pi f)^n + a_{n-1} (j2\pi f)^{n-1} + \dots + a_1 (j2\pi f) + a_0}$$

NOTE.— $H(f)$ or $H(jf)$ or $H(j\omega)$, the transmittance of the system in harmonic conditions, is a rational fraction of variable jf or $j\omega$ of m degrees for the numerator and n for the denominator.

1.2.3. Unilateral Laplace transform of causal systems and study of the various regimes

1.2.3.1. Transform properties

In the broadest cases applicable to all operating conditions, such as used when studying system stability and transient regime, if $x(t)$ does not approach zero when $t \rightarrow +\infty$, the unilateral Laplace transform should be used. It can be deduced from the FT by multiplying the integrand by the unity step $\mathbf{U}(t)$ (zero when $t < 0$, one for $t > 0$), which allows for the introduction of causality, and by an exponential factor $\exp(-\sigma t)$, (with $\sigma > 0$, giving a real negative exponent), thus $\int_{-\infty}^{\infty} y(t)\mathbf{U}(t)\exp[-(\sigma - j2\pi f)t]dt$. These modifications

will ensure convergence by inducing a faster decrease for $t \rightarrow +\infty$. By writing complex variable $s = \sigma + j2\pi f$, we obtain:

$$\text{LT}[y(t)] = Y_L(s) = \int_0^{\infty} y(t) \exp(-st) dt$$

The properties are the same as those indicated for the FT except for the derivation, and we must add (if $X_L(s) = \text{LT}[x(t)]$):

– Symmetry in the complex plane: if $y(t)$ is real $Y_L(\bar{s}) = \overline{Y_L(s)}$ (symmetry relative to the real axis).

– Exponential damping: if $y(t) = x(t)\exp(\lambda t)$ (real λ), $Y_L(s) = X_L(s - \lambda)$ (transposition parallel to the real axis of the LT).

– If a $x(t)$ signal has limited support $[0, T]$ (i.e. zero outside of the interval), the LT of the periodic repetition $y(t) = \sum_{n=0}^{\infty} x(t - nT)$ appears to be

$$Y_L(s) = \frac{X_L(s)}{1 - \exp(-sT)}.$$

– Time derivation and integration: if $y(t) = \frac{dx}{dt}$ then $Y_L(s) = sX_L(s) - x(0^+)$.

More generally, if further derivations are possible:

$$\text{if } y(t) = \frac{d^n x}{dt^n}, \text{ then } Y_L(s) = s^n X_L(s) - \sum_{k=0}^{n-1} s^{n-k-1} \frac{d^k x(0^+)}{dt^k}.$$

$$\text{And if } y(t) = \int_0^t x(\tau) d\tau, \text{ then } Y_L(s) = \frac{X_L(s)}{s}.$$

– Theorems of initial and final values: of the previous properties and of integration by parts, we can deduce:

$$\lim_{s \rightarrow +\infty} s Y_L(s) = y(0^+)$$

and

$$\lim_{s \rightarrow 0} s Y_L(s) = \lim_{t \rightarrow +\infty} y(t)$$

These latter properties are deduced by integration by parts in which the derivative of function $y(t)$ applies. If $y(t)$ is initially discontinuous (but not singular), which is often the case, the LT must be calculated in the open interval $]0 +\infty[$ rather than in the half-closed interval $[0 +\infty[$. This restriction allows the use of the derivative of $y(t)$ in the latter properties while simultaneously needing the assessment of $y(t)$ at $t = 0^+$ rather than at 0 or 0^- . Any other approach would be non-rigorous, leading to serious inconsistencies, particularly when singular functions at the time origin are concerned. Non-continuous functions can only be derived and transformed by the LT in the context of distributions formalism (see Appendix). However, the LT of ordinary functions can be retained for transforming functions with finite discontinuities on condition that they can be obtained by a time translation of one discontinuous function at $t = 0$ and by application of the delay theorem.

1.2.3.2. Application of the Laplace transform to the system's differential equation

By taking the transform of both members of the system's characteristic differential equation $\sum_{r=0}^n a_r \frac{d^r y(t)}{dt^r} = \sum_{p=0}^m b_p \frac{d^p x(t)}{dt^p}$ and accounting for the derivation property, we obtain:

$$\begin{aligned} a_0 Y_L(s) + \sum_{r=1}^n a_r \left(s^r Y_L(s) - \sum_{k=0}^{r-1} s^{r-k-1} \frac{d^k y(0^+)}{dt^k} \right) \\ = b_0 X_L(s) + \sum_{p=1}^m b_p \left(s^p X_L(s) - \sum_{l=0}^{p-1} s^{p-l-1} \frac{d^l x(0^+)}{dt^l} \right) \end{aligned}$$

By transferring all of the independent terms of $Y_L(s)$ to the second member, we discover that the response $Y_L(s)$ can be shared into two parts: one depending on the initial conditions at $t = 0^+$ that corresponds to the system's proper (or free) regime $Y_P(s)$, and one that does not depend on this and that thus corresponds to the forced or steady-state regime $Y_F(s)$, with $Y_L(s) = Y_P(s) + Y_F(s)$. $Y_P(s)$ also corresponds to the LT of the solution of the differential equation without the second member:

$$Y_p(p) = \frac{\sum_{r=1}^n a_r \left(\sum_{k=0}^{r-1} s^{r-k-1} \frac{d^k y(0^+)}{dt^k} \right) - \sum_{p=1}^m b_p \left(\sum_{l=0}^{p-1} s^{p-l-1} \frac{d^l x(0^+)}{dt^l} \right)}{\sum_{r=0}^n a_r s^r}$$

while $Y_F(s)$ is given by the result of the product of the transmittance $H(s)$ by $X_L(s)$:

$$Y_F(s) = \frac{\sum_{p=0}^m b_p s^p}{\sum_{r=0}^n a_r s^r} X_L(s) = H(s) X_L(s)$$

However, it should be noted that the denominator is the same for both signals, which would suggest characteristics of the same nature, as addressed below in this section.

The properties of the convolution and ordinary products are also applied to the LT; one can deduced that, since the LT and FT of $y(t)$ are given by an ordinary product, $y(t)$ is given by a convolution product of $x(t)$ with a characteristic function of the system.

Furthermore, the expression of $H(s)$ is strictly identical to that deduced in harmonic conditions obtained by replacing $j\omega$ by the complex variables.

CONCLUSIONS.— *Transmittance $H(s)$ is a rational fraction whose polynomials have only real coefficients b_p , in numerator and a_r in denominator, which are, respectively, the p th and r th order derivative coefficients of the input and output signals in the system's differential equation. The roots are thus necessarily real or complex conjugates.*

Moreover, there is complete identity for the expressions of $H(s)$ and $H(j\omega)$ obtained, respectively, by the ratio of the Laplace transforms for steady-state input and output signals and the ratio of FTs for input and output signals.

The roots of the numerator are called zeros, noted as z_i and those of the denominator poles, noted as s_k :

$$H(s) = H_0 \left(\frac{s}{\omega_0} \right)^q \frac{(s - z_1)(s - z_2)(s - z_3) \cdots}{(s - s_1)(s - s_2)(s - s_3) \cdots},$$

which can also be written by grouping the terms whose roots are complex conjugates (with H_0 or H_0' real constants) and by factoring all of the roots:

$$H(s) = H_0' \left(\frac{s}{\omega_0} \right)^q \frac{\left(1 + \frac{s}{\omega_{11}}\right) \left(1 + \frac{s}{\omega_{12}}\right) \cdots \left(1 + 2\zeta_{21} \frac{s}{\omega_{21}} + \frac{s^2}{\omega_{21}^2}\right) \left(1 + 2\zeta_{22} \frac{s}{\omega_{22}} + \frac{s^2}{\omega_{22}^2}\right) \cdots}{\left(1 + \frac{s}{\omega_{31}}\right) \left(1 + \frac{s}{\omega_{32}}\right) \cdots \left(1 + 2\zeta_{41} \frac{s}{\omega_{41}} + \frac{s^2}{\omega_{41}^2}\right) \left(1 + 2\zeta_{42} \frac{s}{\omega_{42}} + \frac{s^2}{\omega_{42}^2}\right) \cdots}$$

This expression is written in reference to cases in which the roots have a real negative part, a property of stable systems as seen further. Here, the three characteristic factors of elementary transmittance may be found: 1) s^q corresponding to a pole at infinity if $q \geq 1$ and at origin if $q \leq -1$, single if $q = \pm 1$, multiple if $|q| > 1$; 2) the first degree polynomials give first-order transmittances, with a real and negative root, so that $-\omega_{11}$, $-\omega_{12}$, $-\omega_{31}$, $-\omega_{32} \dots$; 3) second-degree polynomials give second-order transmittances, with two complex conjugate roots $-\omega_{21} \left(\zeta_{21} \pm j\sqrt{1 - \zeta_{21}^2} \right)$, $-\omega_{22} \left(\zeta_{22} \pm j\sqrt{1 - \zeta_{22}^2} \right)$, $-\omega_{41} \left(\zeta_{41} \pm j\sqrt{1 - \zeta_{41}^2} \right)$, $-\omega_{42} \left(\zeta_{42} \pm j\sqrt{1 - \zeta_{42}^2} \right)$, where the ζ_{ij} are the damping coefficients....

1.2.3.3. Properties of elementary transmittances in harmonic regime

In the harmonic regime, s is replaced by $j2\pi f = j\omega$ and again we find the three types of elementary transmittances, corresponding to: 1) monomials; (2) first-degree polynomials and 3) second-degree polynomials in which 2ζ (where ζ is the damping coefficient) can be replaced by $1/Q$, the reverse of the quality coefficient. Each is characterized by a break frequency $f_c = \omega_c/2\pi$.

The study is performed in the Bode plane, that is in logarithmic coordinates or in decibels (=dB) for $|H(j\omega)|$ or $|H(j2\pi f)|$ and in semilogarithmic coordinates for $\text{Arg}\{H(j\omega)\}$ or $\text{Arg}\{H(j2\pi f)\}$. The logarithm of the whole transmittance is then easily obtained by means of the total of elementary transmittance logarithms and the argument of the whole transmittance by the totals and differences of individual arguments according to the position of the numerator or denominator of each elementary

transmittance. If K is the modulus of the logarithmic scale, $K \log |H(j2\pi f)|$ is plotted according to $K \log(f)$ or alternatively, for elementary transmittances, we can work with the reduced frequency $u = f/f_{ij}$, and do plots as a function of $U = K \log(f/f_{ij})$. K can be equal to 20 dB (decibel) and in this case, the vertical scale becomes linear with a dB graduation of 20 dB for a decade.

For a first approximation, the study is performed by means of asymptotic diagrams in which only the predominant term is considered, which amounts to studying only $K \log |H(j2\pi f)|$ in relation to $K \log(f)$, so $K \log |H(u)| = K \log \left(\frac{f}{f_{ij}} \right)^\mu = \mu K \log(u) = \mu U$ line of slope μ in the valid region of the asymptotic approximation, so for $u < 1$ or alternatively $u > 1$, that is $f < f_{ij}$ or $f > f_{ij}$.

Another graphical representation is performed when plotting the complex number $H(j\omega)$ in the complex plane. This is the Nyquist diagram, in which frequency plays the role of a variable parameter, taking values from 0 to infinity. This graph has the advantage of clearly showing the position of the image of the complex number representing transmittance in the complex plane and thus facilitating the visualization of its modulus in linear coordinates and moreover its argument. However, we should add graduations indicating frequency or u on the curve if we also require information concerning frequency.

The elementary first- and second-order transmittances are presented in detail in the following:

– In this case (2), writing $H_1(u) = 1 + ju$; and for the inverse, corresponding to the low-pass filter $[H_1(u)]^{-1} = \frac{1}{1 + ju}$, the plots are obtained as shown in

Figure 1.5.

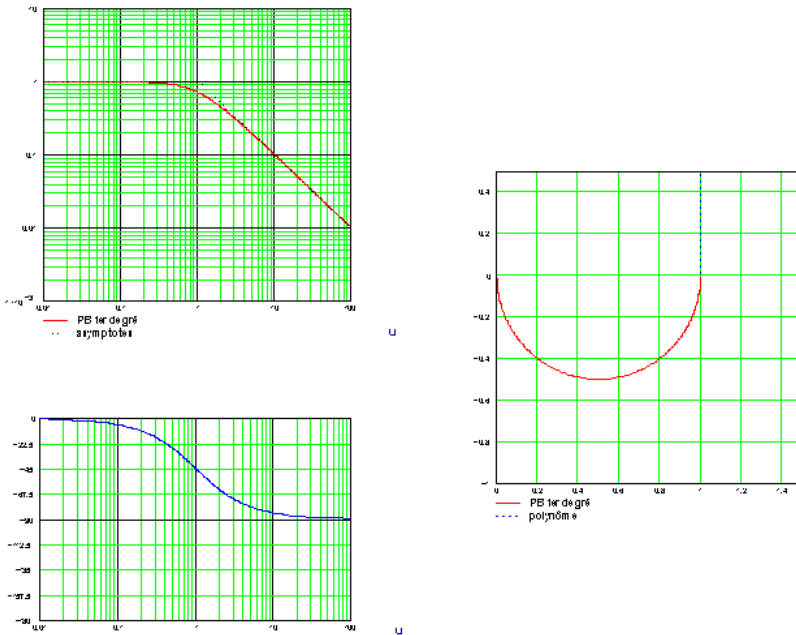


Figure 1.5. Bode and Nyquist diagrams of a first-order low-pass filter $[H_1(u)]^{-1}$ in full lines and $H_1(u)$ as a dotted line in the complex plane. For a color version of this figure, see www.iste.co.uk/muret/electronics2.zip

For $u = 1$ where $f = f_c$ (cut-off frequency), we obtain: $|H_1|^{-1} = 1/\sqrt{2}$ where $20 \log|H_1|^{-1} = -3$ dB and $\text{Arg}\{H_1^{-1}\} = -45^\circ$, while the signs are reversed for H_1 .

– In this case (3), we write: $H_2(u) = 1 - u^2 + 2j\zeta u$ where $f_n = \omega_n/2\pi$ (natural frequency) and $u = f/f_n$. We then have: $[H_2(u)]^{-1} = \frac{1}{1 - u^2 + 2j\zeta u}$, the second-order low-pass filter transmittance. Bode and Nyquist diagrams of $[H_2]^{-1}$ are shown in Figure 1.6.

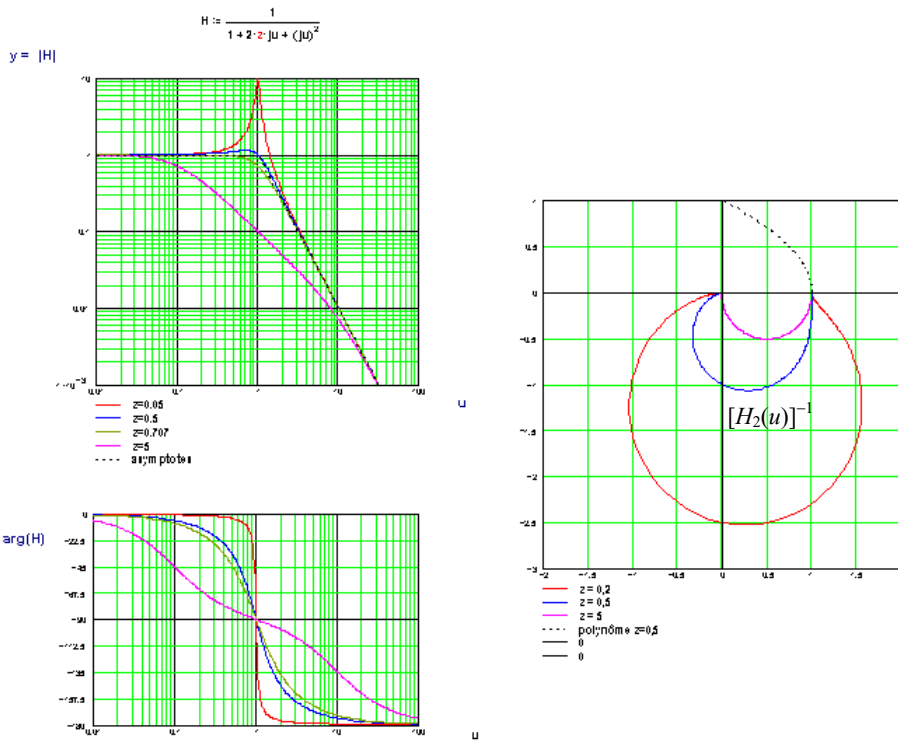


Figure 1.6. Bode and Nyquist diagrams of a second-order low-pass filter with transmittance $[H_2(u)]^{-1}$ (from the highest to the lowest curve, the ζ values, displayed as z inside the figure, are 0.05, 0.5, 0.707, 5 in the Bode diagrams at left and from the lowest to the highest 0.2, 0.5, 5 in the Nyquist diagram at right). $H_2(u)$ is plotted in the case $\zeta = 0.5$ as a dotted line in the complex plane. For a color version of this figure, see www.iste.co.uk/muret/electronics2.zip

If $\zeta > 1$ (or $Q < 1/2$), $H_2(u)$ is decomposed into a product of two elementary first-order transmittances:

$$\left[1 + ju(\zeta + \sqrt{\zeta^2 - 1})\right] \left[1 + ju(\zeta - \sqrt{\zeta^2 - 1})\right]$$

or alternatively

$$\left[1 + \frac{ju}{(\zeta - \sqrt{\zeta^2 - 1})}\right] \cdot \left[1 + \frac{ju}{(\zeta + \sqrt{\zeta^2 - 1})}\right]$$

thus returning to the previous case of the first-degree polynomials.

In any case, when $u = 1$, $|H_2| = 2\zeta = 1 / Q$ and $\text{Arg}\{H_2(u)\} = 90^\circ$. Furthermore, $\text{atan}\left(\frac{2\zeta u}{1-u^2}\right) = 45^\circ$ or 135° when $\frac{2\zeta u}{1-u^2} = \pm 1$ that is for $u_{1,2} = \sqrt{\zeta^2 + 1} \pm \zeta$.

Distance $|u_2 - u_1|$ between these last two values is equal to $2\zeta = 1/Q$ and allows for ζ to be determined knowing f_n according to the previous property: $\text{Arg}\{T_2(u)\} = 90^\circ$ for $u = 1$, that is $f = f_n$.

The smaller the damping coefficient ζ , the less the deviation $|u_2 - u_1|$ (phase variation faster as damping is smaller and also as resonance is greater when Q is higher).

If $\zeta < \frac{1}{\sqrt{2}}$ (or $Q > \frac{1}{\sqrt{2}}$), the minimum value of $|H_2|$ occurs for $u_r = \sqrt{1-2\zeta^2}$ and in this case $|H_2|_{\min} = 2\zeta\sqrt{1-\zeta^2}$ (resonance). In electronics, the expression of $H_2(u)$ is often rewritten in a more symmetrical form as: $H_2(u) = \frac{ju}{Q} \left[1 + jQ \left(u - \frac{1}{u} \right) \right]$.

Other elementary transmittances are as follows:

– Band-pass filter:
$$H_3(u) = \frac{ju}{1-u^2 + \frac{j}{Q}u} = \frac{Q}{1 + jQ \left[u - \frac{1}{u} \right]}$$

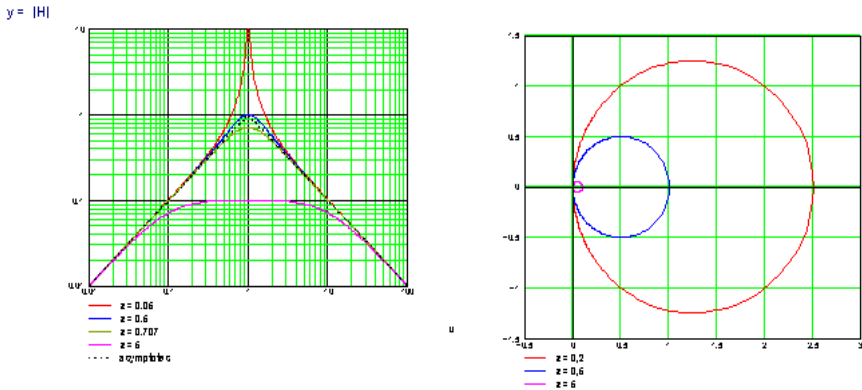


Figure 1.7. Bode and Nyquist diagrams of a second-order band-pass filter (from the highest to the lowest curves, the ζ values are 0.06, 0.6, 0.707, 6 in the Bode diagram at left and 0.2, 0.6, 6 in the Nyquist diagram at right). For a color version of this figure, see www.iste.co.uk/muret/electronics2.zip

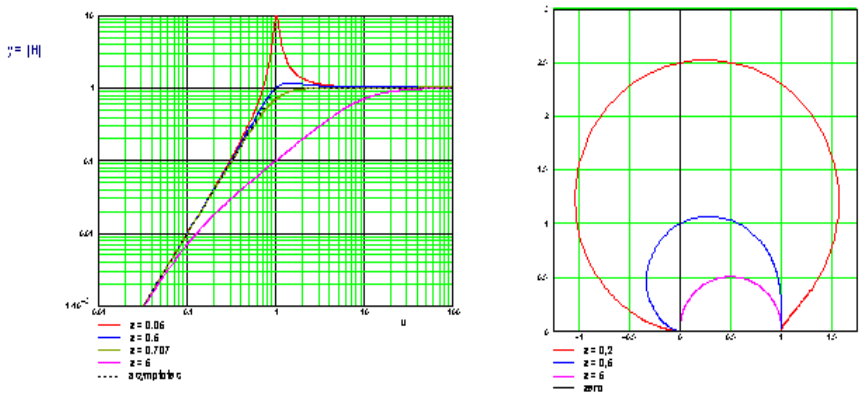


Figure 1.8. Bode and Nyquist diagrams of a second-order high-pass circuit (from the highest to the lowest curves, the ζ values are 0.06, 0.6, 0.707, 6 in the Bode diagram at left and 0.2, 0.6, 6 in the Nyquist diagram at right). For a color version of this figure, see www.iste.co.uk/muret/electronics2.zip

Transmittance $H_3(u)$ is Q (real) for $u = 1$ (resonance). A symmetry of $|H_3(u)|$ relative to the vertical axis at $u = 1$ occurs in the Bode plot while a symmetry of $H_3(u)$ relative to the real axis exists in the Nyquist plot. Phase is deduced from that of the low-pass by adding $+90^\circ$ (or $\pi/2$ rad) to the

argument of the numerator, inducing a symmetry of $\text{Arg}\{H_3(u)\}$ relative to the origin located at $\text{Arg}\{H_3(1)\} = 0$.

$$\text{– High-pass filter: } H_4(u) = \frac{-u^2}{1-u^2 + \frac{j}{Q}u} = \frac{jQu}{1+jQ\left[u - \frac{1}{u}\right]}$$

The maximum value of $|H_4(u)|$ here occurs for $u'_r = \frac{1}{\sqrt{1-2\zeta^2}}$ in cases

where $\zeta < \frac{1}{\sqrt{2}}$ and is $|H_4(u'_r)| = \frac{1}{2\zeta\sqrt{1-\zeta^2}}$. Phase is deduced from that of the

low-pass by adding 180° (or π rad) to the numerator's argument.



1.2.3.4. *Transient responses to a causal-type excitation ($x(t) = 0$ for $t < 0$)*

Transform $Y_L(s)$ is calculated from the general expression given in section 1.2.3.1, and then searching for the original exponential responses in $y(t)$ after partial fraction decomposition over the reals into fractions with linear and quadratic denominators and the use of a dictionary of Laplace transforms (see below).

It should be noted that the denominator $D(s)$ is the same for both terms $Y_P(s)$ (proper regime) and $Y_F(s)$ (forced regime) and that, as a consequence, the transmittance poles are the same and of fundamental significance. They determine the aspect of the transient response by means of coefficient λ of exponent λt appearing in the exponential functions contained in $y(t)$.

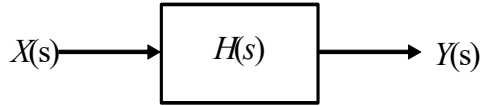
We can rewrite the denominator $D(s)$ from section 1.2.3.2 in the form of a s polynomial factorized in the first-degree polynomials, and in second degree only for those with complex poles (i.e. if $\zeta < 1$ or $Q > 1/2$):
 $D(s) = (s + \omega_{31})(s + \omega_{32}) \cdots (s^2 + 2\zeta_{41}\omega_{41}s + \omega_{41}^2)(s^2 + 2\zeta_{42}\omega_{42}s + \omega_{42}^2) \cdots$

The map of poles, that is the roots of $D(s)$, in the complex plane is those composed of negative real values (or exceptionally positive, however the system is unstable in this case) $-\omega_{31}$, $-\omega_{32}$, ... and complex conjugated roots, that are symmetrical relative to the real axis $-\omega_{41} (\zeta_{41} \pm j\sqrt{1-\zeta_{41}^2})$, $-\omega_{42} (\zeta_{42} \pm j\sqrt{1-\zeta_{42}^2})$, ... with $\omega_j > 0$.

Type	$H(s)$	Step response at $t > 0$
1 st order low-pass	$\frac{1}{1 + \frac{s}{\omega_1}}$	$1 - \exp(-\omega_1 t)$ 
1 st order high-pass	$\frac{\frac{s}{\omega_1}}{1 + \frac{s}{\omega_1}}$	$\exp(-\omega_1 t)$ 
2 nd order low-pass ($\zeta < 1$)	$\frac{1}{1 + 2\zeta \frac{s}{\omega_n} + \left(\frac{s}{\omega_n}\right)^2}$	$1 - \frac{\exp(-\zeta\omega_n t)}{\sqrt{1-\zeta^2}} \cos[\omega_n \sqrt{1-\zeta^2} t - \varphi_0]$ with $\sin(\varphi_0) = \zeta$
2 nd order passband ($\zeta < 1$)	$\frac{\frac{s}{\omega_n}}{1 + 2\zeta \frac{s}{\omega_n} + \left(\frac{s}{\omega_n}\right)^2}$	$\frac{\exp(-\zeta\omega_n t)}{\sqrt{1-\zeta^2}} \sin[\omega_n \sqrt{1-\zeta^2} t]$
2 nd order high-pass ($\zeta < 1$)	$\frac{\left(\frac{s}{\omega_n}\right)^2}{1 + 2\zeta \frac{s}{\omega_n} + \left(\frac{s}{\omega_n}\right)^2}$	$\frac{\exp(-\zeta\omega_n t)}{\sqrt{1-\zeta^2}} \cos[\omega_n \sqrt{1-\zeta^2} t + \varphi_0]$

NOTE.— The step response for the products of the transmittances above is obtained by the convolution of the individual time responses if the numerator and denominator are under the form of first- and second-degree polynomial products. If the rational fraction has been completely decomposed into a sum of fractions with first- and second-degree denominators (total of elementary transmittances), we must simply add the corresponding step responses. When one wants to explicitly introduce the unit step $U(t)$, the rules of the distribution for LT (see Appendix) must be applied, which makes the Dirac impulse appear after derivation in the time domain, in the case of high-pass transmittances (see Chapter 2).

Let us return to the system equation replaced by a block diagram in which transmittance $H(s) = N(s) / D(s)$ is set, which allows for $Y(s) = H(s) X(s)$ to be obtained if the initial conditions ($y(0^+)$ and its derivatives) are zero and in harmonic state by replacing s by $j\omega$ or $j2\pi f$:



In the case where $x(t)$ is a unit step $U(t)$ (zero for $t < 0$, =1 for $t > 0$), the step response is obtained after searching in $H(s)/s$ the original exponential elementary functions of the transmittances presented in the previous table.

1.2.3.5. Pole map in the complex plane and interpretation

The transmittance poles are the roots of the denominator $D(s) = (s + \omega_{31})(s + \omega_{32}) \cdots (s^2 + 2\zeta_{41}\omega_{41}s + \omega_{41}^2)(s^2 + 2\zeta_{42}\omega_{42}s + \omega_{42}^2) \cdots$, that are $-\omega_{31}$, $-\omega_{32}$, ... in first-degree polynomials and $-\omega_{41} \left(\zeta_{41} \pm j\sqrt{1-\zeta_{41}^2} \right)$, $-\omega_{42} \left(\zeta_{42} \pm j\sqrt{1-\zeta_{42}^2} \right)$, ... in the second-degree polynomials. As seen in the previous section, only the poles have an influence on the transient response since the roots of the numerator (the zeros) no longer appear as special values after partial fraction expansion of the rational fraction $H(s)$. The presence of simple real poles suggests non-oscillating and exponentially damped responses, while complex conjugate poles leads to exponentially damped oscillating responses. For a complex pole $-\omega_{41} \left(\zeta_{41} \pm j\sqrt{1-\zeta_{41}^2} \right)$, with natural angular frequency ω_{41} , the modulus is constant and equal to ω_{41} irrespective of ζ_{41} (Figure 1.9). The argument is equal to $\pi \pm \text{Acos}\zeta_{41}$, corresponding to a vector whose extremity is located in the left half-plane since the real part is negative. When ζ_{41} goes from 0 to 1, both conjugate poles then describe a quarter circle of radius ω_{41} in the complex plane. If the damping coefficient increases above 1, the poles will become real and move away on both sides from value $-\omega_{41}$ located on the real axis, with values $\omega_{31}, \omega_{32} = \omega_{41} \left(\zeta_{41} \pm \sqrt{\zeta_{41}^2 - 1} \right)$ (Figure 1.9).

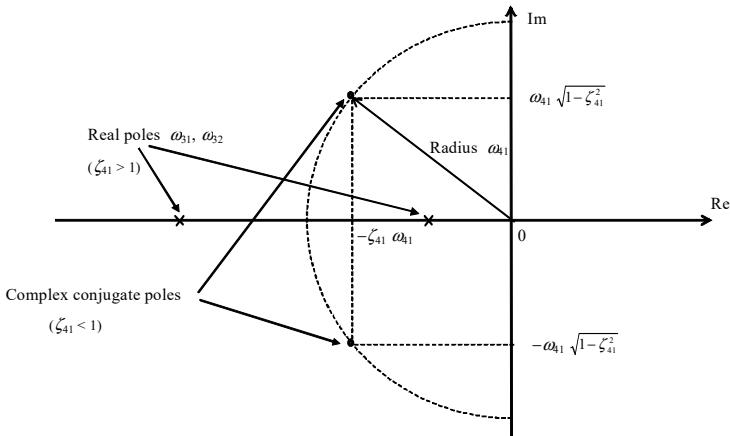


Figure 1.9. Map of transmittance poles

1.3. Negative feedback

Many analog electronic systems are made by means of negative feedback that allows for certain properties to be improved and for the development of new systems. Considering only forced conditions, a one-input-one-output system with negative feedback can be represented by the following functional diagram (or block diagram) in which all the quantities are dependent on the complex variable s .

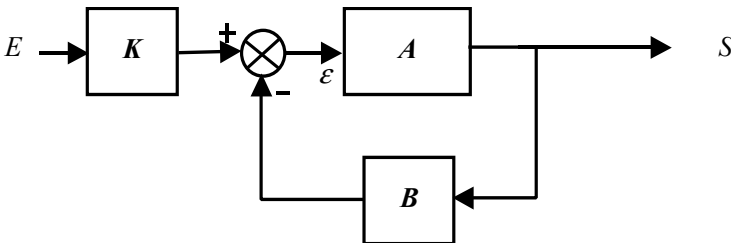


Figure 1.10. Block diagram of a negative feedback system

Signal $\varepsilon = KE - BS$ is multiplied by A to give $S = A(KE - BS) = KAE - ABS$, then:

$$S = E \frac{KA}{1 + AB} \text{ or alternatively } \frac{S}{E} = H = \frac{KA}{1 + AB}$$

where A is the open loop gain, AB is the loop gain and H is the closed loop gain.

1.3.1. Inversion of a transfer function

It should suffice that $AB \gg 1$ so that $S \approx E \frac{K}{B}$, which is reduced to $S \approx E \frac{1}{B}$ if $K = 1$.

The transfer function is $H = \frac{S}{E} = \frac{K}{B}$ and since $KE \approx BS$, we have $\epsilon \approx BS - BS = 0$.

This is the basis of operational amplifier systems, which have high A gain in open loop, but prone to variation, which can be escaped by means of negative feedback. For example, a voltage amplifier can be obtained in closed loop by reversing the voltage divider function $B = \frac{R_1}{R_1 + R_2}$.

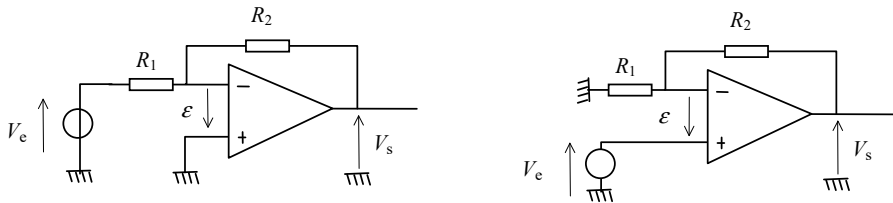


Figure 1.11. Inverting amplifier (left) and non-inverter (right) circuit

Neglecting input currents: $-\epsilon = BV_s + (1 - B)V_e = -\frac{V_s}{A}$ for the inverter and $\epsilon = V_e - BV_s = \frac{V_s}{A}$ for the non-inverter; hence the deduction in the general case, and since $AB \gg 1$:

$$\frac{V_s}{V_e} = \frac{A(B-1)}{1+AB} \rightarrow 1 - \frac{1}{B} = -\frac{R_2}{R_1}$$

for the inverter and $\frac{V_s}{V_e} = \frac{A}{1+AB} \rightarrow \frac{1}{B} = 1 + \frac{R_2}{R_1}$ for the non-inverter. These results can be obtained directly by initially assuming $\varepsilon = 0$.

This operation can be applied to nonlinear functions to obtain the reciprocal function. For example, multiplication or raising to square placed in the return loop provides an analog division or a square root function (assuming $\varepsilon = 0$ initially):

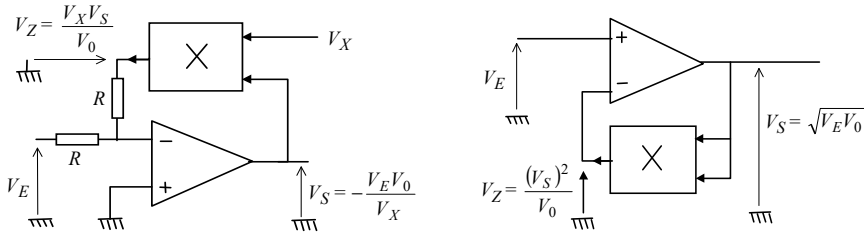


Figure 1.12. Divider (left) and square root function (right), with V_0 as a constant voltage

CONCLUSION.— Negative feedback leads to implementation of the reverse function or of the reciprocal function to that present in the return loop if the modulus of the loop gain is much greater than 1.

1.3.2. Linearization of a nonlinear system

The relation between closed-loop transfer function variations and their open loop counterparts is deduced from the logarithmic derivation of H :

$$\frac{dH}{H} = d(\text{Log}H) = \frac{dA}{A} - \frac{BdA}{1+AB} = \frac{dA}{A} \cdot \frac{1}{1+AB}$$

The relative variation of A is divided by $1 + AB \gg 1$ and the nonlinearity can then be reduced in the same proportion. In terms of applications use, we can point to feedback in B or AB class amplifiers working to reduce distortion at the zero crossing of the output current, the

suppression of diode threshold in rectification (see Figure 1.13) and improvement of operational amplifier linearity.

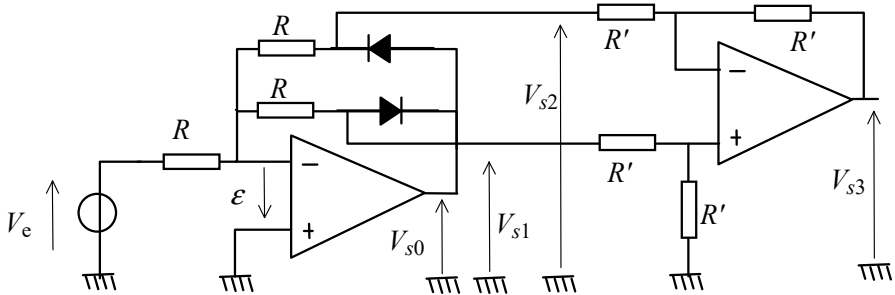


Figure 1.13. "No threshold" rectification

1.3.3. Gain-bandwidth product for first-order low-pass systems

If $A(jf) = \frac{A_0}{1 + j\frac{f}{f_1}}$ where A_0 is real, the open loop gain is $A^{BF} = A_0$ at $f \ll f_1$

and the high-frequency asymptote is $A^{HF} = \frac{A_0 f_1}{jf}$. This is produced for operational amplifiers with unity gain compensation that results in a -20 dB/decade slope until the frequency $A_0 f_1$.

If the feedback coefficient is real, being $B = B_0$:

$$H = \frac{A}{1 + AB} = \frac{A_0}{1 + j\frac{f}{f_1} + A_0 B_0} \approx \frac{1}{B_0} \frac{1}{1 + j\frac{f}{A_0 B_0 f_1}} \text{ if } A_0 B_0 \gg 1$$

which shows that $H^{LF} = 1/B_0$ at low frequency (LF) and that the high frequency (HF) asymptote is still $H^{HF} = \frac{A_0 f_1}{jf}$.

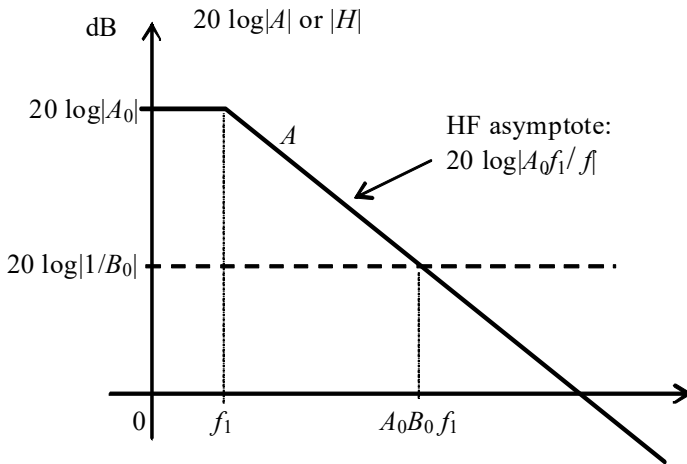


Figure 1.14. Asymptotic Bode diagram of operational amplifier circuit gains

The high-frequency asymptote remains the same in closed loop as in open loop or, in other words, the gain-bandwidth product (= LF gain \times upper cutoff frequency), equal to $A_0 f_1$ is likewise unchanged.

In some cases, this rule is not accurately set, particularly when the number of parameters is greater than 3 (here the parameters are only A_0 , f_1 and B_0); nonetheless, negative feedback always increases bandwidth.

1.3.4. Simultaneous negative and positive feedback

This situation can be found in operational amplifier impedance converters fitted with two return loops, one on the inverter input and the other on the non-inverter input. Input impedance can be calculated from the evaluation of

I_e and the elimination of V_s and ε using relations $V_s \frac{Z_b}{Z_a + Z_b} = V_e + \varepsilon$,

$V_s = A \varepsilon$ and $Z_2 I_e = V_e - V_s$.

After calculation this gives:
$$\frac{V_e}{I_e} = \frac{Z_2}{1 - \frac{A(1 + Z_a/Z_b)}{A - (1 + Z_a/Z_b)}}$$

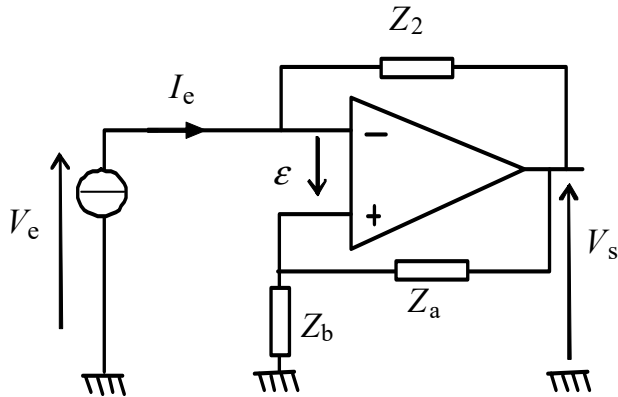


Figure 1.15. Impedance converter circuit

It is evident that this positive feedback has entailed a difference in the denominator. Inside the bandwidth, $A \gg |1 + Z_a/Z_b|$ and consequently:

$$\frac{V_e}{I_e} \approx -\frac{Z_2 Z_a}{Z_b}$$

In the simple case where $Z_a = Z_b = R$, input impedance is Z_2 with changed sign. This circuit can work to create negative resistance, providing energy to the external circuit when it is crossed by a current and is used in oscillator circuits. Feedback coefficient B depends on the circuit into which the converter is inserted. In particular, if an impedance Z_1 is positioned in series with the negative input, for $V_e = 0$: $\frac{\varepsilon}{V_s} = \frac{Z_b}{Z_b + Z_a} - \frac{Z_1}{Z_2 + Z_1} = B$. The path of the complex number AB in the complex plane will be the system's stability or instability determinant, as addressed in the following.

1.4. Study of system stability

Systems are strictly *stable* if the output $y(t)$ tends to zero asymptotic value after the return to zero of a transient excitation $x(t)$ on the input.

In contrast, systems are *unstable* if, under the same input conditions, output diverges or alternatively leads to a limited signal that does not however approach zero.

1.4.1. Time response: pole mapping

As discussed in section 1.2.3.1, the LT of $y(t)$ is composed of the proper response $Y_P(s)$ and forced response $Y_F(s) = H(s) X_L(s)$, which is proportional to input LT[$x(t)$]:

$$Y_L(s) = \frac{\sum_{r=1}^n a_r \left(\sum_{k=0}^{r-1} s^{r-k-1} \frac{d^k y(0^+)}{dt^k} \right) - \sum_{p=1}^m b_s \left(\sum_{l=0}^{p-1} s^{p-l-1} \frac{d^l x(0^+)}{dt^l} \right)}{\sum_{r=0}^n a_r s^r} + \frac{\sum_{p=0}^m b_p s^p}{\sum_{r=0}^n a_r s^r} X_L(s)$$

The initial conditions are only non-zero in the first fraction if the system has enough energy stored in capacitances or inductances to dissipate. Thus, nothing prevents a study of the possibility of an output divergence from zero initial conditions, which is more severe. Moreover, it is evident that the denominator, whose roots (the poles) determine the time response, is the same for both terms. Accordingly, only the following is studied:

$$Y_F(s) = \frac{\sum_{p=0}^m b_p s^p}{\sum_{r=0}^n a_r s^r} X_L(s) = H(s) X_L(s)$$

Following the same reasoning, the case of excitation with a Dirac impulse, whose LT is 1, may be considered, yielding a more straightforward

conclusion. Hence, it should suffice to study $H(s) = \frac{\sum_{p=0}^m b_p s^p}{\sum_{r=0}^n a_r s^r}$ whose inverse

Laplace transform LT^{-1} is the impulse response. According to the convergence or non-convergence of the output signal $\text{LT}^{-1}[H(s)]$ toward zero, the system will be stable or unstable.

Once the poles have been determined, we can then deduce the integer part after division of both polynomials if $m \geq n$, and the following rational fractions by partial fraction expansion into fractions with first- and second-degree denominators:

$$H(s) = \frac{N(s)}{D(s)} = \frac{\sum_{p=0}^m b_p s^p}{\sum_{r=0}^n a_r s^r} = \frac{b_m}{a_n} \left[\sum_{i=0}^{m-n} s^i + \sum_{r=1}^{n'} \frac{A_r}{s - s_r} + \sum_{k=n'+1}^2 \frac{B_k s + C_k}{(s - s_k)^2 + \omega_k^2} \right]$$

where poles s_r are real, possibly multiples of total number n' ; s_k and ω_k are, respectively, the real part and the imaginary part of the complex conjugate poles. The natural frequency is then the pole modulus, that is $\sqrt{\omega_k^2 + s_k^2}$. When s_r and s_k have negative values, we obtain positive signs if the denominators are expressed with positive numerical coefficients.

The table below presents the original or LT^{-1} of each term, with s_r as a real pole, s_k the real part of a complex pole, $\mathcal{U}(t)$ the step function and $\delta(t)$ the Dirac distribution if needed:

$F(s)$	$f(t) = \text{TL}^{-1}\{F(s)\}$
$\frac{1}{s^n}$ with $n > 0$	$\frac{t^{n-1}}{(n-1)!} \mathcal{U}(t)$
$\frac{1}{s^2}$	$t \mathcal{U}(t)$
$\frac{1}{s}$	$\mathcal{U}(t)$
1	$\delta(t)$ *
s^n	$\delta^{(n)}(t)$ *
$\frac{1}{s - s_r}$	$\exp(s_r t) \mathcal{U}(t)$
$\frac{1}{(s - s_r)^2}$	$t \exp(s_r t) \mathcal{U}(t)$
$\frac{1}{(s - s_r)^n}$ with $n > 0$	$\frac{t^{n-1} \exp(s_r t)}{(n-1)!} \mathcal{U}(t)$
$\frac{\omega_k}{(s - s_k)^2 + \omega_k^2}$	$\exp(s_k t) \sin(\omega_k t) \mathcal{U}(t)$
$\frac{s}{(s - s_k)^2 + \omega_k^2}$	$\exp(s_k t) \cos(\omega_k t) \mathcal{U}(t)$

*In terms of distributions (see Appendix).

The LT^{-1} of the integer part (if $m \geq n$) corresponds to the Dirac impulse and their derivatives, which contribute nothing when $t > 0^+$. Accordingly, only rational fractions need to be examined here.

Among the LT^{-1} of $\frac{b_m}{a_n} \sum_{r=1}^{n'} \frac{A_r}{(s-s_r)}$, some are systematically divergent

(in cases of a multiple pole at origin, that is when $s_r = 0$); and others only if s_r or s_k is positive due to factor $\exp(s_r t)$ or $\exp(s_k t)$ present in the time response. And conversely:

THEOREM 1.1. – *A system is stable if all the poles of its transfer function are located on the left half plane (strictly negative real part) of the complex plane.*

The polynomial of the denominator is in this case known as a Hurwitz polynomial.

1.4.2. Nyquist criterion in general case

If the roots of numerator $N(s)$ of degree m and denominator $D(s)$ of

degree n in the rational fraction $H(s) = \frac{\sum_{p=0}^m b_p s^p}{\sum_{r=0}^n a_r s^r} = \frac{N(s)}{D(s)}$ are not known,

nonetheless their number is known, m and n . Then, the Nyquist criterion is based on the Cauchy theorem.

THEOREM 1.2.–

$H(s)$ is supposed to be a function of the complex variable s , holomorphic inside a closed contour C (i.e. single-valued and derivable), except in a certain number of poles (singular points). If image P of s describes C in one direction, image H of $H(s)$ describes closed contour Γ in the same direction with a variation of the argument of $H(s)$ equal to $2\pi(m_1 - n_1)$, where m_1 and n_1 are, respectively, the number of zeros and poles of $H(s)$ included in contour C .

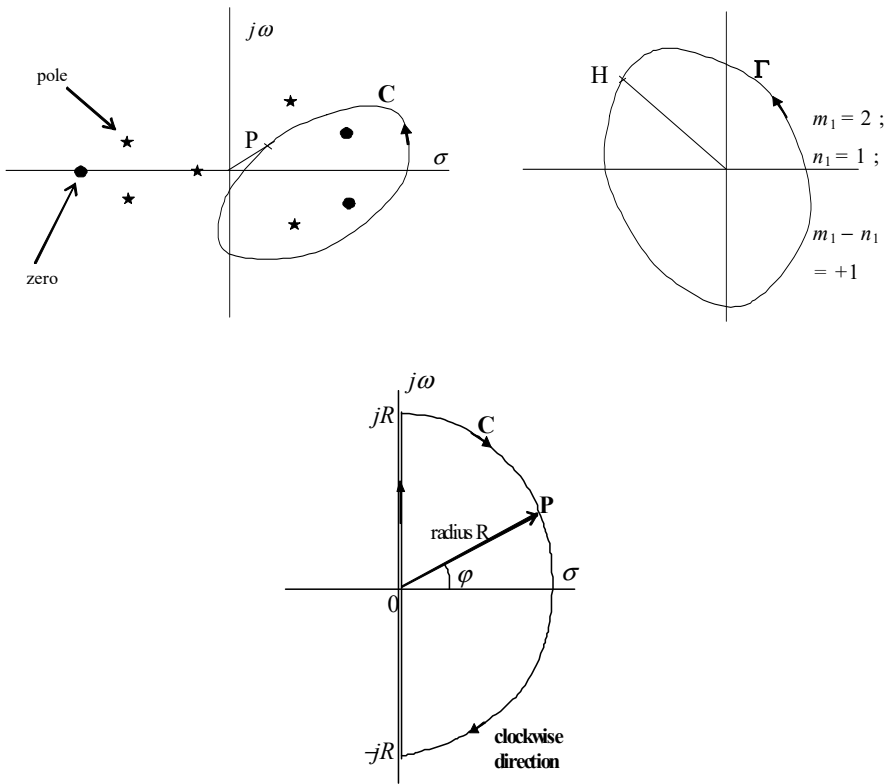


Figure 1.16. Nyquist diagrams of the complex variable $s = \sigma + j\omega$ and of the transfer function $H(s)$

CONVENTION.— *The direction of rotation giving positive angles measured relative to the real positive axis is that indicated in the upper parts of Figure 1.16, which is called counter-clockwise direction, whereas the opposite rotation direction is called clockwise or direct.*

If P follows closed contour C that encircles the right half-plane of the complex plane (Nyquist contour) when radius R approaches infinity, in the clockwise direction (as shown here) and if the number of zeros m of $H(s)$ is known in this right half-plane, the number of turns k done by H on Γ in the

same direction is equal to $m - n > 0$, where n is the number of poles in the right half-plane. Accordingly, if $k > 0$, the number of poles in this same right half-plane may be deduced as equal to $m - k$ (if, however, H follows Γ in the counter-clockwise direction k times around the origin, this is an indication that $n > m$). However, since the system is only stable if $n = 0$, the Nyquist rule may be deduced.

THEOREM 1.3. – *A system is stable if the Nyquist diagram of its transfer function $H(s)$ encircles the origin in the clockwise direction as many times as $H(s)$ has zeros with real positive part. Where there are none, the system is stable if the Nyquist diagram does not surround the origin.*

Note that when P is on the imaginary axis, $s = \pm j\omega$, so $H(s) = H(\pm j\omega)$, which can be studied with the Bode diagram by making ω go from 0 to ∞ . When P is on the circle of constant radius R , $s = R \exp(j\varphi)$. But if $R \rightarrow \infty$, simple elements $\frac{b_m}{a_n} \sum_{i=1}^n \frac{A_i}{(s - s_i)}$ approach zero if $|s| \rightarrow \infty$, whether it is pure or complex imaginary and as a consequence, no new information is supplied. Thus, it should suffice to study the contour followed by $H(j\omega)$, from $H(-j\infty)$ to $H(+j\infty)$. This is the reason for which the clockwise direction was chosen, since the path of radius R is then made in this way. However, it is often difficult to verify if H encircles the origin or not when $H(j\omega) \rightarrow 0$ for $\omega \rightarrow \infty$, which is always the case for physical systems that never have infinite bandwidth (the integer part of $H(s)$ is zero). Furthermore, systems are very regularly built by feedback from subsystems themselves stable. Accordingly, it would be more useful to study this case.

1.4.3. Stability of looped systems assumed stable in open loop: Nyquist and Bode criteria

Here, $H(s) = \frac{N(s)}{D(s)} = \frac{A(s)}{1 + A(s)B(s)}$ and the poles of $H(s)$ are the roots of

$D(s)$, that is the zeros of $1 + A(s)B(s)$, which only has poles with negative real part if it is assumed that the system is stable in open loop. Thus, it is sufficient that the denominator $1 + A(s)B(s)$ also has no root with real positive part. When applying the Nyquist criterion to $1 + A(s)B(s)$ in order for the system to be stable, the Nyquist diagram of $1 + A(j\omega)B(j\omega)$ must not

encircle the origin in the clockwise direction when ω goes from 0 to infinity or in more usual words.

THEOREM 1.4. – *For system stable in open loop to be stable in closed loop, the Nyquist diagram of the loop transmittance $A(j\omega)B(j\omega)$ must not surround point -1 (located on the real axis) in the clockwise direction when ω goes from 0 to infinity.*

If the Nyquist diagram of $A(j\omega)B(j\omega)$ crosses point -1 , the stability limit has been reached and the denominator $D(j\omega) = 1 + A(j\omega)B(j\omega)$ crosses through 0 for the special frequency ω_0 , which is the oscillator frequency in steady-state regime. Condition $A(j\omega_0)B(j\omega_0) = -1$ is written alternatively:

$$\text{Arg}\{A(j\omega_0)B(j\omega_0)\} = (2k+1)\pi \quad (k \text{ integer}) \text{ and } |A(j\omega_0)B(j\omega_0)| = 1$$

If modulus $|A(j\omega_0)B(j\omega_0)| > 1$, the image of $A(j\omega)B(j\omega)$ goes beyond point -1 on the left side of the negative real numbers and the system is thus unstable. So, the Bode criterion can be deduced.

THEOREM 1.5. – *A system including a feedback loop whose loop gain is $A(j\omega)B(j\omega)$ is stable if and only if, when $\text{Arg}\{A(j\omega)B(j\omega)\} = (2k+1)\pi$, we have $|A(j\omega)| < \frac{1}{|B(j\omega)|}$.*

It should suffice then to study the Bode diagrams for $A(j\omega)$ and $1/B(j\omega)$ together.

Furthermore, an unstable system can be stabilized by adding a suitable corrector to reduce $|A(j\omega)|$ or increase $|B(j\omega)|$ in the neighborhood of ω_0 to make a gain margin appear, or alternatively that modifies $\text{Arg}\{A(j\omega)B(j\omega)\}$ in order for the phase stability condition to be met within some phase margin (see Figure 1.17).

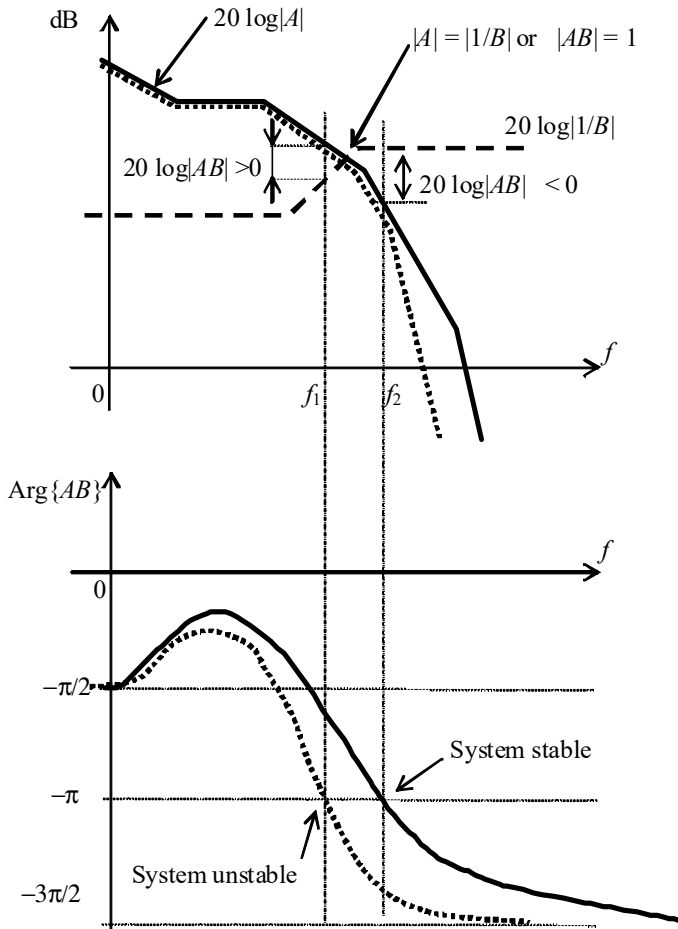


Figure 1.17. Bode diagrams of the gain modulus and the reverse of the feedback coefficient, and loop gain argument, for a closed-loop system stable in open loop (full line, system stable in closed loop since $|1/B| > |A|$ for $f = f_2$; dotted line, system unstable in closed loop since $|1/B| < |A|$ for $f = f_1$; the frequencies corresponding to $\text{Arg}\{AB\} = \pi$ in each case)

1.4.4. Stability of linear and nonlinear networks of any order, analyzed from state variables

In networks comprising passive elements and both independent and current or voltage-dependent sources, formed of b branches and n nodes, we can write $b - n + 1$ independent equations (see Appendix of Volume 1

[MUR 17]), which in general are first-order differential equations in the time domain. Each equation links a voltage or current derivative in a reactance (capacitance or inductance) with the other voltages or currents that are the network state variables. Number $k = b - n + 1$ is the system order, and can be written in matrix form $\frac{d\mathbf{F}}{dt} = \mathbf{A}\mathbf{F} + \mathbf{B}'$, where \mathbf{F} is the column vector of state variables f_i , \mathbf{A} the matrix of coefficients that can be dependent on the \mathbf{F} coefficients when nonlinear elements are present (however stationary, that is, with a response independent of the time origin) and \mathbf{B}' a column vector containing the parameters of external and internal sources, as well as certain nonlinear element parameters. In the case of linear ordinary differential equations, this system can be transformed into the differential equation given in the introduction to this chapter or in section 1.2.1, the order of which will then be k and which will act only on one state variable and one external variable. Application of the Laplace transform to this equation together with partial fraction expansion has already shown that the transmittance poles located in the real positive part half plane of the complex plane lead to existence in the time domain of signal variations or maximum variations like $\exp(+t/\tau)$ (where τ is a positive time constant). Such an exponential growth is a clear indication of the system's instability. The presence of one or several of these factors in the time response of the system can be determined from the previous matrix equation. In the case of a nonlinear system, since it is sufficient to treat small variations around one or several operating points in order to find factors like $\exp(+t/\tau)$, the first-order development of nonlinear function occurring in \mathbf{A} and \mathbf{B}' allows for the conservation of the same differential system though with \mathbf{A} and \mathbf{B}' containing only real constants.

In this approximation, the solution of the differential system is determined through diagonalization of matrix \mathbf{A} . We then find the eigenvalues λ_i and the eigenvectors \mathbf{V}_i so that the characteristic equation $\det(\mathbf{A} - \lambda \mathbf{I}) = 0$ is verified (with $\mathbf{I} =$ unit matrix) for the various eigenvalues $\lambda = \lambda_i$, each assumed distinct. Base change is performed by means of left and right multiplication by square and invertible matrices \mathbf{V}^{-1} and \mathbf{V} , the latter comprising the components of each eigenvector \mathbf{V}_i in each of its columns, in the same order as the corresponding eigenvalues. The initial matrix equation is rewritten introducing $\mathbf{I} = \mathbf{V}\mathbf{V}^{-1}$: $\frac{d\mathbf{F}}{dt} = \mathbf{A}\mathbf{V}\mathbf{V}^{-1}\mathbf{F} + \mathbf{B}'$ then multiplying on the

left side by \mathbf{V}^{-1} , which allows for the production of diagonal matrix $\mathbf{\Lambda} = \mathbf{V}^{-1} \mathbf{A} \mathbf{V}$, containing λ_i : $\frac{d(\mathbf{V}^{-1}\mathbf{F})}{dt} = \mathbf{\Lambda}(\mathbf{V}^{-1}\mathbf{F}) + \mathbf{V}^{-1}\mathbf{B}'$

This matrix equation can be rewritten in the form of a system of independent first-order differential equations, each containing a single new state variable w_i , elements of matrix column $\mathbf{W} = \mathbf{V}^{-1} \mathbf{F}$ and element d_i of $\mathbf{V}^{-1} \mathbf{B}'$, yielding k ordinary differential equations like:

$$\frac{dw_i}{dt} = \lambda_i w_i + d_i \text{ or alternatively } \frac{dw_i}{w_i + d_i / \lambda_i} = \lambda_i dt .$$

Each of these equations has a solution $w_i(t) = c_i \exp(\lambda_i t) - d_i / \lambda_i$ where c_i is an integration constant and where λ_i are the system poles because of the form like $\exp(\lambda_i t)$ of the solutions. The problem becomes here to merely determine whether any of the eigenvalues contain a real positive part, which would be sufficient to provoke system instability from the operating point subject to calculation. Since $\mathbf{F} = \mathbf{V}\mathbf{W}$, the original state variables may be readily found through the linear combination resulting from the matrix product $\mathbf{V}\mathbf{W}$, where $f_i(t) = \sum_{j=1}^{b-n+1} v_{ij} w_j(t)$ if v_{ij} represents \mathbf{V} elements. However, since a single diverging term included in this sum is sufficient to make the operating point in question become unstable, we need only to search for the real part of the eigenvalues. If there are several possible static operating points, some can be stable and others unstable, in which case the system can converge to one of the stable points. If, on the other hand, all of the operating points are unstable, the whole system is unstable.

This is broader and more flexible than previous methods, since it adapts to nonlinear networks and can receive assistance from the eigenvalues evaluation supplied by numerical or symbolic calculation software, in symbolic value up to the fourth order. In addition, it forms the basis of the calculations performed in simulators to determine the time responses, since it is easy to determine how the state variables evolve step by step over a long duration by considering the new operating point reached through the first calculation that ceases to be valid as initial vector for the next calculation and again thereafter (see section 1.5 for more details).

1.5. State space form

In the stability study performed in the previous section using the first-order differential equations system (state equations, numbering k , also the system order) describing the system, the notion of input and output variables is not completely clear. In order to apply this representation to dynamic systems, electronic or otherwise, controlled by one or several input variables and delivering one or several output variables, the equation above must be modified and another must be added. Column vector \mathbf{B}' results from the application of input signals or system inputs, numbering m . As a result, \mathbf{B}' is replaced by $\mathbf{B}\mathbf{X}$, where \mathbf{B} is the control matrix, of format $k \times m$ and \mathbf{X} the column vector of the input variables, with m lines. The second matrix equation allows for the definition of the output(s), numbering p , whose column vector is \mathbf{Y} , depending linearly on state variables \mathbf{F} and input variables \mathbf{X} , by means of observation matrix \mathbf{C} , of format $p \times k$, and at the direct action matrix \mathbf{D} , of format $p \times m$. This results in a system of two matrix equations, which are entirely defined by state matrix \mathbf{A} , of format $k \times k$, whose eigenvalues are the system poles, and matrices \mathbf{B} , \mathbf{C} and \mathbf{D} :

$$\begin{cases} \frac{d\mathbf{F}}{dt} = \mathbf{A}\mathbf{F} + \mathbf{B}\mathbf{X} \\ \mathbf{Y} = \mathbf{C}\mathbf{F} + \mathbf{D}\mathbf{X} \end{cases}$$

For linear and stationary systems, all the elements of matrices \mathbf{A} , \mathbf{B} , \mathbf{C} and \mathbf{D} are constant quantities, independent of time. Of course, it is indeed possible to take the LT of these equations, which corresponds to the system block diagram in Figure 1.18.

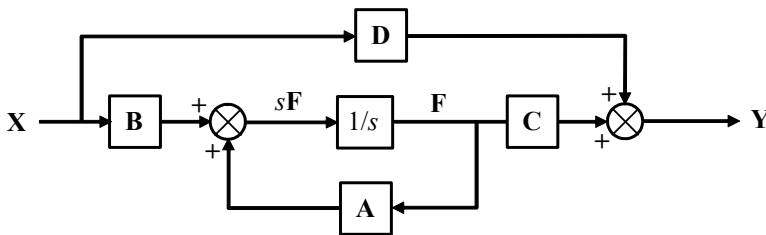


Figure 1.18. Block diagram of a system in state representation

It is obvious that this representation accounts for the internal operation of the system. This can unveil some poles that are referred to as “hidden” if they do not appear in the system’s expression of the transmittance, which is then of an order less than k . Generally speaking, \mathbf{A} , \mathbf{B} , \mathbf{C} and \mathbf{D} are the application matrix acting on vectors \mathbf{X} , \mathbf{Y} and \mathbf{F} , belonging to the vector spaces of respective dimensions m , s and k . Subject to the bases selected, there can be an infinity of system representations with their corresponding matrix. However, as discussed in section 1.4.5, a single base allows for a diagonal representation \mathbf{A}_0 of the application acting on \mathbf{F} , which can be determined by calculating the eigenvalues and eigenvectors of \mathbf{A} . Since the eigenvalues are independent of the selected base and are the system poles, the system is stable if no eigenvalue has positive or zero real part. Integration of the first equation requires the use of matrix exponentials, which are more readily calculated if \mathbf{A} is diagonal. In this respect, it is still possible to assess the time evolution of $\mathbf{F}(t)$ at instant t_f due to a command $\mathbf{X}(t)$ if the state $\mathbf{F}(t_i)$ at the initial instant t_i and all the matrix elements are known by means of a calculation software:

$$\mathbf{F}(t_f) = \mathbf{F}(t_i) \exp(\mathbf{A} \times (t_f - t_i)) + \int_{t_i}^{t_f} \mathbf{B} \mathbf{X}(t) \exp(\mathbf{A} \times (t_f - t)) dt$$

This expression can be used for nonlinear systems in which \mathbf{A} and \mathbf{B} have elements function of \mathbf{F} and \mathbf{X} , and even for non-stationary systems and sampled systems in particular. This representation allows for the introduction and determination of new properties not present in the representation by transfer function, in addition to stability, which are controllability and observability, subject, respectively, to matrix \mathbf{B} and \mathbf{C} and to their product with \mathbf{A} . Since this area is more a concern of automation and robotics, it will not be discussed in detail here. In the case of multiinput and/or multioutput systems, the state-space representation is crucial. Furthermore, matrix calculation programs (MATLAB, SciLab, etc.) include modules adapted to managing signals and systems in both automation and electronics (filtering in particular), which make significant use of the state-space form since it is more general and powerful than representation by transfer function, relying entirely on matrix calculation. More specifically, these programs include the functions necessary to assess the Kalman criteria that allow for controllability and observability to be checked, which occurs if certain square matrices comprising submatrix $\mathbf{B}\mathbf{A}^r$ and $\mathbf{C}\mathbf{A}^r$ ($0 < r < k$) have eigenvalues with no positive or zero real part. In electronics, as soon as the

electrical circuit of the application in question is known, reaching the state-space form is easy by writing, on the one hand, the network equations in number $k = b - n + 1$ as indicated in section 1.4.5 to determine **A** and **B**, and, on the other hand, the equations providing the expression of the outputs (or output) to determine **C** and **D**.

1.6. Oscillators and unstable systems

1.6.1. Sinusoidal oscillators

The creation of a sinusoidal oscillator requires only the presence of two purely imaginary and complex conjugated poles in the transmittance $H(s)$, that is on the imaginary axis. All of the system responses then provide a sinusoidal signal function of time without damping since the real part s_k or ζ that determines the decrease in factors $\exp(s_k t)$ or $\exp(-\zeta\omega_n t)$ due to the first or second degree polynomials of the denominator $D(s)$ of the transmittance will be zero.

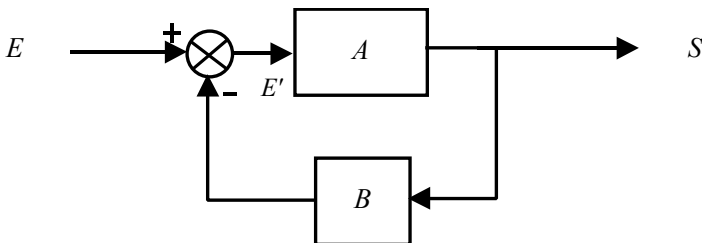
Since here this is a looped system, it may also be defined in this case as a system at its stability limit according to the Bode criterion, that is a system whose loop gain location $A(j\omega)B(j\omega)$ crosses the critical point -1 in the complex plane. Denominator $D(j\omega) = 1 + A(j\omega)B(j\omega)$ then goes through 0 for $\omega = \omega_0$, the oscillator angular frequency.

Angular frequency ω_0 such that $A(j\omega_0)B(j\omega_0) = -1$ defines the condition of oscillation that can be presented either in Cartesian form or in polar form:

$$\text{either } \operatorname{Re}[A(j\omega_0)B(j\omega_0)] = -1 \text{ and } \operatorname{Im}[A(j\omega_0)B(j\omega_0)] = 0;$$

$$\text{or } |A(j\omega_0)B(j\omega_0)| = 1 \text{ and } \operatorname{Arg}\{A(j\omega_0)B(j\omega_0)\} = (2k + 1)\pi$$

In practice, either the amplifier is of the inverter type and the minus sign in the block diagram is verified automatically:



or the return loop generates sign reversal. Nonetheless, oscillators can be made without dephasing because in the above circuit total dephasing is $(2k + 1)\pi$ (due to $\text{Arg}\{A(j\omega)B(j\omega)\}$) to which may be added $\pm\pi$ (due to the minus sign) equal to $2k\pi$ in total, which can be an indication of zero dephasing.

This is the case of the Wien bridge oscillator for example.

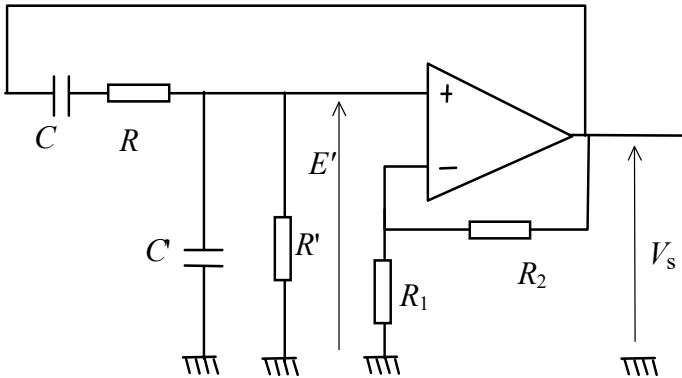


Figure 1.19. *Sinusoidal Wien bridge oscillator*

Input signal E becomes redundant since oscillation begins when a disturbance such as noise occurs, which is always present. So, it may be considered that $E = 0$. Conversely, the amplitude of output signal S is not known since writing $S = A E'$ and $E' = -B S$ results in $(1 + A B) S = 0$, which indicates that $S \neq 0$ when $A B = -1$, however any value of $S \neq 0$ is suitable.

In practice, amplitude is limited by the system's nonlinearity. Or alternatively, if perfectly constant amplitude is required, an amplitude regulator should be added capable of measuring and correcting it by acting on gain A in order to permanently maintain the oscillating state in a precise manner (see below).

– Other circuits with negative gain:

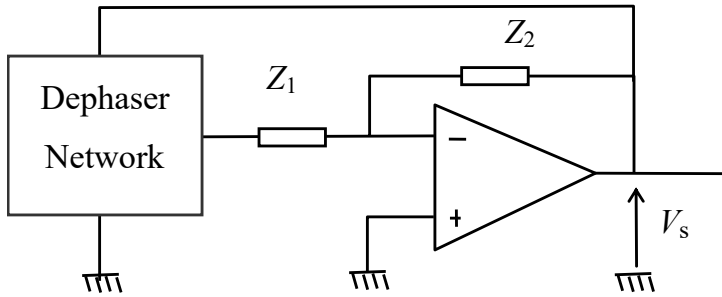


Figure 1.20. Sinusoidal oscillator using an inverter circuit based on an operational amplifier

In the following oscillators, gain is provided by a field effect transistor and the admittance modulus of L_{choke} can be considered weak enough for the load to be comprised exclusively of elements C_1 , L_1 , C_2 . C_l represents a binding capacitance, C_d a decoupling one, with negligible impedances at the oscillation frequency.

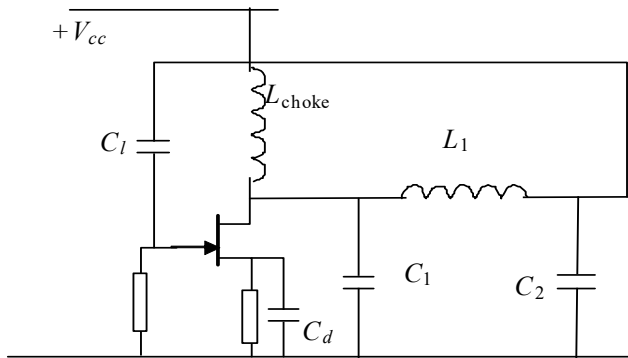


Figure 1.21. Colpitts oscillator

In the Colpitts oscillator, inductance L_1 can be replaced by a quartz resonator, allowing for a highly precise oscillator frequency to be obtained.

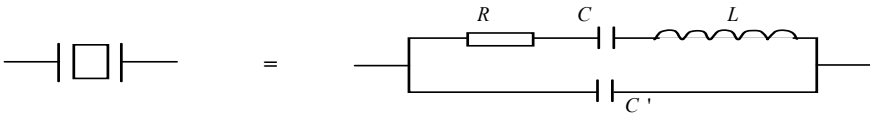


Figure 1.22. Symbol and equivalent circuit of quartz resonator

The quartz equivalent circuit is effectively a dipole with serial resonance frequency (minimum impedance) and very close antiresonance frequency (or parallel resonance with maximum impedance, or alternatively notch effect). In between these two frequencies, the dipole is inductive, whereas outside this interval, it is capacitive (see section 1.7).

– Other oscillator circuits with transistor amplifier (or inverter logic gate):

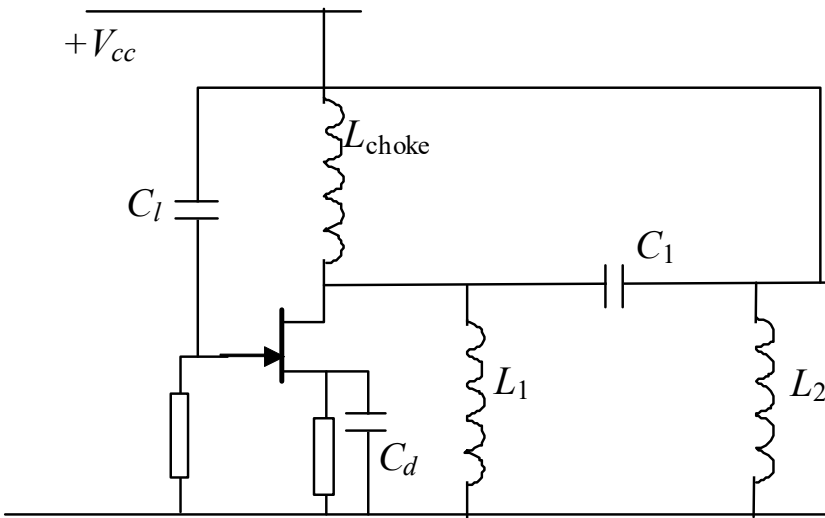


Figure 1.23. Hartley oscillator

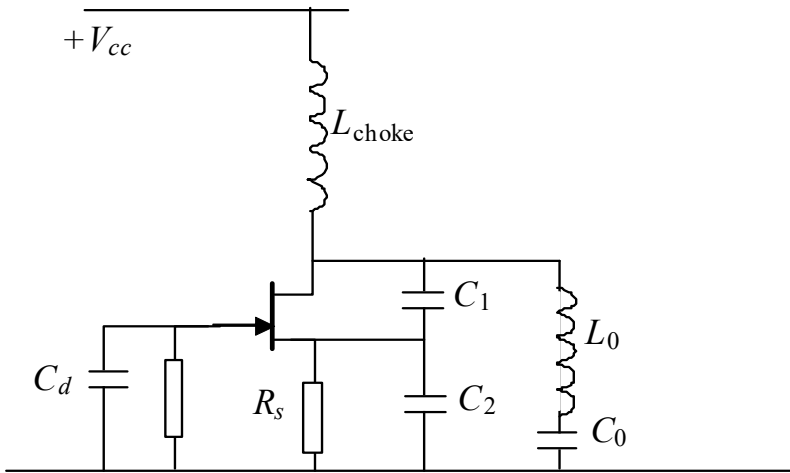


Figure 1.24. Clapp oscillator

In Clapp oscillators, feedback happens at the FET source, with the variable C_0 capacitance allowing for the control of oscillator frequency.

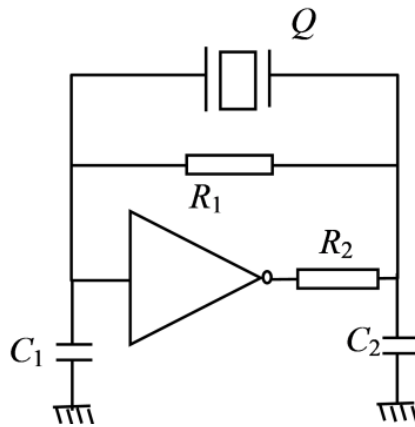


Figure 1.25. Quartz oscillator operating with an inverting logic gate

In quartz oscillators with a CMOS inverting gate as amplifier (Figure 1.25), the $Q - C_1$ network (input capacitance of the gate) constitutes the main part of the return loop. Furthermore, circuit $R_2 - C_2$ supplies the additional

dephasing required to surpass π in the return loop. R_1 allows for the static operating point to be stabilized around the middle of the static characteristic of the inverting gate.

This type of oscillator is used systematically in circuits in which a stable and precise clock frequency, provided by the quartz, is required, with the signal's waveform being of lesser importance. Indeed, the oscillation status is reached at a unique frequency situated in a highly restricted range in which the quartz has an inductive impedance (see section 1.7).

– Regulation of oscillator amplitude:

When the circuit gain is supplied by a transistor, amplitude regulation can be performed by simply dissociating the resistance in series with the source (or with the emitter) into two parts, with one always being decoupled by a filtering capacitor, and the other non-decoupled and connected in parallel with a junction field effect transistor between the drain and the source. The JFET operates as a variable resistance controlled by the rectified output voltage of the oscillator.

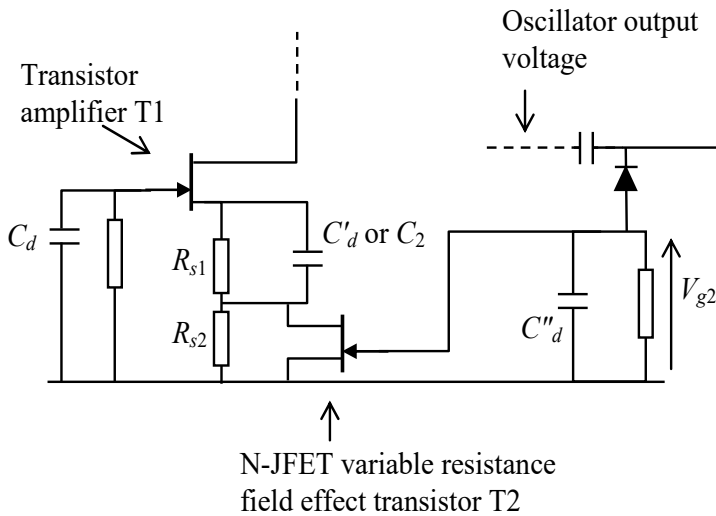


Figure 1.26. Amplitude oscillator stabilization mechanism

Capacitances C_d , C'_d , C''_d act as decoupling ones, presenting negligible impedance at oscillator frequency. When the alternative voltage supplied by the oscillator increases in amplitude, with the rectified voltage V_{g2} being negative, transistor T2 becomes less conductive and the non-decoupled part of the resistance in series with the source of T1 increases and accordingly decreases T1 gain. Accordingly, there is a negative feedback effect together with amplitude oscillator stabilization. Other circuits can act on the T1 gate (or base) or use more efficient rectification in order to reduce the filter time constant, thereby accelerating stabilization.

– Voltage controlled oscillator:

In some circuits like phase-locked loops (see Chapter 1 in Volume 3 [MUR 18]), it is indispensable to control the oscillator frequency using voltage (or current). A frequency-voltage converter can fulfill this role; however, if a sinusoidal signal is required, the sinusoidal oscillator frequency must be modified in the same manner as described previously. In such cases, a “Varicap” diode can be used (see Chapter 1 in Volume 1 [MUR 17]) under reverse polarization given by the control voltage. Then, its capacitance, in parallel with one of the capacitors acting in the resonant circuit where oscillation occurs, can be adjusted, thus involving the control of the oscillator frequency. In theory, the relation frequency-bias voltage is not linear largely due to the square root that appears in $\omega_{oscil} = \frac{1}{\sqrt{LC}}$, but we

can approach linearity on condition that the capacitance excursion, and consequently frequency, is limited. Oscillators made in this way are referred to as voltage controlled oscillators. An amplitude stabilization loop can be added, and in cases where the linearity of the voltage-frequency conversion is indispensable, another feedback loop can also be added on frequency detection according to the principle of reduction of the nonlinearities described in section 1.3.2.

– Stability of oscillator frequency:

The active component generates noise (see Chapter 4 in Volume 1 [MUR 17]) and as all of these oscillators include at least one resistor in the return loop, which is also a source of noise, the loop transmittance is subject to slight fluctuations, in both modulus and phase. These are essentially phase φ fluctuations that determine the stability of oscillator frequency f_0 , that is better as $df_0/d\varphi$ is smaller and consequently as $d\varphi/df_0$ is greater. In the case

of second-order circuits and in accordance with the study of elementary transmittances in harmonic conditions, the argument is $\varphi = \text{Atan}[Q(u - 1/u)]$ where $u = f/f_n$, f_n being the natural frequency, which is indeed very close to f_0 . Deriving $\frac{d\varphi}{du} = \frac{Q(1+1/u^2)}{1+Q^2(u-1/u)^2}$, which is $2Q$ for $u = 1$, in general a condition close to the oscillation frequency. Frequency stability is thus greater as the quality (or overvoltage) coefficient Q is higher. The Wien bridge oscillator for which Q does not exceed $1/2$ is consequently much less stable than resonant circuit oscillators. However, it is the quartz oscillator that ensures the greatest stability since the difference between the two frequencies limiting the range in which quartz is inductive and in which the oscillator frequency is found is extremely narrow (in the order of 1% of oscillator frequency or much less). The calculation of $d\varphi/du$ provides a result depending on the resistance representing dissipation losses in the quartz and the R_2C_2 dephasing network in Figure 1.25 must be adjusted in order to optimize the effective value of the oscillation frequency and its stability.

1.6.2. Relaxation oscillators using a nonlinear dipole and other resonant circuit oscillators

When approximating the linear operation of the active component, this can be modeled by means of negative conductance $-G_a$ in the dynamic circuit of sinusoidal oscillators (with $G_a > 0$). If the conductance of losses G_p is exactly compensated by G_a , the total of both is zero and there is consequently no damping of the oscillating circuit, which, following initial excitation, is the origin of a permanent and non-damped sinusoidal signal. This approximation amounts to the assumption of a linearized current–voltage characteristic with an average negative slope within an amplitude range limited by two thresholds beyond which the dynamic conductance again becomes positive.

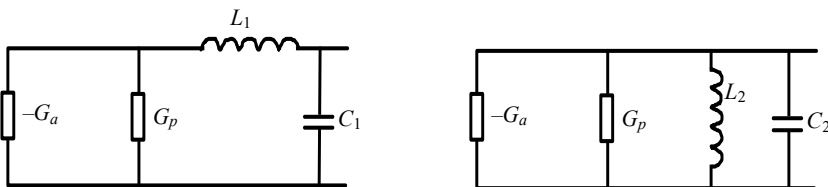


Figure 1.27. Dynamic circuit with negative conductance $-G_a$ and circuit with series (at left) or parallel (at right) resonant network, damped by positive conductance G_p

The effective operation approaches this model when a dipole with negative resistance or conductance is used, such as a tunnel diode, diac, etc. These dipoles are sorted according to two types: with S and N current–voltage characteristic $I_d(V_d)$ (Figure 1.28).

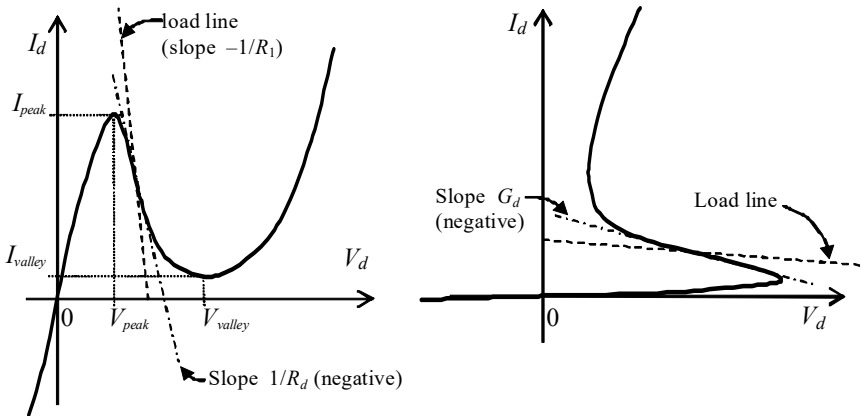


Figure 1.28. Nonlinear dipole N characteristics to the left and S to the right, with negative dynamic resistances and conductance ($1/R_d$ or $G_d = -G_a$), and load lines suited to relaxation oscillator operation

Operation analysis becomes particularly difficult in harmonic conditions and must instead be conducted according to changes in the position of the operating point under the influence of a disturbance. In the case of relaxation oscillators, it is sufficient to add a single reactive element (inductance or capacitance) to a nonlinear dipole for the instability of the operating point to entail cyclical operation around the zone of negative resistance (and conductance), as shown below. Incidentally, it is worth noting that this type of nonlinear dipole cannot contain a semiconductor device but rather a saturable magnetic circuit associated with an inductance or mutual inductance decreasing significantly when the magnetic circuit saturates.

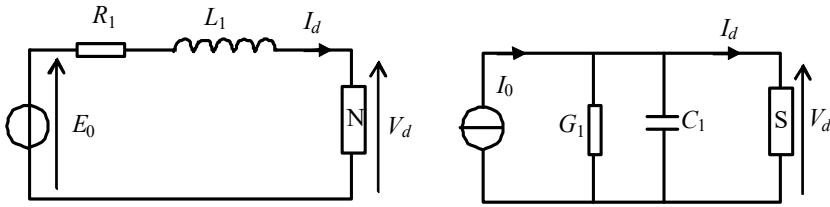


Figure 1.29. Relaxation oscillator circuits with N dipole to the left and S to the right

The circuit to the left in Figure 1.29 under static conditions verifies $E_0 = R_1 I_d + V_d(I_d)$; then, under the influence of disturbance dE : $E_0 + dE = R_1(I_d + dI_d) + L_1 \frac{dI_d}{dt} + V_d(I_d) + R_d dI_d$, where R_d is the dynamic resistance of the N dipole, dependent on I_d . Subtracting static conditions, it remains:

$$dE = R_1 dI_d + L_1 \frac{dI_d}{dt} + R_d dI_d.$$

If the dynamic resistance R_d is sufficiently negative relative to R_1 , that is $R_d + R_1 < 0$, the sign of dI_d should be opposite to that of dE in order for equality to be respected, whether inductance is present or not. This implies a decrease in current when $dE > 0$. When inductance is present, the latter term is also negative in this case, which has the effect of extending the decrease in current down to the operating point at which R_d becomes positive enough again to change the sign of the second member. The evolution will be then reversed, giving rise to a cyclical variation. The operating point becomes therefore unstable since even after the reestablishment of $dE = 0$, the second member can cancel itself without dI_d being zero, due to the inductive term and on condition that $(R_1 + R_d)$ and dI_d are negative in order for the product to be positive and compensated by $L_1 \frac{dI_d}{dt} < 0$. This condition thus requires a

static operating point with a single intersection of the load line with the characteristic $I_d(V_d)$ in the range where R_d is sufficiently negative for condition $(R_1 + R_d) < 0$ to be realized. Otherwise, in the presence of other intersections with stable operating points, the system stops on one of them and oscillation ceases. The half-period may be calculated by integrating the complete equation with $dE = 0$, either analytically by linearizing the characteristic, or more precisely by a numeric integration, between the two

currents limiting the negative resistance zone. In the first case, linearization is equivalent to take R_d between $-\frac{V_{valley} - V_{peak}}{I_{valley} - I_{peak}}$ in Figure 1.28 and the reverse of the maximum slope, that is a value $-|R_{d0}| < 0$. There is then proportionality between I_d and its derivative I_d' according to the variational equation, which implies a solution of the exponential type $I_d = I_{peak} \exp(t/\tau)$ where $\tau = L_1 / (|R_{d0}| - R_1)$.

The oscillation period is then very approximately given by the double of the time taken for current to go from I_{peak} to I_{valley} , that is $T = 2\tau \ln\left(\frac{I_{peak}}{I_{valley}}\right)$.

Precision can be improved by piecewise integration of the whole equation. For the other circuit, operation can analyze symmetrically by searching for the development of voltage under the influence of a current perturbation emanating from the source.

It is clear that these circuits can by no means provide stable and precise frequency oscillation, since it is too dependent on the current–voltage characteristic of the nonlinear dipole, susceptible to dispersion, to being dependent on temperature, etc., and thus can only operate in case of alternative signal generation without any severe demands on the signal's shape or frequency. These relaxation oscillators, whose only advantage is their simplicity, have as a consequence almost disappeared, with the exception of components liable to operate at extremely high frequencies, unattainable for transistors, beyond several tens of gigahertz and up to terahertz. To obtain a more precise oscillator frequency, the principle applied in the circuits of Figure 1.27, comprising a resonance circuit, can be usefully applied again here.

1.6.3. General case of systems comprising a nonlinear dipole and study of oscillation in phase space

Regardless of the oscillator circuit in question, there is always nonlinearity due to the active components. Studying over one or several periods of time can prove insufficient in characterizing long-term operation and in addition does not account for the initial conditions. Since there is always at least one reactance in the oscillator circuit, as shown in the circuits

in Figure 1.27 for instance, it is worthwhile to investigate current and voltage at the terminals of at least one of them, since one of these values is proportional to the derivative of the other. The study in the time domain of one of these quantities can then be replaced by the study of this quantity q and its derivative relative to time \dot{q} (according to the usual mechanical and thermodynamic notation) in the phase plane, with time becoming a parametric variable. This allows for initial oscillation to be studied along with the operating point at which the established oscillation converges. The trajectory of the operating point defined by (q, \dot{q}) in the phase plane then becomes the preferred mean for this type of study that had its beginnings in the mechanical sciences, mathematics and thermodynamics in the 19th Century and has continued until today. For systems comprising a number k of independent variables, the phase plane is replaced by the phase space, which consequently has a dimension equal to $2k$, which is also the number of degrees of freedom of the system.

1.6.3.1. First- and second-degree systems

If q represents the charge on an armature of capacitance C accepting instantaneous voltage v , it is equal to Cv (where $v = q/C$) and the instantaneous current crossing the capacitor is $\dot{q} = dq/dt$. We can study the trajectory of the point (q, \dot{q}) in the phase plane, either from the solution of the differential equation that defines the relation between \dot{q} and q , obtained by algebraic calculation or, as is typically the case, by numeric resolution needed by the nonlinearity of the system, and the initial conditions, or alternatively from the measurement effected on the experimental device if available. If the solution converges to a sinusoidal oscillation, then q is proportional to $\sin(\omega_0 t)$ for example, and as a result, \dot{q} is proportional to $\cos(\omega_0 t)$. The parametric variable t can be eliminated by writing

$$\sin^2(\omega_0 t) + \cos^2(\omega_0 t) = \left(\frac{q}{a}\right)^2 + \left(\frac{\dot{q}}{b}\right)^2 = 1, \text{ which is the equation of an ellipse in}$$

the phase plane, with a and b as constants (Figure 1.30). A distortion of the ideal ellipse appears if the signal is not purely sinusoidal, which in practice is systematically the case due to the amplitude being limited by the intrinsic nonlinearity of the active component, even if it can be minimal and difficult to detect. At the other extreme, in the generator of rectangular signals and squares based on a loop containing an integrator and a hysteresis comparator (see Chapter 4 exercises in Volume 1 [MUR 17]), the capacitance is crossed by a constant current for one half-period and the reverse current for the other

half-period, corresponding to linearly increasing and decreasing voltages at the terminals with two opposite slopes. The resulting cycle for the coordinate points (q, \dot{q}) is thus rectangular. Consequently, relevant information concerning the permanent conditions of the oscillator can be obtained from these observations.

However, the trajectory in the phase plane also advantageously provides information about transient conditions, in particular the beginning of the oscillation, as well as for more complex cycles that can be found in other oscillators such as those addressed below.

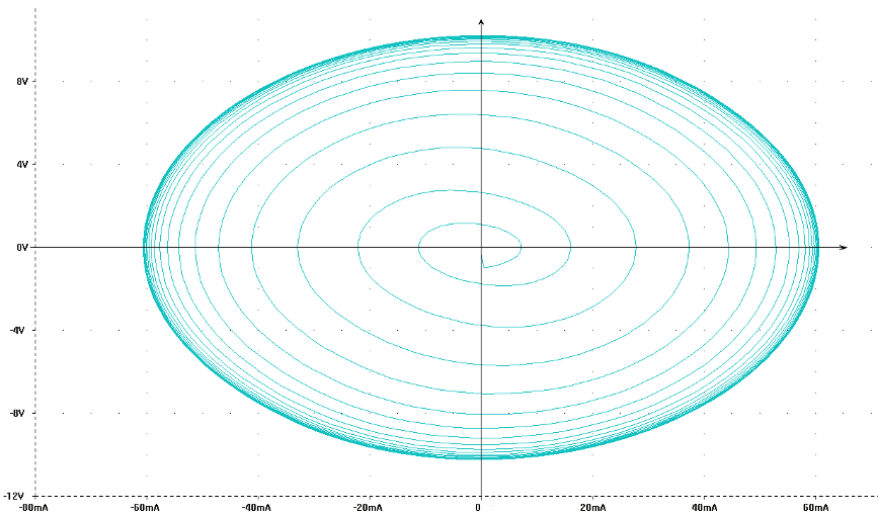


Figure 1.30. Start cycle and limiting cycle of a quasi-sinusoidal oscillator obtained from simulation results

In the case where the circuit shown on the right in Figure 1.27 is taken as example, the law of nodes and the presence of voltage q/C_2 at the terminals

of all elements lead to $L_2 \frac{d}{dt} \left[-\frac{q(G_s - G_a)}{C_2} - \dot{q} \right] = \frac{q}{C_2}$, or alternatively

$$\ddot{q} + \frac{G_s - G_a}{C_2} \dot{q} + \omega_0^2 q = 0 \quad \text{with} \quad \omega_0^2 = \frac{1}{L_2 C_2} \quad (\text{adopting the notation used in}$$

mechanics for the derivations relative to time).

If $G_a - G_p = 0$, the equation becomes that of the harmonic oscillator with a purely sinusoidal solution, with the characteristic equation not having a first-degree term. But in order for the oscillation to start, it must be assumed that the coefficient of \dot{q} is initially negative since in this case

$\exp\left[+\frac{(G_a - G_s)t}{C_2}\right]$ acts as a factor inducing a progressive increase in

amplitude, exponentially up to the cancellation of $G_a - G_p$, from the smallest spontaneous fluctuation due to noise in the resistive elements (see Chapter 4 of [MUR 17]) or in practice, from circuit power up, required to polarize the active element. This evolution is expressed in the phase plane by a trajectory from the coordinate point (q, \dot{q}) that encircles the origin, converging then to an ellipse (Figure 1.30), which comprises the limiting cycle in the case of quasi-sinusoidal oscillation. The limiting cycle can be of different shapes in the case of more complex non-sinusoidal oscillators such as those studied below, and likewise for its center of gravity, known as the attractor, which is not necessarily the origin or can even be plural.

1.6.3.2. Nonlinear systems of order higher than two

The previous method of study is extended here in two steps:

- determination of the static operating point or points from the equation of the load line and the characteristic parameters of the nonlinear elements;

- for small variations around each operating point, the writing of the electrical state equations under given conditions as a function of time and transformed into matrix form $\frac{d\mathbf{F}}{dt} = \mathbf{A}\mathbf{F} + \mathbf{B}'$ as in section 1.4.5. Then, the eigenvalues are calculated for the state matrix \mathbf{A} . The stability (or instability) of the operating points can then be deduced from the existence or absence of poles with positive or zero real part, the poles being the eigenvalues of \mathbf{A} .

A third step can be performed successfully by means of a simulator capable of solving the previous system while accounting for changes in the dynamic parameters of nonlinear elements, consisting of the determination of system changes after a perturbation, and the convergence of state variables to certain types of behavior. Since the solution of a differential system can be highly dependent on the initial conditions, which are renewed each time the simulator has to change parameters, it can evolve either to a phase space trajectory around a single attractor (in the case of a

quasi-sinusoidal oscillator), or around several attractors, if the system is unstable. In this second case, it is possible that the evolution will lead to a deterministic chaos, as Poincaré showed initially, when the phase space trajectory becomes highly complex with a very high number of cycles before returning to the same point. In this case, the signal resembles quasi-random noise more closely than a periodic signal. For example, these various operating conditions can be studied with the Chua oscillator, third-order circuit proposed by Leon Chua in 1983 then revived and simplified in 1984 by T. Matsumoto, and then studied by a great many authors since, including the inventor himself (see the bibliography and history in http://www.scholarpedia.org/article/Chua_circuit). This indicates that these chaotic behaviors can appear from the third order on condition that the circuit comprises a nonlinear conductance, which in the most simple case is that of a dipole presenting a current–voltage characteristic of odd symmetry, with two negative slopes, as shown in Figure 1.32. Another oscillator that can present such behavior is that of Van der Pol, invented in 1927.

The Chua oscillator comprises three reactances, one or two resistances and one D dipole with negative, nonlinear type N conductance (Figure 1.31).

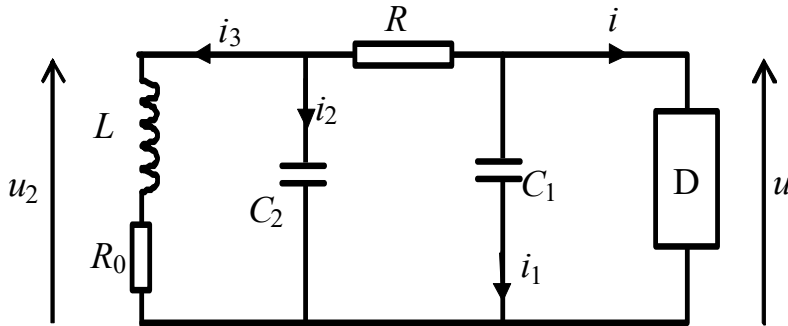


Figure 1.31. Chua oscillator

This can be described as a system comprising a relaxation oscillator composed of D and C_1 , coupled by resistance R to a notch resonant circuit L , R_0 , C_2 . Resistance R_0 is not indispensable but does allow for real losses in inductances to be accounted for, and offers the possibility that an additional parameter may be introduced. Characteristic $i=g(u)$ of dipole D is shown in Figure 1.32 and comprises a negative conductance $-G_a$ around the origin ($G_a > 0$), then for $|u| > u_c$ the conductance becomes $-G_b$ ($G_b > 0$) with

$G_b < G_a$ and finally the conductance (this is also the slope) becomes positive outside of an interval wider than $[-u_c, u_c]$ in order to simulate a real component that can provide only finite energy.

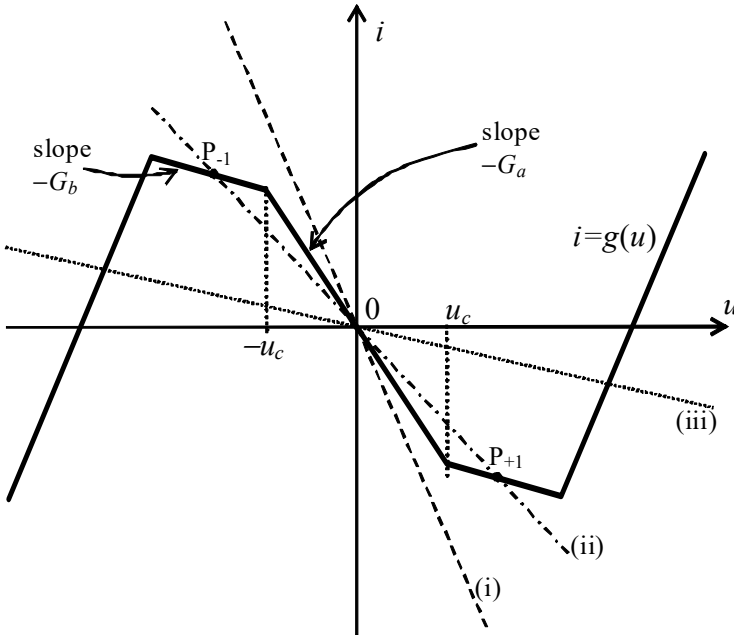


Figure 1.32. Characteristic $i = g(u)$ of dipole D used in the Chua oscillator and load lines corresponding to R equal to (i) R_1 , (ii) R_2 and (iii) R_3

In static conditions, the load line is written as $u = -(R+R_0)i$ or alternatively $i = -G u$, with $G = 1/(R + R_0)$. According to the value of G , three cases may occur: (1) the absolute value of slope G is the greatest, that is $G > G_a$, in which case there is only one static operating point at the origin; (2) $G_b < G < G_a$, and there are three static operating points (P_{-1} , 0 and P_{+1}), all in regions with negative conductance of D ; (3) $G < G_b$, and also three static operating points, one at origin and the other in regions with positive conductance of D . However, in this last case, the operation is inclined toward a relaxation oscillator that is more insulated as R is greater. This will not be addressed here since the perturbation method of current i around one of its operating points allows for its stability to be determined as mentioned in section 1.6.2 (both of the end points are stable and the origin is not).

The second step consists of writing the network equations in transient conditions. As there are five branches and three nodes, the number of independent variables is $5 - 3 + 1 = 3$. Selecting values that are derivatives in the reactances, that is u , u_2 and i_3 , leads directly to a differential system such as the one indicated previously:

$$\begin{cases} \frac{du}{dt} = \frac{1}{C_1} \left(\frac{u_2 - u}{R} - g(u) \right) \\ \frac{du_2}{dt} = \frac{1}{C_2} \left(\frac{u - u_2}{R} - i_3 \right) \\ \frac{di_3}{dt} = \frac{1}{L} (u_2 - R_0 i_3) \end{cases}$$

Around the origin, there is simply $i = g(u) = -G_a u$ for the load line (i); and around the intersection points of the load line (ii), $i = g(u) = -G_b u + (G_b - G_a) u_c \operatorname{sgn}(u)$ where function $\operatorname{sgn}(u) = \pm 1$ according to the sign of u .

In order to reach a system with only state variables and dimensionless parameters, we must make the changes:

$$\theta = \frac{t}{RC_2}; \quad x = \frac{u}{u_c}; \quad y = \frac{u_2}{u_c}; \quad z = \frac{Ri_3}{u_c}$$

for variables;

$$\text{and } \alpha = \frac{C_2}{C_1}; \quad a = RG_a;$$

$$b = RG_b = a \frac{G_b}{G_a}; \quad \beta = \frac{R^2 C_2}{L};$$

$$\gamma = \frac{RR_0 C_2}{L} \text{ for parameters.}$$

Hence the dimensionless system:

$$\begin{cases} \frac{dx}{d\theta} = \alpha \left(y - x - \frac{R}{u_c} g(u) \right) \\ \frac{dy}{d\theta} = x - y - z \\ \frac{dz}{d\theta} = \beta y - \gamma z \end{cases}$$

For load line (i), there is $\frac{R}{u_c} g(u) = \frac{R}{u_c} (-G_a u) = -ax$ around the origin, and this is also true for load line (ii). For operating points P_{-1} and P_{+1} located in the part of the characteristic where conductance is $-G_b$, at the intersection with load line (ii), this can be written as: $\frac{R}{u_c} g(u) =$

$$\frac{R}{u_c} [-G_b u + (G_b - G_a) u_c \operatorname{sgn}(u)] = -bx + (b-a) \operatorname{sgn}(x); \text{ respectively, deducing}$$

$$\text{matrices } \mathbf{A}_i = \begin{bmatrix} -\alpha(1-a) & \alpha & 0 \\ 1 & -1 & -1 \\ 0 & \beta & -\gamma \end{bmatrix} \text{ and } \mathbf{A}_{ii} = \begin{bmatrix} -\alpha(1-b) & \alpha & 0 \\ 1 & -1 & -1 \\ 0 & \beta & -\gamma \end{bmatrix}; \text{ and if}$$

$$\text{required, matrices } \mathbf{B}'_i \text{ (vector column zero) and } \mathbf{B}'_{ii} = \begin{bmatrix} \alpha(a-b) \operatorname{sgn}(x) \\ 0 \\ 0 \end{bmatrix}. \text{ It}$$

should be noted that in case (i), $G_a < G$ leads to $a = RG_a < RG = \frac{R}{R+R_0} < 1$;

and thus $(1-a)$ is always positive in case (i) around the origin. And in case (ii), $b = RG_b < RG < RG_a$ and also $b < \frac{R}{R+R_0} < 1$ for intersection points P_{-1}

and P_{+1} but around the origin, $a > \frac{R}{R+R_0}$. Since R_0 is clearly always smaller

than R , this condition typically leads to $a > 1$ and thus to a positive sign for the element in the first line and the first column of the matrix \mathbf{A}_i .

This step should end with the calculation of eigenvalues for matrices \mathbf{A}_i and \mathbf{A}_{ii} . This could be done with symbolic values since the characteristic equation is of the third degree; however, it leads to long expressions that are difficult to use due to the four parameters involved. It is preferable to set some of these to numeric values using the following considerations.

Since resistance R determines coupling between the two parts of the circuit, any value of C_1 greater than C_2 would significantly alter the resonance frequency of circuit LC_2 in the case of strong coupling, that is when R is weak. So, as to avoid multiplying these changes, it is instead preferable to take $C_1 \ll C_2$ and leave ratio $\alpha = \frac{C_2}{C_1}$ constant, which will be set to 15.6. According to their expressions, parameters β and γ relate to the squared damping coefficients of circuit LC (or the inverse of the squared quality coefficients) and thus have a significant impact on oscillating conditions. The evolution of the eigenvalues may be studied according to β , which is modified by means of L , leaving the other components unaltered and γ initially at zero.

Setting ratio $\chi = \frac{G_b}{G_a} = \frac{b}{a} = \frac{5}{8}$, and considering the two cases of the load

line's intersection with (i) $a = \frac{8}{9}$, and (ii) $a = \frac{8}{7}, b = \frac{5}{7}$; the three eigenvalues of \mathbf{A} are denoted as λ, μ and ν , followed by "i" or "ii" to distinguish the two cases and by 0 or 1 in case (ii) depending whether it concerns the operating point at the origin or at $P_{\pm 1}$.

In case (i), for the only possible static operating point around the origin, for which $a < 1$, the zone for which β is taken between 0 and around 38 comprises one or several eigenvalues with positive real part (Figure 1.33). It follows that the system is unstable.

In case (ii), for the static operating point around the origin, for which $a > 1$, all the eigenvalues have negative real part (Figure 1.34). It follows that this operating point is stable. Conversely, for the static operating points $P_{\pm 1}$ for which $b < 1$, all of the eigenvalues have their positive real part for β from 0 to around 57 (Figure 1.35), which implies that these points are unstable.

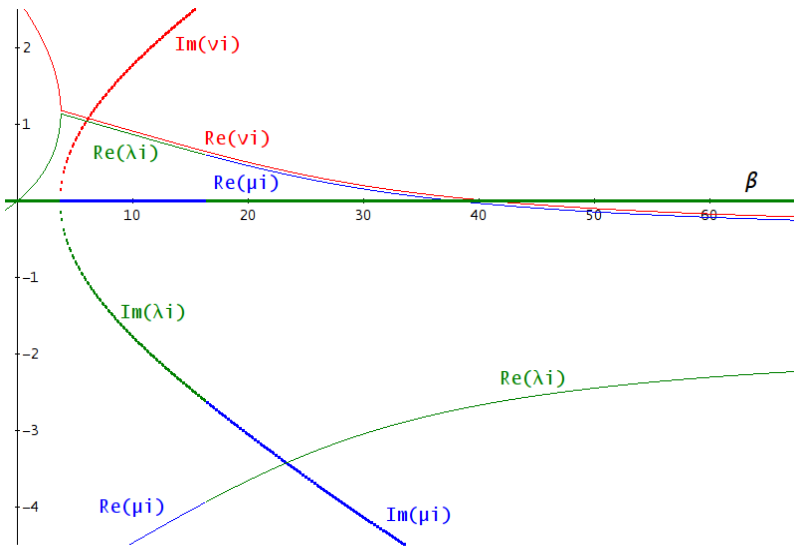


Figure 1.33. Eigenvalues of A in case (i) for the operating point at the origin. For a color version of this figure, see www.iste.co.uk/muret/electronics2.zip

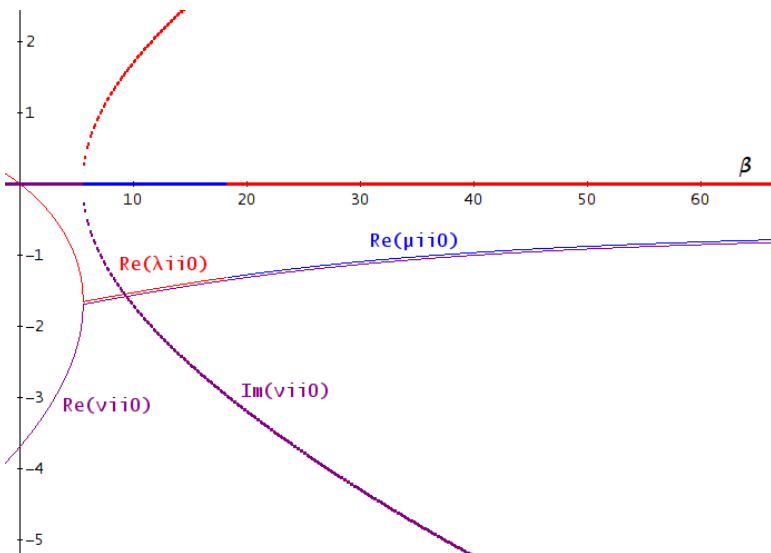


Figure 1.34. Eigenvalues of A in case (ii) for operating point "0" around the origin. For a color version of this figure, see www.iste.co.uk/muret/electronics2.zip

Consequently, it is verified that the unstable operating points can be obtained only when the load line cuts the characteristic of the nonlinear dipole with a conductance $-G$ (or slope) whose absolute value is greater than the absolute value of the dipole conductance (G_a or G_b depending on the operating point), which the qualitative analysis in section 1.6.2 has shown already.

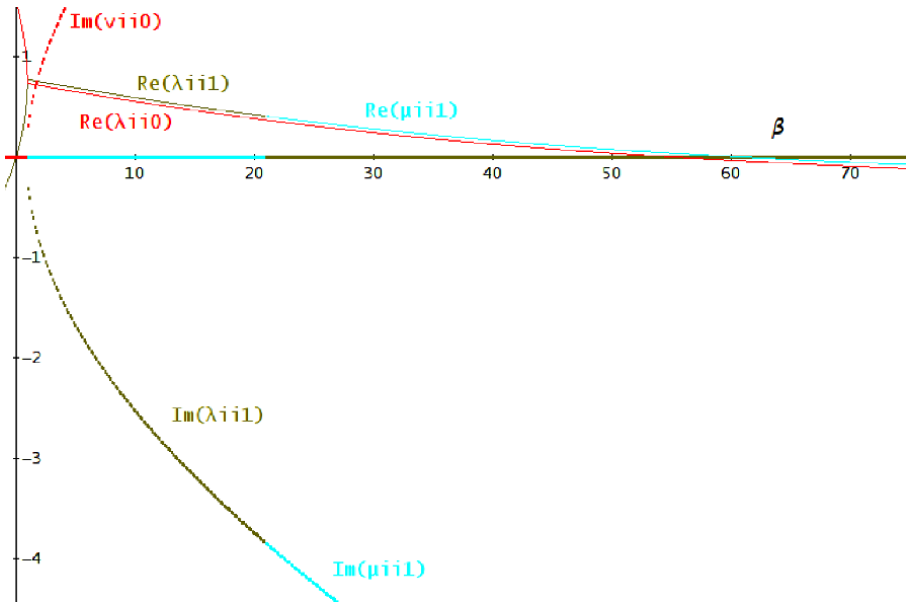


Figure 1.35. Eigenvalues of A in case (ii) for operating points $P_{\pm 1}$. For a color version of this figure, see www.iste.co.uk/muret/electronics2.zip

It should be noted that this system is one of the first dynamic systems that can present a chaotic regime from experimental studies, although the last step of this study is here performed only in simulation. Since the system is of the third order, the phase space has six dimensions. However, it should suffice to plot a state variable relative to one of the capacitors (here u_2) as a function of a state variable relative to the other capacitor (u) or the inductance (i_3) to acquire a sufficiently detailed overview of the oscillator's behavior.

In case (i), where $a < 1$, a quasi-sinusoidal oscillator is obtained together with trajectory $u_2=f(i_3)$ as that represented in Figure 1.30, with a cycle limited by an ellipse.

In case (ii), where $b < 1$, the cycles visible in Figure 1.36 are obtained.

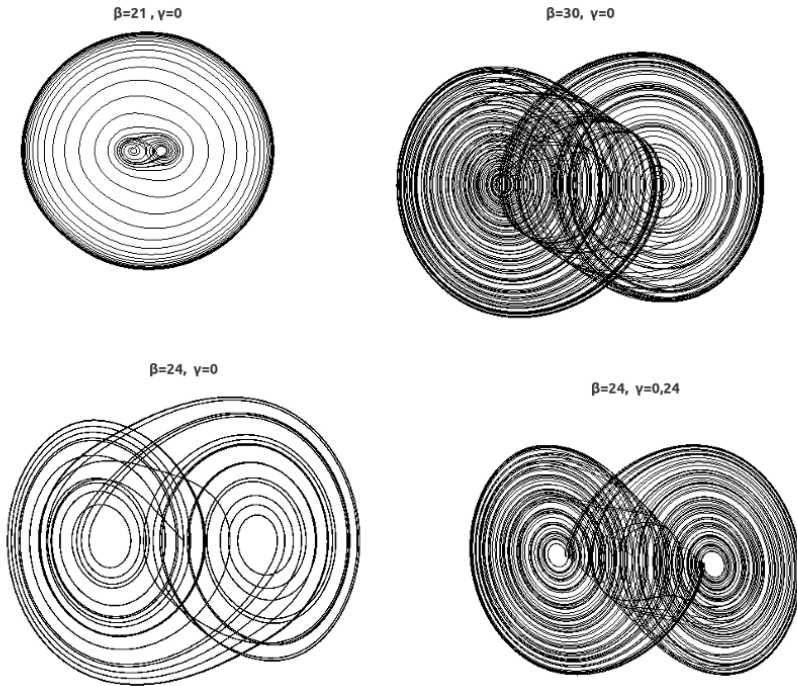


Figure 1.36. Cycles completed by the operating point $u_2(i_3)$ in various conditions

In case $\beta=21$, $\gamma=0$, a limiting cycle representing a quasi-sinusoidal oscillation is reached after one start-up in which the trajectory alternates between both attractors (Figure 1.36). The spectrum includes the odd harmonics of the fundamental frequency around 42 kHz and an erratic spectrum in the lower frequencies corresponding to oscillator start-up (Figure 1.37).

Case $\beta=24$, $\gamma=0$, is unique since the limiting cycle is no longer evident (Figure 1.36); however, the trajectory retains a certain regularity with a period that is multiple of the fundamental one. Observation of the signal or

of its spectrum shows here that the period has been tripled, leading to the appearance of a subharmonic frequency, one near 12 kHz, equal to one-third of the fundamental frequency that is close to 36 kHz, and at fractional harmonics that are $5/3$ and $7/3$ of the fundamental frequency (Figure 1.38). This condition is referred to as a subharmonic cascade.

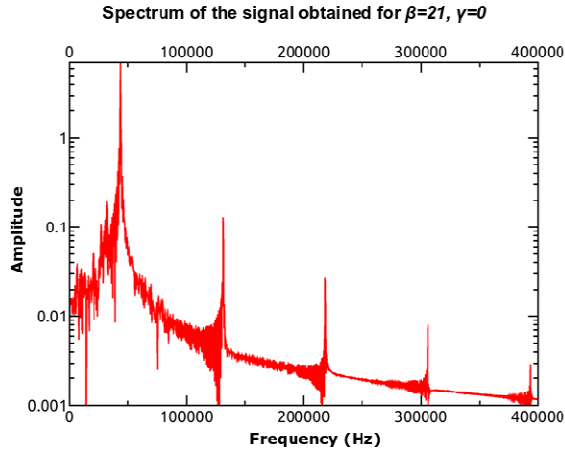


Figure 1.37. FFT of the Chua oscillator signal for $\beta=21$, $\gamma=0$. For a color version of this figure, see www.iste.co.uk/muret/electronics2.zip

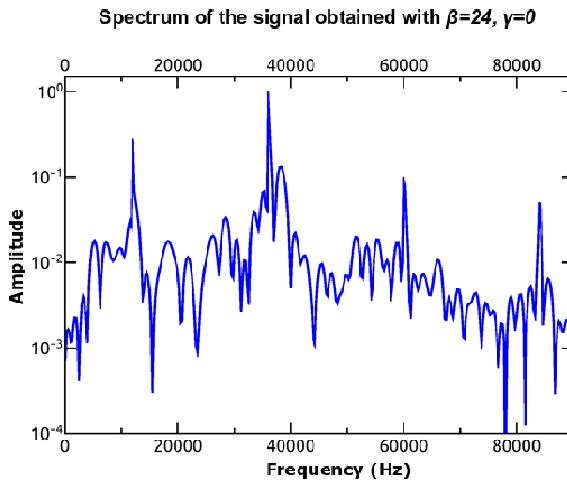


Figure 1.38. FFT of the Chua oscillator signal for $\beta=24$, $\gamma=0$. For a color version of this figure, see www.iste.co.uk/muret/electronics2.zip

In case $\beta=24$, $\gamma=0.24$ and $\beta=30$, $\gamma=0$, the phase space trajectory includes a very high number of different trajectories (several hundred) before returning to the same point alternating around the two attractors that are the two unstable operating points P_{-1} and P_{+1} (Figure 1.36). This is known as a deterministic chaos, since the signal approaches a random signal as its period becomes extremely high relative to the fundamental period. This is illustrated by the signal's spectrum that itself becomes highly chaotic (Figure 1.39), the peak fundamental frequency barely exceeds the continuous, erratic background, or can even disappear completely when parameter γ is no longer zero.

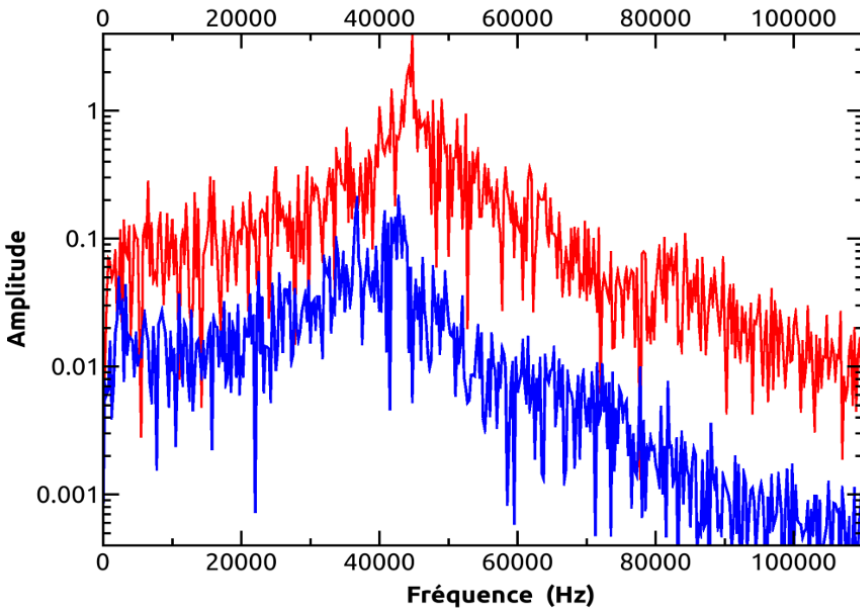


Figure 1.39. FFT of Chua oscillator signals in deterministic chaotic conditions obtained with $\beta=30$, $\gamma=0$ in red (higher spectrum) and with $\beta=24$, $\gamma=0.24$ in blue (lower spectrum). For a color version of this figure, see www.iste.co.uk/muret/electronics2.zip

Numerous applications of this deterministic chaos have emerged since the 1990s in a variety of areas, both in science and art (music, design, etc.).

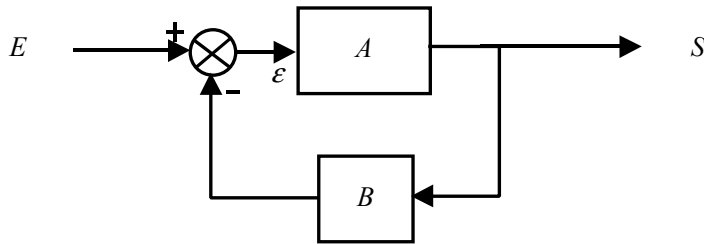
1.7. Exercises

1.7.1. Response and stability of an operational amplifier not compensated until unity gain and loaded by a capacitor

An operational amplifier included in a non-inverter circuit has an open loop gain $A(s)$ for which the approximate expression used is

$$A(s) = \frac{A_0}{\frac{s}{\omega_1} \left(1 + \frac{s}{\omega_2} \right)}$$
 applicable to circular frequencies exceeding ω_1 .

The feedback coefficient is B ; real number belonging to the interval $[1/A_0, 1]$ and the circuit diagram is as follows:



Circular frequency ω_0 is defined by $\omega_0 = A_0 \omega_1$ so that:

$$A(s) = \frac{1}{\frac{s}{\omega_0} \left(1 + \frac{s}{\omega_2} \right)}$$

1) a) Determine the expression of the transfer function in closed loop

$$H(s) = \frac{S(s)}{E(s)} \quad \text{and place it under form} \quad H(s) = \frac{1}{B} \frac{1}{D(s)} \quad \text{where}$$

$$D(s) = 1 + \frac{1}{Q_0} \frac{s}{\omega_n} + \frac{s^2}{\omega_n^2}$$

b) Determine the expressions of the natural circular frequency ω_n and of the quality coefficient Q_0 of $D(s)$ depending on ω_0 , ω_2 and B . For what value of $B \in [1/A_0, 1]$ is quality coefficient Q_0 maximum when $\omega_2 = \omega_0/2$ and what is its numerical value? With this value of B and $\omega_2 = \omega_0/2$, what is then the

maximum value of $20 \log|1/D(j\omega)|$ equal to $20 \log|1/D(j\omega_r)|$ for the resonance angular frequency ω_r ?

2) A capacitive load C is added between output S and the ground, forming a low-pass circuit with the amplifier's output resistance R . The open loop gain then becomes: $A'(s) = \frac{1}{\frac{s}{\omega_0} \left(1 + \frac{s}{\omega_2}\right) \left(1 + \frac{s}{\omega_3}\right)}$ where $\omega_3 = \frac{1}{RC}$.

a) Determine the expression of the argument of $A'(j\omega)$. For what value of circular frequency ω expressed as a function of ω_2 and ω_3 is this argument equal to $-\pi$?

NOTE.— $\text{Atan}(a) + \text{Atan}(b) = \text{Atan}\left(\frac{a+b}{1-ab}\right)$ can be useful here.

b) Determine the condition that must verify the loop gain $A'(j\omega)B$ in order for the circuit to remain stable and the resulting inequality between B , ω_0 , ω_2 and ω_3 . In the case where $\frac{\omega_2}{\omega_0} = \frac{1}{2}$, $B = 1$, $R = 50 \Omega$ and $\omega_0 = 2\pi 10^7$ rd/s, determine the condition on C in numeric value for the circuit to remain stable.

Answer:

1)

$$\text{a) } H(s) = \frac{S(s)}{E(s)} = \frac{A}{1+AB} = \frac{1}{B} \frac{1}{1 + \frac{1}{AB}} = \frac{1}{B} \frac{1}{1 + \frac{s}{B\omega_0} + \frac{s^2}{B\omega_0\omega_2}}$$

b) Hence $\omega_n = \sqrt{B\omega_0\omega_2}$ and $Q_0 = \sqrt{\frac{B\omega_0}{\omega_2}} = \frac{1}{2\zeta}$ maximum when $B = 1$ and

$$Q_0 = \sqrt{2} \text{ when } \omega_2 = \frac{\omega_0}{2}.$$

Resonance occurs at $\omega_r = \omega_n \sqrt{1 - 2\zeta^2} = \omega_n \sqrt{1 - \frac{1}{2Q_0^2}} = \sqrt{B\omega_0\omega_2} \sqrt{1 - \frac{\omega_2}{2B\omega_0}} = \omega_0 \sqrt{\frac{3}{8}}$

providing the value of $|D(j\omega_r)| = 2\zeta \sqrt{1 - \zeta^2}$ (see section 1.2.3.3), where $20 \log |1/D(j\omega_r)| = 3.6$ dB.

2)

a) This is $A'(p) = \frac{1}{\frac{s}{\omega_0} \left(1 + \frac{s}{\omega_2}\right) \left(1 + \frac{s}{\omega_3}\right)}$ hence: $A'(j\omega)$
 $= \frac{1}{\frac{j\omega}{\omega_0} \left(1 + \frac{j\omega}{\omega_2}\right) \left(1 + \frac{j\omega}{\omega_3}\right)}$ in harmonic conditions for which the argument is

$$\text{Arg}\{A'(j\omega)\} = -\frac{\pi}{2} - \text{Atan}\left(\frac{j\omega}{\omega_2}\right) - \text{Atan}\left(\frac{j\omega}{\omega_3}\right) = -\frac{\pi}{2} - \text{Atan}\left(\frac{\frac{\omega}{\omega_2} + \frac{\omega}{\omega_3}}{1 - \frac{\omega^2}{\omega_2\omega_3}}\right).$$

To obtain a total of $-\pi$, the second term must also give $-\pi/2$; therefore, the tangent must approach infinity, where $\omega_i = \sqrt{\omega_2\omega_3}$.

b) To ensure stability, it is necessary that $|A'(j\omega_i)B| < 1$ since $\text{Arg}\{A'(j\omega_i)B\} = -\pi$.

Hence, by replacing ω by $\omega_i = \sqrt{\omega_2\omega_3}$ in $A'(j\omega_i)$, this provides:

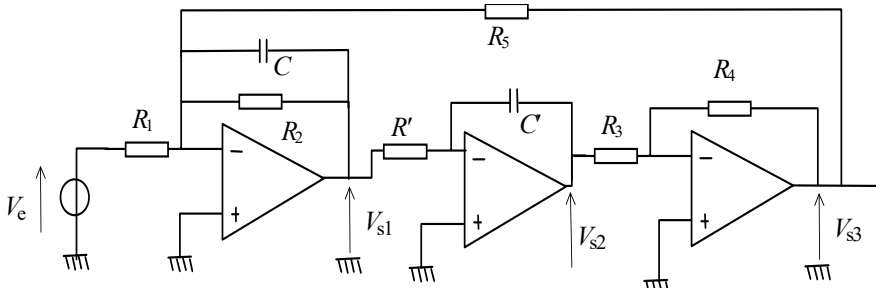
$$\frac{B}{\frac{\sqrt{\omega_2\omega_3}}{\omega_0} \sqrt{1 + \frac{\omega_3}{\omega_2}} \sqrt{1 + \frac{\omega_2}{\omega_3}}} = \frac{B\omega_0}{\omega_2 + \omega_3} < 1$$

Hence, it may be deduced that $C < \frac{2}{R\omega_0} = 640$ pF.

1.7.2. Active filters built with operational amplifiers

1) Butterworth, Bessel or Tchebyshev type active filters

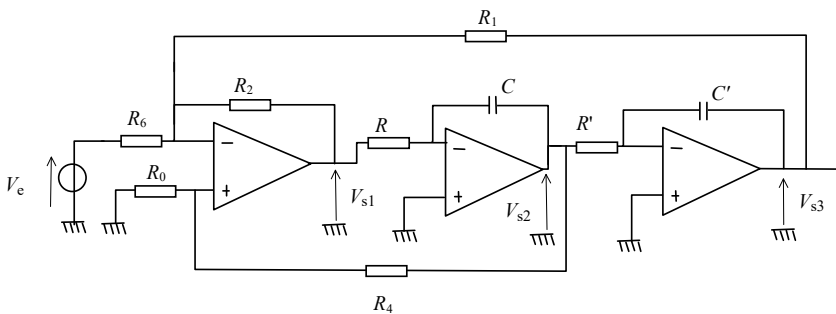
Assuming perfect operational amplifiers, determine V_{s3} according to V_{s1} and the law at the minus input node of the first operational amplifier in the following circuit:



Now deduce from this the transfer function giving V_{s3} / V_e when $R_4 = R_5$; $R_3 = R'$; $C = C'$ and determine the natural circular frequency and damping coefficient. In addition, determine transfer function V_{s1} / V_e and its type.

Indicate which elements are required to set the gain and then the damping factor independently of the natural circular frequency.

Same process for the next filter with V_{s1} as main output; in addition, indicate the type of filter obtained at outputs V_{s2} and V_{s3} .



The equalities $RC = R'C'$; $R_1 = R_2$ can be set here, maintaining however the necessary settings with other independent elements.

Accordingly, which elements are required to set the gain and then the damping factor independently of the natural circular frequency?

One solution that improves the ease of these settings consists of replacing the voltage divider R_4, R_0 with an inverting amplifier whose gain would be $-R_5/R_4$ and connecting its output through a resistance R_3 to the minus input node of the first amplifier whose plus input is then grounded.

2) Elliptic-type filters

In order to obtain a numerator of the same degree as the denominator with zero damping coefficient at the numerator (or equivalently zero transmission at the natural frequency), the solution preserving the settings' independence consists of making the sum of low-pass and high-pass transmittances.

Adding the function indicated above to the previous circuit, deduce the circuit that would provide an elliptic-type second-degree transfer function with independent settings of the natural circular frequency for the denominator and numerator. Give the expression of the transfer function.

Answer:

– Butterworth, Bessel or Tchebyshev type filters

Assuming the operational amplifiers to be perfect, we see:

$$V_{s3} = -\frac{R_4}{R_3} V_{s2} = -\frac{R_4}{R_3} \left(-\frac{1}{R'C'S} \right) V_{s1} \quad \text{and} \quad \frac{V_e}{R_1} + \frac{V_{s3}}{R_5} + \frac{V_{s1}}{R_2} (1 + R_2 C s) = 0$$

Eliminating V_{s1} and V_{s2} provides a second-order low-pass inverter on output 3:

$$\frac{V_{s3}}{V_e} = -\frac{R_5}{R_1} \times \frac{1}{1 + \frac{R_3 R_5}{R_2 R_4} R'C'S + \frac{R_3 R_5}{R_4} R'C'S^2}$$

Accordingly, gain is set by R_1 and R_5 while the other elements set the natural circular frequency ω_n and R_2 independently determines the damping factor ζ .

There is also a band-pass on output 1:

$$\frac{V_{s1}}{V_e} = -\frac{R_3 R_5}{R_4 R_1} \times \frac{R' C' s}{1 + \frac{R_3 R_5}{R_2 R_4} R' C' s + \frac{R_3 R_5}{R_4} R' C' C s^2}$$

with $R_4 = R_5$; $R_3 = R'$; $C = C'$: $\omega_n = \frac{1}{R_3 C}$ and $\zeta = \frac{1}{2} \frac{R_3}{R_2}$.

On output V_{s1} of the second circuit:

$$H(s) = \frac{V_{s1}}{V_e} = -\frac{R_1}{R_6} \times \frac{RCR' C' s^2}{1 + \frac{R_0}{R_0 + R_4} \left[1 + \frac{R_1}{R_6} \left(1 + \frac{R_6}{R_2} \right) \right] R' C' s + \frac{R_1}{R_2} R' C' RC s^2}$$

Taking $RC = R' C'$ and $R_1 = R_2$:

$$H(s) = \frac{V_{s1}}{V_e} = -\frac{R_1}{R_6} \times \frac{(RC s)^2}{1 + \frac{R_0}{R_0 + R_4} \left[2 + \frac{R_1}{R_6} \right] RC s + (RC s)^2}$$

while the numerator becomes 1 instead of $(RCs)^2$ if the output is given in V_{s3} .

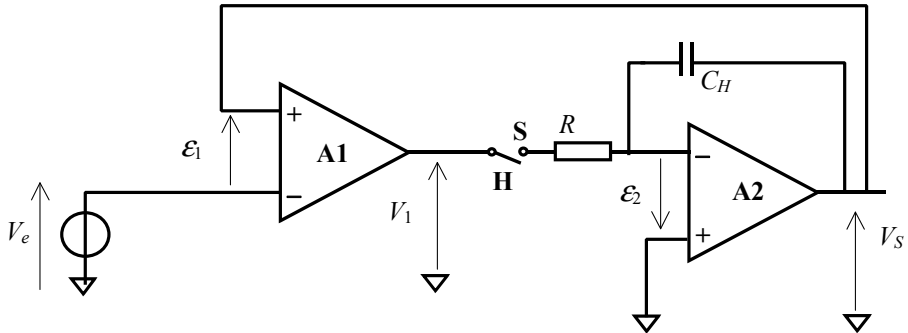
– Making the sum of V_{s3} and V_{s1} on the second filter provides an elliptic-type transmittance by means of a summing and inverting circuit, with V_{s1} being applied on resistance R_7 , V_{s3} on resistance R_8 , and R_9 being the feedback resistance. This provides transmittance:

$$H'(s) = \frac{V_{s4}}{V_e} = \frac{R_1}{R_6} \times \frac{\frac{R_8}{R_9} + \frac{R_7}{R_9} (RC s)^2}{1 + \frac{R_0}{R_0 + R_4} \left[2 + \frac{R_1}{R_6} \right] RC s + (RC s)^2}$$

The natural circular frequencies of both numerator and denominator are then independent and the numerator's damping coefficient is zero (which entails a zero of transmittance situated on the imaginary axis, also known as

an attenuation pole, inducing the cancellation of the transmittance at the corresponding circular frequency in sinusoidal conditions).

1.7.3. Study of a looped system and its stability: sample and hold circuit



It is assumed that the operational amplifiers are compensated until unity gain, that is they have an open loop gain of type: $A(jf) = \frac{A_0}{1 + j \frac{f}{f_1}}$; their input

current and output resistance are neglected.

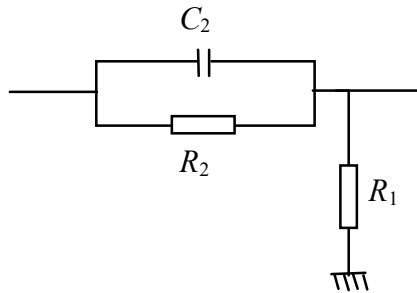
1) Show that the loop gain of an integrator (such as A2, R, C_H) always has an argument between $+\pi/2$ and $-\pi/2$ and as a consequence the integrator is unconditionally stable, since its image on the complex plane can never surround point -1 . Next, make the approximation that A2 is a perfect operational amplified with a loop gain much greater than 1 in modulus (inducing $\varepsilon_2 \approx 0$). Determine the domain of validity of this approximation according to the plot of the Bode diagrams for $|A(f)|$ and $1/|B(f)|$ assuming $A_0 = 10^5$; $f_1 = 500$ Hz; $\frac{1}{2\pi RC_H} = 5 \times 10^5$ Hz; use the new next parameters: $f_0 = A_0 f_1$ and $f_H = \frac{1}{2\pi RC_H}$.

2) Draw the general block diagram of the system and return it to the standard case by changing all the signs. Now determine the expression of the

loop gain and then of the closed loop gain when the switch is closed. By studying the Bode diagram of the loop gain and by calculating quality coefficient Q (or damping coefficient ζ) and natural frequency f_n of the closed loop, show that the system does not oscillate but is very poorly dampened and consequently useless in practice.

3) The real system can be improved by using an operational amplifier for A_1 with the same gain bandwidth product but with much lower DC open loop gain, where, for example, $A_0 = 10^2$ and $f_1 = 5 \times 10^5$ Hz and taking $f_H = 2 \cdot 10^4$ Hz. Recalculate Q , ζ and f_n . Determine the final value of the output voltage when the input signal is a unit step of 1 V and when the capacitance C_H is initially discharged (no free regime). Determine the step response and time taken after step application for output voltage to return within the range of $\pm 10^{-4}$ times the final value calculated previously.

Show that another solution is to introduce a phase lead corrector with transmittance B' in the return loop like below:



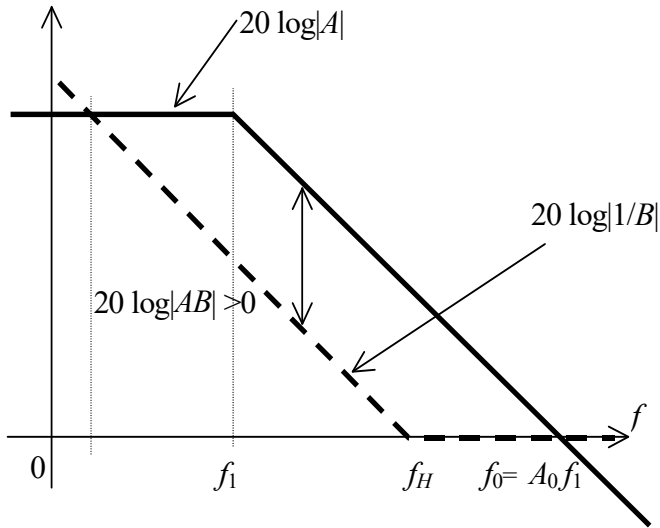
Recalculate the loop gain $A'(f)B'(f)$ where $A'(f)$ is now written as:

$$A'(f) = \frac{A_0}{1 + j \frac{f}{f_1}} \frac{1}{1 + \frac{R_2}{R_1}} = \frac{A'_0}{1 + j \frac{f}{f_1}}; \text{ and with } f_2 = \frac{1}{2\pi R_2 C_2}; f_2' = \frac{1 + \frac{R_2}{R_1}}{2\pi R_2 C_2}. \text{ Plot}$$

its argument qualitatively assuming that $\sqrt{f_2 f_2'}$ is made to correspond with frequency f_n' where $|A'(f_n')B'(f_n')| = 1$. Show that this allows for the loop gain image to be removed farther from point -1 in the complex plane.

Determine f_2 and f_2' to have an additional phase margin of $\pi/4$ when keeping the values of question 2, giving the transmittance argument of the corrector a value of $+\pi/4$ for $f=f_n'$.

Answer:



1) The integrator's return loop transmittance is determined by high-pass voltage divider C_H - R , that is: $\frac{R C_H s}{1 + R C_H s}$. Loop gain in harmonic condition is

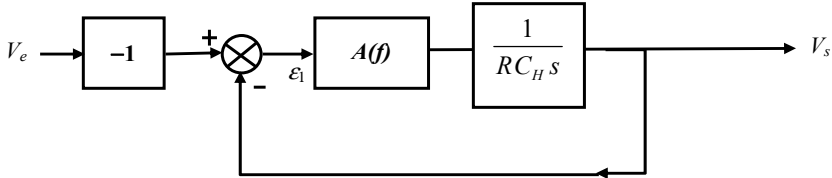
thus $\frac{j \frac{f}{f_H} A_0}{1 + j \frac{f}{f_H} 1 + j \frac{f}{f_1}}$, with asymptotic arguments of $+\pi/2$ in low frequency

and of $-\pi/2$ in high frequency. Loop gain cannot surround point -1 in the complex plane since its image remains in the right half-plane (positive real part). The integrator is thus always stable.

Between the two intersections of $20 \log|A|$ with $20 \log|1/B|$, the loop gain is far greater than 1, validating the use of perfect operational amplifier approximation ($\varepsilon_2 \approx 0$). In the parallelogram visible in the graph, the

intersection frequencies are $f_0 = A_0 f_1 = 5 \times 10^7$ Hz for the higher one, 100 times higher than f_H , and so $f_1/100 = 5$ Hz for the lower frequency.

2) Returning the minus sign of the transmittance of the inverting integrator considered as perfect, with transmittance $-\frac{1}{RC_H s}$, onto the subtractor, provides the following block diagram in forced conditions:



Thus, the loop gain is $\frac{A_0}{1 + \frac{s}{2\pi f_1}} \frac{1}{RC_H s}$, yielding $\frac{A_0}{1 + j \frac{f}{f_1}} \frac{f_H}{j f}$ in harmonic

condition and in closed loop $H(s) = \frac{K A(s)}{1 + A(s)B}$ with $B = 1$ since the feedback loop is unitary:

$$H(s) = \frac{-A_0}{RC_H s \left(1 + \frac{s}{2\pi f_1}\right)} \frac{1}{1 + \frac{A_0}{RC_H s \left(1 + \frac{s}{2\pi f_1}\right)}} = \frac{-1}{1 + \frac{RC_H}{A_0} s + \frac{RC_H}{2\pi f_0} s^2}$$

Its natural frequency is $\sqrt{f_0 f_H}$ and its damping coefficient is $\frac{1}{2A_0} \sqrt{\frac{f_0}{f_H}} = 5 \times 10^{-5}$, an extremely low value. Closed loop transmission is stable nonetheless since the poles have a negative real part $-\frac{RC_H}{2A_0}$; however, the absolute value is too low due to the value of A_0 being too high.

3) The new values provide $f_0 = A_0 f_1 = 5 \times 10^7$ Hz unchanged, a natural frequency $f_n = \sqrt{f_0 f_H} = 10^6$ Hz and a damping coefficient $\zeta = \frac{1}{2A_0} \sqrt{\frac{f_0}{f_H}} = 0.25$.

The final value of the output voltage can be determined by applying the theorem of the final value on the output voltage whose LT may be calculated by the product of $H(s)$ by $1/s$, the LT of the 1 V step:

$$\lim_{t \rightarrow +\infty} V_s(t) = \lim_{s \rightarrow 0} s \frac{H(s)}{s} = \lim_{s \rightarrow 0} H(s) = -1 \text{ V}$$

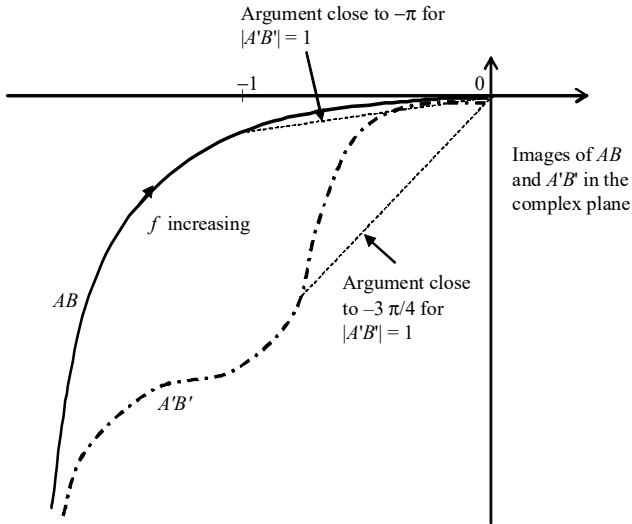
coherent with the sign reversal due to the minus sign present on the input block.

The step response of the second-order low-pass filter representative of $H(s)$ fulfills the expression $1 - \frac{\exp(-\zeta \omega_n t)}{\sqrt{1-\zeta^2}} \cos[\omega_n \sqrt{1-\zeta^2} t - \phi_0]$ multiplied by -1 V. Accordingly, voltage fits into the range of $\pm 10^{-4}$ times the final value when $\frac{\exp(-\zeta \omega_n t)}{\sqrt{1-\zeta^2}}$ becomes lower than 10^{-4} , thus for $t > \frac{1}{\zeta \omega_n} \ln \left[\frac{10^4}{\sqrt{1-\zeta^2}} \right]$ = 5.9 μ s.

4) Feedback loop transmittance is equal to $B'(s) = \frac{R_1}{R_1 + R_2} \frac{1 + \frac{s}{2\pi f_2}}{1 + \frac{s}{2\pi f'_2}}$

The loop gain is thus: $A'(f)B'(f) = \frac{A'_0}{1 + j \frac{f}{f_1}} \frac{f_H}{jf} \frac{1 + j \frac{f}{f_2}}{1 + j \frac{f}{f'_2}}$ in harmonic

condition.



For $f_1 = 500$ Hz, $f_H = 5 \times 10^5$ Hz while accounting for $f'_n = \sqrt{f_2 f'_2}$, $|A'B'|$

$= 1$ and with $f'_n \gg f_1$, the argument of $\frac{1 + j \frac{f}{f_2}}{1 + j \frac{f}{f'_2}}$ must be of $+\pi/4$ in order

to obtain a total $-3\pi/4$.

So:

$$\frac{\pi}{4} = \text{Atan} \left(\frac{f'_n}{f_2} \right) - \text{Atan} \left(\frac{f'_n}{f'_2} \right) = \text{Atan} \left(\frac{\frac{f'_n}{f_2} - \frac{f'_n}{f'_2}}{1 + \frac{f'^2_n}{f_2 f'_2}} \right) = \text{Atan} \left(\frac{\sqrt{\frac{f'_2}{f_2}} - \sqrt{\frac{f_2}{f'_2}}}{2} \right)$$

The tangent must thus be equal to 1. So $x - \frac{1}{x} = 2$ writing $x = \sqrt{\frac{f'_2}{f_2}} > 1$.

The positive root of $x^2 - 2x - 1 = 0$ is $1 + \sqrt{2} = 2.414$, involving $\frac{f'_2}{f_2} = 1 + \frac{R_2}{R_1} = 5.83$.

There remains only to determine frequency f'_n for which $|A'B'| = 1$ while making the approximation $f'_n \gg f_1$, which will be verified below; since

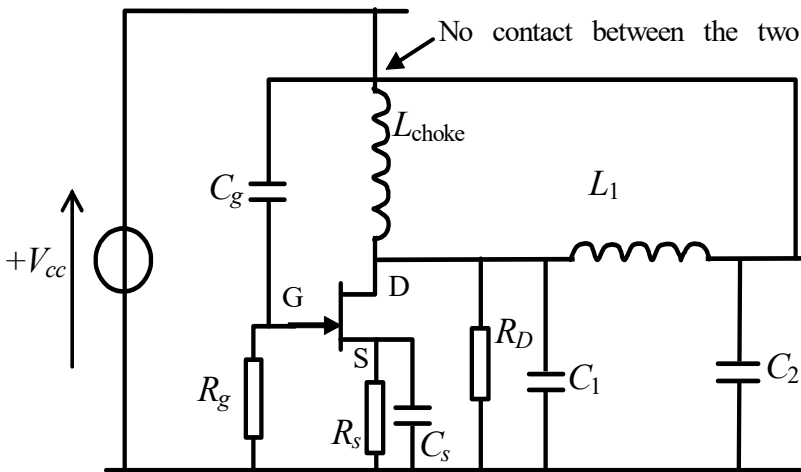
$$1 = \frac{A'_0 f_1 f_H}{f_n'^2} \left| \frac{1 + j \frac{f'_n}{f_2}}{1 + j \frac{f'_n}{f_2'}} \right| = \frac{A'_0 f_1 f_H}{f_n'^2} \left| \frac{1 + j \sqrt{\frac{f_2'}{f_2}}}{1 + j \sqrt{\frac{f_2}{f_2'}}} \right| = \frac{A'_0 f_1 f_H}{f_n'^2} \frac{\sqrt{1 + 5.83}}{\sqrt{1 + \frac{1}{5.83}}}$$

Furthermore, since $A'_0 = \frac{A_0}{1 + \frac{R_2}{R_1}} = \frac{10^5}{5.83}$ then finally

$$f'_n = 3.2 \times 10^6 \text{ Hz} \gg 500 \text{ Hz}, f_2 = 1.3 \times 10^6 \text{ Hz} \quad \text{and} \quad f_2' = 7.7 \times 10^6 \text{ Hz}.$$

1.7.4. Study of a Colpitts oscillator built with a JFET

Let us take the sinusoidal oscillator represented below. The impedances of capacitors C_g and C_s are considered as zero at oscillation frequency and that of inductance L_{choke} as infinite. The conductance of R_g and the transistor's input admittance between G and S are negligible relative to the admittance of C_2 . The transistor is equivalent to a current source $g_m v_{GS}$ between D and S from a dynamic point of view (g_m is the transconductance).



1) In order to obtain an operating point at $I_{DSS} / 2$ (I_{DSS} being the saturation current at $V_{GS} = 0$), there must be a static voltage $V_{GS} = -2$ V. If $I_{DSS} = 2$ mA, calculate R_S , with the static gate current being zero. If $V_{cc} = +5$ V, calculate static V_{DS} .

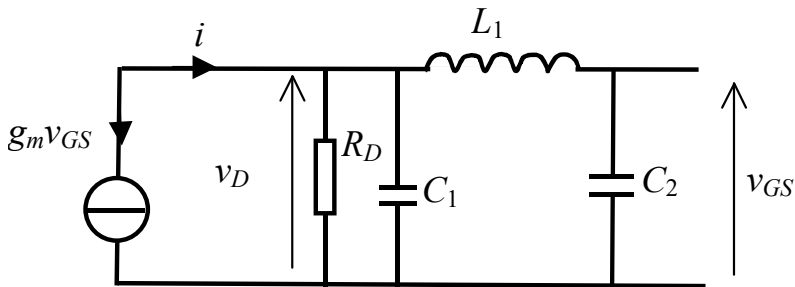
2) Determine the equivalent dynamic circuit while accounting for the hypotheses above.

3) Using the calculation of admittance seen to the right of point D and the AC voltage division performed by L_1 and C_2 , determine the oscillation condition (on the imaginary part and on the real part) and deduce the circular frequency ω_0 for oscillation according to L_1 , C_2 and C_1 , together with the relation between R_D , g_m , C_1 and C_2 . Comment about amplitude stabilization.

Answer:

1) In static condition, there is $V_{GS} = -R_S I_D = -2$ V, then for $I_D = I_{DSS}/2 = 1$ mA, $R_S = 2$ k Ω . And since $V_{DS} = V_{CC} - R_S I_D$; $V_{DS} = 5 - 2 = 3$ V.

2) Accounting for the conditions provided in the presentation, the dynamic operational circuit is made up as follows:



Writing $g_D = 1 / R_D$ and calling $Y(s)$ the admittance of the circuit crossed by current i :

$$Y(s) = g_D + C_1 s + \frac{C_2 s}{1 + L_1 C_2 s^2} \quad \text{and} \quad V_{GS}(s) = V_D(s) \frac{1}{1 + L_1 C_2 s^2}$$

Furthermore, the LT of i reads $I(s) = Y(s)V_D(s) = -g_m V_{GS}(s)$. Replacing s by $j\omega_0$:

$$\left[g_D + j\omega_0 \left(C_1 + \frac{C_2}{1 - L_1 C_2 \omega_0^2} \right) \right] V_D(j\omega_0) + \frac{g_m}{1 - L_1 C_2 \omega_0^2} V_D(j\omega_0) = 0$$

The oscillation condition allows for $V_D(j\omega_0) \neq 0$ only if:

$$g_D + j\omega_0 \left(C_1 + \frac{C_2}{1 - L_1 C_2 \omega_0^2} \right) + \frac{g_m}{1 - L_1 C_2 \omega_0^2} = 0$$

Accordingly, the real part must be zero, and the same for the imaginary part:

$$g_D + \frac{g_m}{1 - L_1 C_2 \omega_0^2} = 0 \quad \text{and} \quad C_1 + \frac{C_2}{1 - L_1 C_2 \omega_0^2} = 0$$

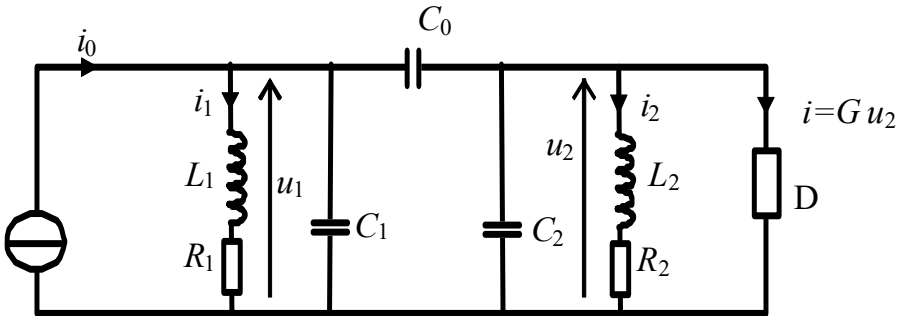
Hence, it may be deduced:

$$\omega_0 = \sqrt{\frac{1}{L_1} \left(\frac{1}{C_1} + \frac{1}{C_2} \right)} \quad \text{and} \quad R_D = \frac{1}{g_D} = \frac{C_2}{C_1 g_m}$$

Stabilization of the amplitude would need a detection circuit controlling the conductance of a second JFET whose drain and source terminals are in parallel on R_s in order to modulate the transconductance of the initial JFET, as described in the lecture of this chapter.

1.7.5. Study of a system in state-space form

The system below, based on two coupled resonant circuits, will now be studied in the aim of determining its poles and its stability. D is a dipole capable of presenting a positive, negative or zero conductance G around the origin, and is nonlinear beyond a certain voltage threshold, as in the Chua oscillator. The independent source of current i_0 can represent the collector or the drain of a transistor.



– Determine the number of nodes and branches in which it is possible to write a relation between voltage and current. From this, deduce the system's number of independent equations (state equations).

– Write the system's state equations, taking the various derivations of the state variables as first members in the order visible in the circuit from left to right. Taking $C_1 = C_2 = C$ and writing $\gamma = \frac{C_0}{C + C_0}$ (coupling coefficient),

resolve the subsystem of equations where the derivations of u_1 and u_2 appear in order to obtain a subsystem in which only one of the two derivations exists in each equation. In addition, since there are still too many settings, it may also be taken that $L_1 = L_2 = L$ and $R_1 = R_2 = R_0$.

– Normalize the system of equations by making the following variable changes: $\theta = \frac{t}{\sqrt{LC}}$; $\zeta = R_0 \sqrt{\frac{C}{L}} \in [0 \ 1]$ (damping coefficient to within a

factor of 2); $\alpha = G \sqrt{\frac{L}{C}} = \frac{GR_0}{\zeta}$; $w = \frac{R_0 i_1}{u_m}$; $x = \frac{u_1}{u_m}$; $y = \frac{u_2}{u_m}$; $z = \frac{R_0 i_2}{u_m}$, u_m being

a constant voltage reference. From this, deduce the dimensionless elements (with the exception of the second term of the second member) in which the column vector of the first member only includes derivatives relative to θ of normalized state variables $\dot{w}, \dot{x}, \dot{y}, \dot{z}$.

– In case $\alpha = 0$, representative of a circuit with no D dipole, determine eigenvalues λ_i of the state matrix \mathbf{A} . It is indicated that the development of the determinant $\det(\mathbf{A} - \lambda \mathbf{I})$, where \mathbf{I} is the unit matrix, leads to equality between two squared expressions for which the square root assigned to the plus or minus sign may readily be taken. Now deduce the expressions of the poles. From the symbolic value of their real part, deduce whether the system

is stable or not. Determine the system's two natural circular frequencies. What is the effect of an increase in the coupling coefficient γ ?

– In the case where $\alpha < 0$, it is possible to obtain a system whose behavior is different; however, the poles can be only be calculated by a numerical method, available in mathematical softwares. For example, for $\zeta = 0.02$ and $\gamma = 0.25$; the eigenvalues of A follow the following laws with a precision better than one thousandth

$$\lambda_{1,2} \approx -\frac{\zeta}{2} - \frac{\alpha}{4} \pm j\sqrt{1 - \frac{\zeta^2}{4}} \quad \text{and} \quad \lambda_{3,4} \approx -\frac{\zeta}{2} - \frac{3\alpha}{20} \pm j\sqrt{\frac{1-\gamma}{1+\gamma} - \frac{\zeta^2}{4}} \quad \text{for } -0.1 \leq \alpha \leq 0.$$

Deduce the value of α allowing the system to oscillate and the oscillation frequency reasoning from the cancellation of the real part of one pole.

Answer:

1) The circuit comprises three nodes and six branches in which it is possible to write a relation between voltage and current, unlike in the case of the ideal source. There are $6 - 3 + 1 = 4$ independent equations.

2) The four state equations are written as:

$$\left\{ \begin{array}{l} L_1 \frac{di_1}{dt} = u_1 - R_1 i_1 \\ C_1 \frac{du_1}{dt} = C_0 \frac{d(u_2 - u_1)}{dt} - i_1 + i_0 \\ C_2 \frac{du_2}{dt} = C_0 \frac{d(u_1 - u_2)}{dt} - i_2 - i \\ L_2 \frac{di_2}{dt} = u_2 - R_2 i_2 \end{array} \right.$$

The subsystem comprised by the second and third equations is resolved after introducing $C_1 = C_2 = C$ and $\gamma = \frac{C_0}{C + C_0}$.

$$\begin{cases} L_1 \frac{di_1}{dt} = u_1 - R_1 i_1 \\ C(1+\gamma) \frac{du_1}{dt} = -\gamma(i_2 + i) - i_1 + i_0 \\ C(1+\gamma) \frac{du_2}{dt} = -i_2 - i + \gamma(i_0 - i_1) \\ L_2 \frac{di_2}{dt} = u_2 - R_2 i_2 \end{cases}$$

3) Making the changes as indicated gives:

$$\begin{bmatrix} \dot{w} \\ \dot{x} \\ \dot{y} \\ \dot{z} \end{bmatrix} = \begin{bmatrix} -\zeta & \zeta & 0 & 0 \\ -1 & 0 & \frac{-\alpha\gamma}{(1+\gamma)} & \frac{-\gamma}{\zeta(1+\gamma)} \\ \zeta(1+\gamma) & 0 & \frac{-\alpha}{(1+\gamma)} & \frac{-1}{\zeta(1+\gamma)} \\ \zeta(1+\gamma) & 0 & \frac{-\alpha}{(1+\gamma)} & \frac{-1}{\zeta(1+\gamma)} \\ 0 & 0 & \zeta & -\zeta \end{bmatrix} \begin{bmatrix} w \\ x \\ y \\ z \end{bmatrix} + \begin{bmatrix} 0 \\ \frac{R_0}{\zeta(1+\gamma)u_m} \\ \frac{\gamma R_0}{\zeta(1+\gamma)u_m} \\ 0 \end{bmatrix} \begin{bmatrix} i_0 \end{bmatrix}$$

that can be condensed into $\dot{\mathbf{F}} = \mathbf{A} \mathbf{F} + \mathbf{B} \mathbf{U}$, where \mathbf{A} is the state matrix. The eigenvalues are the roots of the characteristic equation $\det(\mathbf{A} - \lambda \mathbf{I}) = 0$.

4) In the case of $\alpha = 0$, developing $\det(\mathbf{A} - \lambda \mathbf{I})$ relative to the first line gives: $\det(\mathbf{A} - \lambda \mathbf{I}) = (-\zeta - \lambda) \left[-\lambda^2 (\zeta + \lambda) - \frac{\lambda}{(1+\gamma)} \right] - \zeta \left[\frac{\gamma^2 - 1}{\zeta(1+\gamma)^2} - \frac{\lambda(\zeta + \lambda)}{\zeta(1+\gamma)} \right] = 0$

$$\text{Factoring: } \lambda(\zeta + \lambda) \left[\lambda(\zeta + \lambda) + \frac{2}{(1+\gamma)} \right] + \frac{1 - \gamma^2}{(1+\gamma)^2} = 0$$

Developing: $[\lambda(\zeta + \lambda)]^2 + \frac{2}{(1+\gamma)} \lambda(\zeta + \lambda) + \frac{1}{(1+\gamma)^2} = \frac{\gamma^2}{(1+\gamma)^2}$, equality of two squared expressions, whose square root gives: $\lambda(\zeta + \lambda) + \frac{1}{(1+\gamma)} = \pm \frac{\gamma}{(1+\gamma)}$.

The 4 root solutions can be deduced from $\lambda(\zeta + \lambda) = -1$ and $\lambda(\zeta + \lambda) = -\frac{1-\gamma}{1+\gamma}$:

$$\lambda_{1,2} = -\frac{\zeta}{2} \pm j \sqrt{1 - \frac{\zeta^2}{4}} \quad \text{and} \quad \lambda_{3,4} = -\frac{\zeta}{2} \pm j \sqrt{\frac{1-\gamma}{1+\gamma} - \frac{\zeta^2}{4}}$$

These are the system poles, for which all the real parts are equal to $-\frac{\zeta}{2}$, negative, and as a result, the system is stable. Its free regime is of the form $\sum_i v_i \exp(\lambda_i \theta) = \sum_i v_i \exp\left(\lambda_i \frac{t}{\sqrt{LC}}\right)$ with identical eigenvectors v_i for the complex conjugate poles.

So, the natural circular frequencies are $\frac{1}{\sqrt{LC}} \sqrt{1 - \frac{\zeta^2}{4}}$ and $\frac{1}{\sqrt{LC}} \sqrt{1 + \gamma - \frac{\zeta^2}{4}}$.

5) Starting from $\alpha = 0$ and moving toward $\alpha < 0$, the first pole whose real part reaches zero is $\lambda_{1,2}$ for $\alpha = -0.04$. For this value of α , there will consequently be oscillation at circular frequency $\frac{1}{\sqrt{LC}} \sqrt{1 - \frac{\zeta^2}{4}} = \frac{0.999}{\sqrt{LC}}$ since the sum $\sum_{1,2} v_i \exp\left(\lambda_i \frac{t}{\sqrt{LC}}\right)$ yields a sinusoidal function of time while the other oscillation dampens due to pole $\lambda_{3,4}$ still with negative real part. This operation requires negative conductance G around the origin for dipole D, which is calculable from the value of $\alpha = G \sqrt{\frac{L}{C}} = \frac{GR_0}{\zeta} = -0.04$.

Continuous-time Linear Systems: Quadripoles, Filtering and Filter Synthesis

2.1. Quadripoles or two-port networks

Quadripoles are networks described by a system of two linear equations linking four electric quantities, two currents and two voltages, which can be written in the matrix form, the matrix \mathbf{Q} or \mathbf{T} of the quadripole having to be chosen among six possible combinations of the four electric quantities. By convention, the electric quantities will be written in capital letters because they represent either complex symbolic quantities (with sinusoidal behavior) or Laplace or Fourier transforms of time functions with variable behavior. When the convention about the current directions at the terminal where the potential is highest (tip of the arrow) corresponds to incoming currents, this is a receptor convention (Figure 2.1).

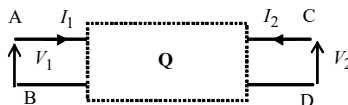


Figure 2.1. *Input and output receptor conventions in a quadripole or two-port network*

In the case of a current leaving the terminal presenting the highest potential, this represents a generator convention, which will be adopted in certain cases. It is assumed that terminals A–B, on the one hand (the left port), and C–D, on the other hand (the right port), are connected to external

dipoles and thus crossed by currents of same name. A–B and C–D pairs are called “ports”.

The interest of quadripoles lies in showing both voltages and currents, which will allow us to perform power calculations. Since filtering can be regarded as an operation that makes the transferred power dependent on the frequency, this issue will be naturally addressed based on the concepts introduced for quadripoles, even when filters make use of circuits that can be represented by block diagrams as in Chapter 1, such as operational amplifier-based circuits.

2.1.1. Quadripoles deduced from dynamic circuits

The four types of quadripoles presented below are simply deduced from the association of two dipoles composed of either a voltage source in series with an impedance, or a current source in parallel with an admittance. The corresponding electrical equations are expressed from the sums of the two voltages in the first case or of the two currents in the second case, giving a relationship for each of the two ports. Each makes it possible to express the characteristic quantity of the dipole according to the other two, one relative to the same terminal and the other relative to the opposite terminal, which offers the possibility of generating electrical couplings between the two ports (direct transfer and inverse transfer). Types II or IV are generally used to describe transistors, type I for standard operational amplifiers, type III for transformers and types I or IV for passive circuits.

type I: with impedance parameters	$\begin{cases} V_1 = Z_{11}I_1 + Z_{12}I_2 \\ V_2 = Z_{21}I_1 + Z_{22}I_2 \end{cases}$	
type II: with hybrid parameters (voltage-current)	$\begin{cases} V_1 = h_{11}I_1 + h_{12}V_2 \\ I_2 = h_{21}I_1 + h_{22}V_2 \end{cases}$	
type III: with hybrid parameters (current-voltage)	$\begin{cases} I_1 = h'_{11}V_1 + h'_{12}I_2 \\ V_2 = h'_{21}V_1 + h'_{22}I_2 \end{cases}$	
type IV: with admittance parameters	$\begin{cases} I_1 = Y_{11}V_1 + Y_{12}V_2 \\ I_2 = Y_{21}V_1 + Y_{22}V_2 \end{cases}$	

The two-equation systems can be written in the matrix form, \mathbf{Z} for type I and \mathbf{Y} for type IV.

In associations of quadripoles, type I will be adopted for associations in series (addition of voltages V_1+V_1' ; V_2+V_2'), that is to say, if currents I_1 and I_2 are common to the homologous ports of both quadripoles, and type IV for the association in parallel (addition of currents I_1+I_1' ; I_2+I_2'), namely if voltages V_1 and V_2 are common to the homologous ports (Figure 2.2). Different associations for both ports will require mixed types II or III.

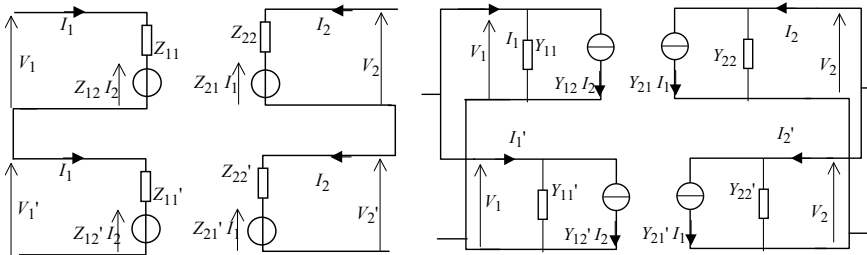


Figure 2.2. Association of quadripoles in series (on the left) and in parallel (on the right), using the appropriate models

Generally speaking, any quadripole can be described by

$$\begin{cases} X_1 = Q_{11}W_1 + Q_{12}X_2 \\ W_2 = Q_{12}W_1 + Q_{22}X_2 \end{cases},$$

where X_1 , X_2 , W_1 and W_2 represent the four electric quantities (two currents and two voltages) and Q_{11} , Q_{12} , Q_{21} and Q_{22} the four parameters (Q_{12} the inverse transfer parameter, Q_{21} the direct transfer parameter). It should be noted that matrices \mathbf{Z} and \mathbf{Y} are inverses of one another and that the same happens for the two types of matrices with hybrid parameters.

2.1.2. Quadripoles and transfer matrices

For a cascading configuration, that is, quadripoles assembled one after the other, quantities V_2 and I_2 (“output port”) must be expressed according to V_1 and I_1 (“input port”), and it should be more convenient to take I_2 outgoing, namely following an output generator convention (Figure 2.3).

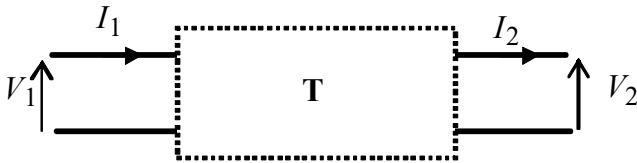


Figure 2.3. Quadripole with receptor convention at left (input) and generator convention at right (output)

It should be denoted by $\begin{cases} V_2 = T_{11}V_1 + T_{12}I_1 \\ I_2 = T_{21}V_1 + T_{22}I_1 \end{cases}$ or in matrix form:

$$\begin{bmatrix} V_2 \\ I_2 \end{bmatrix} = \begin{bmatrix} T_{11} & T_{12} \\ T_{21} & T_{22} \end{bmatrix} \begin{bmatrix} V_1 \\ I_1 \end{bmatrix}.$$

A linear combination of the two characteristic equations of one of the quadripoles deduced from the dynamic circuits (or substitutions) allows for this structure to be obtained, on the condition that the determinant of the initial matrix or some coefficients are non-zero. Therefore, it is not always possible to obtain these two types of quadripoles from one of those in the previous section. Where possible, we can also calculate V_1 and I_1 according to V_2 and I_2 by means of the inverse matrix of matrix \mathbf{T} .

For example, from the admittances (type IV):

$$\begin{cases} V_2 = -\frac{Y_{11}}{Y_{12}}V_1 + \frac{1}{Y_{12}}I_1 \\ I_2 = \frac{\Delta Y}{Y_{12}}V_1 - \frac{Y_{22}}{Y_{12}}I_1 \end{cases}$$

where $\Delta Y = \det Y = Y_{11}Y_{22} - Y_{12}Y_{21}$.

When the calculation is possible, it is then easy to “chain” (or “cascade”) several quadripoles of this type and to execute the calculation of the matrices product by a computer.

2.1.3. Modification of the parameters of the quadripoles using negative feedback

Let the system be $\begin{cases} X_1 = Q_{11}W_1 + Q_{12}X_2 \\ W_2 = Q_{21}W_1 + Q_{22}X_2 \end{cases}$ where $X_1 = V_1$ and $W_1 = I_1$ or vice versa and $X_2 = V_2$ and $W_2 = I_2$ or vice versa.

By applying negative feedback from W_2 onto W_1 , W_1 will be replaced by $W_1 - B W_2$ in both equations. In the second equation, $W_2 = Q_{21}(W_1 - B W_2) + Q_{22}X_2$.

$$\text{Therefore: } \begin{cases} X_1 = \frac{Q_{11}}{1 + BQ_{21}} W_1 + \left(Q_{12} - \frac{BQ_{11}Q_{22}}{1 + BQ_{21}} \right) X_2 \\ W_2 = \frac{Q_{21}}{1 + BQ_{21}} W_1 + \frac{Q_{22}}{1 + BQ_{21}} X_2 \end{cases}$$

It can be observed that the output impedance Q_{22} can be decreased (if X_2 is a current) by a factor $(1 + BQ_{21})$ when the output generator is a voltage generator or the output admittance Q_{22} (if X_2 is a voltage) when the output generator is a current generator; in other words, in both cases it results in a better approximation of an ideal output source.

On input, Q_{11} is also divided by $(1 + BQ_{21})$. This is an impedance if W_1 is a current and an admittance if W_1 is a voltage. It should be noted that this is done at the expense of the direct transfer coefficient Q_{21} , also divided by $(1 + BQ_{21})$.

Replacing X_1 by $X_1 - B'X_2$ is of less interest because only the inverse transfer coefficient is changed into $Q_{12} + B'$ and that of W_1 by $W_1 - B''X_2$ changes Q_{12} into $Q_{12} - B'$ and Q_{22} into $Q_{22} - B'$, which can lead to the instability of the quadripole.

According to the parameter types, the feedback of W_2 onto W_1 is carried out with current or voltage quantities from the output toward the input, with Q_{11} , Q_{21} and Q_{22} divided by $(1 + BQ_{21})$. The type of feedback assumes one of the designations shown in the following table, the first term indicating the output quantity used to develop B and the second term indicating the input quantity onto which the feedback loop acts:

$W_1 =$	I_1	V_1
$W_2 = I_2$	Current–current	Current–voltage
$W_2 = V_2$	Voltage–current	Voltage–voltage

Examples of negative feedback applied onto quadripoles (the quadripoles are usually transistors or associations of transistors or operational amplifiers):

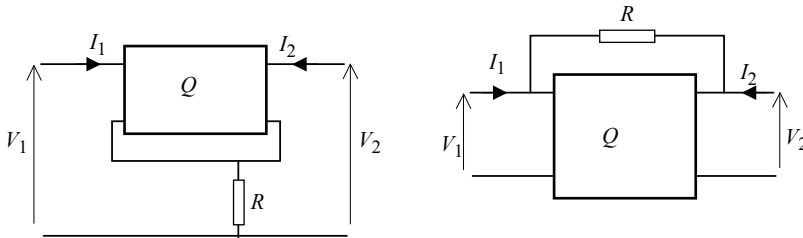


Figure 2.4. Current–voltage feedback on the left and voltage–current feedback on the right

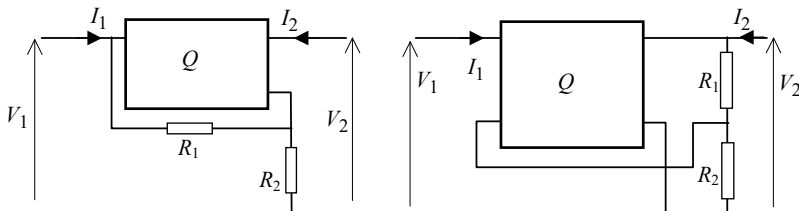


Figure 2.5. Current–current feedback on the left and voltage–voltage feedback on the right

It is essential to write the circuit equations of the aforementioned circuits to obtain exact expressions of the new parameters because the resistances introduced in some cases modify more than one quantity I_1 , V_1 , I_2 or V_2 (except eventually if Q is an ideal operational amplifier), contrary to the assumption made at the beginning of the section. The resistors can also be replaced by impedances, transformers or active components, which offers many possibilities to change the initial properties of a quadripole.

2.1.4. Passive quadripoles

A quadripole is said to be passive if it is possible to find an internal circuit comprising no source.

For example, for type I, the system of equations $\begin{cases} V_1 = Z_{11}I_1 + Z_{12}I_2 \\ V_2 = Z_{21}I_1 + Z_{22}I_2 \end{cases}$ can be transformed into $\begin{cases} V_1 = (Z_{11} - Z_{12})I_1 + Z_{12}(I_2 + I_1) \\ V_2 = (Z_{22} - Z_{12})I_2 + Z_{12}(I_2 + I_1) + (Z_{21} - Z_{12})I_1 \end{cases}$ which can be represented by Figure 2.6.

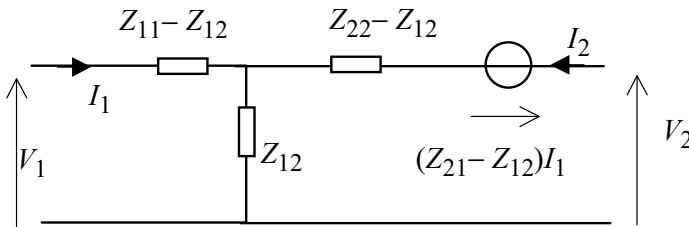


Figure 2.6. Representation of a type I quadripole with a single linked source

Only a single source remains. The only way to make it disappear is to impose $Z_{21} = Z_{12}$.

Then, there are only three independent parameters left for a passive quadripole instead of four for a quadripole in the more general case.

The *reciprocal passive quadripole* is defined, regardless of its type, represented by $\begin{cases} X_1 = Q_{11}W_1 + Q_{12}X_2 \\ W_2 = Q_{21}W_1 + Q_{22}X_2 \end{cases}$, by the equality of non-diagonal coefficients: $Q_{12} = Q_{21}$.

For a reciprocal passive quadripole having a transfer defined by $\begin{cases} V_2 = T_{11}V_1 + T_{12}I_1 \\ I_2 = T_{21}V_1 + T_{22}I_1 \end{cases}$ with the receptor convention on input and generator on output, the determinant Δ is equal to 1 (verify by setting $Y_{12} = Y_{21}$ in the

system in section 2.1.2) and $\Delta = -1$ with the receptor convention on input and output. In addition, if the passive quadripole is *symmetric*, in other words if both ports can be swapped without this having consequences on electrical properties, then $Q_{11} = Q_{22}$ for the quadripoles deduced from the dynamic circuits with the receptor convention on input and output. For symmetric transfer quadripoles, $T_{11} = T_{22}$ with the receptor convention on input and generator on output (or $T_{11} = -T_{22}$ with the receptor convention on input and output).

2.1.5. Dipole impedances and admittances; iterative impedance

2.1.5.1. Impedances or admittances seen at one port, the other being connected to a termination impedance

The input and output impedances, or dipolar impedances (or even “terminated impedances”), are defined for each port, respectively, by $Z_e = V_1/I_1$ and $Z_s = V_2/I_2$ (or admittances by their reciprocals), and by a condition on the parameter related to the opposite port of the quadripole in the equation under consideration, which is obtained by means of the current flow in a termination impedance or admittance. It is therefore possible to admit that the quadripole can be reduced to the dipole whose impedance or admittance is being calculated, the opposite port seeing a condition definitely imposed by the termination impedance or admittance.

In the two extreme cases either corresponding to an open circuit or to a short circuit at the opposite port, we shall add the index *o* or *sc*, respectively. The simplest dipole impedances or admittances are those which are already present in the circuit of the quadripole and that are obtained by canceling the dependent term of the opposite port in each equation:

for type I: $Z_{eo} = Z_{11}$; $Z_{so} = Z_{22}$; for type II: $Z_{esc} = h_{11}$; $Y_{so} = h_{22}$;

for type III: $Y_{eo} = h_{11}'$; $Z_{ssc} = h_{22}'$; for type IV: $Y_{esc} = Y_{11}$; $Y_{ssc} = Y_{22}$.

The others are inferred by canceling the first member of the other equation. Generally speaking, when any quadripole is represented by

$$\begin{cases} X_1 = Q_{11}W_1 + Q_{12}X_2 \\ W_2 = Q_{21}W_1 + Q_{22}X_2 \end{cases}, \text{ we find:}$$

$$\left. \frac{X_1}{W_1} \right|_{W_2=0} = \frac{\det Q}{Q_{22}} \quad \text{and} \quad \left. \frac{W_2}{X_2} \right|_{X_1=0} = \frac{\det Q}{Q_{11}}$$

where $\det Q = Q_{11} Q_{22} - Q_{12} Q_{21}$,

whereas we would have found Q_{11} and Q_{22} for the other two impedances or admittances, the opposite port in open circuit in the case of a voltage dipole or short circuit in the case of a current dipole. There is thus a relation of proportionality between these four parameters, since they depend only on the three quantities Q_{11} , Q_{22} and $\det Q$. Clearly, it can be seen that the Q_{11}/Q_{22} ratio is equal to that of the other two terminated impedances or admittances calculated above.

More generally, the input impedance or admittance is defined with the termination (or load) impedance Z_u connected to the output; and the output impedance or admittance with the termination impedance (or internal impedance of the external generator) Z_g connected to the input. For example, for the previous transfer quadripole, calculations are carried out by imposing the condition corresponding to this impedance connected to the opposite port:

$$Z_{eu} = \left. \frac{V_1}{I_1} \right|_{V_2=Z_u I_2} = \frac{Z_u T_{22} - T_{12}}{T_{11} - Z_u T_{21}} \quad \text{and} \quad Z_{sg} = \left. \frac{V_2}{-I_2} \right|_{V_1=-Z_g I_1} = \frac{T_{12} - Z_g T_{11}}{Z_g T_{21} - T_{22}}.$$

Then, it can easily be found that:

$$Z_{eo} = \left. \frac{V_1}{I_1} \right|_{Z_u = \infty} = -\frac{T_{22}}{T_{21}}; \quad Z_{esc} = \left. \frac{V_1}{I_1} \right|_{Z_u = 0} = -\frac{T_{12}}{T_{11}};$$

$$Z_{so} = \left. \frac{V_2}{-I_2} \right|_{Z_g = \infty} = -\frac{T_{11}}{T_{21}}; \quad Z_{ssc} = \left. \frac{V_2}{-I_2} \right|_{Z_g = 0} = -\frac{T_{12}}{T_{22}},$$

which verifies the relation: $\frac{Z_{eo}}{Z_{esc}} = \frac{Z_{so}}{Z_{ssc}}$, the general relation for all quadripoles, which could be proven independently of their type, as noted in the previous section.

By generalizing to $\begin{cases} X_1 = Q_{11}W_1 + Q_{12}X_2 \\ W_2 = Q_{21}W_1 + Q_{22}X_2 \end{cases}$, it is possible to determine the admittance or the impedance as seen from the input (port no. 1) depending on the termination $Q_u = -\frac{W_2}{X_2}$ at port no. 2, by extracting X_2 from the second equation with respect to W_1 and by deferring it into the first one:

$$\left. \frac{X_1}{W_1} \right|_{W_2 = -Q_u X_2} = \frac{Q_{11}Q_u + \Delta Q}{Q_u + Q_{22}}$$

where $\Delta Q = \det \mathbf{Q}$.

In the same way, we determine (port no. 2) the admittance or impedance as viewed from the output according to the termination $Q_g = -\frac{X_1}{W_1}$ at port no. 1, by extracting X_2 from the first equation with respect to W_1 and by deferring into the second:

$$\left. \frac{W_2}{X_2} \right|_{X_1 = -Q_g W_1} = \frac{Q_{22}Q_g + \Delta Q}{Q_g + Q_{11}}$$

For example, for a quadripole of type I: $Z_e \Big|_{V_2 = -Z_u I_2} = \frac{Z_{11}Z_u + \det \mathbf{Z}}{Z_u + Z_{22}}$

$$\text{and } Z_s \Big|_{V_1 = -Z_g I_1} = \frac{Z_{22}Z_g + \det \mathbf{Z}}{Z_g + Z_{11}}$$

2.1.5.2. Iterative impedance or characteristic impedance

It is the impedance Z_c that, connected to the output, can also be found as input impedance. In other words, this corresponds to the special case where the dipole impedance is the same as the termination impedance connected to

the opposite port. Thereby, we have $Z_c = \left. \frac{V_1}{I_1} \right|_{Z_u = Z_c} = \frac{V_2}{-I_2}$ for a quadripole

following receptor convention on output and $Z_c = \left. \frac{V_1}{I_1} \right|_{Z_u = Z_c} = \frac{V_2}{I_2}$ for a

quadripole with generator convention on output.

In this particular case, the two equations that define the quadripole are no longer independent. In the case of impedance or admittance quadripoles with generator convention on output (types I and IV modified by inverting the direction of I_2), $Y_c = 1/Z_c$ directly represents the eigenvalue with a real positive part of the impedance or admittance matrix.

It is possible to find a general characteristic equation for Z_c using impedances Z_{eo} , Z_{esc} , Z_{so} and Z_{ssc} that can be defined for any quadripole. For example, for the transfer quadripole, we get by setting $Z_u = Z_c = \frac{Z_c T_{22} - T_{12}}{T_{11} - Z_c T_{21}}$, and by replacing the parameters T_{11} , T_{12} , T_{21} and T_{22} by their expressions according to Z_{eo} , Z_{esc} , Z_{so} and Z_{ssc} previously defined:

$$Z_c^2 + (Z_{so} - Z_{eo})Z_c - Z_{ssc}Z_{eo} = 0 \quad \text{or} \quad Z_c^2 + (Z_{so} - Z_{eo})Z_c - Z_{esc}Z_{so} = 0$$

In the general case, Z_c is thus a solution of a second-degree equation and comprises an irrational term because of the square root. This term is therefore not necessarily an impedance achievable with passive elements R , L or C . In the particular case of a *symmetric passive* quadripole, $Z_{so} = Z_{eo}$ and $Z_{ssc} = Z_{esc}$, resulting in:

$$Z_c = \sqrt{Z_{esc}Z_{so}} = \sqrt{Z_{ssc}Z_{eo}}$$

2.1.5.3. *Non-dissipative passive quadripoles: synthesis of diagonal impedances and admittances*

This type of quadripole does not comprise resistance and therefore only uses inductances and capacitances. The functions that it allows to be realized involve matching the impedances and filtering. The properties of such passive quadripoles consisting only of inductances and capacitances are primarily based on those of dipoles existing between the ports when only one term subsists in every system equation describing the quadripole, the other quantity being canceled out, corresponding to the diagonal elements $Z_{ii}(s)$ or $Y_{ii}(s)$ of the matrices:

– impedances $Z_{ii}(s)$ and admittances $Y_{ii}(s)$ are odd functions of the variable s . This directly follows from the fact that the active power consumption is zero and thus $\text{Re}[Z_{ii}(s)] |I|^2 = 0$ for example, in other words $\text{Re}[Z_{ii}(s)] = 0$. In sinusoidal regime, if the real part is zero, it remains $Z_{ii}(j\omega) = jX_{ii}(\omega)$ where $X_{ii}(\omega)$ is the reactance (real number). Thus,

$Z_{ii}(-j\omega) = -j X_{ii}(\omega) = -Z_{ii}(j\omega)$; however, since this relation is an algebraic relation independent of the nature of the variable, purely imaginary or complex, we also get $Z_{ii}(-s) = -Z_{ii}(s)$. $Z_{ii}(-s)$ is called the Hurwitzian conjugate of $Z_{ii}(s)$;

– since these are rational fractions, they are formed by the ratio of two polynomials, one only comprising odd-degree terms and the other only even-degree terms: $Z_{ii}(s)$ or $Y_{ii}(s) = \frac{sV(s^2)}{W(s^2)}$. This comes from the fact that they

are obtained by sums or ratios of terms either proportional to s or to s^{-1} . However, the degrees of the numerator and the denominator differ only by a single unit because the polynomial part of the fraction can only be of degree 1 or -1 , corresponding to an impedance Js , an admittance Cs or their reciprocals; the zero degree is forbidden due to the lack of resistance and the other degrees do not match any feasible passive elements admittance or impedance;

– poles and zeros are alternated on the imaginary axis, and a pole may exist at the origin and/or one at infinity. In fact, according to the foregoing, by means of partial fraction expansion, we get:

$Z_{ii}(s)$ or $Y_{ii}(s) = \frac{A_0}{s} + \frac{A_1 s}{s^2 + \omega_1^2} + \frac{A_2 s}{s^2 + \omega_2^2} + \dots + A_\infty s$, where the coefficients can

only be positive (because they are proportional to products or quotients of positive capacitances or inductances and squared angular frequencies, as seen here below) or equal to zero, particularly the first or the last. In harmonic regime, this corresponds to a reactance or a susceptance (the imaginary part of the admittance):

$$X_{ii}(\omega) \text{ or } B_{ii}(\omega) = -\frac{A_0}{\omega} - \frac{A_1 \omega}{\omega^2 - \omega_1^2} - \frac{A_2 \omega}{\omega^2 - \omega_2^2} - \dots + A_\infty \omega$$

whose derivative $\frac{dX_{ii}(\omega)}{d\omega}$ or $\frac{dB_{ii}(\omega)}{d\omega} = \frac{A_0}{\omega^2} + A_1 \frac{\omega^2 + \omega_1^2}{(\omega^2 - \omega_1^2)^2} + A_2 \frac{\omega^2 + \omega_2^2}{(\omega^2 - \omega_2^2)^2} + \dots + A_\infty$

is always positive. However, when $\omega = \omega_1$, $X_{ii}(\omega)$ brutally shifts from $+\infty$ to $-\infty$ to again reach a value that tends to $+\infty$ at the next pole that will be called ω_2 . Therefore, since reactance is always increasing, it necessarily crosses zero between both poles and so on.

These properties can be used to synthesize a dipole impedance $Z_{ii}(s)$ or admittance $Y_{ii}(s)$ from their expression using two different methods. Foster's synthesis is simply obtained by decomposing the rational fraction over the reals into fractions with linear and quadratic denominators, whereas Caue's synthesis is obtained by decomposing the rational fraction into a continuous fraction through successive Euclidean divisions.

– series Foster's synthesis for $Z_{ii}(s) = \frac{A_0}{s} + \frac{A_1 p}{s^2 + \omega_1^2} + \frac{A_2 s}{s^2 + \omega_2^2} + \dots + Ls$;

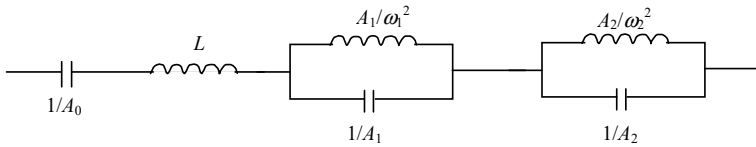


Figure 2.7. Series Foster's synthesis

– parallel Foster's synthesis for $Y_{ii}(s) = \frac{B_0}{s} + \frac{B_1 s}{s^2 + \omega_1^2} + \frac{B_2 s}{s^2 + \omega_2^2} + \dots + Cs$;

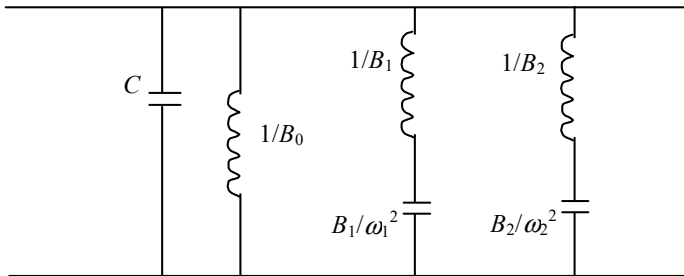


Figure 2.8. Parallel Foster's synthesis

– Caue's synthesis: If in the expression $Z_{ii}(s) = \frac{A_0}{s} + \frac{A_1 s}{s^2 + \omega_1^2} + \frac{A_2 s}{s^2 + \omega_2^2} + \dots + L_1 s$, $L_1 \neq 0$, then $Z_{ii}(s) = L_1 s + Z_2(s)$ can be rewritten, which amounts to placing inductance L_1 in series with a dipole of impedance $Z_2(s)$. Consequently, after transformation into a single fraction, the degree of the numerator of $Z_2(s)$ is a unit less than that of its denominator.

By inverting, it is thus possible to extract a polynomial part corresponding to the admittance of a capacitance in parallel with the admittance $Y_2(s) = 1/Z_2(s) = C_2s + Y_3(s)$, by means of Euclidean division of polynomials and so forth. A “ladder” circuit is then obtained, whose elements are alternatively a branch in series and then a branch connected to the reference potential. These elements are the following, by limiting associations to two elements at most (L and C):

Element(s)	Impedance	Admittance
Inductance L	Ls	$1 / Ls$
Capacitance C	$1 / Cs$	Cs
L and C in parallel	$\frac{Ls}{1+LCs^2}$	$\frac{1+LCs^2}{Ls}$
L and C in series	$\frac{1+LCs^2}{Cs}$	$\frac{Cs}{1+LCs^2}$

Example: by simplifying to the same denominator $Z_{ii}(s) = \frac{A_0}{s} + \frac{A_1s}{s^2 + \omega_1^2} + \frac{A_2s}{s^2 + \omega_2^2} + L_1s$ would give the quotient of a sixth-degree polynomial in the numerator and a fifth-degree polynomial in the denominator.

We can write $Z_{ii}(s) = \frac{A_0}{s} + \frac{A_1s}{s^2 + \omega_1^2} + \frac{A_2s}{s^2 + \omega_2^2} + L_1s = L_1s + Z_2(s)$, where

$$Z_2(s) = \frac{A_0}{s} + \frac{A_1s}{s^2 + \omega_1^2} + \frac{A_2s}{s^2 + \omega_2^2} \quad \text{corresponding to} \quad Y_2(s) = \frac{1}{Z_2(s)} = \frac{s^5 + (\omega_1^2 + \omega_2^2)s^3 + \omega_1^2 \omega_2^2 s}{(A_0 + A_1 + A_2)s^4 + [(A_0 + A_2)\omega_2^2 + (A_0 + A_1)\omega_1^2]s^2 + A_0\omega_1^2 \omega_2^2}$$

which is rewritten as: $Y_2(s) = \frac{1}{Z_2(s)} = \frac{s^5 + (\omega_1^2 + \omega_2^2)s^3 + \omega_1^2 \omega_2^2 s}{\frac{1}{C_2}s^4 + \frac{\omega_3^2}{C_3}s^2 + \frac{1}{C_0}\omega_1^2 \omega_2^2}$ to simplify the notation.

The Euclidean division gives a polynomial part equal to C_2s and $Y_2(s) = C_2s + Y_3(s)$ where:

$$Y_3(s) = \frac{1}{Z_3(s)} = \frac{\left[(\omega_1^2 + \omega_2^2) - \frac{C_2}{C_3} \omega_3^2 \right] s^3 + \omega_1^2 \omega_2^2 \left(1 - \frac{C_2}{C_0} \right) s}{\frac{1}{C_2} s^4 + \frac{\omega_3^2}{C_3} s^2 + \frac{1}{C_0} \omega_1^2 \omega_2^2}$$

The Euclidean division of $Z_3(s)$ gives a polynomial part equal to $\frac{s}{C_2 \left[(\omega_1^2 + \omega_2^2) - \frac{C_2}{C_3} \omega_3^2 \right]}$ and it is deduced that $Z_3(s) = L_3s + Z_4(s)$ where

$$L_3 = \frac{1}{C_2 \left[(\omega_1^2 + \omega_2^2) - \frac{C_2}{C_3} \omega_3^2 \right]} \text{ and where } Y_4(s) = \frac{1}{Z_4(s)} \text{ is an admittance of the}$$

form $\frac{C_4s^3 + C_4\omega_4^2s}{s^2 + \omega_5^2}$ that yields by way of Euclidean division a polynomial

part C_4s added to the quotient of the remainder by the divisor $\frac{C_4(\omega_4^2 - \omega_5^2)s}{s^2 + \omega_5^2}$,

which following the previous table can be associated with the admittance of a capacitance $C_6 = C_4 \left(\frac{\omega_4^2}{\omega_5^2} - 1 \right)$ in series with an inductance

$$L_5 = \frac{1}{C_4(\omega_4^2 - \omega_5^2)}.$$

The corresponding circuit is therefore obtained by combining the following elements, where the order of the last two is arbitrary (C_6 and L_5).

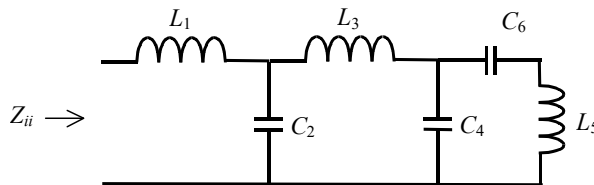


Figure 2.9. Ladder network obtained through Cauer's synthesis, the order of the last two elements L_5 and C_6 being arbitrary

It corresponds to the impedance that is written in the form of a continued fraction:

$$Z_{ii}(s) = L_1 s + \frac{1}{C_2 s + \frac{1}{L_3 s + \frac{1}{C_4 s + \frac{1}{L_5 s + \frac{1}{C_6 s}}}}}$$

There are thus many possible circuits corresponding to a same expression of $Z_{ii}(s)$ according to the type of synthesis that is adopted. It should be noted that Foster's syntheses lead to associations in series or in parallel in which the order of the elements is free, which does not indicate the actual connection for the opposite port in the case of a quadripole, unlike Cauer's synthesis that imposes the order of the elements except for the last two.

Several types of synthesis can also be combined in a decomposition because it may prove necessary to impose a fixed succession of elements according to a ladder structure, in particular for the implementation of band-pass or band-stop filters in which the alternation of capacitances and inductances cannot always be repeated following the same order anywhere in the circuit. In this case, a solution is to perform a Cauer synthesis of $Z_{ii}(s)$ to extract the first part of the elements, and then for the second part of the elements to shift to a Foster synthesis, in series or in parallel, but in which only the extraction of the single term is addressed, having a pole at the origin, after that of the term having a pole at infinity (in other words, the polynomial part). This is possible by factoring the first-degree term in the denominator of the fraction being considered assuming that its degree is odd. Recalling the previous example but by stopping the Cauer synthesis at the element L_3 , we can rewrite:

$$Z_{ii}(s) = L_1 s + \frac{1}{C_2 s + \frac{1}{L_3 s + Z_4(s)}}, \text{ where } Z_4(s) = \frac{1 + L_5 C_6 s^2}{(C_4 + C_6)s + L_5 C_4 C_6 s^3}$$

By factorizing the first term of the denominator and by decomposing it into simple fractions, we get:

$$Z_4(s) = \frac{1}{(C_4 + C_6)s} \frac{1 + L_5 C_6 s^2}{1 + L_5 \frac{C_4 C_6}{C_4 + C_6} s^2} = \frac{1}{(C_4 + C_6)s} + \frac{L_8 s}{1 + L_8 C_9 s^2},$$

where $L_8 = L_5 \frac{C_6^2}{(C_4 + C_6)^2}$, and $C_9 = \frac{(C_4 + C_6)C_4}{C_6}$.

In addition, establishing $C_7 = C_4 + C_6$ yields to an overall impedance:

$$Z_{ii}(s) = L_1 s + \frac{1}{C_2 s + \frac{1}{L_3 s + \frac{1}{C_7 s + \frac{1}{C_9 s + \frac{1}{L_8 s}}}}},$$

which is represented by the following circuit, where the alternation of the last three elements is reversed with regard to the first three, which can be useful when synthesizing a band-pass filter.

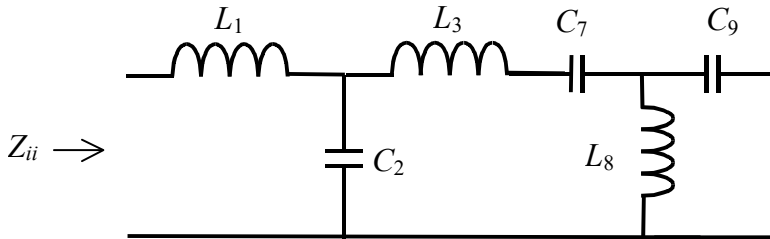


Figure 2.10. Ladder network obtained through Cauer synthesis up to L_3 , then Foster synthesis in series for the element C_7 and finally using Cauer synthesis for the last two

This method can be considered a mixed synthesis because it makes use of both the continued fraction expansion (Cauer's synthesis) and extraction of elements by partial fraction decomposition (Foster's synthesis) restricted to the term exhibiting a pole at the origin.

2.1.6. Scattering matrix (or s-matrix) and transfer matrix

2.1.6.1. General case: incident and reflected waves

This type of representation of quadripoles is useful when it is desirable to study power transfers operated by the quadripole and filtering is one such case. Nonetheless, ideal quadripoles comprise elements such as ideal short circuit, open circuit, perfect transformer ($V_2 = nV_1$; $I_1 = -nI_2$) or gyrator ($V_1 = RI_2$; $V_2 = -RI_1$). Then, some matrices of quadripoles of type I, II, III or IV or transfer matrices cannot be written because shifting from one representation to another always involves a ratio with the determinant or a parameter in the denominator. If one of them is zero, the matrix inversion is impossible.

It is also still possible to write $\mathbf{AV} = \mathbf{BI}$ where \mathbf{A} and \mathbf{B} are 2×2 matrix, with $\mathbf{V} = \begin{bmatrix} V_1 \\ V_2 \end{bmatrix}$ and $\mathbf{I} = \begin{bmatrix} I_1 \\ I_2 \end{bmatrix}$.

For instance, if we have the impedance matrix (type I), matrix \mathbf{A} is simply the unit matrix and matrix \mathbf{B} is the impedance matrix:

$$\begin{bmatrix} 1 & 0 \\ 0 & 1 \end{bmatrix} \begin{bmatrix} V_1 \\ V_2 \end{bmatrix} = \begin{bmatrix} Z_{11} & Z_{12} \\ Z_{21} & Z_{22} \end{bmatrix} \begin{bmatrix} I_1 \\ I_2 \end{bmatrix}. \text{ With the admittance matrix (type IV), we have: } \begin{bmatrix} Y_{11} & Y_{12} \\ Y_{21} & Y_{22} \end{bmatrix} \begin{bmatrix} V_1 \\ V_2 \end{bmatrix} = \begin{bmatrix} 1 & 0 \\ 0 & 1 \end{bmatrix} \begin{bmatrix} I_1 \\ I_2 \end{bmatrix}.$$

And any other matrix equality obtained by multiplying on the left the two members of one of the above expressions also satisfies the general relation $\mathbf{AV} = \mathbf{BI}$.

However, it can happen that \mathbf{A}^{-1} or \mathbf{B}^{-1} may not be computable (as an exercise, write these matrices for the ideal gyrator and the ideal transformer, and show in which case it is possible to calculate or not $\mathbf{V} = \mathbf{A}^{-1}\mathbf{BI}$ and $\mathbf{I} = \mathbf{B}^{-1}\mathbf{AV}$).

This type of problem can be overcome by using s -parameters, which will establish links between new quantities, called incident and reflected waves, themselves in direct relation with the power transfers performed by the quadripole. Consider the case of a termination impedance (load resistance or internal resistance of a generator) equal to R , assumed to be a normalization factor only, and define $\mathbf{v} = \mathbf{V} R^{-1/2}$; $\mathbf{i} = \mathbf{I} R^{1/2}$; $\mathbf{a} = \mathbf{A} R^{1/2}$; $\mathbf{b} = \mathbf{B} R^{-1/2}$ where \mathbf{v} and \mathbf{i} have the dimension of the square root of a power while \mathbf{a} and \mathbf{b} are

dimensionless, which gives place to $\mathbf{a}\mathbf{v} = \mathbf{b}\mathbf{i}$. Define the incident $\mathbf{\alpha} = \mathbf{v} + \mathbf{i}$ and reflected waves $\mathbf{\beta} = \mathbf{v} - \mathbf{i}$, where $\mathbf{\alpha} = \begin{bmatrix} \alpha_1 \\ \alpha_2 \end{bmatrix}$ and $\mathbf{\beta} = \begin{bmatrix} \beta_1 \\ \beta_2 \end{bmatrix}$. In that case: $2\mathbf{v} = \mathbf{\alpha} + \mathbf{\beta}$ and $2\mathbf{i} = \mathbf{\alpha} - \mathbf{\beta}$; from which: $2\mathbf{a}\mathbf{v} = \mathbf{a}(\mathbf{\alpha} + \mathbf{\beta}) = 2\mathbf{b}\mathbf{i} = \mathbf{b}(\mathbf{\alpha} - \mathbf{\beta})$.

We deduce: $(\mathbf{a} + \mathbf{b})\mathbf{\beta} = (\mathbf{b} - \mathbf{a})\mathbf{\alpha}$.

It is shown that the inverse matrix $(\mathbf{a} + \mathbf{b})^{-1}$ exists in all cases (unlike \mathbf{a}^{-1} or \mathbf{b}^{-1} as seen in previous examples), which allows us to write:

$$\mathbf{\beta} = \mathbf{s}\mathbf{\alpha} \text{ where } \mathbf{s} = (\mathbf{b} + \mathbf{a})^{-1}(\mathbf{b} - \mathbf{a})$$

Incident and reflected powers are then, respectively, computed based on the square moduli of α_1, α_2 , on the one hand, and of β_1, β_2 , on the other hand; s_{12}, s_{21} are the transmission coefficients and s_{11}, s_{22} the reflection coefficients.



Figure 2.11. Representations of a quadripole, including currents, voltages and complex parameters on the left and using incident and reflected waves, and s -parameters on the right

However in reality, what represents these incident and reflected powers?

To help clarify this issue, consider, for example, the case of the input of the quadripole assumed to be connected to a generator with internal resistance R . The active power P_1 absorbed by port no. 1 can be calculated based on $\text{Re}[v_1 \bar{i}_1]$ or better with $\frac{1}{2}(v_1 \bar{i}_1 + i_1 \bar{v}_1)$, where we have set $v_1 = V_1 R^{-1/2}$ and $i_1 = I_1 R^{1/2}$. On the other hand, the calculation of the square moduli of $\alpha_1 = v_1 + i_1$ and of $\beta_1 = v_1 - i_1$ gives:

$$|\alpha_1|^2 = (v_1 + i_1)(\bar{v}_1 + \bar{i}_1) = |v_1|^2 + 2P_1 + |i_1|^2$$

$$|\beta_1|^2 = (v_1 - i_1)(\bar{v}_1 - \bar{i}_1) = |v_1|^2 - 2P_1 + |i_1|^2$$

In the particular case where the input impedance of the quadripole V_1/I_1 is resistive and equal to R , that is also $|v_1 / i_1|=1$, the generator provides the sum of the same two powers P_{10} both on input of the quadripole and in its internal resistance. As it will be seen in the following section, this case corresponds to the ideal power match, that is to the maximum power transferred from the generator to the load, which here is the input port of the quadripole. It is obvious that $P_{10} = |v_1|^2 = |i_1|^2$, from which it is finally deduced that:

$$\frac{1}{2}|\alpha_1|^2 = P_{10} + P_1 \text{ and } \frac{1}{2}|\beta_1|^2 = P_{10} - P_1$$

These so-called “incident” and “reflected” half-powers are thus fictional powers, which do not directly correspond to a power dissipated in one of the elements, generators or ports of the quadripole. It is more advantageous to compute the active power actually absorbed by port no.1 of the quadripole in the general case by the difference of the two previous equations:

$$P_1 = \frac{1}{4}(|\alpha_1|^2 - |\beta_1|^2).$$

Similarly, the power absorbed by port no. 2 would be obtained:

$$P_2 = \frac{1}{4}(|\alpha_2|^2 - |\beta_2|^2).$$

These directional powers absorbed by the two ports of the quadripole exactly reflect the diagram showing the incident and the reflected waves (Figure 2.11 on the right).

This description using s -parameters therefore makes it possible to address power transmission and matching problems, and also problems of filtering since filtering is nothing but power transmission depending on the frequency. Matrix¹ $\mathbf{s} = \begin{bmatrix} s_{11} & s_{12} \\ s_{21} & s_{22} \end{bmatrix}$ is either originating from documentation (case of high-frequency active components) or computable from the elements of impedance or admittance matrix (see section 2.1.7.2.) and again we obtain $s_{12} = s_{21}$ for reciprocal passive quadripoles. In addition, this description proves to be very well suited to scattered element systems in which concepts of propagation and termination impedance essentially govern them. This description does not restrict in any way the study to the

¹ The s matrix, written in bold font, and the four elements of the matrix comprising two figure subscripts, must not be confused with the complex variable s

case of termination resistances equal to R , because by applying the same transformation to equations $V_1 = E_g - Z_g I_1$ and $V_2 = -Z_u I_2$, representative of the relations appropriate to a generator with an open-circuit voltage E_g and with an internal impedance Z_g connected on the quadripole input, and to a load Z_u on output, we obtain: $(z_g - 1)\beta_1 = (z_g + 1)\alpha_1 - 2e_g$ and $(z_u - 1)\beta_2 = (z_u + 1)\alpha_2$, where we have established $e_g = \frac{E_g}{\sqrt{R}}$; $z_g = \frac{Z_g}{R}$; $z_u = \frac{Z_u}{R}$.

2.1.6.2. Case where the termination impedance equals the normalization resistance R and impedance matching for maximum power transfer

In the case where $Z_g = R$, we have $e_g = \alpha_1$ and the evaluation of powers can be achieved from $i_1 = \frac{1}{2}(\alpha_1 - \beta_1)$, by calculating the power delivered by the generator: $P_g = \frac{1}{2}(e_g \bar{i}_1 + i_1 e_g) = \frac{1}{4}(2|\alpha_1|^2 - \alpha_1 \bar{\beta}_1 - \alpha_1 \beta_1) = \frac{1}{2}(|\alpha_1|^2 - \text{Re}[\alpha_1 \bar{\beta}_1])$.

Moreover, the power dissipated in the resistance R of the generator is simply $|i_1|^2 = \frac{1}{4}(|\alpha_1|^2 + |\beta_1|^2 - 2\text{Re}[\alpha_1 \bar{\beta}_1])$. Therefore, we finally obtain once more the equality $P_g = |i_1|^2 + P_1 = \frac{1}{4}(|\alpha_1|^2 - 2\text{Re}[\alpha_1 \bar{\beta}_1] + |\beta_1|^2 + |\alpha_1|^2 - |\beta_1|^2) = \frac{1}{2}(|\alpha_1|^2 - \text{Re}[\alpha_1 \bar{\beta}_1])$.

Since $e_g = \alpha_1$ is fixed, the maximal power P_1 transferred in the quadripole is obtained when $\beta_1 = 0$ because the only way to maximize it is to cancel out the second term in the expression $P_1 = \frac{1}{4}(|\alpha_1|^2 - |\beta_1|^2)$.

If the input impedance is equal to Z_1 , we have: $z_1 = \frac{Z_1}{R} = \frac{v_1}{i_1}$. Therefore, we obtain:

$$z_1 i_1 = \frac{z_1}{2}(\alpha_1 - \beta_1) = v_1 = \frac{1}{2}(\alpha_1 + \beta_1)$$

We can thus look for the expression of the reflected wave according to the incident wave:

$$\beta_1 = \frac{z_1 - 1}{z_1 + 1} \alpha_1$$

Therefore, it can be concluded that matching is obtained when $Z_1 = R$ yielding $z_1 = 1$ and $\beta_1 = 0$, which is a reflected wave equal to zero.

On the output side, if $Z_u = R$, then $z_u = 1$ and $(z_u - 1)\beta_2 = (z_u + 1)\alpha_2$ is simplified into $\alpha_2 = 0$. The power reflected by the load is then zero, which indicates that the load dissipates all the power it receives.

2.1.6.3. Cascading quadripoles and chain matrix

When several quadripoles have to be connected in cascade or in chain, it is advantageous to define a system of parameters that enables incident and reflected waves to be obtained at both endpoints of the chain with a matrix product. The system is reorganized, starting from $\begin{bmatrix} \beta_1 \\ \beta_2 \end{bmatrix} = \begin{bmatrix} s_{11} & s_{12} \\ s_{21} & s_{22} \end{bmatrix} \begin{bmatrix} \alpha_1 \\ \alpha_2 \end{bmatrix}$ to obtain $\begin{bmatrix} \beta_1 \\ \alpha_1 \end{bmatrix} = \begin{bmatrix} c_{11} & c_{12} \\ c_{21} & c_{22} \end{bmatrix} \begin{bmatrix} \alpha_2 \\ \beta_2 \end{bmatrix}$, where c_{ij} are the elements of the transfer matrix c . The quantities related to a single port are grouped in the same matrix column as for a transfer matrix but with the difference that incident and reflected waves do not occupy the same row. This makes it possible to effectively obtain the identity of the waves at the ports of the two quadripoles connected in cascade and to perform the calculation of the matrix equivalent to the whole by a matrix product as sketched in Figure 2.12.

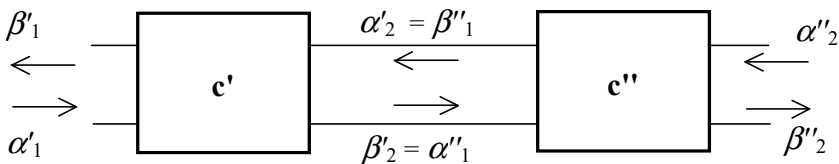


Figure 2.12. Chain of two quadripoles described by their chain parameters, deduced from s -parameters

Since $\alpha'_2 = \beta''_1$ and $\beta'_2 = \alpha''_1$, we infer that

$$\begin{bmatrix} \beta'_1 \\ \alpha'_1 \end{bmatrix} = \begin{bmatrix} c'_{11} & c'_{12} \\ c'_{21} & c'_{22} \end{bmatrix} \begin{bmatrix} c''_{11} & c''_{12} \\ c''_{21} & c''_{22} \end{bmatrix} \begin{bmatrix} \alpha''_2 \\ \beta''_2 \end{bmatrix}. \text{ By combining the two equations of a}$$

system based on the matrix s to obtain the two waves related to the same port according to the waves related to the other port, we obtain the coefficients c_{ij} according to the s_{ij} . The chain matrix is then defined by:

$$\begin{bmatrix} \beta_1 \\ \alpha_1 \end{bmatrix} = \frac{1}{s_{21}} \begin{bmatrix} -\det s & s_{11} \\ -s_{22} & 1 \end{bmatrix} \begin{bmatrix} \alpha_2 \\ \beta_2 \end{bmatrix} \text{ and conversely: } \begin{bmatrix} \alpha_2 \\ \beta_2 \end{bmatrix} = \frac{1}{s_{12}} \begin{bmatrix} 1 & -s_{11} \\ s_{22} & -\det s \end{bmatrix} \begin{bmatrix} \beta_1 \\ \alpha_1 \end{bmatrix}.$$

It is in this way possible to chain quadripoles whose elements are known, or, on the contrary, to decompose a quadripole into a simpler array of elements or extract an element from a quadripole having multiple elements. It should be noted that the determinant of the transfer matrix is equal to s_{12} and the c_{22} element is equal to $(s_{21})^{-1}$.

It will be possible to show as an exercise that in the special case of a quadripole comprising only one impedance in series between the high terminals of each port, with a normalized value z , or still of that including only one admittance in parallel with normalized value y connected between the conductors directly linking the homologous terminals of each port, the chain matrices can be, respectively, written as:

$$\begin{bmatrix} 1-z/2 & z/2 \\ -z/2 & 1+z/2 \end{bmatrix}$$

and $\begin{bmatrix} 1-y/2 & y/2 \\ -y/2 & 1+y/2 \end{bmatrix}$ by splitting into two equal parts the voltage drops or currents flowing on the side of each port, which are matrices whose determinants are equal to 1.

2.1.7. Powers in quadripoles and matching

2.1.7.1. Matching source and load: efficiency

We calculate the power delivered to a load (eventually the input admittance of another quadripole) by a generator (eventually the output circuit of a type II or type IV quadripole).

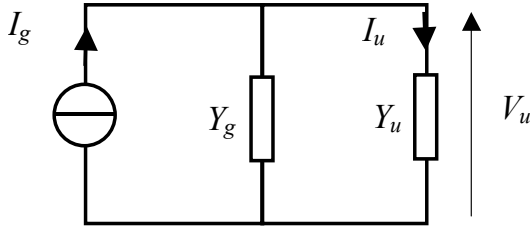


Figure 2.13. Generator with current source and internal admittance Y_g loaded by an admittance Y_u

We then have the equations: $V_u = \frac{I_g}{Y_g + Y_u}$ and $I_u = I_g \frac{Y_u}{Y_g + Y_u}$ from

which the power in Y_u is deduced: $P_u = |I_g|^2 \frac{\text{Re}[Y_u]}{|Y_g + Y_u|^2}$

The maximum of P_u is obtained when $|I_g|^2 / P_u$ is minimum:

$$\begin{aligned} \frac{|I_g|^2}{P_u} &= \frac{(\text{Re}[Y_g] + \text{Re}[Y_u])^2 + (\text{Im}[Y_g] + \text{Im}[Y_u])^2}{\text{Re}[Y_u]} \\ &= 4 \text{Re}[Y_g] + \frac{(\text{Re}[Y_g] - \text{Re}[Y_u])^2 + (\text{Im}[Y_g] + \text{Im}[Y_u])^2}{\text{Re}[Y_u]} \end{aligned}$$

namely when the second term is zero (because it can only be positive or zero), which implies that:

$$\text{Re}[Y_u] = \text{Re}[Y_g] \text{ and } \text{Im}[Y_u] = -\text{Im}[Y_g]$$

These are the power matching conditions. Therefore, we conclude as follows:

Impedance matching or in other words the maximum transfer of power from the generator or the quadripole to the load or termination is obtained when dipolar and termination impedances or admittances are complex conjugates of one another.

It should be noted that in this case: $P_{u \max} = \frac{|I_g|^2}{4 \operatorname{Re}[Y_g]} = \frac{1}{2} P_g$ since both conductances are equal and subject to the same voltage. They thus dissipate the same power, that is an efficiency of 50%, a situation that does not correspond to the maximum performance. As $P_g = |I_g|^2 \operatorname{Re}\left[\frac{1}{Y_g + Y_u}\right] = |I_g|^2 \frac{\operatorname{Re}[Y_g + Y_u]}{|Y_g + Y_u|^2}$, the efficiency $\eta = \frac{P_u}{P_g} = \frac{\operatorname{Re}[Y_u]}{\operatorname{Re}[Y_g] + \operatorname{Re}[Y_u]}$ tends to 1 only if $\operatorname{Re}[Y_g]$ tends toward zero (which avoids dissipating power in the generator conductance). This result can be extended to what follows:

Generally, maximum efficiency is obtained when the generator (voltage or current) supplying the load becomes an ideal source.

CONCLUSION.— *Matching by compensating the imaginary parts of admittances (or impedances) is beneficial for power transfer. We will either choose to make the real parts equal to maximize power transfer when the generator is imposed, or to find an ideal source to maximize efficiency.*

In the case of a quadripole, a full match requires matching both input and output, which can be illustrated in Figure 2.14.

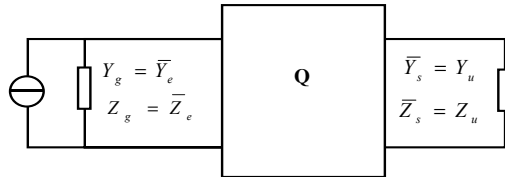


Figure 2.14. Quadripole matched to the input generator and the output load

2.1.7.2. Insertion of an active or passive quadripole: normalized impedances and significance of the parameter s_{21}

A gain of power is obtained by inserting an active quadripole between the generator and the load, with the Y parameters as an example.

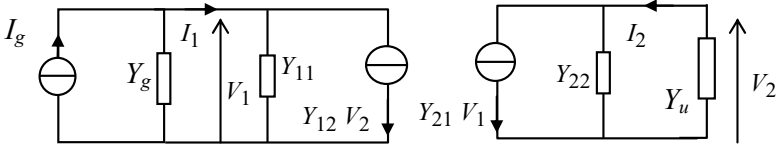


Figure 2.15. Active quadripole described by its parameters Y , inserted between a generator and a load

The useful power on input $P_1 = \text{Re} [I_1 \overline{V_1}]$ is now dissipated in the input admittance Y_e , which can be calculated according to the parameters after having determined the voltage gain.

The power gain is then the ratio of active powers dissipated in the load Y_u , that is $P_2 = \text{Re} [(-I_2) \overline{V_2}]$ and in Y_e that gives:

$$G_p = \frac{|Y_{21}|^2 \text{Re} [Y_u]}{\left(\text{Re} [Y_{11}] - \text{Re} \left[\frac{Y_{12} Y_{21}}{Y_{22} + Y_u} \right] \right) |Y_{22} + Y_u|^2}$$

According to the expression of the denominator, it can be seen that it is advantageous to cancel the imaginary part of $Y_{22} + Y_u$ (matching the output) to maximize this power gain, which moreover is proportional to $|Y_{21}|^2$. To obtain the overall power gain, namely the ratio of P_2 and P_g , the power supplied by the ideal source I_g , it can be shown as an exercise that it suffices to replace Y_{11} by $Y_{11} + Y_g$ in the previous expression.

On the one hand, the insertion gain G_i is the ratio of powers dissipated in the load when the active quadripole is inserted, and, on the other hand, when it is directly connected to the output of the generator:

$$G_i = \frac{|Y_{21}|^2 |Y_g + Y_{ch}|^2}{\left| (Y_{22} + Y_{ch})(Y_g + Y_{11}) - Y_{12} Y_{21} \right|^2}$$

In order to minimize the denominator it can be seen that the input has to be matched: $\text{Re}[Y_g] = \text{Re}[Y_{11}]$; $\text{Im}[Y_g] = -\text{Im}[Y_{11}]$ in addition to matching the output, and also the unilateralization (or neutrodynation), that is $Y_{12} = 0$ or even the lack of feedback from the output onto the input, which is also a condition useful for the stability as will be seen further on.

For reference, two stability criteria can be given, one intrinsic to the quadripole, the other taking into account the load and the source, because they are used in certain documents giving the characteristics of transistors operating at high frequency:

Linville criterion: for $\frac{|Y_{12}Y_{21}|}{2\text{Re}[Y_{11}]\text{Re}[Y_{22}] - \text{Re}[Y_{12}Y_{21}]} < 1$ the quadripole is stable.

Stern criterion: for $\frac{2\text{Re}[Y_{11} + Y_g]\text{Re}[Y_{22} + Y_u]}{|Y_{12}Y_{21}| + \text{Re}[Y_{12}Y_{21}]} > 1$ the quadripole is stable.

The issue of stability will be addressed in greater depth with s -parameters in the following.

Power and power gains measures use as units: decibels (dB) defined by $10 \log G_p$, $10 \log G_i$ for gains and dBW or dBm , respectively, defined by $10 \log P/1W$ or $10 \log P/1mW$ for absolute powers.

Obviously, the s -parameters can be used of course to address in a more general manner these matching issues for maximum power transfer in a quadripole inserted between a source having an internal impedance and a load. To this end, normalized parameters can be defined (dimensionless) initially assuming that this internal impedance and this load are purely resistive, but different: for example, a type I quadripole (Z parameters) inserted between a voltage generator E_g and with an internal resistance R_1 and a load R_2 will be studied (see Figure 2.16).

Second, it will be possible to modify R_1 and R_2 terminations by replacing them with any impedance Z_1 and Z_2 as it will be seen in the following section, the resistors R_1 and R_2 then being used only for the normalization of all the elements including Z_1 and Z_2 .

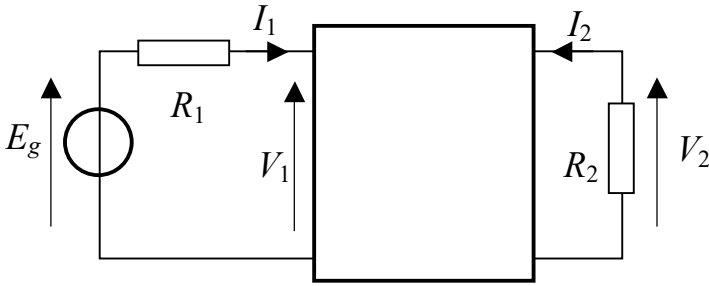


Figure 2.16. Quadripole inserted between a generator and a load for the description by the s -parameters

Starting from $\begin{cases} V_1 = Z_{11}I_1 + Z_{12}I_2 \\ V_2 = Z_{21}I_1 + Z_{22}I_2 \end{cases}$, by multiplying the first equation by $\frac{1}{\sqrt{R_1}}$ and the second equation by $\frac{1}{\sqrt{R_2}}$, we obtain:

$$\begin{cases} \frac{V_1}{\sqrt{R_1}} = \frac{Z_{11}}{R_1} I_1 \sqrt{R_1} + \frac{Z_{12}}{\sqrt{R_1 R_2}} I_2 \sqrt{R_2} \\ \frac{V_2}{\sqrt{R_2}} = \frac{Z_{21}}{\sqrt{R_1 R_2}} I_1 \sqrt{R_1} + \frac{Z_{22}}{R_2} I_2 \sqrt{R_2} \end{cases}.$$

Reduced (or normalized) parameters are defined by establishing:

$$z_{11} = \frac{Z_{11}}{R_1} \quad ; \quad z_{12} = \frac{Z_{12}}{\sqrt{R_1 R_2}} \quad ; \quad z_{21} = \frac{Z_{21}}{\sqrt{R_1 R_2}} \quad ; \quad z_{22} = \frac{Z_{22}}{R_2}$$

$$v_1 = \frac{V_1}{\sqrt{R_1}} \quad ; \quad i_1 = I_1 \sqrt{R_1} \quad ; \quad v_2 = \frac{V_2}{\sqrt{R_2}} \quad ; \quad i_2 = I_2 \sqrt{R_2} \quad ; \quad e_g = \frac{E_g}{\sqrt{R_1}}$$

The z_{ij} parameters (lowercase, but always depending on the complex variable s) are dimensionless.

We can then write: $\begin{bmatrix} 1 & 0 \\ 0 & 1 \end{bmatrix} \begin{bmatrix} v_1 \\ v_2 \end{bmatrix} = \begin{bmatrix} z_{11} & z_{12} \\ z_{21} & z_{22} \end{bmatrix} \begin{bmatrix} i_1 \\ i_2 \end{bmatrix}$ or still denoting by \mathbf{I}_2

(bold character) the unit 2×2 matrix and \mathbf{z} the matrix of parameters z_{ij} : $\mathbf{I}_2 \mathbf{v} = \mathbf{z} \mathbf{i}$.

As previously for the s -parameters: $\boldsymbol{\alpha} = \mathbf{v} + \mathbf{i}$ and $\boldsymbol{\beta} = \mathbf{v} - \mathbf{i}$, that is $\boldsymbol{\alpha} = \mathbf{z} \mathbf{i} + \mathbf{I}_2 \mathbf{i} = (\mathbf{z} + \mathbf{I}_2) \mathbf{i}$ and $\boldsymbol{\beta} = \mathbf{z} \mathbf{i} - \mathbf{I}_2 \mathbf{i} = (\mathbf{z} - \mathbf{I}_2) \mathbf{i}$. We are looking for the matrix \mathbf{s} such that $\boldsymbol{\beta} = \mathbf{s} \boldsymbol{\alpha}$:

$$(\mathbf{z} - \mathbf{I}_2) \mathbf{i} = \mathbf{s} (\mathbf{z} + \mathbf{I}_2) \mathbf{i}$$

and finally:

$$\mathbf{s} = (\mathbf{z} - \mathbf{I}_2) (\mathbf{z} + \mathbf{I}_2)^{-1}$$

NOTE.— Using the same method, it could be demonstrated that $\mathbf{s} = (\mathbf{I}_2 - \mathbf{y}) (\mathbf{I}_2 + \mathbf{y})^{-1}$ with the reduced admittance parameters and conversely that $\mathbf{z} = (\mathbf{I}_2 + \mathbf{s}) (\mathbf{I}_2 - \mathbf{s})^{-1}$ and $\mathbf{y} = (\mathbf{I}_2 - \mathbf{s}) (\mathbf{I}_2 + \mathbf{s})^{-1}$.

Thereby, we can determine the consequences of the insertion of the quadripole between the generator and the load with the matrix equation:

$$\boldsymbol{\beta} = \begin{bmatrix} v_1 - i_1 \\ v_2 - i_2 \end{bmatrix} = \begin{bmatrix} s_{11} & s_{12} \\ s_{21} & s_{22} \end{bmatrix} \begin{bmatrix} v_1 + i_1 \\ v_2 + i_2 \end{bmatrix} = \mathbf{s} \boldsymbol{\alpha}$$

if $V_2 = -R_2 I_2$, $v_2 = -i_2$ and accordingly $\alpha_2 = v_2 + i_2 = 0$, which indicates that there is no power reflected by the load, and $\beta_2 = v_2 - i_2 = 2 v_2$.

On the generator side, $V_1 = E_g - R_1 I_1$ that is $\alpha_1 = v_1 + i_1 = \frac{E_g}{\sqrt{R_1}} = e_g$ and

$\beta_1 = v_1 - i_1 = e_g - 2 i_1 = e_g - 2(e_g - v_1) = 2v_1 - e_g$; thus:

$$\begin{bmatrix} 2v_1 - e_g \\ 2v_2 \end{bmatrix} = \begin{bmatrix} s_{11} & s_{12} \\ s_{21} & s_{22} \end{bmatrix} \begin{bmatrix} e_g \\ 0 \end{bmatrix}$$

Hence, we deduce that $2 v_2 = s_{21} e_g$ and subsequently that $4 |v_2|^2 = |s_{21}|^2 |e_g|^2$, that is:

$$\frac{|V_2|^2}{R_2} = |s_{21}|^2 \frac{|E_g|^2}{4R_1}$$

$|s_{21}|^2$ is thus the ratio of the active power dissipated in the resistive load R_2 to the maximum power likely to be provided by the generator.

This power is actually supplied by the generator only if the input is matched, expressed in equality between R_1 and the real part of the input impedance of the quadripole. Nonetheless in any situation, it appears that s_{21} is a fundamental parameter of the active or passive quadripole, because it determines the power transfer and can therefore be used to size the transmittance of a filter.

2.1.7.3. Gains, dipole impedances and stability of a quadripole inserted between a generator and any load from the s -parameters

In order to determine the properties of the quadripole in the general case, the equations relating to the arbitrary terminations Z_g and Z_u are taken as defined in section 2.1.2 but by normalizing them by R_1 and R_2 as in the previous section:

$$V_1 = E_g - Z_g I_1, V_2 = -Z_u I_2, \text{ with } e_g = \frac{E_g}{\sqrt{R_1}} ; z_g = \frac{Z_g}{R_1} ; z_u = \frac{Z_u}{R_2} .$$

It follows that $(z_g - 1)\beta_1 = (z_g + 1)\alpha_1 - 2e_g$ and $(z_u - 1)\beta_2 = (z_u + 1)\alpha_2$. By analogy with the definitions given in section 2.1.2 for s -parameters, reflection coefficients r_g and r_u are then, respectively, defined onto the generator and the load:

$$r_g = \frac{z_g - 1}{z_g + 1} \text{ and } r_u = \frac{z_u - 1}{z_u + 1}$$

These coefficients are equal to zero when matching is achieved, namely for $Z_g = R_1$ and $Z_u = R_2$, and cannot exceed the unit modulus when z_g and z_u are located in the right half-plane of the complex plane, which is the case for

dissipative impedances, because $|z_g - 1| < |z_g + 1|$ and $|z_u - 1| < |z_u + 1|$, provided that R_1 and R_2 be indeed real and positive resistances.

The previous equations then become: $\alpha_1 = r_g \beta_1 + \frac{2e_g}{z_g + 1}$ and $\alpha_2 = r_u \beta_2$

Waves incident on both terminations are β_1 and β_2 while α_1 and α_2 act as waves reflected by these same terminations, as can be seen in Figure 2.17.

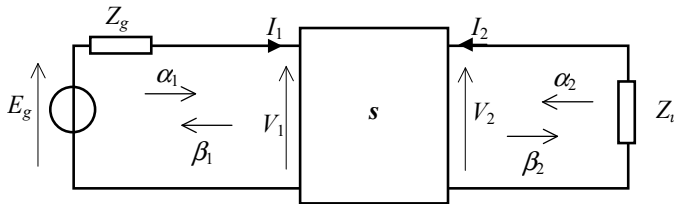


Figure 2.17. Quadripole described by its s -parameters with terminations of any kind

There is therefore a four-equation system that completely defines the four quantities α_1 , α_2 , β_1 and β_2 and is written by establishing $e'_g = \frac{2e_g}{z_g + 1}$:

$$\begin{cases} \alpha_1 - r_g \beta_1 = e'_g & (1) \\ s_{11} \alpha_1 + s_{12} \alpha_2 - \beta_1 = 0 & (2) \\ s_{21} \alpha_1 + s_{22} \alpha_2 - \beta_2 = 0 & (3) \\ \alpha_2 - r_u \beta_2 = 0 & (4) \end{cases}$$

The resolution of this system allows us to write the four waves that all have the same denominator $D_s = (1 - r_g s_{11})(s_{22} r_u - 1) + r_g r_u s_{12} s_{21}$:

$$\begin{cases} \alpha_1 = \frac{r_u s_{22} - 1}{D_s} e'_g & ; & \beta_1 = \frac{r_u (s_{11} s_{22} - s_{12} s_{21}) - s_{11}}{D_s} e'_g \\ \alpha_2 = \frac{-r_u s_{21}}{D_s} e'_g & ; & \beta_2 = \frac{-s_{21}}{D_s} e'_g \end{cases}$$

Starting from $\alpha_1 = v_1 + i_1$, $\beta_1 = v_1 - i_1$, $\alpha_2 = v_2 + i_2$, $\beta_2 = v_2 - i_2$, the v_1 , i_1 , v_2 , i_2 can easily be deduced with a half-sum or half-difference of α_1 , α_2 , β_1 and β_2 :

$$\left\{ \begin{array}{l} v_1 = \frac{(r_u s_{22} - 1)(s_{11} + 1) - r_u s_{12} s_{21}}{2D_s} e'_g \\ i_1 = \frac{(1 - r_u s_{22})(s_{11} - 1) + r_u s_{12} s_{21}}{2D_s} e'_g \\ v_2 = \frac{-s_{21}(1 + r_u)}{2D_s} e'_g \\ i_2 = \frac{s_{21}(1 - r_u)}{2D_s} e'_g \end{array} \right.$$

In addition, voltage, current gains and dipole impedance at port no. 1 can finally be obtained:

$$Z_e = \frac{V_1}{I_1} \Big|_{V_2 = -Z_u I_2} = R_1 \frac{v_1}{i_1} = R_1 \frac{(s_{11} + 1)(r_u s_{22} - 1) - r_u s_{12} s_{21}}{(s_{11} - 1)(1 - r_u s_{11}) + r_u s_{12} s_{21}}.$$

To obtain the dipole impedance at port no. 2, the generator must be placed on the same side and E_g has to be replaced by a short circuit, which amounts to canceling e'_g in equation (1) and defining a second member equal to e'_u in equation (4). After solving the system, we can then compute:

$$Z_s = \frac{V_2}{I_2} \Big|_{V_1 = -Z_g I_1} = R_2 \frac{v_2}{i_2} = R_2 \frac{(s_{22} + 1)(r_g s_{11} - 1) - r_g s_{12} s_{21}}{(s_{22} - 1)(1 - r_g s_{11}) + r_g s_{12} s_{21}}.$$

A further approach consists of defining the new reflexion coefficients that are modified by the terminations on the opposite port when matching occurs

on the port connected to the generator, that is: $\rho_1 = \frac{\beta_1}{e'_g} \Big|_{r_g=0} = s_{11} + \frac{s_{12} s_{21} r_u}{1 - s_{22} r_u}$

and $\rho_2 = \frac{\beta_2}{e'_u} \Big|_{r_u=0} = s_{22} + \frac{s_{12} s_{21} r_g}{1 - s_{11} r_g}$.

The power gain is obtained from powers P_1 and P_2 previously defined, that is:

$$G_p = \frac{-P_2}{P_1} = \frac{|\beta_2|^2 - |\alpha_2|^2}{|\alpha_1|^2 - |\beta_1|^2} = \frac{|s_{21}|^2 (1 - |r_u|^2)}{|s_{22}r_u - 1|^2 - |r_u(s_{11}s_{22} - s_{12}s_{21}) - s_{11}|^2}$$

or even $G_p = \frac{|s_{21}|^2 (1 - |r_u|^2)}{|1 - s_{22}r_u|^2} \frac{1}{1 - \left|s_{11} - \frac{r_u s_{12} s_{21}}{1 - s_{22} r_u}\right|^2}$ independent of r_g .

When it is desirable to determine the overall power gain G_g , taking into account the total power supplied by the generator, the ratio of ($-P_2$) with $P_g = (e_g \bar{i}_1 + \bar{e}_g i_1) / 2$, that is, $P_g = [e'_g (1 + z_g) \bar{i}_1 + \bar{e}'_g (1 + z_g) i_1] / 4$ has to be calculated. Hence, the gain G_g , depending on r_g :

$$G_g = \frac{-P_2}{P_g} = \frac{|s_{21}|^2 (1 - |r_u|^2)}{\operatorname{Re}\left\{(z_g + 1)\left[(1 - r_u s_{22})(s_{11} - 1) + r_u s_{12} s_{21}\right]\left[(1 - r_g s_{11})(s_{22} r_u - 1) + r_g r_u s_{12} s_{21}\right]\right\}}$$

If e'_g is zero, all electric quantities $\alpha_1, \beta_1, \alpha_2, \beta_2, v_1, i_1, v_2, i_2$ are equal to zero, unless the denominator D_s itself is zero, which corresponds to the oscillation condition that is then written as $(1 - r_g s_{11})(s_{22} r_u - 1) + r_g r_u s_{12} s_{21} = 0$.

This condition, which makes instability possible, can be obtained in several ways. The coefficient s_{12} that corresponds to the inverse transfer parameter determines the feedback of the output onto the input, as in all quadripoles. If it is equal to zero, $D_{s0} = (1 - r_g s_{11})(s_{22} r_u - 1)$ and the denominator D_s can in any case be rewritten as:

$$D_s = D_{s0} \left[1 + \frac{r_g r_u s_{12} s_{21}}{(1 - r_g s_{11})(s_{22} r_u - 1)} \right].$$

It is also possible to obtain D_{s0} when r_g or r_u is zero. If none of these parameters are equal to zero, the denominator D_s then takes the same form as that of the closed-loop transmittance of a single-input and single-output system, such as studied in Chapter 1, where $1 + AB$ appears, with A being the direct transmittance and B the feedback coefficient. To ensure stability, it

is necessary to avoid the Nyquist diagram of AB surrounding the point -1 in the complex plane. Therefore, the same rule will be applied here, that is to say that the path of $\frac{r_g r_u s_{12} s_{21}}{(1 - r_g s_{11})(s_{22} r_u - 1)}$ in the Nyquist diagram should not surround the point -1 in the complex plane.

It is remarkable that when there is matching on input and output, r_g and r_u are equal to zero as well as the previous quantity equivalent to AB , which yields $D_s = D_{s0} = -1$, independently of any other parameter and the frequency, if matching does not depend on it. It can thus be concluded that matching the input and the output ensures the unconditional stability of the quadripole. Nonetheless, since most often this matching is only rigorously performed at a single frequency, a comprehensive study should not be ignored.

Another stability criterion is based on the sign of P_1 or P_g , calculable from the previous expressions and from $\frac{1}{4}(|\alpha_1|^2 - |\beta_1|^2)$ for the first one, or from $(e_g \bar{i}_1 + e_g \bar{i}_1)/2$ for the second. As a matter of fact, if one of these powers is negative, there is excess power reflected by the quadripole input with respect to the incident power provided by the generator, which indicates that the quadripole is capable of delivering more power than it absorbs and hence becomes unstable.

Finally, from the previous discussion, one can deduce that the four conditions $|r_g| < 1$; $|r_u| < 1$; $|\rho_1| < 1$; $|\rho_2| < 1$ ensure the unconditional stability of the quadripole if they are simultaneously fulfilled at all frequencies. These conditions can be assessed with the help of plots of the quantities r_g , r_u , ρ_1 , ρ_2 (Smith charts, in polar coordinates), which have to be compared to the circle with unity radius. Notice that ρ_1 and ρ_2 depend on s -parameters.

2.1.8. Image-impedances and image-matching

Quadripoles often need to be assembled in cascade or in chain, by necessity as the passive filters, or to reflect the real situation of a system. Except in cases where internal sources are ideal and internal dipolar impedances are infinite or zero, the connections of a quadripole with external circuits generally cause alterations in the input and output impedances of the overall quadripole, as can be seen in the expressions of Z_e

and Z_s at the end of section 2.1.5.1, most often with a dependency with regard to the frequency. In other words, there is no decoupling or independence of the transfer functions of each quadripole and, as a result, a global transfer function cannot just be obtained from individual transfer functions. In order to overcome this drawback, we can try to satisfy the image-matching conditions at every port, by way of the equality of the dipolar impedances of the quadripole and terminations, as illustrated in Figure 2.18.

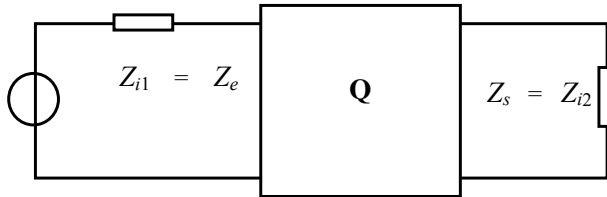


Figure 2.18. Quadripole in a situation of image-matching, where Z_e and Z_s are also, respectively, the input and output impedance of the quadripole

In fact, when symmetrical quadripoles are placed in cascade, the condition for effective matching cannot be satisfied, that is $Z_{i1} = \overline{Z_e}$ and $Z_{i2} = \overline{Z_s}$ with $Z_e = Z_s$ unless we also have $Z_e = \overline{Z_s}$, therefore only if the impedances are real. This is another reason to choose these image-matching conditions as they just have been defined, namely by imposing the two equalities illustrated in Figure 2.18.

A condition is met as soon as the other is also met, which is expressed by two simultaneous equalities for Z_e and Z_s : $Z_{i1} = \frac{Z_{11}Z_{i2} + \det Z}{Z_{i2} + Z_{22}}$ and $Z_{i2} = \frac{Z_{22}Z_{i1} + \det Z}{Z_{i1} + Z_{11}}$.

This system of two equations (nonlinear) defines the image impedances Z_{i1} and Z_{i2} and can be rewritten by expanding:

$$\begin{cases} Z_{i1}Z_{i2} + Z_{i1}Z_{22} = Z_{11}Z_{i2} + \det Z \\ Z_{i2}Z_{i1} + Z_{i2}Z_{11} = Z_{22}Z_{i1} + \det Z \end{cases}$$

By carrying out half the sum and half the difference of the two equations, we simply get:

$$\begin{cases} Z_{i1}Z_{i2} = \det Z \\ Z_{i2}Z_{11} = Z_{i1}Z_{22} \end{cases}$$

We can evaluate Z_{i1} and Z_{i2} separately by eliminating either one in these two equations and it is preferable to replace $(\det Z)/Z_{22}$ and $(\det Z)/Z_{11}$, respectively, by Y_{11} and Y_{22} , which are the admittance parameters of the quadripole (or type IV, see section 2.1.5.1) because Z_{i1} and Z_{i2} are then expressed only according to the diagonal impedances and admittances $Z_{11} = Z_{e0}$, $Z_{22} = Z_{s0}$, $Y_{11} = 1/Z_{esc}$, $Y_{22} = 1/Z_{ssc}$ of the quadripole. The following expressions can be deduced, which define the image impedances of the quadripole:

$$Z_{i1} = \sqrt{\frac{Z_{11}}{Y_{11}}} = \sqrt{Z_{e0}Z_{esc}} \quad \text{and} \quad Z_{i2} = \sqrt{\frac{Z_{22}}{Y_{22}}} = \sqrt{Z_{s0}Z_{ssc}}$$

With these expressions already satisfied for the iterative impedance of symmetric passive quadripoles, this notion is thus generalized to any kind of quadripole distinguishing an image impedance specific to each port. These impedances are not rational and therefore not achievable with passive elements, which however do not prevent them from existing as input or output impedances in a quadripole and thus the possibility that they be used as references. We have chosen here the positive determination for radicals but previous systems of equations can also be satisfied with the negative determination, which can prove useful in some cases as it will be seen with band-pass filters.

Image-matching conditions superimpose onto those of effective matching every time that Z_{i1} and Z_{i2} are real, since in this case the complex conjugation operation no longer has any effect, with nonetheless a dependency from Z_{i1} and Z_{i2} with respect to frequency.

Following the same method as in section 2.1.7.2, we can define the impedance parameters normalized by quadripole image impedances and then calculate the s -parameters:

$$z_{11} = \frac{Z_{11}}{Z_{i1}} \quad ; \quad z_{12} = \frac{Z_{12}}{\sqrt{Z_{i1}Z_{i2}}} \quad ; \quad z_{21} = \frac{Z_{21}}{\sqrt{Z_{i1}Z_{i2}}} \quad ; \quad z_{22} = \frac{Z_{22}}{Z_{i2}}$$

$$v_1 = \frac{V_1}{\sqrt{Z_{i1}}} \quad ; \quad i_1 = I_1 \sqrt{Z_{i1}} \quad ; \quad v_2 = \frac{V_2}{\sqrt{Z_{i2}}} \quad ; \quad i_2 = I_2 \sqrt{Z_{i2}} \quad ; \quad e_g = \frac{E_g}{\sqrt{Z_{i1}}}$$

We then have $\det z = \frac{\det Z}{Z_{i2}Z_{i1}} = 1$ and $z_{11} = z_{22}$ according to the previous

definition relations of image impedances and the general relation $\frac{Z_{eo}}{Z_{esc}} = \frac{Z_{so}}{Z_{ssc}}$

demonstrated in section 2.1.5.1 and valid regardless of the quadripole, passive or not, symmetrical or not.

Based on the matrix expression $\mathbf{s} = (\mathbf{z} - \mathbf{I}_2)(\mathbf{z} + \mathbf{I}_2)^{-1}$, we obtain:

$$\mathbf{s} = \begin{bmatrix} s_{11} & s_{12} \\ s_{21} & s_{22} \end{bmatrix} = \begin{bmatrix} 0 & \frac{z_{12}}{1+z_{11}} \\ \frac{z_{21}}{1+z_{11}} & 0 \end{bmatrix}$$

The diagonal elements s_{11} and s_{22} , which are the reflection coefficients, are therefore zero. We thus have image-matching in the sense where incident waves α_1 and α_2 no longer give place to reflected waves β_1 and β_2 , and there are transmitted waves only because of s_{12} and s_{21} are non-zero.

In such conditions, it proves helpful to determine the elements of the transfer matrix, according to relations $\mathbf{c} = \frac{1}{s_{21}} \begin{bmatrix} -\det \mathbf{s} & s_{11} \\ -s_{22} & 1 \end{bmatrix}$ from section 2.1.6

and $\det \mathbf{s} = -s_{12}s_{21}$. We obtain $\mathbf{c} = \begin{bmatrix} s_{12} & 0 \\ 0 & \frac{1}{s_{21}} \end{bmatrix}$, a diagonal matrix. It is therefore

possible to easily chain quadripoles if image-matching is carried out and to calculate the overall transmittance that directly results from the products of coefficients s_{12} and s_{21} of each quadripole. We thus recover the straightforwardness provided by the transmittances of systems with a single input quantity and single output quantity, which is the main interest of image-matching.

NOTE.— If image-matching is not performed, only s_{12} and s_{21} will have to be recalculated by taking effective terminations into account, s_{11} and s_{22} remaining equal to zero, provided that the normalization of impedance parameters and s -parameters has been achieved with the image impedances.

In the case of reciprocal passive quadripoles, z_{12} and z_{21} are equal and therefore s_{12} and s_{21} too. Then, we outline the image transmittance

$s_i = \frac{z_{21}}{1 + z_{11}} = \exp(-\Gamma)$ and we have $\det s = -s_i^2$. Hence the transfer matrix:

$$c_i = \begin{bmatrix} s_i & 0 \\ 0 & \frac{1}{s_i} \end{bmatrix} = \begin{bmatrix} \exp(-\Gamma) & 0 \\ 0 & \exp(\Gamma) \end{bmatrix},$$

where Γ is defined as the image attenuation complex logarithmic factor and we outline $\Gamma = \gamma + j\delta$, with γ = image attenuation (in Neper, with $1 \text{ Np} = 8.68 \text{ dB}$) and δ = image dephasing. This formalism and the image-matching assumption enable us to address matching and filtering problems, directly from the cascading of quadripoles, with deviations from effective transmittances that generally remain reasonable, and especially with mechanisms close to objectives, such as obtaining a filter template based on fixed criteria.

In that case: $s = \begin{bmatrix} 0 & s_i \\ s_i & 0 \end{bmatrix} = \begin{bmatrix} 0 & e^{-\Gamma} \\ e^{-\Gamma} & 0 \end{bmatrix}$ and according to

$z = (\mathbf{I}_2 + s)(\mathbf{I}_2 - s)^{-1}$ (section 2.1.7.2) we have

$$z = \begin{bmatrix} \coth \Gamma & 1/\sinh \Gamma \\ 1/\sinh \Gamma & \coth \Gamma \end{bmatrix} \text{ and}$$

$$Z = \begin{bmatrix} Z_{i1} \coth \Gamma & \sqrt{Z_{i1} Z_{i2}} / \sinh \Gamma \\ \sqrt{Z_{i1} Z_{i2}} / \sinh \Gamma & Z_{i2} \coth \Gamma \end{bmatrix}.$$

Image transmittance can be advantageously estimated from the diagonal impedances or admittances Z_{11} and Y_{11} or Z_{22} and Y_{22} , for passive quadripoles. In the foregoing, it can be seen that it is helpful to calculate

$\coth(\Gamma)$, then $\exp(\Gamma)$, from $s_i = \frac{z_{21}}{1+z_{11}} = \exp(-\Gamma) = \frac{Z_{i1}Z_{i2}}{\sqrt{Z_{i1}Z_{i2}}(Z_{i1}+Z_{i1})} =$
 $\sqrt{\frac{Z_{i1}}{Z_{i2}}} \frac{Z_{i2}}{Z_{i1}+Z_{i1}} = \frac{Z_{i2}}{\sqrt{\det Z} + \sqrt{Z_{i1}Z_{i2}}}$ then $\coth(\Gamma) = \frac{\exp(\Gamma) + \exp(-\Gamma)}{\exp(\Gamma) - \exp(-\Gamma)} =$
 $\frac{\sqrt{\det Z} + \sqrt{Z_{i1}Z_{i2}}}{Z_{i2}} + \frac{Z_{i2}}{\sqrt{\det Z} + \sqrt{Z_{i1}Z_{i2}}}$, which is simplified after a few
 $\frac{\sqrt{\det Z} + \sqrt{Z_{i1}Z_{i2}}}{Z_{i2}} - \frac{Z_{i2}}{\sqrt{\det Z} + \sqrt{Z_{i1}Z_{i2}}}$
 manipulations into $\coth(\Gamma) = \sqrt{Z_{i1}Y_{i1}} = \sqrt{Z_{i2}Y_{i2}}$.

We obtain:

$$\exp(2\Gamma) = \exp(2\gamma) \exp(2j\delta) = \frac{\coth(\Gamma) + 1}{\coth(\Gamma) - 1} = \frac{\sqrt{Z_{i1}Y_{i1}} + 1}{\sqrt{Z_{i1}Y_{i1}} - 1} = \frac{\sqrt{Z_{i2}Y_{i2}} + 1}{\sqrt{Z_{i2}Y_{i2}} - 1}$$

NOTE.— In AC regime, depending on whether Γ is purely imaginary or not, image attenuation γ is, respectively, zero or non-zero, the first case corresponding to an angular frequency ω in the bandwidth of the system, since there is no attenuation. Conversely, when $\coth(\Gamma)$ is real and positive (and therefore greater than 1), Γ is also in agreement with what is expected of a passive filter for attenuation. If on the other hand, $\coth(\Gamma)$ appear as being real and negative, especially when ω tends to 0 or infinity, which would imply amplification rather than attenuation, it is negative determination that should be used for radicals in order to restore real attenuation, only physically feasible for passive filters.

For non-dissipative passive (or lossless) filters, thus comprising inductors and capacitors only, each parameter Z is such that $Z = jX$ where X is a reactance, and each parameter Y is such that $Y = jB$ where B is a susceptance. If X and B have the same sign, image impedances are thus real according to the expressions previously established, and $\coth(\Gamma)$ is imaginary and equal to ju (u real). It can be deduced that $ju + 1$ and $ju - 1$ having the same modulus, $\exp(2\Gamma)$ has a modulus equal to 1, which implies that the image attenuation γ is zero, which is a characteristic of the bandwidth. If X and B have opposite signs, image impedances are instead imaginary and $\coth\Gamma$ is real with a positive determination as stated above; $\exp(2\Gamma)$ is then also real and greater than 1, yielding an image attenuation larger than 1, which is a characteristic feature of a stopband.

CONCLUSION.— *Important: when the frequency lies in the bandwidth of a non-dissipative passive filter, the image impedance is real and the image attenuation modulus is zero, whereas when the frequency lies in a stopband, the image impedance is imaginary and the image attenuation modulus is greater than 1.*

2.1.9. Representation of quadripoles by block diagrams

Another way of representing equations linking electrical quantities is based on block diagrams. This representation will make it possible to show transfer functions that are useful for the study of stability, for instance. To represent the equation $V = ZI$, we use the operator capable of switching from a current to a voltage, in other words, an impedance $I \longrightarrow Z \longrightarrow V$

or an admittance $V \longrightarrow Y \longrightarrow I$.

Example: Hybrid quadripole (type II)

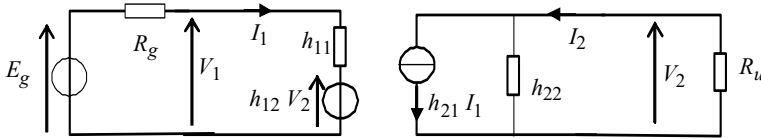


Figure 2.19. Quadripole with hybrid parameters (type II) between a generator and a load

$$\begin{cases} V_1 = h_{11}I_1 + h_{12}V_2 \\ I_2 = h_{21}I_1 + h_{22}V_2 \end{cases} ; I_1 = \frac{E_g - V_1}{R_g} \text{ and } V_2 = -R_u I_2 \text{ can be represented by}$$

Figure 2.20.

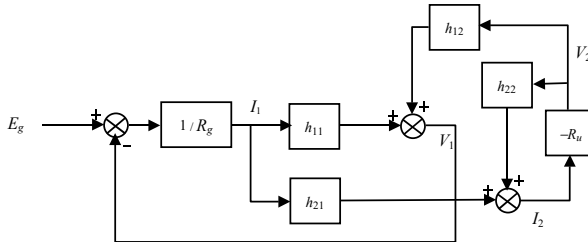
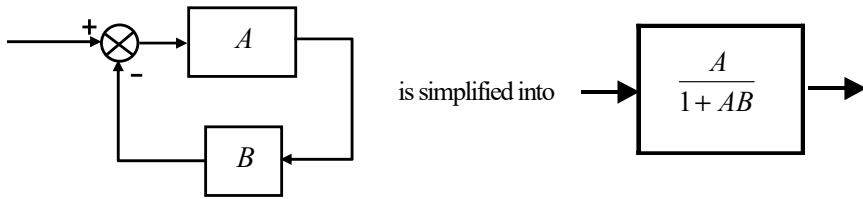


Figure 2.20. Block diagram representing the quadripole and termination elements

It should be recalled that:



NOTE.— If the comparator is an adder namely with two + signs, the transfer function becomes $\frac{A}{1-AB}$.

By way of graphic transformations (or elimination of variables in the equations), it is possible to derive the transfer function that can yield V_2 , for example.

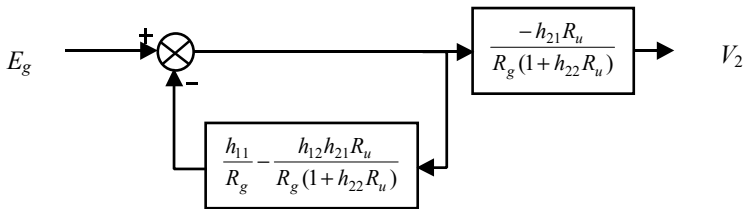


Figure 2.21. Block diagram giving V_2 from E_g for the quadripole and termination elements

The stability of the system is then analyzed with the methods set out in Chapter 1.

Another case where a synthesis between quadripole and block diagram is very useful is that of the “leapfrog” structure, which accounts for ladder networks of passive elements.

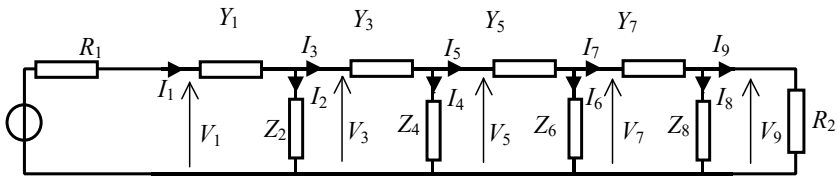


Figure 2.22. Ladder admittance and impedance network

We thus have recurrence equations $I_{2n-1} = (V_{2n-1} - V_{2n+1}) Y_{2n-1}$ and $(I_{2n-1} - I_{2n+1}) Z_{2n} = V_{2n+1}$ that can be translated into the following block diagram with a leapfrog structure.

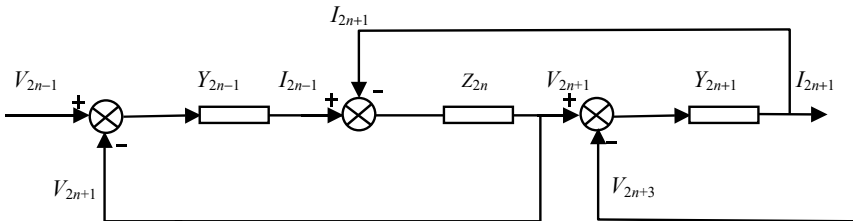


Figure 2.23. Block diagram of an unspecified portion of the ladder network of Figure 2.22

2.2. Analog filters

2.2.1. Definition and impulse response

A filter is a linear and stationary system (or invariant under time translation), stable, of transmittance $H(j\omega)$ or $H(s)$, whose forced response $Y(j\omega)$ or $Y(s)$ at an input $X(j\omega)$ or $X(s)$ is being studied, since the natural response is supposed to be extinct. Provided that we have ordinary products $Y(j\omega) = H(j\omega) X(j\omega)$ and $Y(s) = H(s) X(s)$, we have, according to the properties of the Fourier and Laplace transforms, a convolution product in the time domain, giving the output signal y as function of the input x :

$$y(t) = \int_{-\infty}^{\infty} h(t - \tau)x(\tau)d\tau = \int_{-\infty}^{\infty} h(\tau)x(t - \tau)d\tau .$$

The question is to understand what represents $h(t)$. In order to determine it, it can be assumed that $X(j\omega)$ or $X(s) = 1$. It then follows that $Y(j\omega) = Y_A(j\omega) = H(j\omega)$ and in this case, $x(t) = x_I(t)$ is given by the TF⁻¹ of 1, or $x_I(t) = \int_{-\infty}^{\infty} 1 \cdot \exp[j2\pi ft] df$, which we can guess by taking the limit of:

$$x_I(t) = \lim_{f_0 \rightarrow \infty} \int_{-f_0}^{f_0} \exp[j2\pi ft] df = \lim_{f_0 \rightarrow \infty} \left[2f_0 \frac{\sin(2\pi f_0 t)}{2\pi f_0 t} \right].$$

The function $\text{sinc}(u) = \frac{\sin(u)}{u}$ (sinc function, with here $u = 2\pi f_0 t$) is an impulse, which is maximal and equal to 1 at $t = 0$, an even function, having many secondary extrema decreasing in absolute value on each side of the origin with zeros for $t = k/f_0$ (k integer > 0 or < 0). Therefore, $x_I(t)$ is a pulse centered at the origin whose width tends toward zero and amplitude tends to infinity due to the prefactor $2f_0$ when $f_0 \rightarrow \infty$. It is considered as being analogous to a “Dirac pulse” $\delta(t)$ that has to be addressed using distributions (see Appendix). It can however already be concluded that $h(t)$ represents the impulse response of the system.

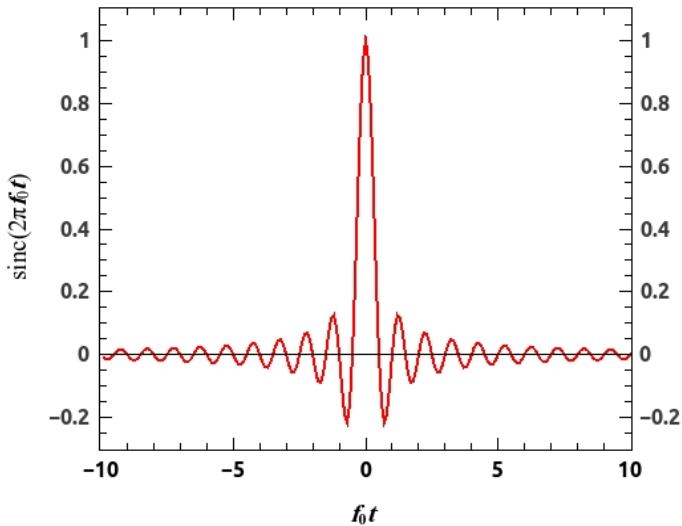


Figure 2.24. Sinc function

NOTE.— The output signal $y(t)$ of a filter is given by the convolution of its impulse (or impact) response $h(t)$ by the input signal $x(t)$.

Conversely, the transmittance or transfer function, obtained by taking the FT or LT of the convolution product defining $y(t)$, is the simple product of the transforms $Y(j\omega) X(j\omega)$ or $Y(s) X(s)$. In the presence of a Dirac pulse on input whose LT or FT is equal to 1, $Y(j\omega) = H(j\omega)$ or $Y(s) = H(s)$.

NOTE.— The transmittance or transfer function $H(j\omega)$ or $H(s)$ is the FT or LT of the impulse response $h(t)$.

There are many cases (passive high-pass and band-stop filters; some low-pass or band-pass filters) in which the transmittance $H(j\omega)$ does not cancel out when ω tends to infinity. This is the case, for example, for all rational transmittance that share the same degree in the numerator and denominator, as for high-pass filters.

This leads to a difficulty in the computation of the impulse response $h(t)$ by the FT⁻¹ $h(t) = \frac{1}{2\pi} \int_{-\infty}^{\infty} H(j\omega) \cdot \exp[j\omega t] d\omega$ because the convergence is not guaranteed at infinite frequencies. The computation can then be divided into two terms:

$$h(t) = \frac{1}{2\pi} \int_{-\infty}^{\infty} [H(j\omega) - H(\infty)] \cdot \exp[j\omega t] d\omega + H(\infty) \int_{-\infty}^{\infty} \exp[j2\pi f t] df .$$

The possibility of convergence of the first term derives from the cancellation of the integrand for ω tending to infinity, whereas similarly to the beginning of the section, the integral contained in the second term can be regarded as the Dirac impulse $\delta(t)$ at the origin. The impulse response $h(t)$ is therefore not always an ordinary, continuous and differentiable function, but often a generalized function comprising a Dirac distribution. If necessary, the first term can be subsequently isolated, which for its part is an ordinary, continuous and differentiable function by establishing:

$$h_{sd}(t) = \frac{1}{2\pi} \int_{-\infty}^{\infty} [H(j\omega) - H(\infty)] \cdot \exp[j\omega t] d\omega .$$

Nonetheless, another difficulty arises if the integrand has no obvious antiderivative (or primitive) analytic expression. Another approach is then

based on the treatment of the time responses in the interval $]-\infty +\infty[$ for the variable t , either based on those already known in the interval $]0 +\infty[$ or based on the differential equation of the system. This requires that distribution properties be applied (see Appendix), which can be summarized in four points: (1) the derivative of the unit step function $U(t)$ is the Dirac pulse $\delta(t)$ within the meaning of distributions and successive derived distributions are denoted by $\delta^{(1)}(t)$, $\delta^{(2)}(t)$, ... $\delta^{(n)}(t)$; (2) the derivation of a function $g(t)$ exhibiting a finite discontinuity Δg at abscissa t_0 is obtained by $g'(t) = g'_{sd}(t) + \Delta g \delta(t - t_0)$ where $g'_{sd}(t)$ represents the derivative of the function without discontinuity; (3) an equation including ordinary functions (continuous and differentiable) and distributions must verify two equalities, one for each type of expression; (4) the product of the variable s by the LT of a function that can have discontinuities and defined in the interval $]-\infty +\infty[$ corresponds to the LT of the derivative of this function within the meaning of distributions. This type of approach is applied here to obtain the impulse response of first- and second-order elementary low-pass filters and then to deduce that of band-pass and high-pass filters.

Type	$H(s)$	Impulse response $h(t)$
First-order low-pass	$\frac{\omega_1}{s + \omega_1}$	$\omega_1 U(t) \exp(-\omega_1 t)$
First-order high-pass	$\frac{s}{s + \omega_1}$	$\delta(t) - \omega_1 U(t) \exp(-\omega_1 t)$
Second-order low-pass ($\zeta < 1$)	$\frac{\omega_n^2}{s^2 + 2\zeta\omega_n s + \omega_n^2}$	$U(t) \frac{\omega_n \exp(-\zeta\omega_n t)}{\sqrt{1-\zeta^2}} \sin\left[\omega_n \sqrt{1-\zeta^2} t\right]$
Second-order band-pass ($\zeta < 1$)	$\frac{s\omega_n}{s^2 + 2\zeta\omega_n s + \omega_n^2}$	$U(t) \frac{\omega_n \exp(-\zeta\omega_n t)}{\sqrt{1-\zeta^2}} \cos\left[\omega_n \sqrt{1-\zeta^2} t + \varphi_0\right]$ with $\sin(\varphi_0) = \zeta$
Second-order high-pass ($\zeta < 1$)	$\frac{s^2}{s^2 + 2\zeta\omega_n s + \omega_n^2}$	$\delta(t) - U(t) \frac{\omega_n \exp(-\zeta\omega_n t)}{\sqrt{1-\zeta^2}} \sin\left[\omega_n \sqrt{1-\zeta^2} t + 2\varphi_0\right]$

In the above table, the impulse response of the low-pass filter transmittance $\frac{\omega_1}{s + \omega_1}$ is deduced from the solution of the differential

equation $\frac{1}{\omega_1} \frac{dh(t)}{dt} + h(t) = \delta(t)$, according to Chapter 1 and in the case of a

Dirac impulse at the system input. By applying the previous rules, the solution can be written as $h_1(t) = \omega_1 \mathbf{U}(t) \exp(-\omega_1 t)$. The verification that involves transcribing this solution into the differential equation shows that in the first member $\delta(t) \exp(-\omega_1 t)$ can be replaced by $\delta(t)$ since $\exp(-\omega_1 t)$ is equal to 1 for $t = 0$, which becomes balanced with the impulse $\delta(t)$ present in the second member. The impulse response of the high-pass filter can be

inferred from the derivation of the previous one since its transmittance is $\frac{s}{\omega_1}$

times that of the low-pass. Furthermore, it can be verified that the differential equation in which only its second member differs from the previous one where the input signal $\delta(t)$ is replaced by its derivative divided by ω_1 or $\delta^{(1)}(t)/\omega_1$ is satisfied because $\delta(t) \exp(-\omega_1 t)$ can be replaced by $\delta(t)$ once the derivation is performed. Concerning the second-order filters, we can similarly look for solutions of the differential equation whose first

member is $\frac{1}{\omega_n^2} \frac{d^2 h(t)}{dt^2} + \frac{2\zeta}{\omega_n} \frac{dh(t)}{dt} + h(t)$ and whose second member is $\delta(t)$,

$\frac{1}{\omega_n} \delta^{(1)}(t)$ or $\frac{1}{\omega_n^2} \delta^{(2)}(t)$, respectively, for the low-pass, band-pass, or high-

pass filter. It is however faster to notice that if a solution $h(t)$ has been already determined for an input $x(t)$, the derivation of the two members of the differential equation leads to the conclusion that $\frac{dh(t)}{dt}$ is a solution

when the second member is equal to $\frac{dx(t)}{dt}$. We can then proceed to these

operations based on the step response of the low-pass filter (see Chapter 1) modified by the factor $\mathbf{U}(t)$ in order for us to work with a function defined in the interval $]-\infty +\infty[$. The first derivation gives the impulse response of the low-pass filter and those of the high-pass and band-pass filters, also taking into account the presence of the factor ω_n or ω_n^2 in the numerator of the corresponding transmittances. It is possible to verify the validity of these solutions by means of rather tedious calculations. It can be noted that the Dirac impulse is present in the impulse response of high-pass filters whose

transmittance modulus tends to a constant beyond the cutoff frequency and up to infinitely large frequencies, which makes it possible to transmit the infinitely rapid variations of this impulse. Note also that its dimension is that of a circular frequency to ensure homogeneity.

2.2.2. Properties of real, causal and stable filters

2.2.2.1. Hermitian and Hurwitzian symmetries of transmittances

The impulse response $h(t)$ being real, $H(\bar{s}) = \overline{H(s)}$, even if $s = j\omega$, therefore: $H(-j\omega) = \overline{H(j\omega)} = \text{Re}[H(j\omega)] - j \text{Im}[H(j\omega)]$ or also: $\text{Re}[H(j\omega)] = \text{Re}[H(-j\omega)]$ and $\text{Im}[H(j\omega)] = -\text{Im}[H(-j\omega)]$.

In the frequency domain, the real part of the transmittance is even while its imaginary part is odd. The modulus of the transmittance is itself also even: $|H(j\omega)| = \sqrt{\text{Re}[H(j\omega)]^2 + \text{Im}[H(j\omega)]^2} = |H(-j\omega)|$, while its argument (or phase shift) is odd. These properties are consequences of the Hermitian symmetry.

In addition, if a stable system described by a differential equation with real and constant coefficients has, as transmittance, a rational fraction $H(s)$ of polynomials having only real or complex conjugated roots, $H(-s)$, called the Hurwitzian conjugate, also denoted by H_* , the poles and zeros of $H(-s)$ are the real or complex numbers opposite to the poles and zeros of $H(s)$ (symmetrical with respect to the origin in the complex plane). In fact, if changing $s \rightarrow -s$ in a polynomial $A_0 s^q (s - s_1)(s - s_2)(s - s_3) \dots$, we get $\pm A_0 s^q (s + s_1)(s + s_2)(s + s_3) \dots$.

2.2.2.2. Causality and Bayard–Bode relations

If the filter is causal, $h(t - \tau)$ is zero for $t - \tau < 0$ that is for $\tau > t$; the infinite upper bound can therefore be replaced by t in the first expression of the convolution product, or alternatively in the second expression of the convolution product, the lower bound can be replaced by 0 since $h(\tau)$ is zero for $\tau < 0$:

$$y(t) = \int_{-\infty}^t h(t - \tau)x(\tau)d\tau = \int_0^{\infty} h(\tau)x(t - \tau)d\tau.$$

Another very important consequence of *causality* is that there is identity between $h(t)$ and $h(t).\text{sgn}(t)$, where $\text{sgn}(t)$ represents the “sign” function equal to -1 for $t < 0$, zero for $t = 0$, and $+1$ for $t > 0$, since $h(t)$ must be zero for $t < 0$: $h(t) = h(t).\text{sgn}(t)$.

Hence, a convolution relation between the Fourier transforms (in Cauchy principal value, see Appendix) is inferred. However, in the case where $h(t)$ is a distribution comprising a Dirac impulse at the time origin, the product $h(t).\text{sgn}(t)$ is indeterminate at $t = 0$. It is then preferable to apply this property to the impulse response from which has been removed a possible Dirac impulse at the origin, and previously named $h_{sD}(t)$. By taking the real (subscript R) and imaginary (subscript I) parts of $\text{TF}\{h_{sD}(t)\} = \text{TF}\{h_{sD}(t).\text{sgn}(t)\}$, we obtain:

$$\begin{aligned} H(j\omega) - H(\infty) &= H_R(\omega) + jH_I(\omega) - H(\infty) \\ &= \int H(ju) \frac{1}{j\pi(\omega-u)} du = \int H_I(u) \frac{1}{\pi(\omega-u)} du - j \int H_R(u) \frac{1}{\pi(\omega-u)} du \end{aligned}$$

calculated from the convolution product of $\text{TF}\{h_{sD}(t)\}$ and $\text{TF}\{\text{sgn}(t)\}$ (see Appendix), yielding the relations between real and imaginary parts:

$$\begin{cases} H_R(\omega) - H(\infty) = \int \frac{H_I(u)}{\pi(\omega-u)} du \\ H_I(\omega) = - \int \frac{H_R(u)}{\pi(\omega-u)} du \end{cases}$$

because, on the one hand, $H(\infty)$ being the asymptotic constant value of $H(j\omega)$, we will verify later that the asymptotic argument and the imaginary part are zero for $\omega \rightarrow \infty$, and, on the other hand, the integrals above are zero when the numerator of the integrand is a constant K :

$$\int \frac{K}{u-\omega} du = K \lim_{u \rightarrow \infty} \left[\ln \left| \frac{u-\omega}{u+\omega} \right| \right] = 0.$$

These expressions, called Bayard–Bode relations, show that the real and imaginary parts of a causal transfer function are dependent on each other.

The real and imaginary parts are Hilbert transforms of one another.

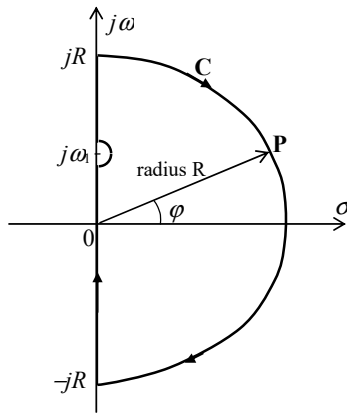


Figure 2.25. Integration contour for the application of the Cauchy theorem to the function $H(j\omega) - H(\infty)$ divided by $s - j\omega_1$

Nonetheless, these relations can be demonstrated from other assumptions, by using the Cauchy theorem and by integrating the transfer function $H(j\omega) - H(\infty)$ divided by $s - j\omega_1$ around the contour of the Figure 2.25 in the complex plane.

If the system is stable (no poles having positive real parts) and does not have zeros with positive real parts either (minimal phase-shifting system), the result of the integration in the complex plane is zero and we obtain exactly the same Bayard–Bode relations by replacing ω_1 with the common variable ω . It can even be accepted that the transfer function is at the limit of stability (oscillator), in other words it has a pair of poles on the imaginary axis that can be avoided in the same way as the pole $j\omega_1$ in the Figure 2.25.

Bayard–Bode relations are therefore also valid for a transfer function with neither poles nor zeros in the right half-plane of the complex plane.

In addition, taking into account the property that $h(t)$ has to be real, which implies that $H_R(\omega)$ is even and $H_I(\omega)$ is odd, we obtain Kramers–Kronig relations, also valid for any representative function $\mathcal{R}(j\omega)$ of the response of a physical system, linear and stationary, in the frequency domain (dielectric, magnetic susceptibilities, etc.):

$$\left\{ \begin{array}{l} H_R(\omega) - H(\infty) = \frac{2}{\pi} \int_0^\infty \frac{uH_I(u)}{\omega^2 - u^2} du \\ H_I(\omega) = -\frac{2\omega}{\pi} \int_0^\infty \frac{H_R(u)}{\omega^2 - u^2} du \end{array} \right. \quad \text{or even} \quad \left\{ \begin{array}{l} \mathcal{R}_{\mathcal{R}}(\omega) - \mathcal{R}(\infty) = \frac{2}{\pi} \int_0^\infty \frac{u\mathcal{R}_I(u)}{\omega^2 - u^2} du \\ \mathcal{R}_I(\omega) = -\frac{2\omega}{\pi} \int_0^\infty \frac{\mathcal{R}_R(u)}{\omega^2 - u^2} du \end{array} \right.$$

However, these relations are not the most helpful for electronics experts who are primarily interested in the modulus and the argument of the transmittance. It is therefore preferable to deduce the link between the modulus of $H(j\omega)$ and its argument $\varphi(\omega)$ that appears as the imaginary part of $\ln[H(j\omega)] = \ln[|H(j\omega)| \exp(j\varphi)] = \ln|H(j\omega)| + j\varphi(\omega)$. If $H(j\omega)$ has neither poles nor zeros in the right half-plane of the complex plane, $\ln[H(j\omega)]$ has no poles in the right half-plane, except potentially at infinity. As a result, the previous relations can be applied and we obtain by defining $\mathcal{R}(j\omega) = \ln[H(j\omega)]$:

$$\left\{ \begin{array}{l} \ln|H(\omega)| - \ln|H(\infty)| = \frac{2}{\pi} \int_0^\infty \frac{u\varphi(u)}{\omega^2 - u^2} du \\ \varphi(\omega) = -\frac{2\omega}{\pi} \int_0^\infty \frac{\ln|H(u)|}{\omega^2 - u^2} du \end{array} \right.$$

The modulus and the argument of a minimal phase-shift transmittance, namely that there are no zeros in the right half-plane of the complex plane, are thus dependent on one another. In particular, the second expression makes it possible to calculate the argument from the modulus. Therefore, this type of transmittance also corresponds to that of a causal system (as is the case for a rational transmittance obtained by the LT of the differential equation of the system), whereas conversely, it cannot be said that the transmittance of any causal system verifies the last two expressions.

2.2.2.3. Stable rational transfer functions

Stable rational transfer functions only have poles with negative real parts (or comprising Hurwitzian polynomials only) and are of the type:

$$H(p) = H_0 \left(\frac{p}{\omega_0} \right)^q \frac{\left(1 + \frac{p}{\omega_{11}} \right) \left(1 + \frac{p}{\omega_{12}} \right) \cdots \left(1 + 2\zeta_{21} \frac{p}{\omega_{21}} + \frac{p^2}{\omega_{21}^2} \right) \left(1 + 2\zeta_{22} \frac{p}{\omega_{22}} + \frac{p^2}{\omega_{22}^2} \right) \cdots}{\left(1 + \frac{p}{\omega_{31}} \right) \left(1 + \frac{p}{\omega_{32}} \right) \cdots \left(1 + 2\zeta_{41} \frac{p}{\omega_{41}} + \frac{p^2}{\omega_{41}^2} \right) \left(1 + 2\zeta_{42} \frac{p}{\omega_{42}} + \frac{p^2}{\omega_{42}^2} \right) \cdots}$$

assuming the angular frequency and damping coefficient parameters are all positive.

The degree of the denominator defines the n order of the filter and the degree of the numerator is at most equal to n . As mentioned in the previous section, two cases ought to be distinguished:

– minimal phase-shift transmittances $H_m(j\omega)$, which only have zeros with negative real parts. Only + signs appear in the numerator when the parameters are expressed from strictly positive quantities. In this case, the asymptotic values of the argument $\text{Arg}\{H_m(j\omega)\}$ are simply $k \frac{\pi}{2}$ if k is the exponent of $s = j\omega$ in the asymptotic expression of $H_m(j\omega)$;

– non-minimal phase-shift transmittances, comprising zeros with positive real part. It is then possible to split the overall transmittance $H(j\omega)$ into a minimal phase-shift transmittance $H_m(j\omega)$ and another transmittance $H_{ap}(j\omega)$ in which all factors $P(s)$ having zeros with positive real parts are grouped together, called an all-pass filter, because it only introduces an additional phase shift without attenuation (or amplification); then

$$H(s) = H_m(s) H_{ap}(s) = H_m(s) \frac{P(s)}{P(-s)}$$

where $P(s)$ is a Hurwitz polynomial, that is to say having roots with negative real parts only. This is especially the case in which the numerator of $H(s)$ shows minus signs when the parameters are expressed from strictly positive quantities, which is a sufficient but not necessary condition (there may be roots with positive real parts even with polynomial coefficients all positive). For non-minimal phase shift transmittances, Bayard–Bode relations do not apply.

All-pass filters can prove useful when it is desirable to correct the phase shift and the group propagation delay (see section 2.2.2.4) of a minimal phase shifting filter. As a matter of fact, in this case, the transmittance modulus is not modified and it is therefore possible to work on modifying the phase shift only, while knowing that the latter will be necessarily increased.

2.2.2.4. Group delay

We define group delay by $t_g(\omega) = -\frac{d[\text{Arg}\{H(j\omega)\}]}{d\omega} = -\frac{d\varphi(\omega)}{d\omega}$ if we establish that $\varphi(\omega) = \text{Arg}\{H(j\omega)\}$.

It gives the variation of the phase shift with respect to the circular frequency. If it is constant and equal to t_{g0} , the phase shift varies linearly with the circular frequency: $\varphi(\omega) = -\omega t_{g0}$, and with the frequency: $\varphi(f) = -2\pi f t_{g0}$.

This last property is useful if it is not desired that a signal with a part of its spectrum inside the bandwidth of the filter be distorted, although the filter induces a frequency-dependent phase shift.

For example, a periodic signal $x_T(t) = c_0 + \lim_{N \rightarrow \infty} 2 \sum_{n=1}^N |c_n| \cos\left[\frac{2\pi n t}{T} + \varphi_n\right]$ will undergo additional phase shift for each of its frequency harmonics $f_n = \frac{2\pi n}{T}$, which will give on the filter output a complex amplitude $c_n H\left(j \frac{2\pi n}{T}\right)$ whose argument will be $\varphi_n - \frac{2\pi n}{T} t_{g0}$. The time delay between harmonics k^{th} and n^{th} will then be: $\left[\frac{T}{2\pi n} \varphi_n - t_{g0}\right] - \left[\frac{T}{2\pi k} \varphi_k - t_{g0}\right] = \frac{T}{2\pi n} \varphi_n - \frac{T}{2\pi k} \varphi_k$, which is the same as for the input signal. It can be concluded that the distortion of the signal will be minimal because the relative delay between each harmonic composing the signal will be preserved in the bandwidth of the filter in the case where the group delay is constant.

For an input signal whose spectrum is $X(j2\pi f)$, the spectrum of the output signal will be $|H(j2\pi f)| \exp[j\varphi(f)] X(j2\pi f) = |H(j2\pi f)| \exp[-j 2\pi f t_{g0}] X(j2\pi f)$ if t_g is constant in the frequency band under consideration, which corresponds to a constant delay and equal to t_{g0} for the output signal compared to the input signal. When this frequency band is the bandwidth of the filter, the same conclusion is attained.

A constant group delay can thereby constitute a fundamental criterion in the selection of a filter when it is desirable to limit the distortion of the signal

by delaying in a uniform manner all signal components that are not attenuated, namely whose frequencies are located within the bandwidth of the filter. If the filter does not have a constant group delay, one can try to approach this property by adding an all-pass filter, with a non-minimal phase shift, intended to correct the phase shift without modifying the overall transmittances module.

2.2.2.5. Types of minimal phase shift filters and templates

Minimal phase-shift transmittances can be categorized into:

- low-pass filter if $20\log|H_m(j\omega)|$ has a negative slope asymptote for $\omega > \omega_c$ the cut-off angular frequency;
- band-pass filter if $20\log|H_m(j\omega)|$ has a positive slope asymptote for $\omega < \omega_{c1}$ and a negative slope asymptote for $\omega > \omega_{c2}$ with $\omega_{c2} > \omega_{c1}$;
- high-pass filter if $20\log|H_m(j\omega)|$ has a positive slope asymptote for $\omega < \omega_c$;
- band-stop or band-rejection filter if $20\log|H_m(j\omega)|$ has a minimum for $\omega = \omega_1$ and horizontal asymptotes for $\omega \rightarrow 0$ and $\omega \rightarrow \infty$.

Filter synthesis is then performed based on a template of the Bode diagram of the reciprocal of the transmittance $[H(j2\pi f)]^{-1}$ of the low-pass filter, whose modulus is called attenuation. If the numerator of $H(j2\pi f)$ is equal to a constant H_0 (frequent case of low-pass filters), $[H(j2\pi f)]^{-1}$ is simply equal to the denominator $D(j2\pi f)$ divided by the constant H_0 . Other types of filters can be deduced by changing variables: $\frac{s}{\omega_c} \rightarrow \frac{\omega_c'}{s}$ to shift to

the high-pass filter with a new cutoff frequency ω_c' ; $\frac{s}{\omega_c} \rightarrow \left(\frac{\omega_0}{s} + \frac{s}{\omega_0}\right) \frac{\omega_0}{\Delta\omega}$ to shift to the band-pass filter with a new central frequency ω_0 and bandwidth $\Delta\omega$; $\frac{s}{\omega_c} \rightarrow \frac{\Delta\omega}{\omega_0} \frac{1}{\left(\frac{\omega_0}{s} + \frac{s}{\omega_0}\right)}$ to switch to the band-stop filter with a new central

frequency ω_0 and bandwidth $\Delta\omega$. The order of the filter is doubled in the last two cases.

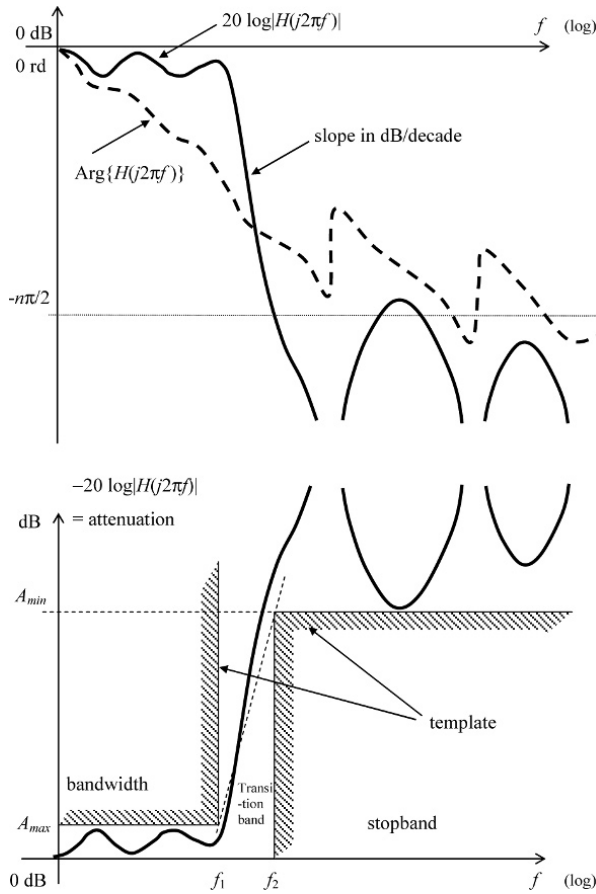


Figure 2.26. Transmittance and attenuation template of a low-pass filter

The filters whose transmittance differs only by the cutoff frequency or center frequency all have the same Bode diagrams which can be deduced by a translation along the logarithmic frequency axis. The study thus only considers a single transmittance called normalized transmittance, for which $\omega_c = \omega_c' = \omega_0 = 1$ rd/s, the circular frequency ω can then be regarded as a normalized (dimensionless) one. The transmittance having a different frequency ω_c or ω_0 can be inferred by the denormalization (or back-normalization) operation as it will be seen further in the text.

The characteristics of the low-pass filter are as follows:

- A_{max} = maximal ripple in the bandwidth;
- f_1 = cutoff frequency (cutoff circular frequency ω_1);
- A_{min} = minimal attenuation in the stopband;
- f_2 = minimal frequency of the stopband (circular frequency ω_2).

The ratio f_2/f_1 measures the attenuation stiffness and the filter requires a degree n of the polynomial $D(j2\pi f)$ that is increasingly higher as this ratio becomes closer to 1, which defines the order of the filter. The slope $d[-20\log|H(j2\pi f)|]/df$ is measured in dB/decade. The frequency range $[f_1, f_2]$ is called transition band. Its width is quantified as a relative value by the ratio $f_2/f_1 = \omega_2/\omega_1$. With normalized circular frequency, $\omega_1 = 1$ rd/s and this ratio then becomes equal to ω_2 .

An example of the response of a low-pass filter and the template used to infer the attenuation is shown in Figure 2.26.

This allows us to visualize all of the characteristics defined at the beginning of this section (A_{max} = maximal ripple in the bandwidth, f_1 = cutoff frequency, A_{min} = minimal attenuation in the bandwidth, f_2 = minimal frequency of the stopband), $[f_1, f_2]$ = transition band). The areas which the attenuation curve must be excluded from are shown with a hatched line, which graphically defines the template of the filter.

2.2.2.6. Approximation criteria of the transmittance of a low-pass filter

To approximate the template, it is necessary to find a polynomial $D(j2\pi f)$ (or a rational fraction $[H(j2\pi f)]^{-1}$ if the numerator $N(j2\pi f)$ is not equal to a constant) that allows $|D(j2\pi f)|$ (or $|H(j2\pi f)|^{-1}$) to stay in the proximity of 1 for $f < f_1$ and to quickly increase for $f_1 < f < f_2$.

Every time $20 \log|H(j2\pi f)|$ crosses 0 dB in the bandwidth for a specific frequency, it is referred to as an attenuation zero; whenever $20 \log|H(j2\pi f)|$ shifts to infinity in the stopband for a particular frequency, it is referred to as an attenuation pole.

The square modulus $|D(j\omega)|^2$ of the polynomial is then of the form $|D(j\omega)|^2 = 1 + R_n(\omega^2)$ where $R_n(\omega^2)$ is a $2n$ -degree polynomial in which even powers of ω only appear in order to ensure the even symmetry of the

modulus $|D(j\omega)|$. Since the imaginary variable $j\omega$ or $j2\pi f$ is a special case of the complex variable s , we will give preference to working with the latter.

There are numerous criteria enabling an approximation of the ideal transmittance to be obtained and one must be chosen as a priority, which implies that the other criteria will not be perfectly satisfied. The four most common cases are detailed below, with the corresponding polynomials, and some extensions are commented thereafter.

– Butterworth polynomials: $|D(j\omega)|^2 = 1 + (-1)^n \omega^{2n}$ has the $2n$ th roots of 1 or -1 . For $|D(s)|^2$, only roots with negative real parts are kept:

$$D(s) = \prod_{k=1}^n (s - s_k) \quad \text{with} \quad s_k = \exp\left(j \frac{\pi}{2} \left[\frac{1+2k}{n} \right]\right), \quad 2k \text{ assuming integer values}$$

such as $\frac{n-1}{2} \leq k \leq \frac{3n-1}{2}$. This type of transmittance is obtained when the criterion giving the flattest possible response in the bandwidth is preferred (this is a filter also known as “flat-top” or “maximally flat”) with an attenuation of 3 dB at the cutoff frequency f_1 and a slope $P \leq 20 n$ dB/decade in the transition band. With normalized circular frequencies, the unique parameter is the order of the filter.

– Bessel polynomials: these filters guarantee a group delay t_g as constant as possible in the bandwidth. We can show that the polynomials defined by the equation $D_n(s) = (2n - 1) D_{n-1}(s) + s^2 D_{n-2}(s)$ with $D_0(s) = 1$ and $D_1(s) = s + 1$ satisfy this criteria. The slope is $P \leq 20 n$ dB/decade in the transition band. With normalized circular frequencies, the unique parameter is the order of the filter. The impulse response of this filter is non-oscillating, unlike all other filters.

– Type I Chebyshev polynomials: $|D(j\omega)|^2 = 1 + [mT_n(\omega)]^2$ where $T_n(\omega)$ oscillates between -1 and $+1$ in the bandwidth ($\omega < 1$ in normalized circular frequency). The oscillation of $|D(j\omega)|$ is therefore from 1 to $\sqrt{1+m^2}$, that is $10\log(1+m^2)$ in dB. This condition leads to the differential

equation:
$$\frac{dT_n}{\sqrt{1-T_n^2}} = n \frac{d\omega}{\sqrt{1-\omega^2}}, \quad \text{which admits the solutions}$$

$T_n(\omega) = \cos[n \operatorname{Arccos}(\omega)]$. Defining $m = 1/\sinh(na)$, the roots of $1 + [mT_n(\omega)]^2$ located in the left half-plane are:

$$s_k = -\sinh(a) \sin \left[(2k-1) \frac{\pi}{2n} \right] + j \cosh(a) \cos \left[(2k-1) \frac{\pi}{2n} \right],$$

distributed over an ellipse centered on the origin in the complex plane. The criterion that is preferred here is the transmittance stiffness in the transition band. The decisive advantage of these filters is based on a cutoff slope $P > 20n$ dB/decade at the beginning of the transition band. On the other hand, there are attenuation zeroes in the bandwidth, which leads to a ripple A_{\max} . With normalized circular frequencies, the two parameters to set are the order of the filter and the ripple in the bandwidth.

The transmittances based on type II Chebyshev polynomials, obtained by replacing $j\omega$ by $1/j\omega$ (in normalized circular frequencies) instead exhibit undulating (or rippling) attenuation in the stopband but a flat response in the bandwidth. This property may make these filters more interesting than those of type I, although the stiffness of the cutoff is less pronounced at the beginning of the transition band. The numerator is also a polynomial of degree equal to the order of the filter.

– Elliptical filters (or Jacobi or Causer or Zolotarev filters): The numerator of $H(s)$ has zeros on the imaginary axis, allowing the increase in the cutoff stiffness ($P > 20n$ dB/decade), at the expense of a finite transmittance undulating in both the bandwidth and the stopband:

$$H(s) = \prod_{k=1}^{n/2} \frac{1 + \frac{s^2}{\omega_k^2}}{1 + 2\zeta_k b_k s + b_k^2 s^2} \quad \text{for } n \text{ even. Here, the preferred criterion is the}$$

reduction of the transition band width by means of the presence of an attenuation pole at circular frequency ω_2 . Parameters ω_k , ζ_k , b_k cannot be directly calculated following an analytical approach because it is necessary to resort to elliptical integrals (hence the name), but can be obtained based on series expansions or by numerical evaluation. There are three parameters necessary to define these filters: the order n , the ripple in the bandwidth A_{\max} and either the minimal attenuation in the stopband A_{\min} or the ratio between the circular frequency of the first attenuation pole ω_2 (or zero of the transmittance) in the stopband and the cutoff circular frequency ω_1 , or still the exact measure of the relative value of the transition band. The attenuation

in the stopband decreases as this last ratio is approaching unity. Therefore, a tradeoff must be decided between these two characteristics.

All these polynomials can be obtained nowadays from the characteristics requested in the template by numerical computation programs, for example in MATLAB in the “signal processing” toolbox (“besselap, buttap, cheb1ap, cheb2ap, ellipap” for normalized transmittances and “lp2lp, lp2bp, lp2hp, lp2bs” for type transformations). Also in MATLAB, operations on polynomials or rational fractions can be performed with “conv, deconv, roots, poly, residue”, respectively, for multiplication, Euclidean division, for calculating the roots, polynomial expansion and the partial fraction expansion of rational functions or conversely the reduction to a single rational fraction. Further in the chapter, all examples will be developed from the polynomials and normalized transmittances available in MATLAB.

Based on a template determined by the synthesis methods of the following sections, it is possible to shift from a low-pass filter to the other types by directly transforming the elements in the circuit of the low-pass filter using the below table.

– In order to obtain a low-pass filter with cut-off pulse ω_c' instead of 1 rd/s, s has simply to be substituted (in fact s/ω_c with $\omega_c = 1$ rd/s) by $\frac{s}{\omega_c'}$.

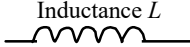
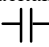
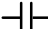


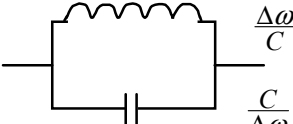
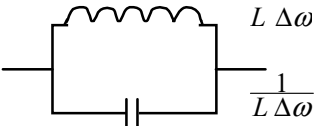

– The transformation to obtain a high-pass filter $\frac{s}{\omega_c} \rightarrow \frac{\omega_c'}{s}$ indicates the replacement of capacitances by inductances and vice versa. Resistances are not affected.

– The transformation for obtaining a band-pass filter $\frac{s}{\omega_c} \rightarrow \left(\frac{\omega_0}{s} + \frac{s}{\omega_0} \right) \frac{\omega_0}{\Delta\omega}$ (where ω_0 is the central circular frequency and $\Delta\omega$ the bandwidth) corresponds to replacing each inductance by an inductance and a capacitance in series, and each capacitance by a capacitance and an inductance in parallel.

– The transformation $\frac{s}{\omega_c} \rightarrow \frac{\Delta\omega}{\omega_0} \frac{1}{\left(\frac{\omega_0}{s} + \frac{s}{\omega_0} \right)}$, namely low-pass

toward band-stop requires replacing each capacitance by an inductance and a capacitance in series, and each inductance by a capacitance and an inductance in parallel.

In summary, these transformations are shown in the following table:

Elements in a low-pass filter	 Inductance L	 Capacitance C
Corresponding elements of the high-pass filter	 $1/L$	 $1/C$
Corresponding elements of the band-pass filter	 $\frac{\Delta\omega}{L}$ $\frac{L}{\Delta\omega}$	 $\frac{\Delta\omega}{C}$ $\frac{C}{\Delta\omega}$
Corresponding elements of the band-stop filter	 $L \Delta\omega$ $\frac{1}{L \Delta\omega}$	 $C \Delta\omega$ $\frac{1}{C \Delta\omega}$

For the normalized transmittances $\omega_c = \omega_c' = \omega_0 = 1$ rd/s and the bandwidth, $\Delta\omega$ is taken as a relative value. Practical central or cutoff frequencies can be subsequently obtained by changing inductances and capacitances according to the denormalization procedure described in section 2.4.1.3.

As a comparison, the Bode diagrams of the modulus of four fourth-order low-pass filters, obtained with different types of polynomials, as well as the group delays are plotted in Figure 2.27 according to the normalized circular frequency (or with the cutoff circular frequency $\omega_c = 1$ rd/s).

In this example, for type I Chebyshev and elliptical filters, the ripple in the bandwidth is set to 1dB and the ratio of the frequency of the first transmittance zero at ω_c is 2 for the elliptical filter. We clearly see that the Bessel filter gives a rather “soft” attenuation in the vicinity of ω_c , but it is the only one to provide a group delay almost constant up to $0.7\omega_c$ and then

decreasing. The other filters all show a ripple of the group delay t_g with a pronounced maximum at ω_c , especially for Chebyshev and elliptical filters, which also causes ripples in the impulse response.

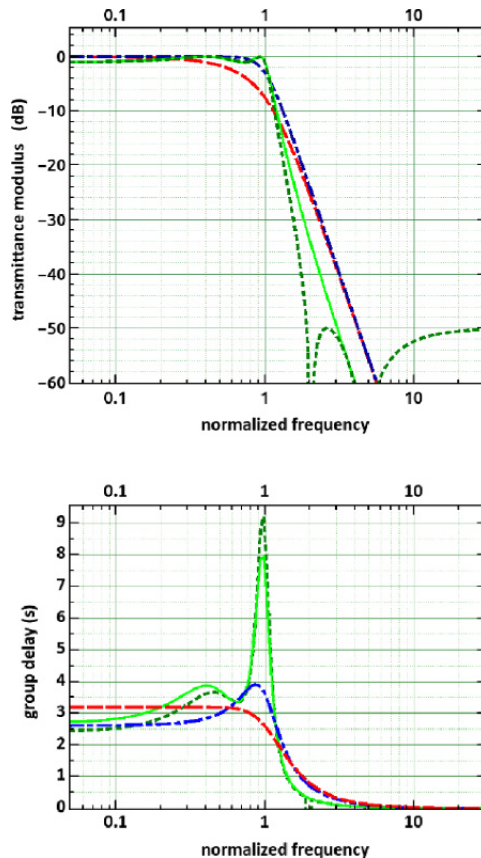


Figure 2.27. Transmittance modulus and group delay for fourth-order low-pass filters (Bessel in red broken line, Butterworth in blue dash-dot line, Chebyshev in full light green line, elliptical in dark green dash). For a color version of this figure, see www.iste.co.uk/muret/electronics2.zip

The Butterworth filter clearly shows a response with a maximal flatness of the modulus in the bandwidth but similarly to the Bessel filter, the stopband slope is limited to $-20n$ dB/dec, where n is the order of the filter (4 here). Conversely, type I Chebyshev and elliptic filters provide a more accentuated slope in the immediate vicinity of ω_c in the transition band. To

reduce the variations of t_g , the solution consists of adding an all-pass filter partly compensating for variations of the phase shift with ω , and thus those of t_g (see section 2.4.2.7).

2.2.2.7. Approximation of any kind of transmittance: Padé approximation and other approximations

The problem is defined in terms of searching for the best approximation to a transmittance $H(j\omega)$ or $H(s)$ with a usable function, which in addition must result in a stable transmittance. If the desired transmittance H_d is known only in a finite number of circular frequencies ω_i , we should employ methods based on the algebra of function spaces used in signal processing and control of systems, which fall outside the scope of this book. In particular, it is often necessary to resort to a system representation using state variables, which are internal variables and not necessarily observable. Nevertheless, they facilitate the description of time responses by a system of first-order differential equations (see Chapter 1 and, for example, [UNS 04]). Interpolation methods (Lagrange polynomials, for instance) may nevertheless constitute a first step in the process for obtaining an analytical approximation.

In the event that there is already an analytical expression, the calculation of a Padé approximation allows us to obtain a first relation in the form of a rational fraction $P(s)/Q(s)$, which is then directly usable for the synthesis of the transmittance. This method is the subject of a large number of mathematical approaches implemented by algorithms, some of which being available in software programs. The sequences of Padé approximates can always be expressed in the form of continued fraction expansion. A first step involves therefore finding an expression for the function $H(s)$, even if it is trivial, in the form of a constant a_0 in addition to a fraction $P_1(s)/Q_1(s)$. If $P_1(s) = s^{n_1}$, the same process is restarted for $Q_1(s)$, which can either indefinitely continue (infinite continued fraction), or stop at a certain order n if $Q_n(s)$ is itself a rational fraction. If $P_1(s)$ is not a power of s , we try to perform a limited expansion of $P_1(s)$ and $Q_1(s)$, then through repeated polynomial division up to a certain order, it also yields a continued fraction. Being restricted to a certain order, the continued fraction can be reduced to a rational fraction. The resulting filter is not considered one of the conventional filters described in section 2.2.2.6, which is also the case for the approximations briefly mentioned hereafter.

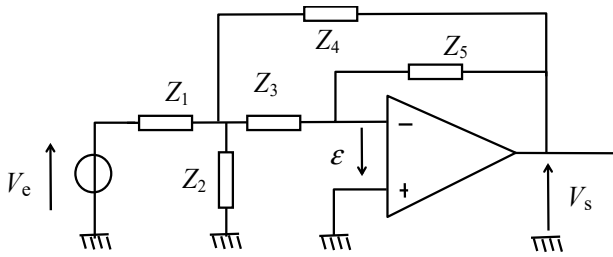
Other methods are possible, which make use of criteria of a different nature. For example, it is possible to use the function “invfreqs” in MATLAB to obtain the numerator and the denominator of a transfer function passing through the points specified in the complex plane. Some options are able to define the tolerance over the deviations, the iteration process, and to ensure the stability of the system. Other methods can be applied primarily to the synthesis of sampled filters but in light of the transformations studied in Volume III, it is possible to find once more the transfer function of an analog filter. The Yule–Walker method is based on the minimization of quadratic deviations between the desired time response, obtained if necessary by means of the inverse Fourier transform of transfer function in the frequency domain, and the synthesized time response (see the function “yulewalk” in MATLAB). The Prony method can be used from the desired impulse response. The corresponding algorithm and others inspired by signal processing methods can be found in the MATLAB “signal processing” toolbox.

2.3. Synthesis of analog active filters using operational amplifiers

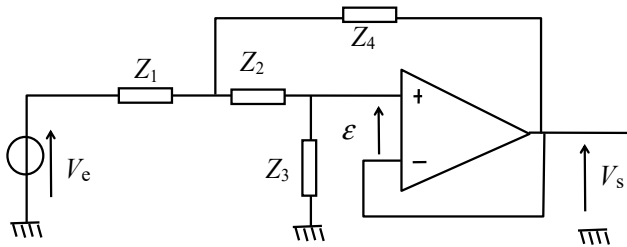
2.3.1. Cascading second-order cell filters

An n -order filter requires $n/2$ second-order cells (or elementary filters) if n is even; $(n-1)/2$ if n is odd in addition to one of the first order. Elementary second-order active filters employing a single operational amplifier are Sallen–Key (non-inverting) or Rauch (inverting) structures (see figure 2.28).

These circuits have the disadvantage of exhibiting interdependent quality coefficients and natural circular frequency. It is thus preferable to use structures in which the quality coefficient can be adjusted independently of the natural circular frequency such as so-called biquadratic structures (second degree) and the simplest is described hereafter (see Figures 2.29, 2.30 and section 1.7.2. in Chapter 1). Other passive or active internal feedback loops can also be added. The various outputs allow for several types of filters (low-pass, band-pass or high-pass).



Rauch structure



Sallen-Key structure

Figure 2.28. Active filters with a single operational amplifier

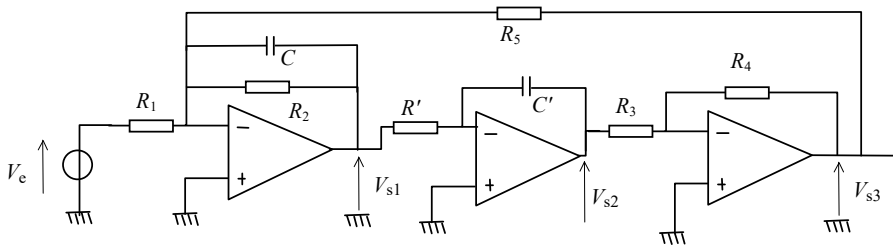


Figure 2.29. Second-order active filter using three operational amplifiers

In order to obtain a second-order transmittance comprising of both a second-degree numerator and a denominator in s (biquadratic), the Delyannis–Friend structure can be employed (see figure 2.30), in which the transmittance parameters can be adjusted without mutual interaction.

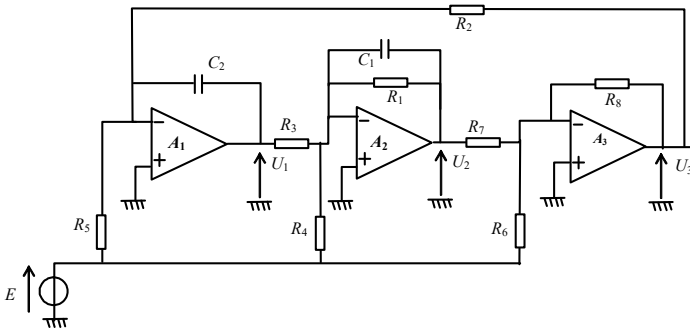


Figure 2.30. *Delyannis–Friend second-order active filter*

The synthesis of operational amplifier-based active filters can easily be achieved from the decomposition of the denominator of the normalized transmittance into a product of second-degree polynomials in s (and possibly a first-degree factor in the case of odd-degree denominator), which can be computed after determining the roots of the denominator and eventually of the numerator (e.g. using the MATLAB function “roots”). Each of them can then be implemented by one of the previous circuits because there is no coupling between one stage and the next. The elements are then calculated by denormalization, by dividing time constants by the ratio of the desired cutoff circular frequency to $\omega_c = 1$ rd/s.

2.3.2. Multiple feedback loop cell

The previous circuits can be generalized through the diagram shown in Figure 2.31, which theoretically allows us to synthesize the transfer function only once.

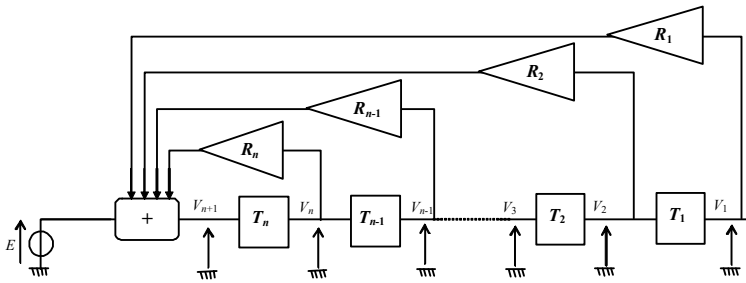


Figure 2.31. Multiple feedback loop cell with forward transmittances $T_n, T_{n-1}, \dots, T_2, T_1$ and feedback transmittances $R_1, R_2, \dots, R_{n-1}, R_n$

The relation between voltages V_i ($i = 1$ to n) and V_{n+1} is written as:

$$V_i = V_{n+1} T_n T_{n-1} \dots T_i = V_{n+1} \prod_{j=i}^n T_j$$

And in addition $V_{n+1} = E + \sum_{i=1}^n R_i V_i$. The transfer function $T = V_1/E$ can

therefore be deduced:

$$T = \frac{V_1}{E} = \frac{\prod_{j=1}^n T_j}{1 - \sum_{i=1}^n R_i \prod_{j=i}^n T_j}$$

The synthesis is carried out from the transfer function T supposed to be of the $2n$ degree and from real numbers with a modulus less than 1 for the R_1, R_2, \dots, R_n using a recursive method. Firstly, we split the diagram into two looped blocks T'_1 and R_1 . Hence $T = \frac{T'_1}{1 - R_1 T'_1}$, which is verified by:

$$T'_1 = \frac{T}{1 + R_1 T}$$

Next, T'_1 is factorized in order to break down this transmittance into a biquadratic transmittance (of the second degree) achieved by an assembly like in section 2.3.1. and a rational fraction T''_1 of degree $2n - 2$. The second step is the repetition of the previous one

but with T''_1 instead of T and R_2 instead of R_1 . The process is then restarted to achieve the final system.

Nonetheless, the stability of the system should be verified, for example based on the state representation, because it can be more problematic than for previous assemblies studied in section 2.3.1.

2.4. Non-dissipative filters synthesis methods

This type of filter assumes that purely reactive elements are being used, such as capacitances, inductances and possibly ideal transformers, excluding any resistance and neglecting Joule losses in reactances. This solution is especially interesting at high frequencies where operational amplifiers can no longer be employed and when it is desirable to minimize active power dissipation. As a matter of fact, only a small number of pure reactances (inductance, capacitance or quartz resonator) are sufficient to synthesize all types of filters previously described. In addition, it is superior to active filters in terms of sensitivity to the value of elements, mentioned at the end of chapter.

These quadripoles are arranged in a chain and are generally terminated by a resistance. Iterative impedance is not always purely resistive and it is preferable to determine recurrence relations between parameters when an element is added to achieve the synthesis of these filters; a second option is to use a more general method that takes termination impedances into account, since the response of the filter depends therefrom. The best model is then the one making use of s -parameters (see sections 2.1.6 and 2.1.7.2), which find a very powerful application below. A first exact method makes it possible to obtain the minimum number of elements from the effective parameters of the filter, themselves calculated based on the transfer function chosen for the transfer coefficient s_{21} . Another method, not fully exact and eventually making use of a larger number of elements, relies on image-matching. It permits to built any filter by cascading passive cells made of capacitors and inductors without mutual interaction like for active filters based on operational amplifiers and studied in the section 2.3.1. It provides good results in the case of narrow-band band-pass filters and allows calculations by hand. These two procedures are described in the following sections.

2.4.1. Synthesis based on effective parameters

2.4.1.1. Zero dissipation condition in the quadripole (unitarity relation)

The zero dissipation condition in the quadripole can be developed from $\beta = s \alpha$, where: $\alpha = v + i$ and $\beta = v - i$ (in matrix notation), that is to say:

$$\beta = \begin{bmatrix} v_1 - i_1 \\ v_2 - i_2 \end{bmatrix} = \begin{bmatrix} s_{11} & s_{12} \\ s_{21} & s_{22} \end{bmatrix} \begin{bmatrix} v_1 + i_1 \\ v_2 + i_2 \end{bmatrix} = s \alpha$$

The power absorbed by the quadripole taking into account its two ports is $\text{Re} \left[v_1 \bar{i}_1 + v_2 \bar{i}_2 \right]$ or in a more symmetrical way:

$$P = \frac{1}{2} \left[v_1 \bar{i}_1 + v_2 \bar{i}_2 + \bar{v}_1 i_1 + \bar{v}_2 i_2 \right].$$

However, $\begin{bmatrix} v_1 & v_2 \end{bmatrix} \begin{bmatrix} \bar{i}_1 \\ \bar{i}_2 \end{bmatrix} = v_1 \bar{i}_1 + v_2 \bar{i}_2 = {}^t v \bar{i}$, where ${}^t v$ is the transpose of matrix v and \bar{i} the complex conjugate matrix of i . Therefore:

$$2P = {}^t v \bar{i} + {}^t \bar{v} i \text{ or even } 2P = {}^t \bar{i} v + {}^t \bar{v} i$$

From sum and difference of $\alpha = v + i$ and $\beta = v - i$, and by establishing $I_2 = \begin{bmatrix} 1 & 0 \\ 0 & 1 \end{bmatrix}$:

$$4 {}^t \bar{v} i = ({}^t \bar{\alpha} + {}^t \bar{\beta})(\alpha - \beta) = {}^t \bar{\alpha} \alpha - {}^t \bar{\beta} \beta + {}^t \bar{\beta} \alpha - {}^t \bar{\alpha} \beta$$

$$4 {}^t \bar{i} v = ({}^t \bar{\alpha} - {}^t \bar{\beta})(\alpha + \beta) = {}^t \bar{\alpha} \alpha - {}^t \bar{\beta} \beta - {}^t \bar{\beta} \alpha + {}^t \bar{\alpha} \beta$$

$$4 ({}^t \bar{v} i + {}^t \bar{i} v) = 2 {}^t \bar{\alpha} \alpha - 2 {}^t \bar{\beta} \beta$$

$$4P = {}^t \bar{\alpha} \alpha - {}^t \bar{\beta} \beta = {}^t \bar{\alpha} I_2 \alpha - {}^t \bar{\alpha} {}^t s s \alpha$$

$$4P = {}^t \bar{\alpha} \alpha - {}^t \bar{\beta} \beta = {}^t \bar{\alpha} \left[I_2 - {}^t s s \right] \alpha$$

The cancellation of this power P thus implies that:

$$\boxed{{}^t s s = I_2 \quad \text{or alternatively} \quad \overline{{}^t s} = s^{-I}}$$

thereby making matrices explicit:

$$\begin{bmatrix} \overline{s_{11}} & \overline{s_{21}} \\ \overline{s_{12}} & \overline{s_{22}} \end{bmatrix} \begin{bmatrix} s_{11} & s_{12} \\ s_{21} & s_{22} \end{bmatrix} = \begin{bmatrix} |s_{11}|^2 + |s_{21}|^2 & \overline{s_{11}}s_{12} + \overline{s_{21}}s_{22} \\ \overline{s_{12}}s_{11} + \overline{s_{22}}s_{21} & |s_{12}|^2 + |s_{22}|^2 \end{bmatrix} = \begin{bmatrix} 1 & 0 \\ 0 & 1 \end{bmatrix},$$

which gives the Feldkeller relations: $|s_{12}|^2 + |s_{22}|^2 = |s_{11}|^2 + |s_{21}|^2 = 1$ and a dependency relation between the four coefficients $\overline{s_{11}}s_{12} + \overline{s_{21}}s_{22} = 0$, which is normal for a passive quadripole.

All of these coefficients are actually rational fractions of polynomials that depend on the variable s in the same way as the variable $j\omega$ and therefore the conjugate complexes can be replaced by Hurwitzian conjugates in all these expressions. The equality $\overline{{}^t s} = s^{-1}$ then implies the equality of determinants, which is expressed by $(\det s)_* (\det s) = 1$, which is a characteristic property

of an all-pass transmittance of the $\det s = \mp \frac{g_*}{g}$ type, where g is a Hurwitzian

polynomial. Since g appears in the denominator of the determinant of s , it is necessarily part of the denominator of the coefficients of the matrix s . This allows us to write the previous matrix relation $\overline{{}^t s} = s^{-1}$ after simplification of common polynomial factors in the form:

$$\frac{1}{g_*} \begin{bmatrix} n_{11*} & n_{21*} \\ n_{12*} & n_{22*} \end{bmatrix} = \frac{1}{g \det s} \begin{bmatrix} n_{22} & -n_{12} \\ -n_{21} & n_{11} \end{bmatrix},$$

where the n_{ij} represent the polynomials of the numerators of coefficients s_{ij} , and g the polynomial common to their denominator. After simplification by g and g_* , this yields equalities $n_{11*} = \mp n_{22}$, $n_{21*} = \pm n_{12}$ and $n_{12*} = \pm n_{21}$, which properly verify $s_{11*} s_{12} + s_{21*} s_{22} = 0$. Finally, there are only three distinct polynomials remaining, g for the common denominator and we will denote $h = n_{11}$ and $f = n_{12}$ for the numerators. The matrix s then takes the form:

$$\boxed{s = \frac{1}{g} \begin{bmatrix} h & f \\ \pm f_* & \mp h_* \end{bmatrix}},$$

where $\pm f_* = n_{21}$ and $\mp h_* = n_{22}$ are, respectively, replaced by f and $-h$ for reciprocal quadripoles, which is the case for passive circuits including only inductances and capacitances.

Since $\det \mathbf{s} = \mp \frac{g_*}{g}$, the computation of $\det \mathbf{s}$ leads to the “unitarity relation”:

$$\boxed{gg_* = hh_* + ff_*}$$

This relation constitutes the basis for the synthesis of these filters, since $s_{12} = s_{21} = \frac{f}{g}$ is determined from the transmittance desired for the filter, its power gain being proportional to $|S_{21}|^2$ (see section 2.1.7.2). This transmittance is itself sized based on the template and the two polynomials f and g are thus known. The unitarity relation makes it possible to deduce the third polynomial h , which gives the diagonal coefficients of the matrix \mathbf{S} .

We can therefore deduce matrices $\mathbf{z} = (\mathbf{I}_2 + \mathbf{s})(\mathbf{I}_2 - \mathbf{s})^{-1}$ and $\mathbf{y} = (\mathbf{I}_2 - \mathbf{s})(\mathbf{I}_2 + \mathbf{s})^{-1}$ and especially impedances z_{11} and z_{22} or admittances y_{11} and y_{22} , which give access to the circuit diagram of the quadripole based on impedance or admittance synthesis as seen in section 2.1.5.3. It follows that:

$$z_{11} = \frac{(g \pm g_*) + (h \pm h_*)}{(g \mp g_*) - (h \mp h_*)}; \quad z_{22} = \frac{(g \pm g_*) - (h \pm h_*)}{(g \mp g_*) - (h \mp h_*)};$$

$$z_{12} = z_{21} = \frac{2f}{(g \mp g_*) - (h \mp h_*)};$$

$$y_{11} = \frac{(g \pm g_*) - (h \pm h_*)}{(g \mp g_*) + (h \mp h_*)}; \quad y_{22} = \frac{(g \pm g_*) + (h \pm h_*)}{(g \mp g_*) + (h \mp h_*)}.$$

It can be observed that z_{11} , z_{22} , y_{11} and y_{22} only involve sums and differences of two polynomials and their Hurwitzian conjugate, which automatically gives rise to polynomials with either even or odd degree, as

this is necessary for impedances z_{ii} or admittances y_{ii} comprising reactive elements only (inductances and capacitances). The number of reactive passive elements is directly related to the order of the filter. The elements are numbered in the order of the branches encountered from the input to the output as in the following example (Figure 2.32).

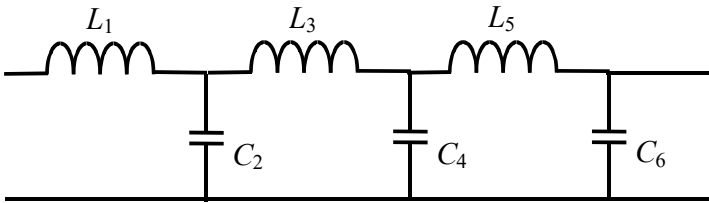


Figure 2.32. Ladder sixth-order low-pass filter

The different possibilities of assembling the inductances and capacitances either correspond to filters of the same transmittance, which can be implemented in different ways if different syntheses are used (Foster, Cauer or mixed), or to the filters of different types (low-pass, band-pass, high-pass or band-stop). Therefore in the second case, the right configuration has to be chosen according to the requested type, mainly by placing inductances and capacitances to achieve the desired low-frequency and high-frequency behaviors (see section 2.1.5.3). However, it is generally easier to synthesize the low-pass filter and then to deduce the elements of the filter of the desired type by the transformations specified in section 2.2.2.5.

EXAMPLE.— Eighth-order band-pass filter synthesized from the fourth-order low-pass filter.

Consider the fourth-order Chebyshev low-pass filter giving a ripple of 0.1 dB in the bandwidth, with normalized transmittance $\frac{0.819}{s^4 + 1.804s^3 + 2.627s^2 + 2.026s + 0.8285} = \frac{f}{g}$. With the unitarity relation, we get $h = s^4 + s^2 + 0.125$. The diagram can be synthesized in the form shown in the previous circuit (Figure 2.32) with four elements only: $L_1 = 1.109$; $C_2 = 1.306$; $L_3 = 1.77$; $C_4 = 0.818$ from the Cauer's synthesis (section 2.1.5.3.). The low-pass \rightarrow band-pass transformation (section 2.2.2.5) with a

reduced bandwidth $\Delta\omega = 0.3$, for example, gives the network, as shown in Figure 2.33.

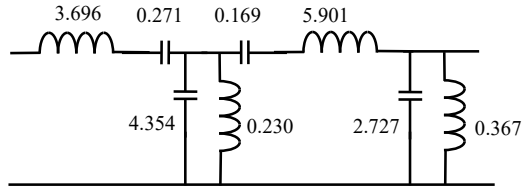


Figure 2.33. Network of the normalized Chebyshev filter obtained after the transformation low-pass to band-pass with a normalized bandwidth $\Delta\omega = 0.3$ and a ripple of 0.1 dB within the bandwidth

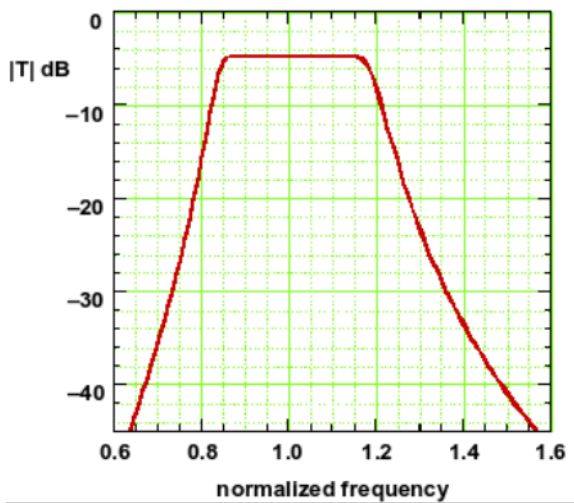


Figure 2.34. Transmittance modulus of the eighth-order Chebyshev band-pass filter with normalized bandwidth equal to 0.3 and a ripple of 0.1 dB within the bandwidth

This corresponds to the transmittance:

$$\frac{6.63 \times 10^{-3} s^4}{s^8 + 0.5411s^7 + 4.2364s^6 + 1.6781s^5 + 6.4795s^4 + 1.6781s^3 + 4.2364s^2 + 0.5411s + 1}$$

The latter would result in a more complicated direct synthesis because the impedances z_{ii} and admittances y_{ii} obtained by the expressions previously provided are composed of polynomials of the seventh-degree at most and thus do not make it possible to deduce the value of all elements at once.

The Bode diagram simulated from the filter response whose network is given above shows breaks located around 0.84 and 1.18 (corresponding in fact to $\Delta\omega = 0.34$) and an almost flat response in the bandwidth according to the original specifications (0.1 dB ripple). The practical implementation, however, generates a response more distant from the template, because the ratio of two elements of the same kind can reach 20, which turns the condition of negligible dissipation problematic in all elements. An even narrower bandwidth would enhance this flaw.

2.4.1.2. Elliptic filters

There are, nonetheless, cases where the syntheses exposed in section 2.1.5.3 do not allow us to obtain the transfer function corresponding to the transmission parameter $s_{21} = f/g$. This is the case if the polynomial f of the numerator includes zeros (or roots), as in elliptical or Jacobi filters (see section 2.2.2.5). In effect, in this case the circuit requires LC-series resonant branches in parallel or LC-parallel antiresonant branches in series, as in Figure 2.35, in order to cause, respectively, a short circuit or an open circuit at every angular frequency $\omega_j = 1/\sqrt{L_j C_j^r}$.

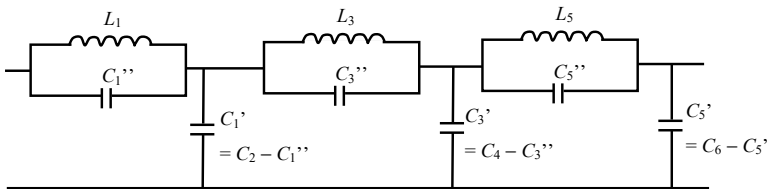


Figure 2.35. Sixth-order low-pass elliptic filter

The synthesis then requires one additional step that consists of achieving a partial extraction of an element of the network shown in Figure 2.32 in order to carry forward the residual element (capacitance or inductance) onto the previous element, of opposite nature (respectively, inductance or capacitance), as shown in Figure 2.35.

Let a normalized impedance or a admittance be $x_{ii} = z_{ii}$ or y_{ii} whose synthesis is achieved using the Cauer method: $x_{ii} = \tau_1 p + \frac{N_2(p)}{D_2(p)}$, where τ_1

represents the time constant of either an inductance if $x_{ii} = z_{ii}$ or a capacitance if $x_{ii} = y_{ii}$, and where $N_2(p)$ has a degree $k - 1$, one unit lower than that of $D_2(p)$, which has a degree k . The partial extraction consists of breaking down τ_1 into $\tau_1 + \tau_1''$ in order to carry forward and to combine $\tau_2 s$ with the fraction $\frac{N_2(s)}{D_2(s)}$ so that its denominator is now

$$\frac{\tau_2 s}{1 + \frac{s^2}{\omega_0^2}}$$

instead of $\tau_2 s$, thus corresponding to a resonant or antiresonant branch at angular frequency ω_0 . Hence, the sequence of the following operations:

$$x_{ii} = \tau_1 s + \frac{N_2(s)}{D_2(s)} = \tau_1 s + \tau_1'' s + \frac{N_2(s)}{D_2(s)} = \tau_1 s + \frac{\tau_1'' s D_2(s) + N_2(s)}{D_2(s)},$$

which makes it possible to obtain a $k+1$ -degree numerator for the last fraction, denoted by x_{ii}'' .

How can the value of τ_1'' be calculated?

It derives from the next stage of Cauer's synthesis that consists of expressing the reciprocal of the last fraction in the form $\frac{1}{x_{ii}''} = \frac{D_2(s)}{\tau_1'' s D_2(s) + N_2(s)} = \frac{\tau_2 s}{1 + \frac{s^2}{\omega_0^2}} + \frac{D_3(s)}{N_3(s)}$, which has thus two poles at

$$s = \pm j\omega_0.$$

Therefore, $\frac{1}{x_{ii}''(\pm j\omega_0)} \rightarrow \infty$, or still $x_{ii}''(\pm j\omega_0) = 0$, which implies that

$$j\omega_0 \tau_1'' D_2(j\omega_0) + N_2(j\omega_0) = 0, \quad \text{that is: } \tau_1'' = j \frac{N_2(j\omega_0)}{\omega_0 D_2(j\omega_0)}$$

and τ_1'' can be inferred by $\tau_1 - \tau_1''$.

This time constant is real since one of the polynomials is of odd degree, it is imaginary, and the other is of even degree, thereby is real. However, if $\tau_1'' < 0$ or if $\tau_1'' > \tau_1$ the synthesis is impossible. If it is possible, the result is,

for example, the previous network where each capacitance C'' is calculated from an angular frequency corresponding to a zero of the polynomial f and every capacitance C' is obtained by $C - C''$, where C represents the capacitance previously found by the complete synthesis.

EXAMPLE.— Fourth-order elliptic low-pass filter

A fourth-order low-pass elliptic filter, providing a ripple of 1 dB in the bandwidth and a minimum of 52 dB of stop band attenuation, has a normalized transmittance (from MATLAB “ellipap” function):

$$\frac{f}{g} = \frac{0.002539(s^2 + 24.227)(s^2 + 4.5933)}{s^4 + 0.9455ps^3 + 1.4831s^2 + 0.7753s + 0.3170}$$

The unitarity relation provides the polynomial $h = s^4 + 1.0338s^2 + 0.1426$, then the one giving y_{22} and the complete Cauey synthesis lead to:

$$y_{22} = \frac{4s^4 + 5.0339s^2 + 0.9193}{1.981s^3 + 1.5506s} = 2.1153s + \frac{1.7538s^2 + 0.9193}{1.981s^3 + 1.5506s} \text{ or:}$$

$$y_{22} = 2.1153s + \frac{1}{1.078s + \frac{1}{3.135s + \frac{1}{0.6086s}}}$$

; next, the zeros of f

($\omega_{01} = 4.922$ and $\omega_{02} = 2.143$) allow us to change the ladder network to add the capacitances that unveil the two antiresonant circuits in Figure 2.36 and which have to be subtracted from initial capacitances.

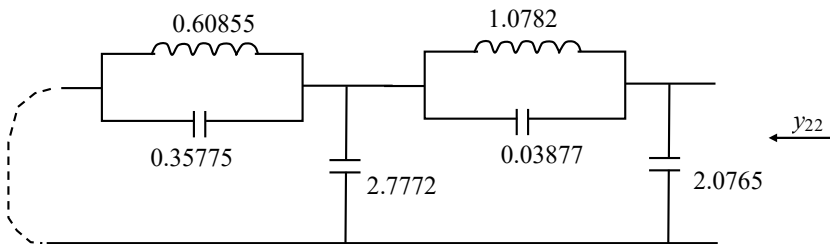


Figure 2.36. Fourth-order elliptic filter synthesis based on its normalized admittance y_{22}

EXERCISE.– Check coherency of the elements value with y_{22} , ω_{01} and ω_{02} . The Bode diagram of this elliptical filter transmittance can be seen at the end of section 2.2.2.5.

2.4.1.3. Development of the filter network and denormalization

Given that impedances $z_{ii}(s)$ and admittances $y_{ii}(s)$ are normalized (dimensionless), the coefficients appearing in their expressions are actually time constants, expressed in seconds, which leads to a notation making use of an expansion into successive fractions (for instance for a sixth-order low-pass filter) for diagonal impedances:

$$z_{ii}(s) = \tau_1 s + \frac{1}{\tau_2 s + \frac{1}{\tau_3 s + \frac{1}{\tau_4 s + \frac{1}{\tau_5 s + \frac{1}{\tau_6 s}}}}}$$

(using Euclidean polynomial division to obtain the integer part of the fraction, and then that of the denominator, etc).

Because of the symmetry of the roots on each side of the real axis for the polynomials f , g and h , certain combinations existing in the numerators and denominators of $z_{11}(s)$, $z_{22}(s)$, $y_{11}(s)$, $y_{22}(s)$ yield identical results. Two identical expressions are then found for $z_{11}(s)$ and $y_{22}(s)$, for example (or for $y_{11}(s)$ and $z_{22}(s)$), which can be represented for the ladder low-pass filter (Figures 2.37 and 2.38) by applying the valid definitions for the impedance or admittance quadripole.

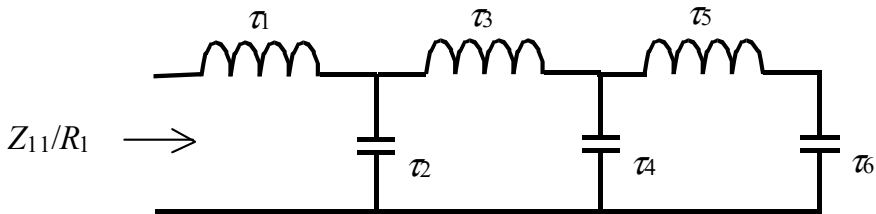


Figure 2.37. Low-pass filter synthesis based on its normalized impedance $z_{11} = Z_{11}/R_1$

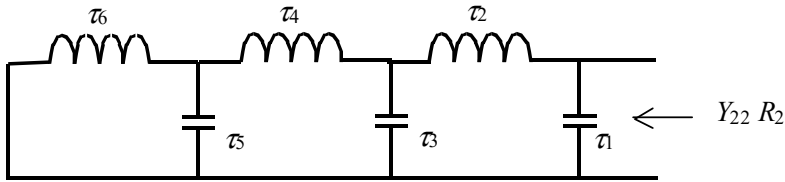


Figure 2.38. Low-pass filter synthesis based on its normalized admittance $y_{22} = Y_{22} R_2$

Based on these time constants, the final network is shown in Figure 2.39.

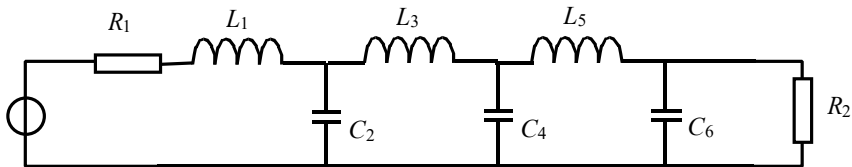


Figure 2.39. Full filter

By matching the identical elements of previous diagrams, we obtain the identities: $\tau_1 = \frac{L_1}{R_1} = R_2 C_6$; $\tau_2 = R_1 C_2 = \frac{L_5}{R_2}$; $\tau_3 = \frac{L_3}{R_1} = R_2 C_4$; $\tau_4 = R_1 C_4 = \frac{L_3}{R_2}$; $\tau_5 = \frac{L_5}{R_1} = R_2 C_2$; $\tau_6 = R_1 C_6 = \frac{L_1}{R_2}$, which by dividing each member in both expressions giving L_1, C_2, L_3, C_4 , etc, implies that:

$$r_R = \frac{R_2}{R_1} = \frac{\tau_1}{\tau_6} = \frac{\tau_3}{\tau_4} = \frac{\tau_5}{\tau_2}$$

and more generally for an n th-order ladder filter:

$$r_R = \frac{R_2}{R_1} = \frac{\tau_1}{\tau_n} = \frac{\tau_3}{\tau_{n-2}} = \frac{\tau_5}{\tau_{n-4}} = \dots$$

Nevertheless, the consistency of the ratios of the various time constants may not be rigorously ensured in some cases. We will then refer to the completed impedance method exposed later in this section.

In the case of elliptic filters for which the transmittance has zeros, the circuit has to be modified by extracting some of the capacitances to carry them forward in parallel onto the inductances in order to identify notch circuits at frequencies corresponding to the zeros of the transmittance, as mentioned in the previous section.

Finally, it is important to consider changing the cutoff angular frequency of the filter, which so far was $\omega_c = 1$ rd/s in the normalized transmittance, to obtain the final circuit. The cutoff angular frequency can be modified in two ways, by altering inductances with the ratio k and by fiddling with capacitances with the ratio m :

– if inductances L are changed into $\frac{L}{k}$ Ls becomes

$$L's = \frac{Ls}{k} = L\sqrt{\frac{m}{k}} \frac{s}{\sqrt{mk}};$$

– if capacitances C are changed into $\frac{C}{m}$ Cs becomes

$$C's = \frac{Cs}{m} = C\sqrt{\frac{k}{m}} \frac{s}{\sqrt{mk}}.$$

The variable s is therefore divided by \sqrt{mk} (and similarly for $j\omega$) in both cases, while impedances are all multiplied by $\sqrt{\frac{m}{k}}$. In order to find the same variation with frequency than with the normalized transmittance, larger angular frequencies by a factor \sqrt{mk} have to be used, which leads to sizing $\sqrt{mk} = r_f$ so as to be equal to the desired cutoff angular frequency $\omega_c' = r_f \omega_c$ with $\omega_c = 1$ rd/s (Note: the new cutoff frequency is then $f_c' = \frac{r_f}{2\pi}$ Hz) and thus to divide all the time constants by r_f to obtain the new time constants $\tau_1' = \frac{\tau_1}{r_f}$; $\tau_2' = \frac{\tau_2}{r_f}$; $\tau_3' = \frac{\tau_3}{r_f}$; etc.

Since the impedances are multiplied by $\sqrt{\frac{m}{k}}$, the resistances R_1 and R_2 also become the new resistances $R_1' = \sqrt{\frac{m}{k}}R_1$, $R_2' = \sqrt{\frac{m}{k}}R_2$ and $\frac{R_2'}{R_1'} = r_R$.

Then, either R_1' , or R_2' has to be chosen (or possibly a capacitance or an inductance).

The new capacitances and inductances are then inferred from:
 $L_1' = \frac{\tau_1 R_1'}{r_f} = \frac{\tau_n R_2'}{r_f}$; $C_2' = \frac{\tau_2}{r_f R_1'} = \frac{\tau_{n-1}}{r_f R_2'}$; $L_3' = \frac{\tau_3 R_1'}{r_f} = \frac{\tau_{n-2} R_2'}{r_f}$; $C_4' = \frac{\tau_4}{r_f R_1'} = \frac{\tau_{n-3}}{r_f R_2'}$; etc.

If the object is not a low-pass filter, the appropriate transformations of initial inductances and capacitances are performed to obtain the desired filter type.

EXAMPLE— Sixth-order type-1 Chebyshev low-pass filter giving a 0.2 dB ripple in the bandwidth.

The calculation achieved with help of the relevant functions available in MATLAB gives:

$$g = s^6 + 1.4708s^5 + 2.5816s^4 + 2.2082s^3 + 1.6029s^2 + 0.6611s + 0.1473.$$

The numerator $f = 0.1439$ is a constant in the case of a low-pass filter. From the unitarity relation, it follows $h = s^6 + 1.5s^4 + 0.5625s^2 + 0.0313$, then a normalized impedance $z_{11} = \frac{4s^6 + 8,1632s^4 + 4.3308s^2 + 0.3571}{2.9416s^5 + 4.4163s^3 + 1.3222s}$ that can be synthesized using the Cauer method (Figure 2.40).

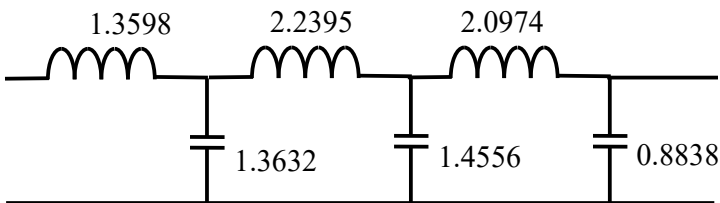


Figure 2.40. Low-pass filter synthesized from its normalized impedance z_{11}

NOTE.— Important: a number of useful MATLAB files for performing these computations based on the expression of the two polynomials f and g have been developed by the author. They can be found at the Mathworks site (<http://www.mathworks.fr/matlabcentral>) in user communities proposing file exchanges: hurwitz.m for the Hurwitzian conjugate of a polynomial; unitarh.m to determine the polynomial h ; z11sh.m; z22sh.m; z11sb.m; z22sb.m; y11sh.m; y22sh.m; y11sb.m; y22sb.m to determine the normalized elements of the ladder structure based on the result of the function chosen among the last eight and giving the maximum amount of elements.

The equivalent network to calculate $z_{11} = \frac{Z_{11}}{R_1}$ is then the following (Figure 2.41).

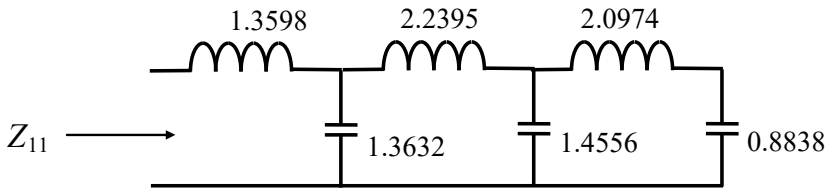


Figure 2.41. Z_{11} computation network

But we also find that $y_{22} = Y_{22}R_2$ corresponds to network shown in Figure 2.42.

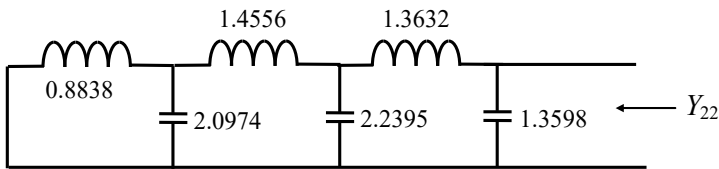


Figure 2.42. Y_{22} computation network

This implies that $r_R = \frac{R_2}{R_1} = \frac{\tau_1}{\tau_6} = \frac{\tau_3}{\tau_4} = \frac{\tau_5}{\tau_2} = 1.539$. Imposing, for example, R_1' at 140Ω and the new cutoff frequency $f_c' = 11.1 \text{ MHz}$, the final network is fully determined and sketched in Figure 2.43.

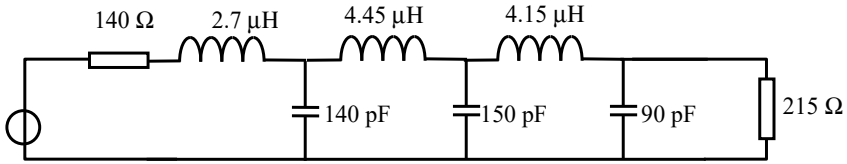


Figure 2.43. Final network of the Chebyshev sixth-order low-pass filter

EXERCISE.– Check the previous calculations.

A more rigorous and more general method for the determination of termination resistances ratio r_R relies on the computation of input and output impedances or “terminated impedances”.

In the matrix expression $\beta = s \alpha$, terminating the quadripole with the resistance R_2 yields $v_2 = -i_2$ and we still get $v_1 + i_1 = e_g$. Since $2 v_1 = e_g (1 + s_{11})$, the input impedance is deduced:

$$Z_{in} = \left. \frac{V_1}{I_1} \right|_{V_2 = -R_2 I_2} = R_1 \frac{1 + s_{11}}{1 - s_{11}} = R_1 \frac{g + h}{g - h}$$

Similarly for the output impedance at $E_g = 0$, we get $v_1 = -i_1$ and $v_2 - i_2 = s_{22} (v_2 + i_2)$. Hence:

$$Z_{out} = \left. \frac{V_2}{I_2} \right|_{V_1 = -R_1 I_1} = R_2 \frac{1 + s_{22}}{1 - s_{22}} = R_2 \frac{g \mp h_*}{g \pm h_*}$$

The polynomials appearing in these two terminated impedances are, at least for one of the two factors of the quotient, neither even nor odd. This corresponds to impedances that are not purely reactive, which is quite expected, since R_2 is included in Z_{in} and R_1 in Z_{out} . The signs to be considered for reciprocal quadripoles are the higher signs in the expression of Z_{out} . If we reason about the polynomials g and $h = h^*$ specific to the template of the low-pass filter, the zero angular frequency limit of Z_{in} or Z_{out} corresponds to a purely resistive impedance because there are only terms of degree zero in the numerator and denominator, the others being cancelled. These are obviously R_2 in the first case and R_1 in the second. Hence, a direct evaluation has been

done of the ratio r_R , which leads to the same expression both from Z_{in} and Z_{out} (higher signs):

$$r_R = \frac{R_2}{R_1} = \lim_{s=0} \left[\frac{g+h}{g-h} \right]$$

If in practice the two resistances are imposed, one will be set to the desired value and the other will be completed by adding a resistance in series (or in parallel) to bring the overall termination resistance on the port opposite to the value calculated from the ratio r_R . If none are imposed, we will be able to set any one capacitance or inductance chosen among all and then deduce the two termination resistances.

In all cases, once the template f/g is established and the synthesis achieved in normalized values, only two degrees of freedom will remain: one to choose the new cutoff frequency or center frequency, the other to choose a single element among the two resistances, or among the inductances or capacitances. Therefrom, all other elements will be computable. These two degrees of freedom derive from the independence of only two of the three polynomials f , g and h , and from the unitarity relation.

In conclusion, it is remarkable that the method exposed here makes it possible to simultaneously solve the filtering problem by synthesizing the filter that satisfies a template; and in addition, it also solves the problem of impedance matching since the elements can be calculated by taking into account the termination resistances whose ratio is, nevertheless, imposed by the nature of the filter chosen through the expression of s_{21} . Subsequently, this last restriction may be lifted by adding an ideal transformer, except for low-pass filters. In the case of narrow-band band-pass filters, the reduced bandwidth $\Delta\omega$ plays a role in the determination of the elements during the band-pass \rightarrow low-pass transformation and gives place to elements that are in a ratio close to $1/\Delta\omega^2$ (see section 2.2.2.5). This leads to filters unfeasible in practice if $\Delta\omega < 0.25$ due to the difficulty in implementing elements absolutely lossless with very different values. The impedance-image method exposed hereafter is a means to size such filters at the cost of an approximation, which is largely offset by the efficiency of the implementation and by solving the previous difficulty.

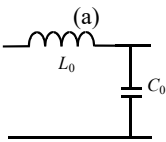
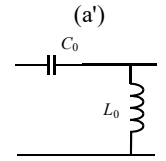
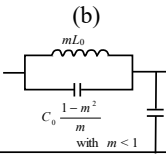
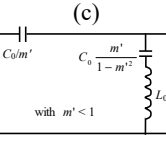
2.4.2. Synthesis based on image parameters

This method relies on the search for a device able to define an overall transfer function from the chaining of elementary quadripoles, called “elementary cells” in the following: their transmittances are themselves known and easily computable without the help of software programs. This device is image-matching and has been described in section 2.1.8. Image impedances are generally not rational and thus not implementable using passive elements. However, this does not prevent us from using them to ensure image-matching between the input and the output of two cascading elementary cells. The problem only actually appears for termination impedances for which the image-matching condition can only be approximately satisfied with the exception of certain frequencies. In the following, the characteristics of elementary low-pass, high-pass and band-pass cells will be first calculated, namely image impedances $Z_{i1} = \sqrt{\frac{Z_{11}}{Y_{11}}} = \sqrt{Z_{e0} Z_{esc}}$ and $Z_{i2} = \sqrt{\frac{Z_{22}}{Y_{22}}} = \sqrt{Z_{s0} Z_{ssc}}$ at each port and the corresponding transmission coefficients $s_i = \exp[-\Gamma] = \exp[-(\gamma + j\delta)]$ by evaluating image attenuations γ and image phase-shifts δ from $\exp[2\Gamma]$ (see section 2.1.8).

The frequency band in which we simultaneously have $\gamma = 0$ and real image impedances will be systematically assimilated to a bandwidth, whereas it will be assimilated to a stop band otherwise.

2.4.2.1. Low-pass and high-pass elementary cells

The simplest elementary cells are obviously those involving only two reactive elements. However, they have the disadvantage of presenting image impedances that vary a lot in the bandwidth and since there are no adjustable parameters, we are always driven to repeat the same cell for a low-pass or high-pass type of filter. This solution is certainly not optimal. Since image-matching must be ensured at both ports of each cell, type (a) or (a') cells should moreover be grouped together in the following table following a “head-to-tail” assembly, either in T or in Π , in order to obtain symmetrical cells presenting the same image impedance at both ports and an image attenuation Γ , which is twice that of the initial cell. It is generally preferred to also have recourse to cells presenting a resonant or antiresonant (b)- or (c)-type circuit, which combine several advantages. The network and image properties of these four cells are grouped in the following table.

Elementary cell	Z_{i1}	Z_{i2}	$\exp(\Gamma)$	Case $\omega < 1$	Case $\omega > 1$
 <p>(a)</p>	$\sqrt{s^2 + 1}$	$\frac{1}{\sqrt{s^2 + 1}}$	$\sqrt{s^2 + 1} + s$	$\gamma = 0$ $\delta = \text{asin}\omega$	$\gamma = \ln\left[\sqrt{\omega^2 - 1} + \omega\right]$ $\delta = \pi/2$
 <p>(a')</p>	$\frac{\sqrt{s^2 + 1}}{s}$	$\frac{s}{\sqrt{s^2 + 1}}$	$\frac{\sqrt{s^2 + 1} + 1}{s}$	$\gamma = \ln\left[\sqrt{\omega^2 - 1} + \omega\right]$ $\delta = -\pi/2$	$\gamma = 0$ $\delta = -\text{asin}(1/\omega)$
 <p>(b)</p>	$\frac{\sqrt{s^2 + 1}}{1 + (1 - m^2)s^2}$	$\frac{1}{\sqrt{s^2 + 1}}$	$\frac{\sqrt{s^2 + 1} + ms}{\sqrt{s^2 + 1} - ms}$	$\gamma = 0$ $\delta = \text{atan}\frac{m\omega}{\sqrt{1 - \omega^2}}$	$2\gamma = \ln\left \frac{\sqrt{\omega^2 - 1} + m\omega}{\sqrt{\omega^2 - 1} - m\omega}\right $ $\delta = \pi/2$ if $1 < \omega < \omega_\infty$ $\delta = 0$ if $\omega > \omega_\infty$
 <p>(c)</p>	$\frac{\sqrt{s^2 + 1}}{s}$	$\frac{s^2 + (1 - m'^2)}{s\sqrt{s^2 + 1}}$	$\frac{\sqrt{s^2 + 1} + m'}{\sqrt{s^2 + 1} - m'}$	$2\gamma = \ln\left \frac{\sqrt{1 - \omega^2} + m'}{\sqrt{1 - \omega^2} - m'}\right $ $\delta = 0$ if $\omega < \omega'_\infty$ $\delta = -\pi/2$ if $\omega'_\infty < \omega < 1$	$\gamma = 0$ $\delta = \text{atan}\frac{\sqrt{\omega^2 - 1}}{m'}$

Type (b) and (c) cells enable for each of them that an attenuation pole ω_∞ or ω'_∞ be introduced (or transmittance zero), whose position can be adjusted, and they present impedance images approaching a constant in the bandwidth, as this will be detailed in the following. For low-pass filters, it is possible to place elementary (a)- and (b)-cells in cascade provided that only Z_{i2} is used as image impedance, which requires the combination of two (a)-

or (b)-cells grouped in a “head-to-tail” fashion. In addition, it proves more advantageous to assemble (b)-type cells whose image impedance Z_{i1} can be much closer to a constant resistance in the bandwidth (see Figures 2.45 and 2.46), directly connected with a termination resistance. Generally speaking, if the letter “i” is added to indicate the interchanging of both ports with regard to the cells presented in the table, the logical sequence for the low-pass filter can be read as (b) (ai) (a) (bi) in Figure 2.44.

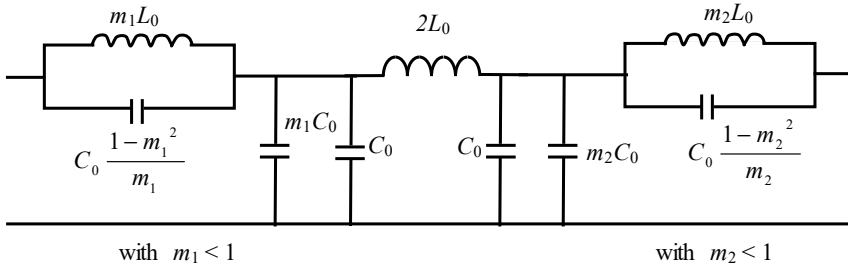


Figure 2.44. Four-cell low-pass filter, two of each type, with the same image impedance at each port, given by the expression of Z_{i1} in the previous table, provided that $m_2 = m_1$

It is also possible to use (b) (bi) (b) (bi) ... (b) (bi) in the case it is desirable to benefit from finite-frequency attenuation poles in preference to those placed at zero and infinite frequencies. Capacitances in parallel will be obviously grouped.

For high-pass cells denoted by (a'), (a'i), (c) and (ci), image-matching must use Z_{i1} . This leads to the sequence (a'i), (c), (ci) and (a'), which imposes the same parameter m' for the two central (c)- and (ci)-type cells.

The image impedances and transmittances of the table are normalized with $\omega_c = \omega_0 = 1$ rd/s as usual in this chapter. The parameters of the cell (a') are inferred from those of the cell (a) by way of the usual low-pass to high-pass transformation, namely by replacing s by $1/s$, because the capacitance and the inductance have been inverted. Conversely, this transformation is not the one that allows switching from (b) to (c) cells. The normalized attenuation poles for (b) and (c) are, respectively, $\omega_\infty = \frac{1}{\sqrt{1-m^2}}$ and $\omega'_\infty = \sqrt{1-m'^2}$, giving rise to zero transmittance.

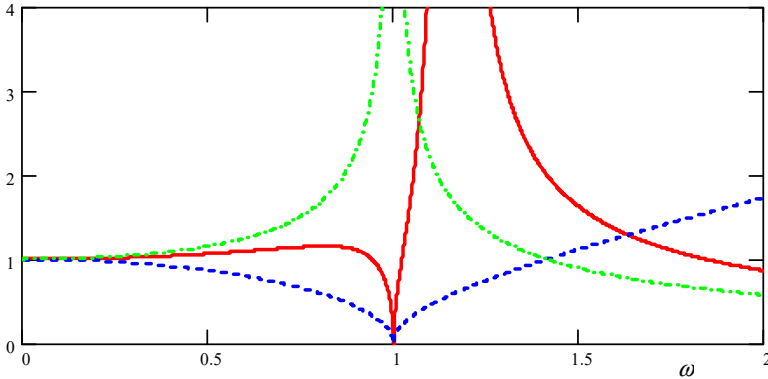


Figure 2.45. Modulus of image impedances normalized by the characteristic impedance R_0 for the low-pass (a) and (b) cells (real if $\omega < 1$, imaginary if $\omega > 1$): $Z_{i1}(b)$ in solid lines for $m = 0.5$; $Z_{i1}(a)$ in dotted line and $Z_{i2}(a) = Z_{i2}(b)$ in dash-dotted line. For a color version of this figure, see www.iste.co.uk/muret/electronics2.zip

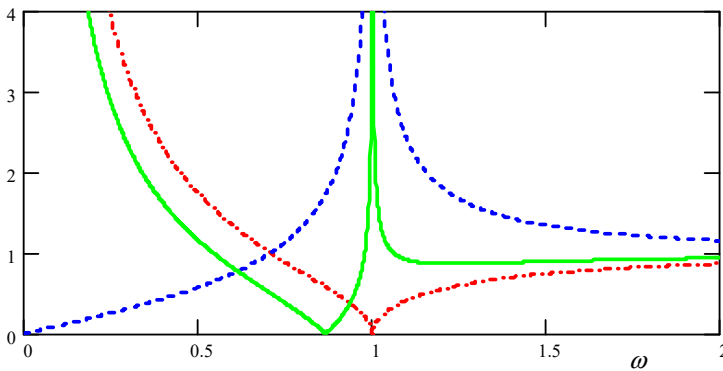


Figure 2.46. Modulus of the image impedances normalized by the characteristic impedance R_0 for high-pass cells (a') and (c) (imaginary for $\omega < 1$, real for $\omega > 1$): $Z_{i2}(c)$ in solid lines for $m' = 0.5$; $Z_{i1}(c) = Z_{i1}(a')$ in dash-dotted line and $Z_{i2}(a')$ in dotted line. For a color version of this figure, see www.iste.co.uk/muret/electronics2.zip

As it can be observed in Figures 2.45 and 2.46, the normalized impedance images in the bandwidth $Z_{ilb} = \frac{\sqrt{1-\omega^2}}{1-(1-m^2)\omega^2}$ for cell (b) and

$Z_{i2c} = \frac{\omega^2 - (1 - m'^2)}{\omega\sqrt{\omega^2 - 1}}$ for cell (c) constitute excellent approximations to a

constant resistance in 90% of the bandwidth, provided that we take $m = 0.5 = m'$. These cells will thus be systematically adopted as ending cells with values for parameters m and m' very close to $1/2$ or equal to $1/2$.

2.4.2.2. Denormalization and filter synthesis

In order to denormalize image impedances and image transmittances, the change in variable has to be carried out by shifting from ω to ω/ω_0 where $\omega_0 = 1/\sqrt{L_0 C_0}$, and by multiplying the image impedances by the characteristic impedance $R_0 = \sqrt{L_0/C_0}$. This last factor and ω_0 , the cutoff angular frequency, thus allow sizing L_0 and C_0 from the image impedance in the bandwidth, which is purely resistive, and the cutoff frequency $\omega_0/2\pi$, which determines: $C_0 = \frac{1}{R_0 \omega_0}$ and $L_0 = \frac{R_0}{\omega_0}$. Nevertheless, this operation will be carried out as a last step, once the effective attenuation is adjusted onto the template.

The main operation of the synthesis consists of determining the number and the type of cells and to choose the value of the adjustable parameter(s) m or m' . From a desired template, the procedure will be to achieve successive approximations consisting of initially determining the image attenuation that needs for a certain number of cells placed in cascade. This is achieved by analogy with Chebyshev or elliptic low-pass or high-pass filters through the matching of the number of branches of the circuit and the order of the filter and by anticipating a margin of safety with respect to the effective attenuation that needs to be achieved. Ultimately, we will verify through simulation the deviation of the actual response with those from the image impedances and the template method, and an extra iteration will be executed if deviations become too significant. In all cases, it is important to first carry out an evaluation of maximum deviations between ideal values of image attenuations obtained from s_{21} and their effective values.

In order to try to evaluate certain bounds of the deviations between the gain or the attenuation resulting from the approximation of image impedances and the same quantities that will actually be obtained, all general expressions of s -parameters (section 2.1.6) and gain or impedance (section 2.1.7.3) can be used with the image impedance normalization, except for

power calculations which will have to be excluded when image impedances are not real, which is the case in the stop band. That being said, the decisive advantage of this method is to enable us to simultaneously consider all the cells placed in cascade to evaluate an overall parameter $s_{12} = s_{21} = e^{-\Gamma}$ since normalization using image impedances implies that $s_{11} = s_{22} = 0$. Nevertheless, it is important to properly note that Z_{i2} and Z_{i1} , the image impedances to be considered, are supposed to match those of ending cells found at every port of the overall filter (therefore in the network, Figure 2.44, we have the image impedance Z_{i1} of cell (b) at each port) during the synthesis, which is not exactly the reality.

The voltage gain V_2/E_g is obtained from the expression given for v_2 according to e'_g in section 2.17.3, taking into account z_g to calculate e_g :

$$\frac{V_2}{E_g} = \sqrt{\frac{Z_{i2}}{Z_{i1}}} \frac{s_{21}}{1 - r_g r_u s_{12} s_{21}} \frac{r_u + 1}{z_g + 1}.$$

The mismatching factor of the voltage gain $\lambda_v = \sqrt{\frac{Z_{i2}}{Z_{i1}}} \frac{1}{1 - r_g r_u s_{12} s_{21}} \frac{r_u + 1}{z_g + 1}$

relative to s_{21} is equal to $\frac{1}{2} \sqrt{\frac{Z_{i2}}{Z_{i1}}}$ when the image-matching is implemented, as a result of $r_g = r_u = 0$ and $z_g = 1$.

It is also possible to evaluate the current gain from the ratio i_2/i_1 given in section 2.1.7.3, still with $s_{11} = s_{22} = 0$: $\frac{I_2}{I_1} = \sqrt{\frac{Z_{i1}}{Z_{i2}}} \frac{s_{21}(1 - r_u)}{1 - r_u s_{12} s_{21}}$. The deviation

with respect to s_{21} is measured using the mismatching factor of the current gain $\lambda_i = \sqrt{\frac{Z_{i1}}{Z_{i2}}} \frac{1 - r_u}{1 - r_u s_{12} s_{21}}$, which can be reduced to $\sqrt{\frac{Z_{i1}}{Z_{i2}}}$ when matching

occurs. The product of these two factors will affect the overall power gain and thus will be equal to $\frac{1}{2}$ in the event of a match $R_u = Z_{i2}$ and $R_g = Z_{i1}$,

which is equivalent to the result $\frac{|V_2|^2}{R_2} = |s_{21}|^2 \frac{|E_g|^2}{4R_1}$ mentioned in section 2.1.7.2

in the case of the match $R_g = Z_{i1} = R_1$ and $R_u = Z_{i2} = R_2$ because then $|I_1| = |E_g|/(2R_1)$ and $|I_2| = |V_2|/R_2$. If the modulus of their product is larger than

$\frac{1}{2}$, the true power gain will be increased and the true attenuation will be reduced with regard to the image values or, on the other hand, vice versa.

In general, for the calculation of these two mismatch factors, it will be necessary to take into account effective termination impedances that should

be assumed to be real, equal to R_g and R_u , which gives $z_g = \frac{R_g}{Z_{i1}}$; $z_u = \frac{R_u}{Z_{i2}}$;

$r_g = \frac{R_g - Z_{i1}}{R_g + Z_{i1}}$; $r_u = \frac{R_u - Z_{i2}}{R_u + Z_{i2}}$ from which it can be inferred that:

$$\lambda_v = \frac{2R_u}{R_u + Z_{i2}} \frac{\sqrt{Z_{i1}Z_{i2}}}{R_g + Z_{i1}} \frac{1}{1 - r_g r_u e^{-2\Gamma}}$$

$$\lambda_i = \sqrt{\frac{Z_{i1}}{Z_{i2}}} \frac{1 - r_u}{1 - r_u s_{12} s_{21}} = \frac{2\sqrt{Z_{i1}Z_{i2}}}{R_u + Z_{i2}} \frac{1}{1 - r_u e^{-2\Gamma}}$$

NOTE.— Important: These factors and previous gains become meaningless at the cutoff frequency, because the normalization enabling the computation of the s -parameters has been made using Z_{i1} and Z_{i2} , which become either zero or infinite. On the other hand, outside of this particular frequency, the analysis of deviations between effective attenuation and image attenuation can be performed, differently however, depending on whether the bandwidth or the stop band is under consideration.

In the stop band, impedances Z_{i1} and Z_{i2} are purely imaginary and accordingly the power gain is not given by the product between voltage and current gains, but this does not prevent an estimate of the mismatch factors in modulus being obtained for each of them. Since the image attenuation e^Γ is much larger than 1, the factors $1 - r_g r_u e^{-2\Gamma}$ and $1 - r_u e^{-2\Gamma}$ are close to 1. We define that $Z_{i1} = jX_1$ and $Z_{i2} = jX_2$, which leads to

$$|\lambda_v| = 2\sqrt{\frac{R_u}{R_g}} \frac{\sqrt{R_g X_1}}{\sqrt{R_g^2 + X_1^2}} \frac{\sqrt{R_u X_2}}{\sqrt{R_u^2 + X_2^2}}, \text{ which is maximum when } R_g = X_1 \text{ and } R_u =$$

$$X_2 \text{ and is equal to } \sqrt{\frac{R_u}{R_g}}. \text{ Similarly, } |\lambda_i| = 2\sqrt{\frac{X_1}{R_u}} \frac{\sqrt{R_u X_2}}{\sqrt{R_u^2 + X_2^2}} \text{ equals } \sqrt{2} \sqrt{\frac{R_g}{R_u}} \text{ at}$$

the maximum under the same conditions. The product of the two thus gives

an overall factor $\sqrt{2}$ which is $2\sqrt{2}$ times larger than the factor $\frac{1}{2}$ that we get when there is a match and reflects an effective attenuation deficit of $10\log(2\sqrt{2}) = 4.5$ dB compared to the image attenuation. This would require the anticipation of a safety margin with respect to the desired final template. In fact, since conditions $R_g = X_1$ and $R_u = X_2$ take place very close to the cut-off frequency, as it can be seen in Figures 2.45 and 2.46, because R_g and R_u are very close to R_0 for a later-discussed reason, the most important consequence is that this attenuation deficit with regard to the image attenuation may push the cut-off frequency toward higher values for the low-pass filter or toward lower ones for the high-pass filter. It will thus be necessary to be cautious when addressing the assessment of the image cutoff frequency compared to the one desired in reality. On the other hand, when ratios R_g/X_1 and R_u/X_2 or inverse ratios exceed about $\sqrt{2}$, a true attenuation greater than the image attenuation is obtained and it is no longer necessary to take a safety margin. It can thus be concluded that in reality, a cutoff frequency offset and a transition band should appear between the bandwidth and the stop band that did not exist in the image attenuation.

NOTE.— Important: This conclusion, however, must be tempered by the approximate nature of the correction affected with mismatching factors that do not take into account the presence of terminations other than constant resistances in the previous computation. Moreover, this is only achieved in the case of a single-cell filter since, for a multiple-cell filter, the terminations of each cell are the dipole impedances of adjacent cells, except at the ends of the filter. Therefore, less severe corrections are expected as well as a performance that better approximates the actual attenuation to the image attenuation, as we will see in the practical examples that follow.

In the case of a filter solely made up of (b)- or (c)-cells, it is important to know the asymptotic value of the image attenuation, which can be derived from the stop band values of γ given in the table of the previous section. For a set of n pairs of (b)(bi)-cells with parameter $m_1, m_2, \dots, m_i \dots, m_n$ and with ω tending to infinity, a total image attenuation of $20\sum_{i=1}^n \log \frac{1+m_i}{1-m_i}$ is obtained, taking into account the proportionality of the power gain to $|s_i|^2$, after converting into decibels. It is therefore helpful to choose values for the parameter m_i close to 1 to increase the stop band image attenuation.

In the bandwidth, the impedances Z_{i1} and Z_{i2} are real and it is therefore possible to carry out an accurate calculation of mismatch factors that will reflect the effective ripple, the image attenuation being zero as well as its ripple. As a first step, we can find out what the frequencies make the modulus of the overall mismatch factor equal to 1/2. As previously seen, these frequencies correspond, on the one hand, to the match $R_u = Z_{i2}$ and $R_g = Z_{i1}$. To obtain this match and thus to benefit from an additional finite-frequency attenuation zero, we will place R_g and R_u slightly above R_0 in the case of the low-pass filter whose end cells are (b) and (bi), that is $R_g = R_u = \mu R_0$ (with $\mu > 1$) or slightly below in the case of the high-pass, namely $R_g = R_u = \mu' R_0$ (with $\mu' < 1$), which will also impose two identical parameters m_1 or m_1' identical at the ends of the filter, therefore two symmetric end cells. Coefficients r_g and r_u will be close to zero, much smaller than 1 in absolute value. In addition, since the image impedance is very close to a constant value and equal to R_0 when m_1 or m_1' is equal to 0.5, this numerical value will be retained, at least as a first approximation.

On the other hand, additional attenuation zeros appear due to the presence of factors $1 - r_g r_u e^{-2\Gamma}$ and $1 - r_u e^{-2\Gamma}$, which cannot be neglected in the denominators of λ_v and λ_i in the bandwidth. Since the image attenuation γ is zero in the exponents of $\exp[-2\Gamma] = \exp[-2(\gamma + j\delta)]$, the exponent is purely imaginary and corresponds to the single image phase-shift, which allows us to write:

$$\lambda_v \lambda_i = \frac{1}{z_g + 1} \frac{1 + r_u}{1 - r_g r_u e^{-2j\delta}} \frac{1 - r_u}{1 - r_u e^{-2j\delta}}$$

As seen in the previous section, r_g and r_u are real and less than 1 in absolute value in the bandwidth. The factors existing in the denominator thus oscillate between $1 - r_g r_u$ and $1 + r_g r_u$ for the first, $1 - r_u$ and $1 + r_u$ for the second, respectively, for $\delta = k\pi$ and for $\delta = (2k+1)\frac{\pi}{2}$. It can be concluded therefore that there will be increasingly more effective attenuation oscillations as the variation of the image phase-shift will be larger in the bandwidth, in other words when the number of cells will be more significant. For symmetrical terminal cells (Z_{i1} of cell b) and for equal termination resistances ($R_u = R_g$), we obtain with $\delta = k\pi$:

$$[\lambda_v \lambda_i]_{\delta=k\pi} = \frac{1+r_u}{1+z_g} \frac{1}{1-r_g r_u} = \frac{R_u Z_{i1}}{R_u Z_{i1} + R_g Z_{i2}} = \frac{1}{2}$$

as in the image-matching case. In the case where $\delta = (2k+1)\frac{\pi}{2}$:

$$[\lambda_v \lambda_i]_{\delta=(2k+1)\pi/2} = \frac{1}{1+z_g} \frac{1-r_u}{1+r_g r_u} = \frac{Z_{i1} Z_{i2}}{Z_{i1} Z_{i2} + R_g R_u} = \left(1 + \mu^2 \frac{[1 - (1-m^2)\omega^2]^2}{1-\omega^2} \right)^{-1},$$

the last equality applying to the case of the (b)- and (bi)-type cell of the low-pass filter.

The envelope of the ripple in the bandwidth is thus computable using the ratio of the product of the mismatch factors for image phase-shifts $\delta=k\pi$

and $\delta=(2k+1)\frac{\pi}{2}$. We get: $\Omega = \frac{1}{2} \left\{ 1 + \mu^2 \frac{[1 - (1-m^2)\omega^2]^2}{1-\omega^2} \right\}$, which takes the

value 1 at each image-matching case, occurring twice in the bandwidth as it can be observed in Figure 2.47. Nevertheless, in addition, $\lambda_v \lambda_i$ will also assume the value 1/2, resulting in an attenuation zero, every time the phase-shift image will be equal to $\delta=k\pi$. This phase shift either corresponds to a direct link (k is even or zero, as for $\omega = 0$), or to crossing connections between the two ports of the quadripole (k is odd) since the image attenuation is zero. It is then logical that effective attenuation be also zero for these angular frequencies that are called antiphase zeros.

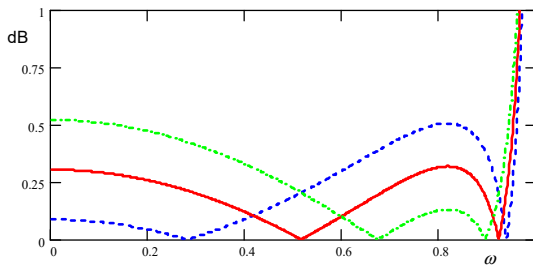


Figure 2.47. Ripple envelope in the bandwidth of low-pass filters of parameter $m_1 = 0.5$ characterizing the end cells for three values of the parameter $\mu = 1.02; 1.07; 1.12$ in ascending order of the values at $\omega = 0$ (respectively, in dotted line, solid line and dash-dotted line). For a color version of this figure, see www.iste.co.uk/muret/electronics2.zip

The absolute value of 10 times the decimal logarithm of Ω gives the envelope of the ripple in the bandwidth, which does not exceed 0.3 dB in the interval of normalized angular frequency $[0; 0.9]$ in the most favorable case. This corresponds to a choice of the ratio of termination resistances and the characteristic impedance $\mu = 1.07$ when $m_1 = 0.5$ as it can be seen in Figure 2.47. The antiphase zeros are increasingly tightened as the normalized angular frequency progresses from zero to one, because of the expression of the total image phase shift, corresponding to $2 \sum_{i=1}^n \operatorname{atan} \left(\frac{m_i \omega}{\sqrt{1-\omega^2}} \right)$ for n pairs of cells of type (b)-(bi). The value of each term $\operatorname{atan} \left(\frac{m_i \omega}{\sqrt{1-\omega^2}} \right)$ for $\omega = 1$ being $\frac{\pi}{2}$, there will be n antiphase zeros in the bandwidth, namely as many as cell pairs, the first being still located at $\omega = 0$.

Nonetheless, here again, this calculation of the ripple in the bandwidth has been obtained assuming that for each cell, the two termination resistances were constant. This is, however, no longer achieved when the number of cells is greater than one, because each cell is then terminated by the impedance presented by the neighboring cell at one of the ports, or even at both ports. Furthermore, we thus approach the ideal condition of termination impedance identical to the image impedance with a number of cells that increases proportionally as the number of cells itself becomes more significant. As a result, it can be concluded that the previous calculation of the ripple indicates an upper bound of the actual ripple and that it gives an all the more pessimistic indication with more significant numbers of cells. In other words:

NOTE.— The actual attenuation ripple in the bandwidth will be the smallest compared to Ω with a greater number of cells.

EXAMPLE.— Low-pass filter with pairs of cells of type (b) (bi)

Given a template enforcing an effective attenuation of 52 dB above the normalized angular frequency $\omega_2 = 1.5$ and an actual ripple not exceeding 0.2 dB in the bandwidth. This last condition is stricter than in the example addressed with the exact method of effective parameters, in which a fourth-order elliptic filter had been employed, giving a ripple of 1 dB. If the value

$m_1 = 0.5$ is retained for both terminal cells with the aim of ensuring the best possible match to the end ports, we obtain $20 \log \frac{1+m_1}{1-m_1} = 9.4$ dB of attenuation with infinite angular frequency and an attenuation pole at $\omega_{\infty 1} = 1.15$. Therefore, 43 dB are missing which would be difficult to recover by solely adding a pair of cells. We therefore prefer to rely on the following network (Figure 2.48), which includes three pairs of cells of types (b) (bi).

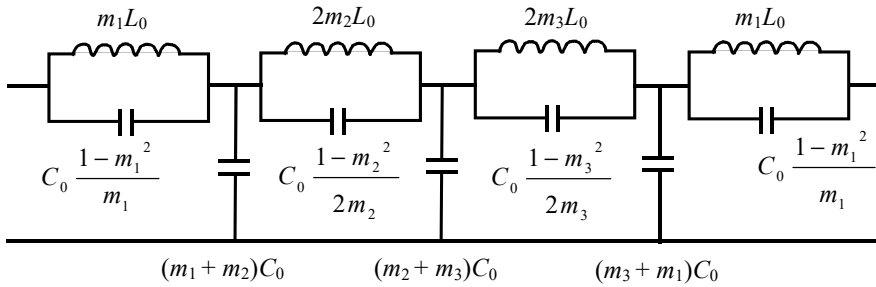


Figure 2.48. Schematic of a low-pass filter, symmetrical and composed of two doubled cells of type (b)-(bi) and two simple terminal (b) and (bi) cells. Terminations are not illustrated

It is useful to place an attenuation pole in the vicinity of ω_2 , which results in a value of m_2 close to 0.7, providing an additional 15 dB of attenuation. There are 28 dB that remain to be attributed to the cell characterized by a parameter m_3 , which then assumes the value 0.92.

The final step is denormalization which is performed based on the characteristic impedance inferred from $R_g = R_u = \mu R_0$ (with $\mu = 1.07$), $R_0 = \sqrt{L_0/C_0}$ and the cutoff frequency $\omega_0 = 1/\sqrt{L_0 C_0}$ which is to be obtained. If for example we have $R_g = R_u = 75 \Omega$ and $\omega_0 = 2\pi \times (6 \text{ MHz})$, it is deduced that $R_0 = 70 \Omega$, and it is calculated that $L_0 = 1.859 \mu\text{H}$ and $C_0 = 378.4 \text{ pF}$; then all the elements shown in Figure 2.48 from the expressions included in it as well as the numeric value of the parameters. The Bode diagram calculated from the image attenuation and that obtained through simulation is shown in Figure 2.49.

It can be noted that the template that imposed at least 52 dB of attenuation in the stop band beyond the reduced frequency 1.5 is enforced since we have -58 dB at most for the highest lobe of the transmittance, compared to -6 dB in the bandwidth, and that this is obtained from the reduced frequency of 1.2. The simulation gives a normalized cutoff frequency for a 3 dB relative attenuation (that is to say for an absolute transmittance of -9 dB) of 0.996; namely only 4% of deviation from the theoretical value, and therefore, it is not necessary to redo a calculation of the elements by applying a correction. The improvement of the ripple in the bandwidth with regard to the upper bound given by the ratio Ω is very significant, as shown in Figure 2.50, since the actual maximal ripple is only 0.04 dB within 95% of the bandwidth against a theoretical value approximately 10 times larger, as shown in Figure 2.47.

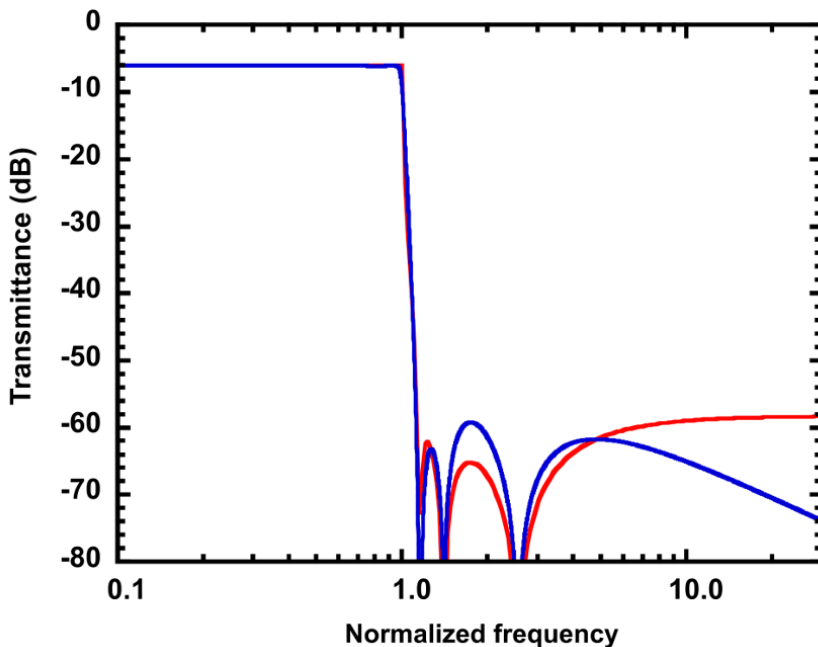


Figure 2.49. Image-transmittance in red and actual transmittance in blue for the low-pass filter synthesized in this section. For a color version of this figure, see www.iste.co.uk/muret/electronics2.zip

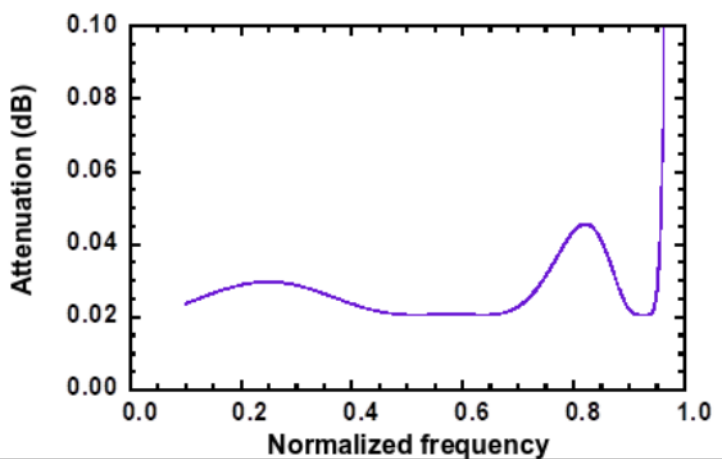


Figure 2.50. Deviation of the actual attenuation in the bandwidth with respect to 6 dB for the low-pass filter synthesized in this section

2.4.2.3. Elementary band-pass cells

These cells make it possible to define a bandwidth between the upper cutoff angular frequency ω_{sup} and the lower cutoff frequency ω_{inf} and in addition to introduce an attenuation pole located either in the lower stop band, or in the upper stop band. They are symmetric, which simplifies matching since the image impedances are the same at each port. According to the desired template, we will either be able to combine them or not and add them to additional low-pass or high-pass cells studied in the following section if we want to benefit from attenuation poles at zero and/or infinite frequencies. The first cell, denoted by (d), is drawn in Figure 2.51.

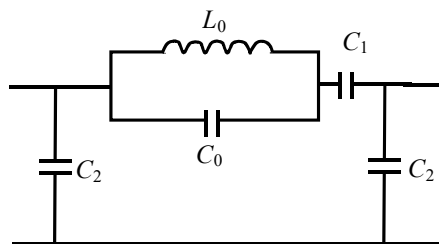


Figure 2.51. Elementary type-(d) band-pass cell, with an attenuation pole in the upper lateral stop band

Let $a_1 = C_1/C_0$; $a_2 = C_2/C_0$; the attenuation pole $\omega_\infty = 1/\sqrt{L_0 C_0}$; and the image-impedance is determined from Z_{11} and Y_{11} :

$$Z_{id} = Z_{i1} = Z_{i2} = \frac{1}{\sqrt{C_1 C_2} s} \sqrt{\frac{(1+a_1)s^2 + \omega_\infty^2}{\left(2+a_2 + \frac{a_2}{a_1}\right)s^2 + \left(2 + \frac{a_2}{a_1}\right)\omega_\infty^2}}$$

$$\text{then } \coth \Gamma_d = \frac{a_1 + a_2 + a_1 a_2}{\sqrt{a_1 a_2} \sqrt{1+a_1}} \frac{s^2 + \omega_1^2}{\sqrt{\left(2+a_2 + \frac{a_2}{a_1}\right)s^2 + \left(2 + \frac{a_2}{a_1}\right)\omega_\infty^2}}$$

$$\text{with } \omega_1^2 = \omega_\infty^2 \frac{a_1 + a_2}{a_1 + a_2 + a_1 a_2}; \quad \omega_2^2 = \omega_\infty^2 \frac{2a_1 + a_2}{2a_1 + a_2 + a_1 a_2}; \quad \omega_3^2 = \frac{\omega_\infty^2}{1+a_1}.$$

The squared image attenuation is:

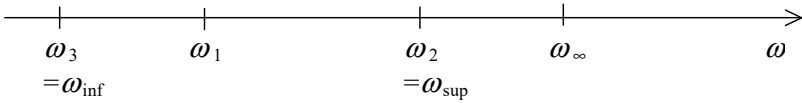
$$\exp(2\Gamma_d) = \frac{K_d (\omega_1^2 - \omega^2) + \sqrt{(\omega_2^2 - \omega^2)(\omega_3^2 - \omega^2)}}{K_d (\omega_1^2 - \omega^2) - \sqrt{(\omega_2^2 - \omega^2)(\omega_3^2 - \omega^2)}}$$

(with eventual change of sign from terms including K_d factor) where it is established that:

$$K_d = \frac{a_1 + a_2 + a_1 a_2}{\sqrt{(a_2 + a_1 a_2)(2a_1 + a_2 + a_1 a_2)}} = \frac{C_1 C_0 + C_2 C_0 + C_1 C_2}{\sqrt{(C_2 C_0 + C_1 C_2)(2C_1 C_0 + C_2 C_0 + C_1 C_2)}}.$$

Due to the previous expressions of angular frequency, the conditions are the following: $\omega_3 < \omega < \omega_2 < \omega_\infty$ as sketched further.

With harmonic behavior, when $\omega_3 < \omega < \omega_2$, $\exp(2\Gamma_d)$ is complex, with modulus equal to 1 because square roots are imaginary and therefore numerator and denominator are complex conjugates. There is thus no image attenuation between angular frequencies ω_3 and ω_2 , which then define bandwidth $[\omega_3, \omega_2] = [\omega_{\text{inf}}, \omega_{\text{sup}}]$:



Conversely, outside the bandwidth $[\omega_3, \omega_2]$, the differences under the radicals of $\exp(2\Gamma_d)$ have the same sign, therefore the radicals are real and so is $\exp(2\Gamma_d)$, hence an image attenuation $\gamma = \frac{1}{2} \ln[e^{2\Gamma_d}]$. Therefore, let $\omega_3 = \omega_{\text{inf}}$, $\omega_2 = \omega_{\text{sup}}$ and $\exp(2\Gamma_d)$ is rewritten as: $\exp(2\Gamma_d) = \frac{\pm K_d (\omega_1^2 - \omega^2) + \sqrt{(\omega_{\text{sup}}^2 - \omega^2)(\omega_{\text{inf}}^2 - \omega^2)}}{\pm K_d (\omega_1^2 - \omega^2) - \sqrt{(\omega_{\text{sup}}^2 - \omega^2)(\omega_{\text{inf}}^2 - \omega^2)}}$, the chosen determination has to ensure $\Gamma_d > 0$ in each stop band.

The image impedance takes the form

$$Z_{id} = \sqrt{\frac{C_0 + C_1}{C_2(C_0 C_2 + C_1 C_2 + 2C_1 C_0)}} \frac{1}{s} \sqrt{\frac{s^2 + \omega_{\text{inf}}^2}{s^2 + \omega_{\text{sup}}^2}}$$

In the bandwidth with harmonic behavior: $Z_{id}(\omega) = Z_{i0} \frac{\omega_{\text{sup}}}{\omega} \sqrt{\frac{\omega^2 - \omega_{\text{inf}}^2}{\omega_{\text{sup}}^2 - \omega^2}}$ where

we have defined $\omega_0^2 = \omega_3 \omega_2 = \omega_{\text{inf}} \omega_{\text{sup}}$ and $Z_{i0} = Z_{id}(\omega_0) = \sqrt{\frac{(C_0 + C_1)L_0}{C_2(C_2 + 2C_1)}}$. The

angular frequency ω_1 gives an effective attenuation equal to zero in the bandwidth by analogy with the case of the antiphase zeros described in the (b)-(bi)-type cells, because the image phase-shift equals $\frac{\pi}{2}$ for $\omega = \omega_1$. This implies that there are effective transmittance ripples in the bandwidth. Outside the bandwidth, the denominator and the numerator of the last radical have the same sign. The two radicals are thus real and the factor $1/j\omega$ makes the image impedance purely imaginary.

We must address in a similar way the type (e) band-pass cell, with an attenuation pole in the lower lateral stop band, as shown in Figure 2.52. Let us establish $a'_1 = C'_1/C'_0$; $a'_2 = C'_2/C'_0$; $\omega'_\infty = 1/\sqrt{L'_0 C'_0}$.

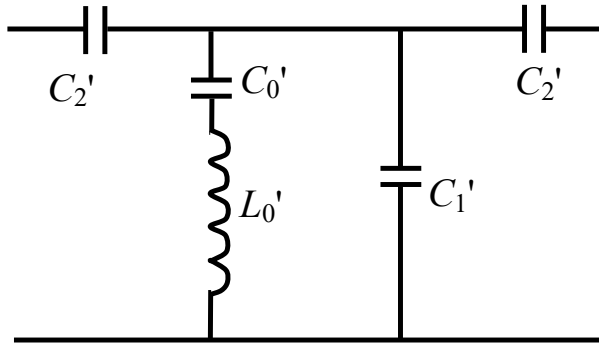


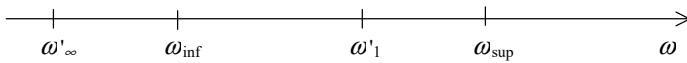
Figure 2.52. Elementary type (e) band-pass cell, with an attenuation pole in the lower lateral stop band

Similarly to the previous case (d), it is determined that:

$$Z_{ie} = \frac{1}{C_2' s} \sqrt{\frac{(a_1' + 2a_2')s^2 + (1 + a_1' + 2a_2')\omega_\infty'^2}{a_1's^2 + (1 + a_1')\omega_\infty'^2}} = \frac{1}{C_2' s} \sqrt{\frac{C_1' + 2C_2'}{C_1'}} \sqrt{\frac{s^2 + \omega_{\text{inf}}'^2}{s^2 + \omega_{\text{sup}}'^2}}$$

with $\omega_\infty'^2 = \frac{1}{L_0' C_0'}$; $\omega_1'^2 = \omega_\infty'^2 \frac{C_0' + C_1' + C_2'}{C_1' + C_2'}$; $\omega_{\text{inf}}'^2 = \omega_\infty'^2 \frac{C_0' + C_1' + 2C_2'}{C_1' + 2C_2'}$;

$\omega_{\text{sup}}'^2 = \omega_\infty'^2 \frac{C_0' + C_1'}{C_1'}$ and the following order according to the various angular frequencies:



We also obtain:

$$\coth \Gamma_e = K_e \frac{s^2 + \omega_1'^2}{\sqrt{(s^2 + \omega_{\text{sup}}'^2)(s^2 + \omega_{\text{inf}}'^2)}} \quad \text{with} \quad K_e = \frac{a_1' + a_2'}{\sqrt{a_1'(a_1' + 2a_2')}} = \frac{C_1' + C_2'}{\sqrt{C_1'(C_1' + 2C_2')}}$$

In the harmonic regime: $Z_{ie}(\omega) = Z'_{i0} \frac{\omega_{\text{sup}}}{\omega} \sqrt{\frac{\omega^2 - \omega_{\text{inf}}^2}{\omega_{\text{sup}}^2 - \omega^2}}$ where we have

$$\text{defined } Z'_{i0} = Z_{ie}(\omega_0) = \sqrt{\frac{C'_0(C'_1 + 2C'_2)L'_0}{C_2'^2(C'_0 + C'_1)}} \text{ and } \omega_0'^2 = \omega_{\text{inf}}\omega_{\text{sup}}.$$

The squared image attenuation is calculated as previously from $\coth(\Gamma_e)$ by replacing s by $j\omega$ and is written as:

$$\exp(2\Gamma_e) = \frac{\pm K_e(\omega_1'^2 - \omega^2) + \sqrt{(\omega_{\text{sup}}^2 - \omega^2)(\omega_{\text{inf}}^2 - \omega^2)}}{\pm K_e(\omega_1'^2 - \omega^2) - \sqrt{(\omega_{\text{sup}}^2 - \omega^2)(\omega_{\text{inf}}^2 - \omega^2)}}, \text{ by choosing the sign}$$

that renders Γ_e positive in every stop band.

The expressions of image attenuation and image impedance are then highly similar for the two (d) and (e) cells regarding the dependence with respect to the variable ω and only differ by certain constants. The angular frequencies ω_{inf} and ω_{sup} that define the bandwidth $[\omega_{\text{inf}}, \omega_{\text{sup}}]$ obviously must be the same for both cells.

The image adaptation between the two cells then requires the equality:

$$Z_{i0} = Z'_{i0} = R_0,$$

where R_0 will represent the effective termination resistance at each port, which can be described also as iterative resistance.

The effective adaptation will be achieved only for $\omega = \omega_0 = \omega_0' = \sqrt{\omega_{\text{inf}}\omega_{\text{sup}}}$, while $Z_i(\omega) = Z_{id}(\omega) = Z_{ie}(\omega)$ will be smaller than R_0 between ω_{inf} and ω_0 (zero value for $\omega = \omega_{\text{inf}}$) and will be larger than R_0 between ω_0 and ω_{sup} (infinite value for $\omega = \omega_{\text{sup}}$).

Since there are four passive elements in each cell, if we set the iterative resistance R_0 and the two angular frequencies ω_{inf} and ω_{sup} , only a single free parameter remains, which is obviously the attenuation pole of the cell, that is to say ω_{∞} or ω_{∞}' . It is then possible to directly establish the expressions of the elements based on the values of the four parameters R_0 , ω_{inf} , ω_{sup} and ω_{∞} or ω_{∞}' from the previous equations.

For the cell of type (d), with an attenuation pole in the upper stop band, we find:

$$C_0 = \frac{\omega_{\text{inf}}}{2R_0(\omega_{\infty}^2 - \omega_{\text{inf}}^2)} \left[\frac{\omega_{\text{sup}}}{\omega_{\text{inf}}} \sqrt{\frac{\omega_{\infty}^2 - \omega_{\text{inf}}^2}{\omega_{\infty}^2 - \omega_{\text{sup}}^2}} - \frac{\omega_{\text{inf}}}{\omega_{\text{sup}}} \sqrt{\frac{\omega_{\infty}^2 - \omega_{\text{sup}}^2}{\omega_{\infty}^2 - \omega_{\text{inf}}^2}} \right];$$

$$C_1 = \frac{1}{2R_0\omega_{\text{inf}}} \left[\frac{\omega_{\text{sup}}}{\omega_{\text{inf}}} \sqrt{\frac{\omega_{\infty}^2 - \omega_{\text{inf}}^2}{\omega_{\infty}^2 - \omega_{\text{sup}}^2}} - \frac{\omega_{\text{inf}}}{\omega_{\text{sup}}} \sqrt{\frac{\omega_{\infty}^2 - \omega_{\text{sup}}^2}{\omega_{\infty}^2 - \omega_{\text{inf}}^2}} \right];$$

$$C_2 = \frac{1}{R_0\omega_{\text{sup}}} \sqrt{\frac{\omega_{\infty}^2 - \omega_{\text{sup}}^2}{\omega_{\infty}^2 - \omega_{\text{inf}}^2}}; \quad L_0 = \frac{1}{C_0\omega_{\infty}^2}.$$

For the cell of type (e), with an attenuation pole in the lower stop band, we get:

$$C'_0 = \frac{2}{R_0\omega'_{\infty}} \left[\frac{\omega_{\text{sup}}}{\omega'_{\infty}} - \frac{\omega'_{\infty}}{\omega_{\text{sup}}} \right] \sqrt{\frac{(\omega_{\text{sup}}^2 - \omega_{\infty}'^2)(\omega_{\text{inf}}^2 - \omega_{\infty}'^2)}{(\omega_{\text{sup}}^2 - \omega_{\text{inf}}^2)}};$$

$$C'_1 = \frac{2\sqrt{(\omega_{\text{sup}}^2 - \omega_{\infty}'^2)(\omega_{\text{inf}}^2 - \omega_{\infty}'^2)}}{R_0\omega_{\text{sup}}(\omega_{\text{sup}}^2 - \omega_{\text{inf}}^2)};$$

$$C'_2 = \frac{1}{R_0\omega_{\text{sup}}} \sqrt{\frac{\omega_{\text{sup}}^2 - \omega_{\infty}'^2}{\omega_{\text{inf}}^2 - \omega_{\infty}'^2}}; \quad L'_0 = \frac{1}{C'_0\omega_{\infty}'^2}.$$

These expressions therefore allow us to size the elements in each cell based on the parameters chosen for the bandwidth, the iterative resistance and the attenuation pole.

In return, the expressions of the necessary parameters to calculate the image attenuations can be determined according to the angular frequencies, that only define the filters, that is to say the boundaries of the bandwidth ω_{inf} , ω_{sup} and the attenuation pole ω_{∞} or ω'_{∞} .

$$\text{For type (d): } K_d = \frac{2\omega_{\infty}^2 - \omega_{\text{inf}}^2 - \omega_{\text{sup}}^2}{2\sqrt{(\omega_{\infty}^2 - \omega_{\text{inf}}^2)(\omega_{\infty}^2 - \omega_{\text{sup}}^2)}} \quad \text{and} \quad \omega_1 = \sqrt{\frac{\omega_{\infty}^2(\omega_{\text{sup}}^2 + \omega_{\text{inf}}^2) - 2\omega_{\text{sup}}^2\omega_{\text{inf}}^2}{2\omega_{\infty}^2 - \omega_{\text{inf}}^2 - \omega_{\text{sup}}^2}}.$$

$$\text{For type (e): } K_e = \frac{\omega_{\text{inf}}^2 + \omega_{\text{sup}}^2 - 2\omega_{\infty}^2}{2\sqrt{(\omega_{\text{inf}}^2 - \omega_{\infty}^2)(\omega_{\text{sup}}^2 - \omega_{\infty}^2)}} \text{ and } \omega_1 = \sqrt{\frac{2\omega_{\text{inf}}^2\omega_{\text{sup}}^2 - \omega_{\infty}^2(\omega_{\text{sup}}^2 + \omega_{\text{inf}}^2)}{\omega_{\text{inf}}^2 + \omega_{\text{sup}}^2 - 2\omega_{\infty}^2}}.$$

Based on these expressions, it is easy to determine the asymptotic behaviors of the image attenuation in the stop bands. For type (d), when $\omega \rightarrow 0$:

$$\exp(2\Gamma_{d0}) = \frac{K_d\omega_1^2 + \omega_{\text{sup}}\omega_{\text{inf}}}{K_d\omega_1^2 - \omega_{\text{sup}}\omega_{\text{inf}}} \text{ gives } \exp(\Gamma_{d0}) = \frac{\frac{\omega_{\text{sup}}}{\omega_{\text{inf}}}\sqrt{\frac{\omega_{\infty}^2 - \omega_{\text{inf}}^2}{\omega_{\infty}^2 - \omega_{\text{sup}}^2}} + 1}{\frac{\omega_{\text{sup}}}{\omega_{\text{inf}}}\sqrt{\frac{\omega_{\infty}^2 - \omega_{\text{inf}}^2}{\omega_{\infty}^2 - \omega_{\text{sup}}^2}} - 1}$$

For $\omega \rightarrow \infty$, we simply get $\exp(2\Gamma_{d\infty}) = \frac{K_d + 1}{K_d - 1}$ by choosing the negative determination in front of K_d in the general expression, which yields

$$\exp(\Gamma_{d\infty}) = \frac{\sqrt{\frac{\omega_{\infty}^2 - \omega_{\text{inf}}^2}{\omega_{\infty}^2 - \omega_{\text{sup}}^2}} + 1}{\sqrt{\frac{\omega_{\infty}^2 - \omega_{\text{inf}}^2}{\omega_{\infty}^2 - \omega_{\text{sup}}^2}} - 1}.$$

$$\text{For type (e), where } \omega \rightarrow 0: \exp(\Gamma_{e0}) = \frac{\frac{\omega_{\text{inf}}}{\omega_{\text{sup}}}\sqrt{\frac{\omega_{\text{sup}}^2 - \omega_{\infty}^2}{\omega_{\text{inf}}^2 - \omega_{\infty}^2}} + 1}{\frac{\omega_{\text{inf}}}{\omega_{\text{sup}}}\sqrt{\frac{\omega_{\text{sup}}^2 - \omega_{\infty}^2}{\omega_{\text{inf}}^2 - \omega_{\infty}^2}} - 1}; \text{ and when}$$

$$\omega \rightarrow \infty, \exp(\Gamma_{e\infty}) = \frac{\sqrt{\frac{\omega_{\text{sup}}^2 - \omega_{\infty}^2}{\omega_{\text{inf}}^2 - \omega_{\infty}^2}} + 1}{\sqrt{\frac{\omega_{\text{sup}}^2 - \omega_{\infty}^2}{\omega_{\text{inf}}^2 - \omega_{\infty}^2}} - 1}.$$

The asymptotic image attenuations in dB are therefore obtained by taking 20 times the decimal logarithm of the previous quantities, which are nothing other than the asymptotic expressions of the $|S_{21}|$ of the image transmittance.

2.4.2.4. Complementary low-pass and high-pass cells adapted to the band-pass cells

These cells provide a means to add a zero or infinite frequency attenuation pole. They must have one of their image impedances identical to that of the previous band-pass cells, namely $Z_i(\omega)$. The networks that satisfy this condition are shown in Figure 2.53.

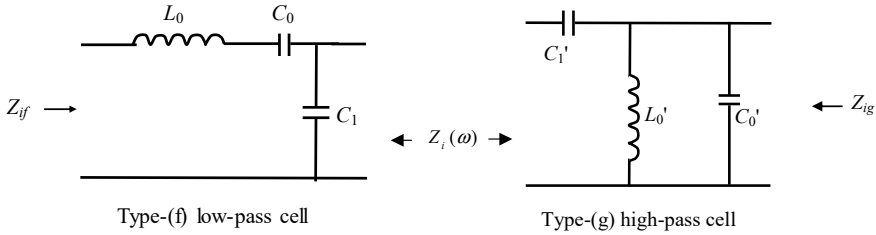


Figure 2.53. Complementary cells of band-pass cells

As a matter of fact, if we establish $\omega_4 = \frac{1}{L_0 C_0}$; $\omega_3 = \omega_4 \sqrt{\frac{C_0 + C_1}{C_1}}$;

$\omega_6 = \frac{1}{L_0 C_0}$; $\omega_7 = \omega_6 \sqrt{\frac{C_0'}{C_0' + C_1'}}$, we obtain $Z_i = \frac{1}{C_1 s} \sqrt{\frac{s^2 + \omega_4^2}{s^2 + \omega_3^2}}$ for type (f) and

$Z_i = \sqrt{1 + \frac{C_1'}{C_0'}} \frac{1}{C_1' s} \sqrt{\frac{s^2 + \omega_7^2}{s^2 + \omega_6^2}}$ for type (g). It is therefore necessary to impose

$\omega_4 = \omega_{inf}$, $\omega_5 = \omega_{sup}$; $\omega_7 = \omega_{inf}$; $\omega_6 = \omega_{sup}$ to find an expression that depends on ω similarly to the image impedance $Z_i(\omega)$ of cells (d) and (e), with

$$R_0 = \frac{1}{C_1 \omega_{sup}} = \frac{1}{C_1' \omega_{sup}} \sqrt{1 + \frac{C_1'}{C_0'}}$$

in addition.

The external image impedances, shown in Figure 2.53, are in the general

case: $Z_{if} = \frac{1}{C_0 s} \frac{\sqrt{(s^2 + \omega_{inf}^2)(s^2 + \omega_{sup}^2)}}{\omega_{inf}^2}$ for type (f) at the left port and

$$Z_{ig} = \frac{1}{C_0' s} \sqrt{\frac{C_0'}{C_0' + C_1'}} \frac{s^2}{\sqrt{(s^2 + \omega_{inf}^2)(s^2 + \omega_{sup}^2)}}$$

for type (g) at the right port. They

are real in the bandwidth of the corresponding band-pass filter, that is for

$$\omega_{\text{inf}} < \omega < \omega_{\text{sup}} \text{ and are, respectively, equal to } Z_{jf}(\omega) = \frac{1}{C_0 \omega} \frac{\sqrt{(\omega_{\text{sup}}^2 - \omega^2)(\omega^2 - \omega_{\text{inf}}^2)}}{\omega_{\text{inf}}^2}$$

$$\text{for type (f) and } Z_{ig}(\omega) = \sqrt{\frac{1}{C_0'(C_0' + C_1')}} \frac{\omega}{\sqrt{(\omega_{\text{sup}}^2 - \omega^2)(\omega^2 - \omega_{\text{inf}}^2)}} \text{ for type (g).}$$

The first one crosses a maximum equal to $R_0 \frac{\omega_{\text{sup}}}{\omega_{\text{sup}} + \omega_{\text{inf}}}$, neighboring $\frac{R_0}{2}$ for a narrow bandwidth, for $\omega = \omega_0 = \sqrt{\omega_{\text{inf}} \omega_{\text{sup}}}$ and always remains smaller than this value in the bandwidth, tending toward zero at both ends. The second one crosses a minimum equal to $R_0 \frac{\omega_{\text{sup}} + \omega_{\text{inf}}}{\omega_{\text{sup}}}$, neighboring $2R_0$ for a narrow bandwidth, for $\omega = \omega_0 = \sqrt{\omega_{\text{inf}} \omega_{\text{sup}}}$ and always remains larger than this value in the bandwidth, tending toward infinity at both ends.

If it is desirable to find an image impedance equal to $Z_i(\omega)$, each of these cells can be doubled by assembling them upside down (head-to-tail), as in type (b) low-pass or type (c) high-pass cells.

The calculation of the elements for both of these cells derives from the identifications made previously and gives:

$$C_0 = \frac{\omega_{\text{sup}}^2 - \omega_{\text{inf}}^2}{R_0 \omega_{\text{sup}} \omega_{\text{inf}}^2}; \quad C_1 = \frac{1}{R_0 \omega_{\text{sup}}}; \quad L_0 = \frac{R_0 \omega_{\text{sup}}}{\omega_{\text{sup}}^2 - \omega_{\text{inf}}^2} \text{ for type (f);}$$

$$C_0' = \frac{\omega_{\text{inf}}}{R_0 (\omega_{\text{sup}}^2 - \omega_{\text{inf}}^2)}; \quad C_1' = \frac{1}{R_0 \omega_{\text{inf}}}; \quad L_0' = \frac{R_0 (\omega_{\text{sup}}^2 - \omega_{\text{inf}}^2)}{\omega_{\text{sup}}^2 \omega_{\text{inf}}} \text{ for type (g).}$$

The image attenuations can be evaluated from $\coth(\Gamma) = \sqrt{Z_{11} Y_{11}} = \sqrt{Z_{22} Y_{22}}$ then from $\exp(2\Gamma) = \frac{\coth(\Gamma) + 1}{\coth(\Gamma) - 1}$. For type (f): $Z_{22} = \frac{1}{C_1 p}$

$$\text{and } Y_{22} = C_1 s + \frac{C_0 s}{1 + \frac{s^2}{\omega_{\text{inf}}^2}}; \quad \text{where from } \coth(\Gamma_f) = \sqrt{\frac{\omega^2 - \omega_{\text{sup}}^2}{\omega^2 - \omega_{\text{inf}}^2}} \text{ and}$$

$$\exp(2\Gamma_f) = \frac{\sqrt{\frac{\omega^2 - \omega_{\text{sup}}^2}{\omega^2 - \omega_{\text{inf}}^2} + 1}}{\sqrt{\frac{\omega^2 - \omega_{\text{sup}}^2}{\omega^2 - \omega_{\text{inf}}^2} - 1}} \quad \text{are deduced in the upper stop band } (\omega > \underline{\omega}_{\text{sup}})$$

using the expressions found above.

For type (g), $Y_{11} = C_1' s$ and $Z_{11} = \frac{1}{C_1' s} + \frac{s}{C_0' (s^2 + \omega_{\text{sup}}^2)}$, from which it can

$$\text{inferred that } \coth(\Gamma_g) = \sqrt{\frac{\omega_{\text{sup}}^2}{\omega_{\text{inf}}^2} \frac{\omega_{\text{inf}}^2 - \omega^2}{\omega_{\text{sup}}^2 - \omega^2}} \quad \text{and } \exp(2\Gamma_g) = \frac{\sqrt{\frac{\omega_{\text{sup}}^2}{\omega_{\text{inf}}^2} \frac{\omega_{\text{inf}}^2 - \omega^2}{\omega_{\text{sup}}^2 - \omega^2} + 1}}{\sqrt{\frac{\omega_{\text{sup}}^2}{\omega_{\text{inf}}^2} \frac{\omega_{\text{inf}}^2 - \omega^2}{\omega_{\text{sup}}^2 - \omega^2} - 1}} \quad \text{in}$$

the lower stop band ($\omega < \underline{\omega}_{\text{inf}}$).

When using two “head-to-tail” cells, the image attenuations calculated in dB must obviously be doubled.

2.4.2.5. Synthesis of band-pass filters

It is therefore possible to build a full band-pass filter in various ways by combining (d)- and/or (e)-type band-pass cells, and eventually complementary (f)-type low-pass and/or (g)-type high-pass cells, doubled or not. If these complementary cells are used without doubling them, one will need to be placed at the beginning and the other at the end of the filter and, in this case, the termination impedances should be close to $\frac{R_0}{2}$, or even lower for the (f)-type cell, and to $2R_0$, or even higher, for the (g)-type cell. This solution thus implies asymmetry. If on the contrary, we want symmetrical termination resistances R_1 and R_2 equal to R_0 , we should choose to only use band-pass-based cells or also doubled complementary cells assembled head-to-tail if one or more attenuation poles are imposed at the origin or at infinity. According to the theory of image-matching developed in this section, these elementary cells will be assembled in cascade as in the following operation schematic.

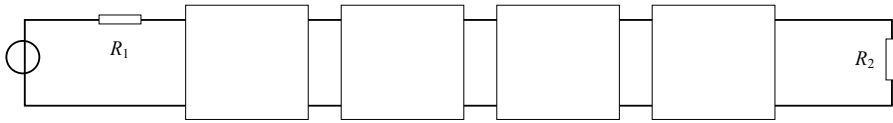


Figure 2.54. *Image-matching filter, composed of cascading cells represented by rectangles, with their termination resistances*

The synthesis in itself consists of determining the nature and the number of cells needed to satisfy a template, and then the position of the attenuation pole for each cell. However, the calculations that can precisely predict the effective attenuation based on all these data are generally complex since for each cell they must take into account a termination impedance that is different from both the image impedance assumed in theory and also from the iterative resistance R_0 if this is not involving the first or the last cell. As a result, here we will only consider an approximated method to be implemented in two stages:

1) the template will be first approximated by the asymptotic image attenuation after the choice of the number of cells and of their type determined according to the symmetry or asymmetry of terminations, the number of finite-frequency attenuation poles and the existence of attenuation poles at zero and/or infinite frequency. It will be possible to evaluate a limit of the ripple in the bandwidth compared with the standard-type elliptical filter that gives the same finite-frequency attenuation poles and a stop band attenuation similar to that of the template;

2) the result of the simulation of the effective attenuation with the desired template will allow us to rectify the previous choices, and to possibly modify the cutoff frequencies to take account of the effect of the attenuation factors whose expressions have been determined independently of the type of filter (section 2.4.2.2), for a single cell however. Therefore, their actual impact may be very different in multiple-cell-based filters, with most often a real decrease in the bandwidth compared with the image bandwidth.

EXAMPLE.— Two (d) cells and two (e) cells band-pass filter, providing two attenuation poles in the lower stop band and two in the upper stop band.

In this example the template requires a normalized cutoff angular frequency of 0.95 and 1.05 as well as attenuation poles at angular frequencies 0.6, 0.8, 1.25 and 1.5 between symmetrical terminations, with a minimal stop band attenuation of 82 dB. Based on the asymptotic expressions of image attenuation, it can be verified that a filter made up of two (d) cells and two (e) cells is suitable. When looking for the eighth-order elliptical filter giving the minimal attenuation and neighboring attenuation poles (0.6, 0.8, 1.25 and 1.7) using MATLAB, we find that the ripple in the passband is 1.5 dB. Then, the elements are determined based on the expressions of the previous two sections. The plots of the moduli of the image attenuation and simulated attenuation are presented in Figure 2.55 (the simulation has been achieved for symmetrical termination resistances R_1 and R_2 and equal to $R_0 = 50 \Omega$ and frequencies identical to the normalized values but expressed in MHz).

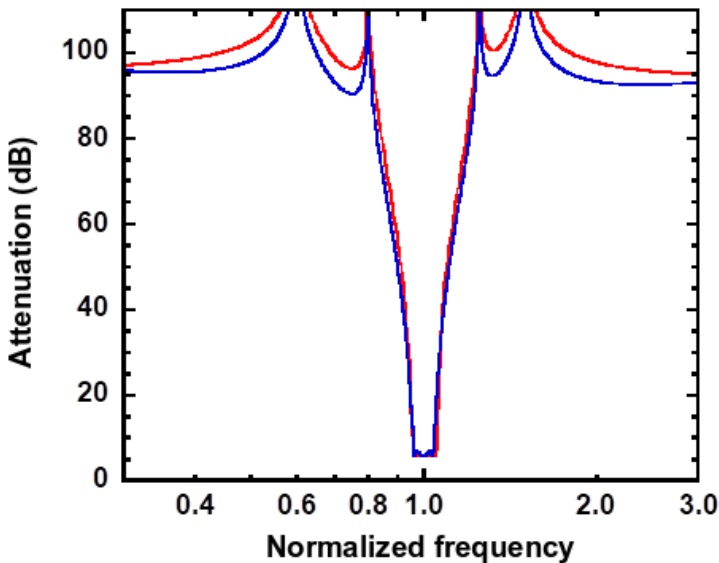


Figure 2.55. Image attenuation in red and effective attenuation in blue, obtained by simulation, for the filter whose template is defined in the example above. For a color version of this figure, see www.iste.co.uk/muret/electronics2.zip

The cutoff frequencies normalized at -3 dB are 0.958 instead of 0.950 and 1.041 instead of 1.050, which is equivalent to a reduction of 17% of the bandwidth. This would therefore require us to recalculate the elements

starting from an image bandwidth about 17% higher, therefore with normalized cutoff frequencies of 0.942 and 1.059. The minimum stop band attenuation is 84 dB above the 6 dB specific to the bandwidth, about 6 dB less than the image attenuation in the area of the lobes, the deviation decreasing when moving away from external attenuation poles, to achieve an attenuation of the order of 90 dB above that in the bandwidth. The template is thus satisfied in the stop bands. The actual ripple in the bandwidth is 0.9 dB, with 2 minima and 3 maxima, smaller than that of the elliptical filter that has been previously considered. With the exception of the bandwidth that can be easily rectified, the performances of this filter are thus superior to those of an elliptic filter with equivalent order.

The effective ripple of the order of 1 dB in the bandwidth is explained by the fact that for the external (d)- and (e)-type cells, the image impedance is equal to the termination resistances only at the center of the bandwidth and moves considerably away at their boundaries where it tends either toward zero, or to infinity. From the perspective of image-matching, the simple cells of type (f) and (g) are more interesting if one accepts a dissymmetry of the terminations because matching can be twice achieved at each port in the bandwidth. This would significantly enable the ripple in the bandwidth to be decreased.

EXERCISE.– Check all the steps of the previous synthesis in a quantitative way.

2.4.2.6. Band-pass filter based on quartz or ceramic resonator: lattice filters

An equivalent circuit of a piezoelectric quartz resonator, obtained by neglecting the damping resistance (Joule losses), is shown in Figure 2.56.

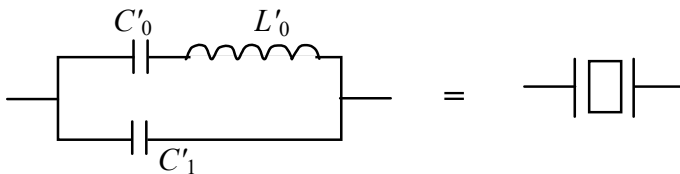


Figure 2.56. *Equivalent circuit and symbol of the quartz resonator, where the damping resistance (Joule losses) is neglected*

A distinction is made between series or resonance angular frequency ω_S and parallel or antiresonance angular frequency $\omega_{//}$. The circuit is identical to the central part of the previous (e)-type cell whose admittance is written as $Y_Q(s) = (C'_0 + C'_1)s \frac{1 + s^2/\omega_{//}^2}{1 + s^2/\omega_S^2}$ with $\omega_S^2 = \frac{1}{L'_0 C'_0} = \omega_\infty^2$ and $\omega_{//}^2 = \omega_\infty^2 \frac{C'_0 + C'_1}{C'_1} = \omega_{\text{sup}}^2$, the two extreme angular frequencies of the (e) cell. The bandwidth of a filter built with such a resonator and an (e)-type circuit is thus necessarily smaller than the interval $[\omega_S, \omega_{//}]$. To give an order of magnitude, the relative difference between ω_S and $\omega_{//}$ is of the order of 0.05 % if the ratio C'_1/C'_0 is close to 1,000, which is a minimum for quartz, in which ratio up to several times 10^6 can be reached. This bandwidth can be extended by resorting either to ceramic resonators with smaller ratios C'_1/C'_0 but also presenting greater losses than quartz crystals, or to specially designed quartz resonators with an enhanced parallel capacitance C'_1 . A different network such as the lattice filter can also be adopted.

The equivalent diagram can also be that of the central part of the (d)-cell (Figure 2.57) whose admittance is $Y_Q(s) = C_1 s \frac{1 + s^2/\omega_\infty^2}{1 + s^2/\omega_{\text{inf}}^2}$ and angular frequencies are those previously defined for the same cell. Here again, the bandwidth is necessarily smaller than the interval that is defined by these two angular frequencies in the band-pass filter synthesized by the image impedance method, which remains still applicable for ladder filters.

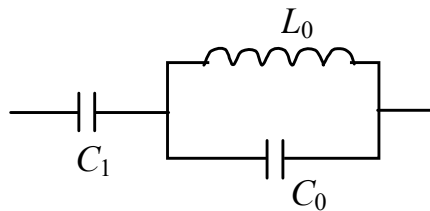


Figure 2.57. Another equivalent circuit of the quartz resonator

Another solution consists of using symmetrical lattice filters whose operation circuit is illustrated in Figure 2.58.

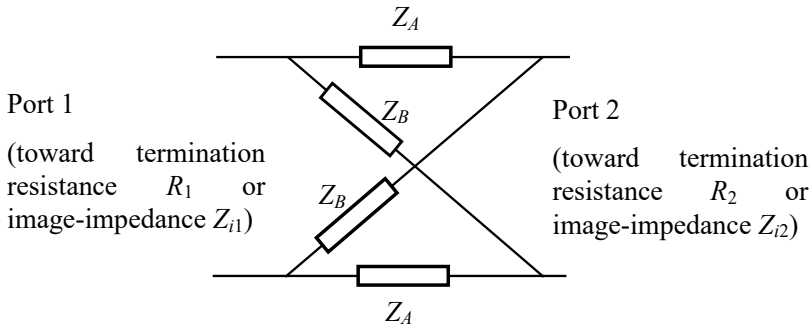


Figure 2.58. Lattice filter

It can be shown (see section 2.5) that parameters Z_{ij} of the corresponding quadripole are given by $Z_{11} = Z_{22} = \frac{Z_B + Z_A}{2}$; $Z_{12} = Z_{21} = \frac{Z_B - Z_A}{2}$ and $\det Z = Z_A Z_B$; the image impedances are given by $Z_{i1} = Z_{i2} = \sqrt{Z_A Z_B}$. Under

image-matching conditions, the matrix of normalized z -parameters is $\mathbf{z} = \begin{bmatrix} \coth \Gamma & 1/\sinh \Gamma \\ 1/\sinh \Gamma & \coth \Gamma \end{bmatrix}$ and the parameters $s_{21} = s_i$ and Γ are computable by

$$s_i = \frac{z_{21}}{1 + z_{11}} = \exp(-\Gamma) = \frac{Z_{12}}{\sqrt{\det Z} + \sqrt{Z_{11} Z_{22}}}$$

and Z_{i2} are real, Z_{11} and Z_{21} are purely imaginary, it is because Z_A and Z_B are also imaginary (in other words, Z_A and Z_B are reactances). If these reactances are opposite in nature (one capacitive, the other inductive), the logarithmic image attenuation factor Γ is thus also imaginary and accordingly the image attenuation γ is zero. This case thus corresponds to the bandwidth, which is consequently determined by the frequency domain where Z_A and Z_B are reactances of opposite nature, one being inductive, the other capacitive. This is achieved in the lattice if Z_A is the impedance of a resonator and Z_B that of a capacitance (see section 2.5) in all the frequency domain where the resonator is inductive. Lattice filters also have the advantage of exhibiting an attenuation pole determined by the angular frequency ω_{AB} where $Z_A = Z_B$ (which cancels out Z_{12} and Z_{21}) and therefore ω_{AB} is independent of the characteristic frequencies of impedances Z_A and Z_B such as ω_s and $\omega_{//}$.

2.4.2.7. All-pass lattice or bridged-T filter structure

It is easy to turn the lattice filter mentioned previously into an all-pass filter whose bandwidth by definition ranges from the zero frequency to infinite frequencies. Furthermore, since the image impedance $Z_{i1} = Z_{i2} = \sqrt{Z_A Z_B}$ is real in the bandwidth, it simply suffices to impose that it remains always real by means of the condition $Z_A Z_B = R_0^2$, verified regardless of the frequency. It can be shown that R_0 is then the effective iterative resistance (and not only the image impedance) by deferring Z_{11} and Z_{12} into the expression of the terminated input impedance with $Z_u = R_0$

(according to section 2.1.5.2): $Z_e|_{V_2=-Z_u I_2} = \frac{Z_{11} Z_u + \det Z}{Z_u + Z_{22}}$, which is simplified into R_0 taking $Z_A Z_B = R_0^2$ into account. Moreover, the voltage gain of the quadripole loaded by R_0 is equal to $G_v|_{V_2=-R_0 I_2} = \frac{Z_{21} R_0}{Z_{11} R_0 + \det Z}$ giving

$G_v|_{V_2=-R_0 I_2} = \frac{R_0 - Z_A}{R_0 + Z_A}$ after simplification. Therefore, we can easily get a

first-order all-pass transmittance with an inductance L for Z_A , which implies a capacitance $C = L/R_0^2$ for Z_B , in order to satisfy the condition $Z_A Z_B = R_0^2$. Nevertheless, the second-order all-pass is often more useful and requires then that an inductance L and a capacitance C be placed in parallel for Z_A (see section 2.5). In this case, a transmittance can be obtained

$G_v(s) = \frac{s^2 - 2\zeta\omega_n s + \omega_n^2}{s^2 + 2\zeta\omega_n s + \omega_n^2}$. Under a certain condition, it is possible to transform

the lattice into a bridged-T structure (see section 2.5).

An all-pass filter or a cascade of all-pass filters enable the correction of the phase of a first minimal phase-shift filter for which the synthesis was carried out based on a template of the modulus of the desired transmittance. For example, it may be useful to reduce group delay variations by at least partially compensating for the strong variations of the phase shift introduced by the first filter in order to approximate an overall linear phase shift with frequency. To this end, we can add with no major problem an all-pass filter to the first filter such as those described above with a value of R_0 equal to that provided for the termination resistance of the first filter since the iterative resistance of all-pass filters itself is R_0 , regardless of the synthesis method employed for the first filter. The synthesis of the all-pass filter consists of finding a phase shift whose variations with the angular frequency

are shifted relatively to that of the first filter so as to minimize the derivative of the overall phase shift, namely the group delay, with respect to a constant value. This search requires software-based simulation.

Other circuits (double T, circuits comprising a transformer) can be implemented to synthesize passive filters, including RC circuits. It is also possible to make use of active elements such as gyrators or negative resistances. Since the latter have mainly an historical interest, they will not be addressed here. For more information and further theoretical study, the reader can refer to [DED 96].

2.4.3. Filter sensitivity and Orchard's argument

The sensitivity of a filter can be defined as the derivative of one of the basic parameters of the filter, such as its cutoff frequency or its central frequency, its ripple in the bandwidth, etc., with respect to the value of a passive element from which it is built, or with respect to termination resistances. With the emergence of operational amplifiers, it has been noted that this sensitivity is much less significant when the filter includes passive elements only. Moreover, this has resulted in a renewed interest for passive filters because lower sensitivity with regard to the dispersion of element values constitutes a decisive advantage in industrial production.

The phenomenon was explained by Orchard in 1966 with the following reasoning.

As seen in section 2.1.8 for image adaptation, the modulus of the parameter S_{21} is equal to 1 in the bandwidth and the attenuation $1/|S_{21}|^2$ is also equal to 1. The first derivative of this attenuation with respect to frequency in the bandwidth is therefore zero. However then, it is also with respect to the values of capacitive and inductive elements, respectively, C_i and L_i , of the passive filter because L_i or C_i play a dual frequency role since they define frequencies specific to the filter or their square root; the same occurs for termination resistances that fall within the definition of time constants. We could also reason by stating the fact that the attenuation $1/|S_{21}|^2$ reaches its absolute minimum because its derivative is also zero with respect to the same variables. At the first order, the sensibility of a passive filter with respect to its elements is therefore zero in the bandwidth. The same cannot be said if energy is supplied (active elements) within the quadripole because the previous argument is no longer valid. The argument applies all the more when the attenuation is lower (close to the unity, or

0 dB) in the bandwidth, when the ripple in the bandwidth is lower and when the filter is inserted between terminations with non-zero resistances, because in the case where the resistance is too close to zero, it is no longer possible to consider that the aforementioned derivatives are zero with respect to a termination resistance zero. This shows the superiority of doubly terminated filters and having termination resistances not too distant from one another compared to simply terminated filters, that is to say supplied by an ideal voltage or current generator. All-pass filters equally display a nature more sensitive to variations of elements because one of the parameters depends on the difference of two impedances, whose derivative tends to infinity when this difference is cancelled out. For this reason, these filters can prove to be good detectors, as well as bridged circuits, because in this case high sensitivity becomes an advantage.

2.5. Exercises

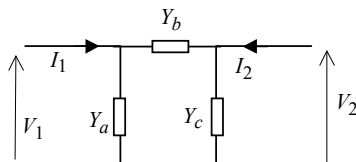
2.5.1. Impedance matching by means of passive two-port networks; application to class B push-pull power RF amplifier with MOS transistors

This exercise is based on the circuit described in Philips application note NCO8701 (see the complete circuit at the end of the exercise).

1) Matching on input

a) Rewrite the admittance equations of a two-port network $\begin{cases} I_1 = Y_{11}V_1 + Y_{12}V_2 \\ I_2 = Y_{21}V_1 + Y_{22}V_2 \end{cases}$ using the term $\pm Y_{12}(V_1 - V_2)$ in both equations so that the circuit contains only one source and one admittance $-Y_{12}$ subject to voltage $(V_1 - V_2)$. From this, deduce the condition necessary for the two-port network to be passive (no source).

b) Find the flow relations between Y_{11} , Y_{12} , Y_{22} and the electrical quantities of the following Π two-port network:



c) Find the circuit and relations that allow matching of a generator with an internal resistance $R_g = 25 \Omega$ using a passive Π two-port network with the input of a field effect transistor (BLF244). Here, its input impedance is purely capacitive ($C_u = 117 \text{ pF}$) but is completed by adding a parallel resistance R_u . The working frequency is $f_1 = 55 \text{ MHz} = \omega_1/2\pi$ (central frequency of useable bandwidth). Each admittance of the passive two-port network will be purely reactive to avoid consuming active power, comprising only one element (capacitance or inductance). For Y_b , a pure inductance L_b is selected.

Show that, in this case, Y_a has to be a capacitance C_a . Determine L_b , C_a and L_c (assuming that Y_c must be the admittance of a pure inductance L_c) in relation to R_u , R_g , C_u and ω_1 . Write $L' = \frac{L_b L_c}{L_b + L_c}$, also calculating its algebraic expression.

d) Determine transfer function $T = V_2 / V_1$, its natural frequency f_n and its quality coefficient Q relative to R_u , C_u , ω_1 . Assuming that at a frequency of 110 MHz, a variation of -10 dB is accepted relative to low-frequency conditions, determine the value of Q , showing that if $R_u = R_g$, the previous hypothesis on Y_c (where Y_c is the admittance of a pure inductance L_c) is justified. What is the relative value of $|T|$ in dB at 55 MHz relative to low-frequency conditions?

2) Matching on output using transformer between the transistors of the push-pull stage (class B) and load $R_{load} = 50 \Omega$

a) Modeling the presumably linear transformer: primary composed of resistance R_1 in series with inductance L_1 , secondary composed of resistance R_2 in series with inductance L_2 , with both inductances coupled by mutual inductance M .

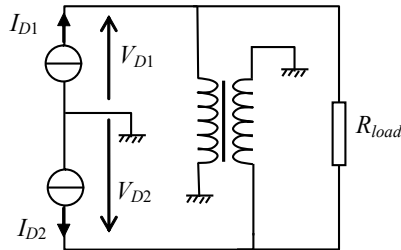
Write $n = \sqrt{\frac{L_2}{L_1}}$ and $k = \frac{M}{\sqrt{L_1 L_2}}$. Write out the system of characteristic

equations for an impedance two-port network, that is V_1, V_2 relative to I_1, I_2 . Next, transform it into a system with hybrid parameters of type III: I_1, V_2 relative to V_1, I_2 , establishing the equivalent electrical circuit.

What happens to the equations and the circuit if the transformer has no losses, that is if $R_1 = R_2 = 0$? And if in addition the coupling is unitary: $k = 1$?

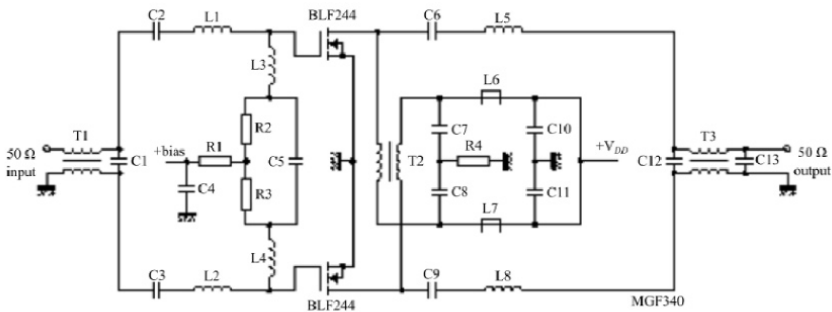
In the latter case, determine the input impedance (or impedance brought to primary) when the secondary is loaded by impedance Z_{ch} .

b) Show that the amplifier allows (disregarding the reactive elements as a first approximation and considering the MOS drain as an ideal source of current) for the use of a half-load, $R_{load}/2$, as internal source resistance and the other half as load resistance.



Deduce the theoretical yield if matching is perfect (compensated reactance).

In reference to the previous results, analyze and comment on the full circuit shown below.



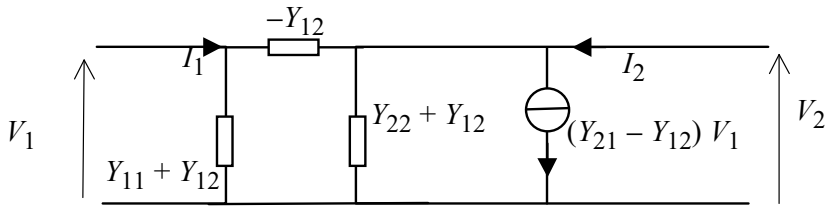
Answer:

1) Matching on input

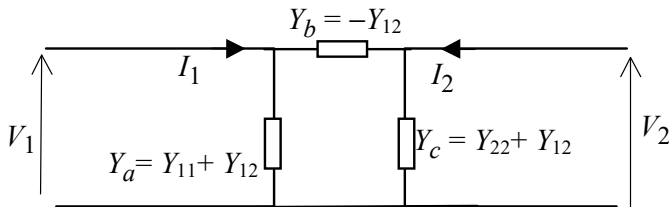
a) Adding and subtracting term $Y_{12}V_1$ to and from the first equation, and term $Y_{12}(V_1 - V_2)$ to the second, provides:

$$\begin{cases} I_1 = (Y_{11} + Y_{12})V_1 + (-Y_{12})(V_1 - V_2) \\ I_2 = (Y_{21} - Y_{12})V_1 + (-Y_{12})(V_2 - V_1) + (Y_{22} + Y_{12})V_2 \end{cases}$$

Corresponding to:



If $Y_{12} = Y_{21}$, this provides a passive two-port network:



b) With:
$$\begin{cases} Y_{11} = Y_a + Y_b \\ Y_{21} = Y_{12} = -Y_b \\ Y_{22} = Y_c + Y_b \end{cases}$$

therefore:
$$\begin{cases} I_1 = (Y_a + Y_b)V_1 - Y_b V_2 \\ I_2 = -Y_b V_1 + (Y_c + Y_b)V_2 \end{cases}$$

c) If the output of the two-port network is loaded by admittance Y_u , this gives $Y_u V_2 = -I_2$ that, when carried into the second equation, provides:

$V_2 = \frac{Y_b}{Y_b + Y_c + Y_u} V_1$ and by carrying this into the first:

$Y_e = \frac{I_1}{V_1} = Y_a + Y_b - \frac{Y_b^2}{Y_b + Y_c + Y_u}$ where Y_a, Y_b, Y_c are pure susceptances. Taking

$Y_u = G_u + j B_u$ where $G_u = 1/R_u, B_u = C_u \omega$ and setting $Y_b = \frac{1}{jL_b \omega}$.

Clearly, to obtain the real Y_e , we should set $Y_a + Y_b = 0$ and $Y_b + Y_c + jB_u = 0$.

Y_b^2 is then a real negative quantity. Furthermore, for matching at the generator, we must set $Y_e = \frac{|Y_b|^2}{G_u} = |Y_b|^2 R_u = \frac{1}{R_g}$.

Hence: $|Y_b| = \frac{1}{\sqrt{R_u R_g}}$ where $L_b \omega = \sqrt{R_u R_g}$ at $\omega = \omega_1 = 2\pi f_1$ or alternatively

$$L_b = \frac{\sqrt{R_u R_g}}{\omega_1}.$$

It is deduced that $Y_a = -Y_b$ must be capacitive $jC_a \omega_1 = -\frac{1}{jL_b \omega_1} = \frac{j}{\sqrt{R_u R_g}}$;

hence:

$$C_a = \frac{1}{\omega_1 \sqrt{R_u R_g}}.$$

So $Y_c = -Y_b - jC_u \omega_1 = -\frac{1}{jL_b \omega_1} - jC_u \omega_1 = j \left[\frac{1}{L_b \omega_1} - C_u \omega_1 \right]$. If the bracket is positive, it is a capacitive admittance, otherwise inductive, where

$L_c = \frac{L_b}{L_b C_u \omega_1^2 - 1}$ in the latter case where there is also $\frac{1}{L'} = \frac{1}{L_b} + \frac{1}{L_c} = C_u \omega_1^2$ and $L_b \omega_1 = \sqrt{R_u R_g}$.

d) Transmittance T is given by:

$$\frac{V_2}{V_1} = \frac{Y_b}{Y_b + Y_c + Y_u} = \frac{\frac{1}{jL_b\omega}}{\frac{1}{jL_b\omega} + \frac{1}{jL_c\omega} + jC_u\omega + \frac{1}{R_u}} = \frac{L_c}{L_c + L_b} \frac{1}{1 + j \frac{1}{R_u C_u \omega_1} \frac{\omega}{\omega_1} - \left(\frac{\omega}{\omega_1}\right)^2}$$

Where natural frequency $\omega_n = \omega_1$ and quality coefficient $Q = R_u C_u \omega_1$.

To obtain $L_b C_u \omega_1^2 - 1 > 0$, there must be $Q \sqrt{\frac{R_g}{R_u}} > 1$. Writing $u = \omega / \omega_1$:

$$T(u) = \frac{L_c}{L_c + L_b} \frac{1}{1 + j \frac{u}{Q} - u^2}; \text{ hence } |T(u)| = \frac{L_c}{L_c + L_b} \frac{1}{\sqrt{(1-u^2)^2 + \frac{u^2}{Q^2}}}$$

For $u = 2$, there is $20 \log \frac{|T(2)|}{|T(0)|} = -10$ dB resulting in $Q = 2$. Inequality

$Q \sqrt{\frac{R_g}{R_u}} > 1$ is then verified with $R_g = R_u$.

This provides $20 \log \frac{|T(1)|}{|T(0)|} = +6$ dB. This solution thus leads to a variation

of 16 dB between $f_1 = 55$ MHz and $f_n = 2 f_1 = 110$ MHz, which is high for an amplifier supposed to have an approximately flat response in its bandwidth. To improve this response, a more complex solution should be used in which admittances Y_b and Y_c are not reduced to purely reactive elements but rather to associations, as per the real circuit provided at the end of the introduction of this exercise.

2) Matching on output using a transformer between the transistors of the push-pull stage (class B) and load $R_{load} = 50 \Omega$

a) For the transformer, set:
$$\begin{cases} V_1 = (R_1 + jL_1\omega)I_1 + jM\omega I_2 \\ V_2 = (R_2 + jL_2\omega)I_2 + jM\omega I_1 \end{cases}$$

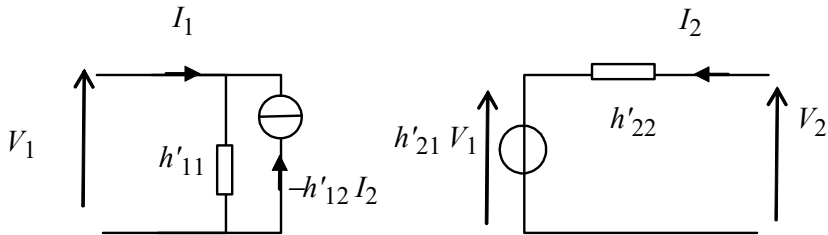
Write $k = \frac{M}{\sqrt{L_1 L_2}}$, $n = \sqrt{\frac{L_2}{L_1}}$ and $R'_2 = \frac{R_2}{n^2}$. Hence:

$$\begin{cases} V_1 = (R_1 + jL_1\omega)I_1 + jnkL_1\omega I_2 \\ V_2 = jnkL_1\omega I_1 + n^2(R'_2 + jL_1\omega)I_2 \end{cases}$$

Dividing the first equation by $(R_1 + jL_1\omega)$ and carrying it over to the second provides a system with type III hybrid parameters:

$$\begin{cases} I_1 = \frac{V_1}{R_1 + jL_1\omega} - nk \frac{jL_1\omega}{R_1 + jL_1\omega} I_2 \\ V_2 = nk \frac{jL_1\omega}{R_1 + jL_1\omega} V_1 + \left[\frac{(nkL_1\omega)^2}{R_1 + jL_1\omega} + n^2(R'_2 + jL_1\omega) \right] I_2 \end{cases}$$

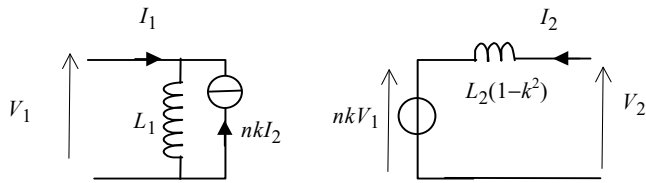
The equivalent circuit then becomes:



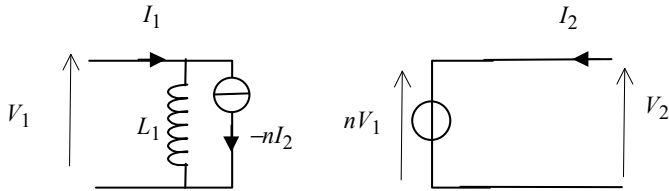
$$\text{with } \begin{cases} h'_{11} = \frac{1}{R_1 + jL_1\omega} & ; & h'_{22} = \frac{(nkL_1\omega)^2}{R_1 + jL_1\omega} + R_2 + jL_2\omega \\ h'_{21} = nk \frac{jL_1\omega}{R_1 + jL_1\omega} & ; & -h'_{12} = nk \frac{jL_1\omega}{R_1 + jL_1\omega} \end{cases}$$

where h'_{11} and h'_{22} are, respectively, an admittance and an impedance.

For the transformer with no losses, $R_1 = R_2 = 0$, which provides:



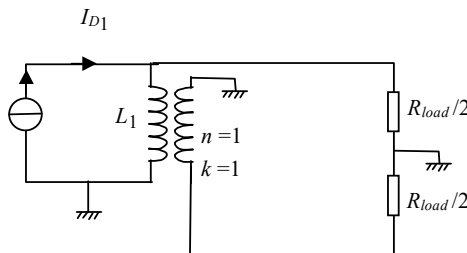
If in addition the coupling is worth 1:



NOTE.— In this case, the secondary cannot be transformed into a current source and the quadripole passed to the admittance parameters system.

If $V_2 = n V_1 = -Z_{ch} I_2$, the current source inside the primary becomes $-nI_2 = \frac{n^2 V_1}{Z_{ch}}$, which is equivalent to a primary comprising L_1 in parallel with impedance $\frac{Z_{ch}}{n^2}$.

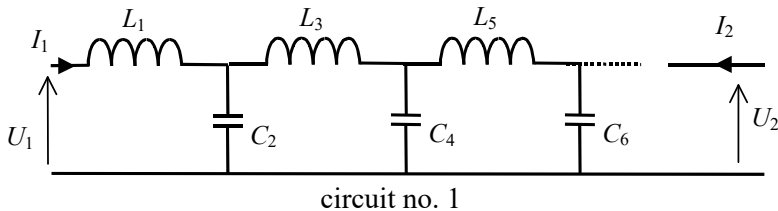
b) Disregarding the reactive elements, since the circuit is symmetrical, R_{load} can be separated into two resistances equal to $R_{load}/2$, and when the higher transistor is conductive with a current I_{D1} , the equivalent circuit becomes:



where the current source I_{D1} is loaded by $R_{load}/4$ since the lower resistance $R_{load}/2$ occurs in parallel on the other by means of the transformer, as if it played the role of the internal resistance of the generator supplying current to the higher resistance. Thus, no power is lost since the two half-load resistances each receive half of the total power. This system avoids half power loss in the internal resistance of the generator, reaching maximum yield for the class B circuit (78%), or even more when class C is used. An LC network should be added at the secondary to compensate the reactances due to the output capacitances of the transistors, as in the full circuit shown previously.

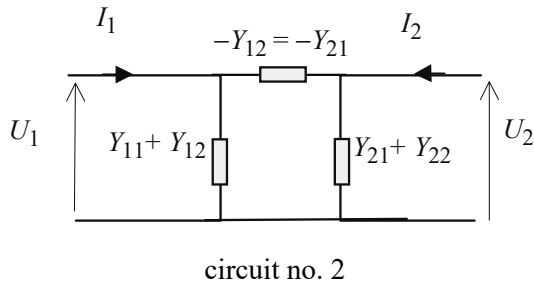
2.5.2. Passive low-pass filtering of an ideal voltage source by a two-port network built with an LC ladder (single-ended ladder filter)

A ladder network LC- n is a passive two-port network comprising n elements (with as many inductances as capacitances when n is even and one more inductance than capacitance when n is odd) responding to the following circuit:



The inductances are numbered with odd integers and the capacitances with even integers. The two-port network comprising n elements is described by the admittance matrix. Assuming that parameters $Y_{12,n}$ and $Y_{22,n}$ are written $Y_{21,n} = Y_{12,n} = \frac{-1}{sQ_n(s^2)}$ and $Y_{22,n} = \frac{S_n(s^2)}{sQ_n(s^2)}$ where $Q_n(s^2)$ and $S_n(s^2)$ are polynomials in s^2 (of the type $b_0 + b_1s^2 + b_2s^4 + \dots$), a property addressed through recurrence in question 3.

1) Any passive two-port network can be represented by the following circuit in which Y_{ij} represents admittance (inverse of impedance) and $Y_{21} = Y_{12}$:



a) Using circuit no. 2, find the equations providing I_1 and I_2 relative to U_1 and U_2 for a passive two-port network described by the previous admittances.

b) How can two distinct elements of admittance Y_a and Y_b be arranged so that the global admittance is equal to $Y_a + Y_b$ and what is then the fraction of the total current going into Y_a ?

2) a) Determine transmittance $T_n(p) = \frac{U_2}{U_1}$ when ladder LC- n represented by circuit no. 2 is closed on a resistance for which conductance is G (for this, write the relation between I_2 and U_2) first relative to $Y_{21,n}$, $Y_{22,n}$, and then $S_n(s^2)$, $Q_n(s^2)$, G and s .

b) In order to implement transmittance filter $T_5(s) = \frac{1}{a_0 + a_1s + a_2s^2 + a_3s^3 + a_4s^4 + a_5s^5}$ find G , $Q_5(s^2)$ and $S_5(s^2)$ relative to the terms of denominator of $T_5(s)$.

3) Try to prove the relations giving $Y_{12,n}$ and $Y_{22,n}$ relative to the polynomials $Q_n(s^2)$ and $S_n(s^2)$ by recurrence. Draw the circuits corresponding to both cases below using circuit no. 2, when $U_1 = 0$:

a) When adding inductance L_{n+1} to ladder LC- n , find the relations providing I_1 and U_2 relative to I_2 , $Y_{21,n}$, $Y_{22,n}$ and $L_{n+1}s$ when $U_1 = 0$. Deduce $Y_{21,n+1}$ and $Y_{22,n+1}$ relative to $Y_{21,n}$, $Y_{22,n}$ and $L_{n+1}s$ then relative to $Q_n(s^2)$, $S_n(s^2)$, L_{n+1} and s .

b) When adding a capacitance C_{n+1} to ladder LC- n , find the relations providing I_1 and U_2 relative to I_2 , $Y_{21,n}$, $Y_{22,n}$ and $C_{n+1}s$ when $U_1 = 0$.

Deduce $Y_{21,n+1}$ and $Y_{22,n+1}$ relative to $Y_{21,n}$, $Y_{22,n}$ and $C_{n+1}s$ then relative to $Q_n(s^2)$, $S_n(s^2)$, C_{n+1} and s . Which is the admittance that remains unchanged?

c) Deduce that $Y_{21,n+1}$ and $Y_{22,n+1}$ retain the same properties as $Y_{21,n}$ and $Y_{22,n}$, and that as a general rule:

$$\text{- for } n = 2k+1, \text{ odd : } S_{2k+1}(s^2) = S_{2k}(s^2) = S_{2k-1}(s^2) + s^2 C_{2k} Q_{2k-1}(s^2)$$

$$\text{- for } n = 2k, \text{ even : } Q_{2k}(s^2) = Q_{2k-1}(s^2) = Q_{2k-2}(s^2) + L_{2k-1} S_{2k-2}(s^2)$$

4) a) Show from circuit no. 1, using the elements of impedance associated in series and the elements of admittance associated in parallel, that $Y_{22,5}$ occurs in the form of a continued fraction:

$$Y_{22,5} = \frac{1}{K_5 p + \frac{1}{K_4 p + \frac{1}{K_3 p + \frac{1}{K_2 p + \frac{1}{K_1 p}}}}}$$

What do K_5, K_4, K_3, K_2, K_1 represent, respectively?

b) Using the relation giving $Y_{22,n}$ at the beginning of question 3, $n = 5$, and the result of 2) b), show by performing successive division (no more than 2) of the denominator or the remainder of the previous division by the numerator of $Y_{22,n}$ according to decreasing powers of s , that $Y_{22,5}$ can be written in the previous form with coefficients, K_5, K_4, K_3, K_2, K_1 functions of $a_5, a_4, a_3, a_2, a_1, a_0$. Use this method to deduce expressions of K_5 and K_4 .

Answer:

1) a) The equations relative to circuit no. 2 are written as:

$$\begin{cases} I_1 = (Y_{11} + Y_{12})U_1 + (-Y_{12})(U_1 - U_2) = Y_{11}U_1 + Y_{12}U_2 \\ I_2 = (Y_{21} + Y_{22})U_2 + (-Y_{21})(U_2 - U_1) = Y_{21}U_1 + Y_{22}U_2 \end{cases}$$

here again are the definition equations of the admittance two-port network after simplification.

b) The product of an admittance $Y_a + Y_b$ by unique voltage V gives current $I = (Y_a + Y_b) V$, which is the total of two currents. Both elements are necessarily in parallel because they undergo the same voltage V and the ratio of currents $Y_a V$ over $(Y_a + Y_b)V$ gives a fraction $\frac{Y_a}{Y_a + Y_b}$ of the total current in the element with admittance Y_a .

2) a) When the port no. 2 of ladder LC- n is closed on a resistance whose conductance is G , there is $I_2 = -G U_2$; so carrying this into the equation gives $I_2: I_2 = -G U_2 = Y_{21,n} U_1 + Y_{22,n} U_2$

$$\text{Hence: } T_n(s) = \frac{U_2}{U_1} = -\frac{Y_{21,n}}{G + Y_{22,n}}$$

that can be rewritten by replacing the admittances by their expressions according to polynomials $Q_n(s^2)$ and $S_n(s^2)$:

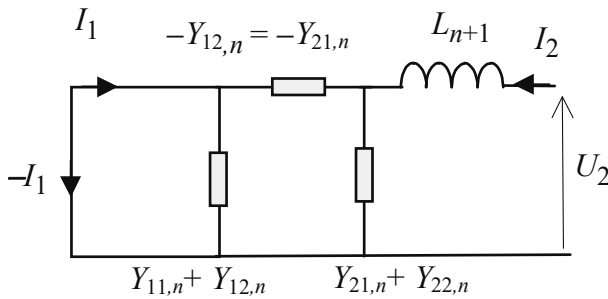
$$T_n(s) = \frac{U_2}{U_1} = \frac{1}{sQ_n(s^2) \left[G + \frac{S_n(s^2)}{sQ_n(s^2)} \right]}$$

$$\text{resulting in: } T_n(s) = \frac{1}{GsQ_n(s^2) + S_n(s^2)}$$

b) $G s Q_5(s^2)$ can be identified with the odd degree terms of the denominator of $T_5(s)$ (that is $a_0 + a_1s + a_2s^2 + a_3s^3 + a_4s^4 + a_5s^5$) while $S_5(s^2)$ with the polynomial's terms of even degree which provides:

$$\begin{cases} GsQ_5(s^2) = a_1s + a_3s^3 + a_5s^5 \\ S_5(s^2) = a_0 + a_2s^2 + a_4s^4 \end{cases}$$

3) a) When inductance L_{n+1} is added and when $U_1 = 0$, circuit no. 2 becomes:



Hence the current division ratio (with $Y_{11,n} + Y_{12,n}$ short circuited, thus cancelling the current through it): $-I_1 = \frac{-Y_{12,n}}{-Y_{12,n} + Y_{12,n} + Y_{22,n}} I_2$ leading to

$$I_1 = \frac{Y_{12,n}}{Y_{22,n}} I_2$$

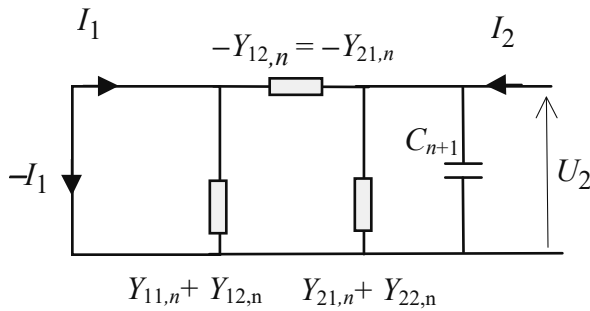
and $U_2 = L_{n+1} s I_2 + \frac{I_2}{-Y_{21,n} + Y_{21,n} + Y_{22,n}} = L_{n+1} s I_2 + \frac{I_2}{Y_{22,n}}$

deducing:
$$\begin{cases} Y_{21,n+1} = \left. \frac{I_1}{U_2} \right|_{U_1=0} = \frac{Y_{21,n}}{1 + L_{n+1} s Y_{22,n}} \\ Y_{22,n+1} = \left. \frac{I_2}{U_2} \right|_{U_1=0} = \frac{Y_{22,n}}{1 + L_{n+1} s Y_{22,n}} \end{cases}$$

Carrying the admittance values relative to the polynomials $Q_n(s^2)$ and $S_n(s^2)$:

$$\begin{cases} Y_{21,n+1} = \frac{-1}{s[Q_n(s^2) + L_{n+1} S_n(s^2)]} \\ Y_{22,n+1} = \frac{S_n(s^2)}{s[Q_n(s^2) + L_{n+1} S_n(s^2)]} \end{cases}$$

b) When capacitance C_{n+1} is added and when $U_1 = 0$, circuit no. 2 becomes:



Hence, the current division ratio is: $-I_1 = \frac{-Y_{12,n}}{-Y_{12,n} + Y_{12,n} + Y_{22,n} + C_{n+1}s} I_2$

leading to $I_1 = \frac{Y_{12,n}}{Y_{22,n} + C_{n+1}s} I_2$

and $U_2 = \frac{I_2}{Y_{22,n} + C_{n+1}s}$

deducing:
$$\begin{cases} Y_{21,n+1} = \left. \frac{I_1}{U_2} \right|_{U_1=0} = Y_{21,n} \\ Y_{22,n+1} = \left. \frac{I_2}{U_2} \right|_{U_1=0} = Y_{22,n} + C_{n+1}s \end{cases}$$

Carrying the admittance expressions function of the polynomials $Q_n(s^2)$

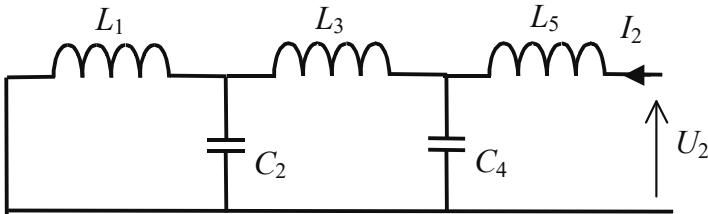
and $S_n(s^2)$:
$$\begin{cases} Y_{21,n+1} = \frac{-1}{s Q_n(s^2)} \\ Y_{22,n+1} = \frac{S_n(s^2)}{s Q_n(s^2)} + C_{n+1}s = \frac{S_n(s^2) + s^2 C_{n+1} Q_n(s^2)}{s Q_n(s^2)} \end{cases}$$

c) When adding a capacitance C_{n+1} , $n+1$ is even and thus n odd. Note in the numerator of $Y_{22,n+1}$ that $S_n(s^2)$ is replaced by $S_n(s^2) + s^2 C_{n+1} Q_n(s^2)$; so for odd $n = 2k-1$: $S_{2k}(s^2) = S_{2k-1}(s^2) + s^2 C_{2k} Q_{2k-1}(s^2)$. Since for the next integer, no capacitance is added, there is also $S_{2k+1}(s^2) = S_{2k}(s^2)$.

When adding an inductance L_{n+1} , $n+1$ is odd and n even. Note in the denominator of $Y_{21,n+1}$ and of $Y_{22,n+1}$ that $Q_n(s^2)$ is replaced by

$Q_n(s^2) + s^2 L_{n+1} S_n(s^2)$; so for even $n = 2k-2$: $Q_{2k-1}(s^2) = Q_{2k-2}(s^2) + L_{2k-1} S_{2k-2}(s^2)$. Since for the next integer, no inductance is added, there is also $Q_{2k}(s^2) = Q_{2k-1}(s^2)$.

4) a) When closing the port no. 1 of ladder LC- n on short-circuit $U_1 = 0$, $Y_{22,5}$ can be assessed directly by the ratio I_2/U_2 , that is the equivalent admittance observed between the output terminals where voltage U_2 is applied.



Going from the left, L_1 and C_2 are in parallel, giving an admittance $C_2 s + \frac{1}{L_1 s}$, occurring in series with L_3 , with an impedance $L_3 s + \frac{1}{C_2 s + \frac{1}{L_1 s}}$,

which occurs in parallel on C_4 , yielding an admittance $C_4 s + \frac{1}{L_3 s + \frac{1}{C_2 s + \frac{1}{L_1 s}}}$,

which occurs in series with L_5 to provide an impedance $L_5 s + \frac{1}{C_4 s + \frac{1}{L_3 s + \frac{1}{C_2 s + \frac{1}{L_1 s}}}}$, which may simply be reversed to provide

admittance $Y_{22,5}$.

Thus, identifying $K_5 = L_5$, $K_4 = C_4$, $K_3 = L_3$, $K_2 = C_2$, $K_1 = L_1$.

b) According to questions 2 and 3(b): $Y_{22,5} = \frac{S_n(s^2)}{s Q_n(s^2)} = \frac{a_0 + a_2 s^2 + a_4 s^4}{a_1 s + a_3 s^3 + a_5 s^5} G$

Division of $a_5s^5 + a_3s^3 + a_1s$ by $a_4s^4 + a_2s^2 + a_0$ provides $\frac{a_5}{a_4}s$ as quotient and $\left(a_3 - \frac{a_2a_5}{a_4}\right)s^3 + \left(a_1 - \frac{a_5}{a_4}\right)s$ as remainder. Hence, $L_5 = \frac{a_5}{a_4G}$.

Division of $a_4s^4 + a_2s^2 + a_0$ by remainder $\left(a_3 - \frac{a_2a_5}{a_4}\right)s^3 + \left(a_1 - \frac{a_5}{a_4}\right)s$ provides a quotient $\frac{a_4s}{a_3 - \frac{a_2a_5}{a_4}}$. Hence $C_4 = \frac{a_4G}{a_3 - \frac{a_2a_5}{a_4}}$; etc.

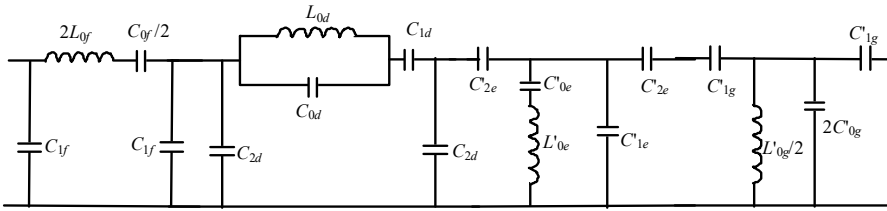
2.5.3. Dual-ended passive filter, synthesized by the image-impedance method

The aim is to create a band-pass filter with normalized angular cut-off frequencies 0.97 and 1.03, and additionally with attenuation poles at circular frequencies zero; infinite; 0.8 and 1.25. Resistance terminations are symmetrical and equal to $R_0 = 50 \Omega$. Minimum attenuation in stop band has to be 58 dB greater than that in pass band. The central frequency must be of 10.7 MHz.

- 1) Choose the type of cell to be used and their arrangement. Define the network.
- 2) Find the value of the components, with termination resistances being equal to R_0 .
- 3) Verify the minimum attenuation in stop band with help of asymptotic expressions.

Answer:

1) For the conditions applied, the choice is a (d) cell and an (e) cell used, respectively, to help the attenuation poles in the higher and lower stop bands. These are surrounded (f) and (g) cells redoubled and symmetrized for the attenuation poles at zero and infinite frequencies:



2) The termination resistances are noted R_0 (not shown on the figure).

The cutoff frequencies of cells (d) and (e) must be the same, noting the symmetrical attenuation poles $\omega'_{\infty\text{inf}}$ and $\omega_{\infty\text{sup}}$, which leads to:

$$C_{0d} = \frac{\omega_{\text{inf}}}{2R_0(\omega_{\infty\text{sup}}^2 - \omega_{\text{inf}}^2)} \left[\frac{\omega_{\text{sup}}}{\omega_{\text{inf}}} \sqrt{\frac{\omega_{\infty\text{sup}}^2 - \omega_{\text{inf}}^2}{\omega_{\infty\text{sup}}^2 - \omega_{\text{sup}}^2}} - \frac{\omega_{\text{inf}}}{\omega_{\text{sup}}} \sqrt{\frac{\omega_{\infty\text{sup}}^2 - \omega_{\text{sup}}^2}{\omega_{\infty\text{sup}}^2 - \omega_{\text{inf}}^2}} \right];$$

$$L_{0d} = \frac{1}{C_0 \omega_{\infty\text{sup}}^2}; \quad C_{2d} = \frac{1}{R_0 \omega_{\text{sup}}} \sqrt{\frac{\omega_{\infty\text{sup}}^2 - \omega_{\text{sup}}^2}{\omega_{\infty\text{sup}}^2 - \omega_{\text{inf}}^2}};$$

$$C_{1d} = \frac{1}{2R_0 \omega_{\text{inf}}} \left[\frac{\omega_{\text{sup}}}{\omega_{\text{inf}}} \sqrt{\frac{\omega_{\infty\text{sup}}^2 - \omega_{\text{inf}}^2}{\omega_{\infty\text{sup}}^2 - \omega_{\text{sup}}^2}} - \frac{\omega_{\text{inf}}}{\omega_{\text{sup}}} \sqrt{\frac{\omega_{\infty\text{sup}}^2 - \omega_{\text{sup}}^2}{\omega_{\infty\text{sup}}^2 - \omega_{\text{inf}}^2}} \right];$$

$$C'_{0e} = \frac{2}{R_0 \omega'_{\infty\text{inf}}} \left[\frac{\omega_{\text{sup}}}{\omega'_{\infty\text{inf}}} - \frac{\omega'_{\infty\text{inf}}}{\omega_{\text{sup}}} \right] \frac{\sqrt{(\omega_{\text{sup}}^2 - \omega_{\infty\text{inf}}^2)(\omega_{\text{inf}}^2 - \omega_{\infty\text{inf}}^2)}}{(\omega_{\text{sup}}^2 - \omega_{\text{inf}}^2)}; \quad L'_{0e} = \frac{1}{C'_0 \omega_{\infty\text{inf}}^2};$$

$$C'_{2e} = \frac{1}{R_0 \omega_{\text{sup}}} \sqrt{\frac{\omega_{\text{sup}}^2 - \omega_{\infty\text{inf}}^2}{\omega_{\text{inf}}^2 - \omega_{\infty\text{inf}}^2}}; \quad C'_{1e} = \frac{2\sqrt{(\omega_{\text{sup}}^2 - \omega_{\infty\text{inf}}^2)(\omega_{\text{inf}}^2 - \omega_{\infty\text{inf}}^2)}}{R_0 \omega_{\text{sup}} (\omega_{\text{sup}}^2 - \omega_{\text{inf}}^2)}.$$

Then, determine the components of cells (f) and (g) by:

$$C_{0f} = \frac{\omega_{\text{sup}}^2 - \omega_{\text{inf}}^2}{R_0 \omega_{\text{sup}} \omega_{\text{inf}}^2}; \quad C_{1f} = \frac{1}{R_0 \omega_{\text{sup}}}; \quad L_{0f} = \frac{R_0 \omega_{\text{sup}}}{\omega_{\text{sup}}^2 - \omega_{\text{inf}}^2} \text{ for type (f);}$$

$$C'_{0g} = \frac{\omega_{\text{inf}}}{R_0 (\omega_{\text{sup}}^2 - \omega_{\text{inf}}^2)}; \quad C'_{1g} = \frac{1}{R_0 \omega_{\text{inf}}}; \quad L'_{0g} = \frac{R_0 (\omega_{\text{sup}}^2 - \omega_{\text{inf}}^2)}{\omega_{\text{sup}}^2 \omega_{\text{inf}}}$$

for type (g).

Numerical application provides:

$$C_{0d} = 78 \text{ pF}; C_{1d} = 51.5 \text{ pF}; C_{2d} = 259 \text{ pF}; L_{0d} = 1.81 \text{ } \mu\text{H};$$

$$C'_{0e} = 1.12 \text{ nF}; C'_{1e} = 1.71 \text{ nF}; C'_{2ed} = 341 \text{ pF}; L'_{0e} = 0.307 \text{ } \mu\text{H};$$

$$C_{0f} = 37 \text{ pF}; C_{1f} = 289 \text{ pF}; L_{0d} = 6.38 \text{ } \mu\text{H};$$

$$C'_{0g} = 2.40 \text{ nF}; C'_{1g} = 289 \text{ pF}; C'_{2g} = 259 \text{ pF}; L'_{0g} = 87 \text{ nH}.$$

Of course, capacitances in parallel or in series are merged into a single one by the usual formula.

3) Zero and infinite frequency asymptotic image-attenuations for cells (d) and (e) are calculated from the following expressions by $20 \log(\Gamma)$:

$$\exp(\Gamma_{d0}) = \frac{\frac{\omega_{\text{sup}}}{\omega_{\text{inf}}} \sqrt{\frac{\omega_{\infty}^2 - \omega_{\text{inf}}^2}{\omega_{\infty}^2 - \omega_{\text{sup}}^2}} + 1}{\frac{\omega_{\text{sup}}}{\omega_{\text{inf}}} \sqrt{\frac{\omega_{\infty}^2 - \omega_{\text{inf}}^2}{\omega_{\infty}^2 - \omega_{\text{sup}}^2}} - 1}; \quad \exp(\Gamma_{d\infty}) = \frac{\sqrt{\frac{\omega_{\infty}^2 - \omega_{\text{inf}}^2}{\omega_{\infty}^2 - \omega_{\text{sup}}^2}} + 1}{\sqrt{\frac{\omega_{\infty}^2 - \omega_{\text{inf}}^2}{\omega_{\infty}^2 - \omega_{\text{sup}}^2}} - 1};$$

$$\exp(\Gamma_{e0}) = \frac{\frac{\omega_{\text{inf}}}{\omega_{\text{sup}}} \sqrt{\frac{\omega_{\text{sup}}^2 - \omega_{\infty}^2}{\omega_{\text{inf}}^2 - \omega_{\infty}^2}} + 1}{\frac{\omega_{\text{inf}}}{\omega_{\text{sup}}} \sqrt{\frac{\omega_{\text{sup}}^2 - \omega_{\infty}^2}{\omega_{\text{inf}}^2 - \omega_{\infty}^2}} - 1}; \quad \exp(\Gamma_{e\infty}) = \frac{\sqrt{\frac{\omega_{\text{sup}}^2 - \omega_{\infty}^2}{\omega_{\text{inf}}^2 - \omega_{\infty}^2}} + 1}{\sqrt{\frac{\omega_{\text{sup}}^2 - \omega_{\infty}^2}{\omega_{\text{inf}}^2 - \omega_{\infty}^2}} - 1}$$

Providing 47 dB for the two asymptotic values. The image attenuation

must be added twice:
$$\exp(2\Gamma_f) = \frac{\sqrt{\frac{\omega^2 - \omega_{\text{sup}}^2}{\omega^2 - \omega_{\text{inf}}^2}} + 1}{\sqrt{\frac{\omega^2 - \omega_{\text{sup}}^2}{\omega^2 - \omega_{\text{inf}}^2}} - 1} \quad \text{for } \underline{\omega} > \underline{\omega}_{\text{sup}} \text{ and}$$

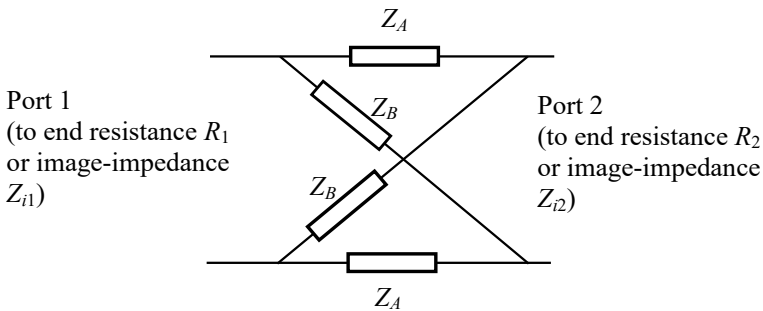
$$\exp(2\Gamma_g) = \frac{\sqrt{\frac{\omega_{\text{sup}}^2 - \omega_{\text{inf}}^2}{\omega_{\text{sup}}^2 - \omega^2}} + 1}{\sqrt{\frac{\omega_{\text{sup}}^2 - \omega_{\text{inf}}^2}{\omega_{\text{sup}}^2 - \omega^2}} - 1} \quad \text{for } \underline{\omega} < \underline{\omega}_{\text{inf}}, \text{ for cells (f) and (g), which}$$

quickly tend to a constant that can be evaluated quite precisely for $\omega = 10 \omega_{\text{sup}}$ and $\omega = \omega_{\text{inf}}/10$.

Using these expressions, the $40 \log(\Gamma)$ image-attenuations can be deduced, finding 13 dB for both 47 dB cells (f) and (g). Adding to the image-attenuations of cells (d) and (e) provides 60 dB, which is greater than the requirement.

2.5.4. Lattice filter

The circuit of the symmetrical lattice is provided below:



1) Show that the reference potential (ground) can be placed so that the potentials are made antisymmetric relative to the median horizontal axis. Deduce the consequence of this for the currents.

2) Deduce parameters Z and Y as a function of Z_A and Z_B , then the image-impedances.

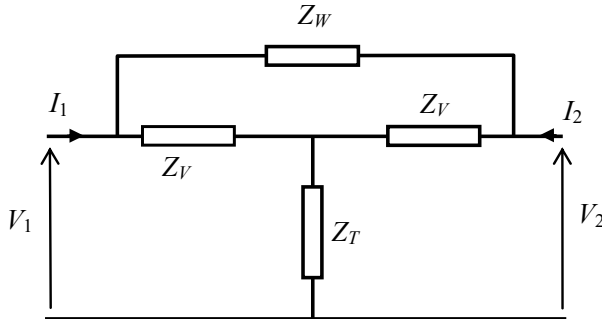
3) In the case where Z_A is the impedance of a quartz resonator (with the series capacitance C_0 much larger than the parallel one C_1) and Z_B that of a capacitor C_2 , find the function of the two-port network as well as its image-parameters (characteristic frequencies, bandwidth, asymptotic attenuations). Is the response curve symmetric in the frequency domain? How should the image-attenuation in the stop bands be designed?

4) Show that the frequency of the attenuation pole can be set independently by calculating the voltage gain for a resistive load R_l .

5) By keeping the lattice structure but loaded by the iterative resistance R_0 , apply the expressions provided in the course for voltage gain G_v and

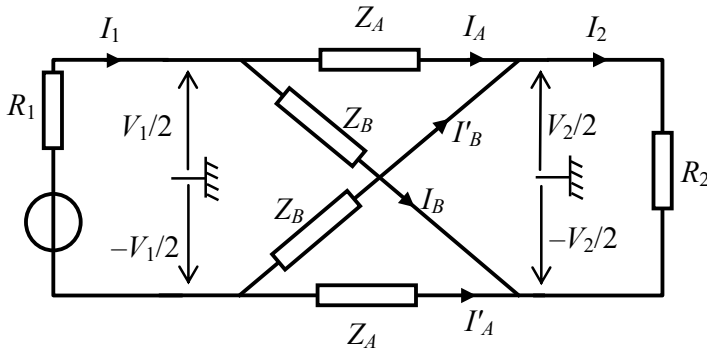
input impedance, then determine the elements necessary to obtain voltage gain with all-pass transmittance $G_v(s) = \frac{s^2 - 2\zeta\omega_n s + \omega_n^2}{s^2 + 2\zeta\omega_n s + \omega_n^2}$.

6) Show that a bridged-T structure such as the one below can, under a certain condition (to be defined), have the same parameters (Z for example) as the previous all-pass-type lattice filter.



Answer:

1) Applying the ground in order to divide V_1 into 2 parts equal in modulus and opposites, where $V_1 = V_1/2 - (-V_1/2)$, and similarly for V_2 , providing:



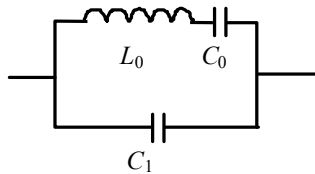
By symmetry relative to the median horizontal axis, since the voltages are antisymmetric, the currents must be likewise: $I'_A = -I_A$; $I'_B = -I_B$ since currents are related to voltages by means of a system of linear equations.

2) With $I_2 = 0$, current I_1 divides into two equal parts in two identical branches in parallel with impedance $Z_A + Z_B$, where $Z_{11} = \frac{Z_B + Z_A}{2} = Z_{22}$ due to the symmetry relative to the median vertical axis. Similarly, $Z_{21} = V_2 / I_1$ can be calculated by means of the two voltage dividers Z_A, Z_B : $V_2 = \left(\frac{Z_B}{Z_B + Z_A} - \frac{Z_A}{Z_B + Z_A} \right) V_1 = (Z_B - Z_A) \frac{V_1}{Z_B + Z_A} = (Z_B - Z_A) \frac{I_1}{2}$. Hence, $Z_{21} = \frac{Z_B - Z_A}{2} = Z_{12}$ by symmetry relative to the median vertical axis.

For the Y parameters, with $V_2 = 0$, the Z_A and Z_B parameters are in parallel and two cells $Z_A // Z_B$ are placed in series, thus $Y_{11} = \frac{Z_B + Z_A}{2Z_B Z_A} = Y_{22}$. The same condition allows for the calculation of $I_2 = I_A - I_B = \left[\frac{Z_B}{(Z_B + Z_A)} - \frac{Z_A}{(Z_B + Z_A)} \right] I_1 = \left[\frac{Z_B}{(Z_B + Z_A)} - \frac{Z_A}{(Z_B + Z_A)} \right] Y_{11} V_1$, accounting for the current dividers, which leads to $Y_{21} = \frac{Z_B - Z_A}{2Z_B Z_A} = Y_{12}$.

The image-impedance (symmetrical relative to the median vertical axis) is calculated by $Z_{iT} = \sqrt{\frac{Z_{11}}{Y_{11}}} = \sqrt{Z_A Z_B}$.

3) Simulating the quartz resonator with the following schematics,



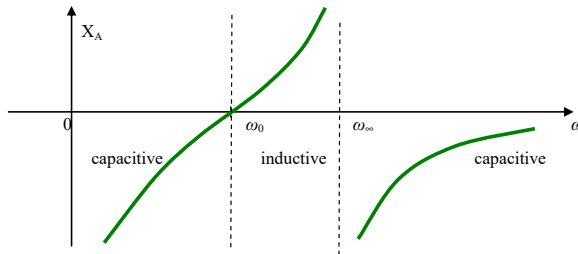
its impedance turns out to be:

$$\begin{aligned}
 Z_A &= \frac{1}{C_1 s + \frac{C_0 s}{L_0 C_0 s^2 + 1}} = \frac{L_0 C_0 s^2 + 1}{(C_0 + C_1) s \left[1 + L_0 \frac{C_0 C_1}{C_0 + C_1} s^2 \right]} \\
 &= \frac{1 + \frac{s^2}{\omega_0^2}}{(C_0 + C_1) s \left[1 + \frac{s^2}{\omega_\infty^2} \right]}
 \end{aligned}$$

writing $\omega_0^2 = \frac{1}{L_0 C_0}$ and $\omega_\infty^2 = \frac{C_0 + C_1}{L_0 C_0 C_1} = (1 + a_1) \omega_0^2$ where $a_1 = \frac{C_0}{C_1} \ll 1$.

Impedance $Z_A = j X_A$ with reactance $X_A = -\frac{1 - \frac{\omega^2}{\omega_0^2}}{(C_0 + C_1) \omega \left[1 - \frac{\omega^2}{\omega_\infty^2} \right]}$ under

sinusoidal conditions always results in the following response in linear scales:



If Z_B is the impedance of a capacitor C_2 , the image-impedance is $\sqrt{Z_A Z_B} = \sqrt{\frac{X_A}{C_2 \omega}}$, real when X_A is positive (inductive Z_A) and imaginary when X_A is negative (capacitive Z_A). The bandwidth is thus the interval $[\omega_0, \omega_\infty]$, surrounded by two stop bands; accordingly this is a band-pass. Its image-attenuation Γ_T is provided by $\coth(\Gamma_T) = \sqrt{Z_{11} Y_{11}} = \frac{Z_A + Z_B}{2\sqrt{Z_A Z_B}}$, which is real when X_A is negative (capacitive Z_A), corresponding to the stop bands. The full expression is:

$$\coth(\Gamma_T) = \frac{1}{2} \sqrt{\frac{C_2 \left[1 - \frac{\omega^2}{\omega_0^2}\right]}{(C_0 + C_1) \left[1 - \frac{\omega^2}{\omega_\infty^2}\right]}} + \frac{1}{2} \sqrt{\frac{(C_0 + C_1) \left[1 - \frac{\omega^2}{\omega_\infty^2}\right]}{C_2 \left[1 - \frac{\omega^2}{\omega_0^2}\right]}}$$

approaching $\frac{1}{2} \sqrt{\frac{C_2}{(C_0 + C_1)}} + \frac{1}{2} \sqrt{\frac{(C_0 + C_1)}{C_2}}$ for $\omega \rightarrow 0$ and approaching

$$\frac{1}{2} \sqrt{\frac{C_2}{C_1}} + \frac{1}{2} \sqrt{\frac{C_1}{C_2}} \text{ for } \omega \rightarrow \infty.$$

Since C_0 is much lower than C_1 in quartz, the two previous limits are very close to each other. Consequently, the response curve is almost symmetric. Since both of these asymptotic values contain the total of a quantity and its opposite, thus providing a minimum value when both quantities are equal, it is worthwhile to favor either one term or the other in each, for example with either $C_2 \gg C_1$, or the opposite. Then, image-attenuation can be designed

with $\coth(\Gamma_T) \approx \exp(\Gamma_T) \approx \frac{1}{2} \sqrt{\frac{C_2}{C_1}}$ in the first case. In order to augment this,

several identical filters may be placed in cascade, which has the further effect of minimizing deviations between the image response curve and the real response curve in so far as the intermediate dipolar impedances approach the image-impedances.

4) The voltage gain can be easily obtained from the Z parameters:

$$G_v = \frac{Z_{21} R_l}{\det Z + Z_{11} R_l}, \quad \text{that is} \quad G_v = \frac{Z_B - Z_A}{2} \frac{R_l}{Z_B Z_A + \frac{Z_B + Z_A}{2} R_l} = \frac{(Z_B - Z_A) R_l}{2 Z_B Z_A + (Z_B + Z_A) R_l}.$$

There is thus zero transmittance or attenuation pole at the frequency where $Z_A = Z_B$, independently of the characteristic frequencies of the previous question.

5) Returning to the previous expression in which $Z_A Z_B$ is replaced by R_0^2 :

$$\begin{aligned}
 G_v &= \frac{Z_B - Z_A}{2R_0 + (Z_B + Z_A)} = \frac{R_0^2 / Z_A - Z_A}{2R_0 + (R_0^2 / Z_A + Z_A)} \\
 &= \frac{R_0^2 - Z_A^2}{Z_A^2 + 2R_0 Z_A + R_0^2} = \frac{R_0 - Z_A}{R_0 + Z_A}
 \end{aligned}$$

and using the input impedance given at the end of section 2.1.5.1:

$$\begin{aligned}
 Z_e \Big|_{V_2 = -R_0 I_2} &= \frac{Z_{11} R_0 + \det Z}{R_0 + Z_{22}} \\
 Z_e &= \frac{R_0 (Z_A + Z_B) + 2Z_A Z_B}{2R_0 + Z_A + Z_B} = \frac{R_0 (Z_A + R_0^2 / Z_A) + 2R_0^2}{2R_0 + Z_A + R_0^2 / Z_A} \\
 &= R_0 \frac{Z_A^2 + R_0^2 + 2R_0 Z_A}{Z_A^2 + R_0^2 + 2R_0 Z_A} = R_0
 \end{aligned}$$

An inductance L and capacitance C placed in parallel for Z_A provide

$$Z_A = \frac{1}{Cs + \frac{1}{Ls}} = \frac{Ls}{LCs^2 + 1}, \text{ which sets } G_v = \frac{R_0 (LCs^2 + 1) - Ls}{R_0 (LCs^2 + 1) + Ls} = \frac{s^2 - \frac{s}{R_0 C} + \frac{1}{LC}}{s^2 + \frac{s}{R_0 C} + \frac{1}{LC}}$$

that is identified with the form of the all-pass transmittance of the second order if $\omega_n = \frac{1}{\sqrt{LC}}$ and if the damping coefficient is $\zeta = \frac{1}{2R_0} \sqrt{\frac{L}{C}}$. The

elements can be calculated by $C = \frac{1}{2\zeta\omega_n R_0}$ and $L = \frac{2\zeta R_0}{\omega_n}$. Lastly,

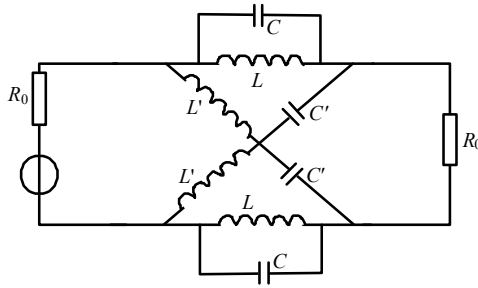
establishing the expression of impedance Z_B :

$$Z_B = \frac{R_0^2}{Z_A} = \frac{R_0^2}{Ls} (LCs^2 + 1) = R_0^2 Cs + \frac{R_0^2}{Ls}.$$

It is thus the serial association of an

inductance $L' = R_0^2 C = \frac{R_0}{2\zeta\omega_n}$ and a capacitance $C' = \frac{L}{R_0^2} = \frac{2\zeta}{R_0\omega_n}$. Hence the

filter circuit:



6) Parameters Z_{11} and Z_{12} of the T-bridge two-port network can be determined by calculating the impedance of the associations that appear in the circuit for $I_2=0$ in the first case and $I_1=0$ in the second:

$$Z_{11} = \left. \frac{V_1}{I_1} \right|_{I_2=0} = Z_T + Z_V // (Z_V + Z_W) = Z_T + \frac{Z_V (Z_V + Z_W)}{2Z_V + Z_W}$$

$Z_{12} = \left. \frac{V_1}{I_2} \right|_{I_1=0}$ is deduced from the calculation of

$$V_1 = (V_2 - Z_T I_2) \frac{Z_V}{Z_V + Z_W} + Z_T I_2 = \frac{V_2 Z_V + Z_W Z_T I_2}{Z_V + Z_W} \quad \text{and of} \quad V_2 = Z_{22} I_2 = Z_{11} I_2.$$

Carrying over the expression of V_2 into that of V_1 , after simplification, provides $Z_{12} = Z_T + \frac{Z_V^2}{2Z_V + Z_W}$. Note that $Z_{11} = Z_{12} + \frac{Z_V Z_W}{2Z_V + Z_W}$.

For the lattice, according to the response to question 2, $Z_A = Z_{11} - Z_{12} = \frac{Z_V Z_W}{2Z_V + Z_W}$ thus Z_V in parallel with $Z_W/2$. Since Z_A itself comprises two branches in parallel, there is clearly either Z_V with $jL\omega$ and $Z_W/2$ with $1/jC\omega$ (case 1), or Z_V with $1/jC\omega$ and $Z_W/2$ with $jL\omega$ (case 2). Next, calculate $Z_B = Z_{11} + Z_{12}$ which after simplification gives $Z_B = 2Z_T + Z_V$.

Hence the deduction $Z_T = \frac{1}{2}(Z_B - Z_V)$ when possible.

In the first case, $Z_V = jL\omega$; $Z_W = \frac{2}{jC\omega}$;

$$Z_T = \frac{1}{2} \left(jL'\omega + \frac{1}{jC'\omega} - jL\omega \right) = j \frac{L'-L}{2} \omega + \frac{1}{jC'\omega}$$

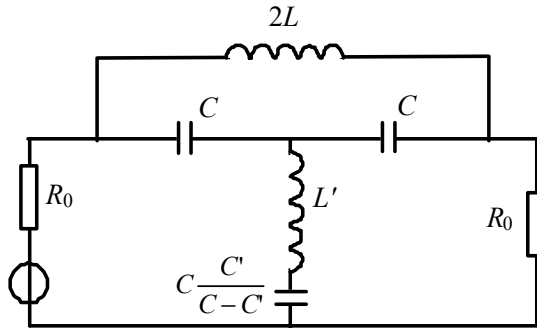
and in the second case

$$Z_V = \frac{1}{jC\omega}; Z_W = 2jL\omega;$$

$$Z_T = \frac{1}{2} \left(jL'\omega + \frac{1}{jC'\omega} - \frac{1}{jC\omega} \right) = jL'\omega + \frac{1}{jC\omega} \frac{C-C'}{C'}$$

In both cases, the difference must be positive, which requires $\frac{1}{2\zeta} > 2\zeta$ using the expressions of C, C' or L, L' from question 5, implying $\zeta < \frac{1}{2}$.

This condition is often applied for an all-pass filter group delay corrector since the significant variations of the derivative of the phase for one filter are due to factors of the second order presenting a low damping coefficient, which requires compensation by means of the all-pass transmittance. The second version is to be favored, in which there are only two inductances (the R_0 terminations can be replaced by iterative resistance cells or identical image-resistance):



Appendix

Notions of Distribution and Operating Properties

While a function establishes a correspondence between a set of numbers and another set of numbers, a T functional (or form) is an application that maps a set of numbers (end set) to a set of functions or operators g (start set) belonging to a vector space by means of a function ϕ that should be indefinitely differentiable with bounded support or, alternatively, quickly decreasing.

A distribution is a linear functional with respect to ϕ and g , which is calculated like a scalar product if g is assumed to be locally integrable, that is to say integrable as defined by Lebesgue, on any bounded interval (or support):

$$\langle T_g, \phi \rangle = \int_{-\infty}^{\infty} g(x)\phi(x)dx$$

For measurable subsets of \mathbb{R} , for which a length can be defined, Lebesgue's integration approaches the result by summing "slices" with height dy , where y are the ordinates, in contrast to Riemann's integration that approximates the result by summing rectangles of width dx , where x represents abscissa. These subsets, called X , form a σ -algebra if they have a complement, if the empty subset exists and if countable unions and intersections still generate another subset; therefore, a measure $\mu(X)$, which is related to the size of the "slices", can be defined and enables us to

calculate the Lebesgue integral. In the following example we will only focus on the distributions that are useful for signal processing.

A.1. Dirac distribution or Dirac impulse δ_a or $\delta(x - a)$

The Dirac impulse δ_a can be understood as *an operator that makes obtaining the value of the function ϕ at point a possible*. In general, it can be written in the following form:

$$\langle T_{\delta_a}, \phi \rangle = \int_{-\infty}^{\infty} \delta(x-a)\phi(x)dx = \phi(a)$$

The generally adopted notation $\delta(x - a)$ suggests that it is a function; this is, however, not the case. The integral must be taken within the meaning of distributions. It makes sense if it is a Lebesgue integral, which is defined if the integrand can be integrated (it is then part of the vector space of summable functions denoted by L^1), and in order to make g integrable, it is necessary and sufficient that $|g|$ is so, that is to say that the integral be absolutely convergent.

This implies that $g(x) \rightarrow 0$ when $x \rightarrow \pm\infty$ or that the *support* of the function or of the operator $g(x)$ be *bounded* (g equal to zero outside of one or more closed intervals). In the case of the Dirac impulse, the support is reduced to a single point at the abscissa $x = a$ (the size along x is zero) and the measure $\mu(X) = \int \delta_a d\mu = \int_{-\infty}^{\infty} \delta(x-a)dx = 1$ is unitary.

– Application to the convolution product:

$$\int_{-\infty}^{\infty} h(t-\tau)\delta(\tau)d\tau = \int_{-\infty}^{\infty} h(\tau)\delta(t-\tau)d\tau = h(t)$$

The Dirac impulse is the neutral element of the convolution product.

NOTE.– If the integration interval is $[b, c]$ instead of $]-\infty, \infty[$, the result is the same when the support a is included in $[b, c]$ or $b \leq a \leq c$. Otherwise, the result is zero.

– Application to the Fourier and Laplace transforms of the Dirac impulse:

$$\int_{-\infty}^{\infty} \exp[-j2\pi ft] \delta(t) dt = 1 \quad \text{and} \quad \int_{-\infty}^{\infty} \exp[-pt] \delta(t) dt = 1.$$

It can be shown that any pulse sequence $f_n(x)$ (rectangular, triangular, sinc, Gaussian, etc.) whose amplitude $f_n(0)$ tends to infinity and the width to zero while maintaining the area under the curve equal to 1, that is $\int f_n(x) dx = 1$ when $n \rightarrow \infty$, converges toward the Dirac distribution. This is the case of:

$$\text{TF}^{-1}[1] = \lim_{n \rightarrow \infty} \int_{-nf_0}^{nf_0} \exp[j2\pi ft] df = \lim_{n \rightarrow \infty} \left[2nf_0 \frac{\sin(2\pi nf_0 t)}{2\pi nf_0 t} \right] \rightarrow \delta(t) \quad \text{and}$$

$$\text{symmetrically } \text{TF}[1] = \lim_{n \rightarrow \infty} \int_{-nT_0}^{nT_0} \exp[-j2\pi ft] dt = \lim_{n \rightarrow \infty} \left[2nT_0 \frac{\sin(2\pi nT_0 f)}{2\pi nT_0 f} \right] \rightarrow \delta(f)$$

$$\text{In summary: } \begin{cases} \delta(t) \xrightarrow{\text{FT}} 1 & 1 \xrightarrow{\text{FT}^{-1}} \delta(t) \\ \delta(f) \xrightarrow{\text{FT}^{-1}} 1 & 1 \xrightarrow{\text{FT}} \delta(f) \end{cases}$$

Meanwhile, the replacement of $\delta(x)$ with $f_n(x)$ in $\int_{-\infty}^{\infty} f_n(x) \phi(x) dx$ does not necessarily lead to a converging integral. But it can be shown that $f_n(x) = \lim_{n \rightarrow \infty} \left[\frac{1}{2\pi n} \left(\frac{\sin(nx/2)}{\sin(x/2)} \right)^2 \right]$ involves convergence for all continuous functions $\phi(x)$ on a compact support.

By extension, the infinite and periodic suites of Dirac impulses, known as Dirac “combs” $\sum_{k=-\infty}^{+\infty} \delta(t - kT_0)$ with a period T_0 in the time domain and $\sum_{n=-\infty}^{+\infty} \delta(f - nf_0)$ with a period f_0 in the frequency domain can be devised.

A.2. Derivation of a distribution and derivation of discontinuous functions

The derivative of a distribution $\langle T_g, \phi \rangle$ is obtained by the distribution associated with g' , the derivative of the function: $\langle T_{g'}, \phi \rangle = \int_{-\infty}^{\infty} g'(x)\phi(x)dx$.

Since g' is not necessarily defined, it is useful to calculate the result of the integration by parts:

$$\begin{aligned} \int_{-\infty}^{\infty} g'(x)\phi(x)dx &= [g(x)\phi(x)]_{-\infty}^{\infty} - \int_{-\infty}^{\infty} g(x)\phi'(x)dx = - \int_{-\infty}^{\infty} g(x)\phi'(x)dx \\ &= - \langle T_g, \phi' \rangle \end{aligned}$$

because $g(x) \rightarrow 0$ when $x \rightarrow \pm\infty$.

Therefore by definition, it is established that: $\langle T_{g'}, \phi \rangle = - \langle T_g, \phi' \rangle$.

For δ_a' : $\langle T_{\delta'}, \phi \rangle = - \langle T_{\delta}, \phi' \rangle = - \phi'(a)$. δ_a' is therefore an operator that makes it possible to obtain the value of the derivative of the function ϕ at the abscissa point a , with changed sign.

More generally, the n th derivatives of the Dirac distribution $\delta_a^{(n)}$ are defined by:

$$\int_{-\infty}^{\infty} \delta^{(n)}(x-a)\phi(x)dx = (-1)^n \phi^{(n)}(a)$$

NOTE.— The Dirac distribution and its n th derivatives $\delta_a^{(n)}$ are operators that provide the value of the function ϕ or of its n th derivatives $\times (-1)^n$ at point a when the product $\phi \delta_a^{(n)}$ is integrated on an interval including abscissa a .

If a function $g(x)$ exhibits 1st-kind discontinuity at $x = b$ with a step Δg , we look for the derivative of the distribution associated with g and we use two integrations by parts:

$$\begin{aligned} - \langle T_{g'}, \phi \rangle &= \langle T_g, \phi' \rangle = \int_{-\infty}^{b-} g(x)\phi'(x)dx + \int_{b+}^{\infty} g(x)\phi'(x)dx = [g(x)\phi(x)]_{-\infty}^{b-} \\ &- \int_{-\infty}^{b-} g'(x)\phi(x)dx + [g(x)\phi(x)]_{b+}^{\infty} - \int_{b+}^{\infty} g'(x)\phi(x)dx = -[g(b_+) - g(b_-)]\phi(b) \\ &- \int_{-\infty}^{\infty} g_{md}'(x)\phi(x)dx = -\Delta g \phi(b) - \int_{-\infty}^{\infty} g_{md}'(x)\phi(x)dx, \end{aligned}$$

where $g_{md}'(x)$ is the derivative of the function minus the discontinuity Δg $U(t)$. Then

$$\langle T_{g'}, \phi \rangle = \Delta g \langle T_{\delta_b}, \phi \rangle + \langle T_{g_{md}'}, \phi \rangle$$

or to simplify the notation, but still within the definition of distributions:

$$g' = g_{md}' + \Delta g \delta_b = g_{md}' + \Delta g \delta(x - b)$$

By extension to the case of the second derivative:

$$g'' = g_{md}'' + \Delta g \delta'(x - b) + \Delta g' \delta(x - b)$$

– Application to the derivative of the unit step function $U(t)$:
 $U'(t) = 0 + 1 \delta(t) = \delta(t)$.

The derivative of the Heaviside step function within the sense of distributions is equal to the Dirac impulse.

A.3. Laplace transform of distributions

Let $T_f^{(n)}$ be a distribution associated with the n th derivative of a function $f(t)$ within the meaning of distributions. Let $F(s)$ be the Laplace transform of $f(t)$. By definition, it is defined that the LT of the distribution $T_f^{(n)}$ is equal to $s^n F(s)$.

The $LT[\delta(t)]$ is then simply $LT[\delta(t)] = s \frac{1}{s} = 1$.

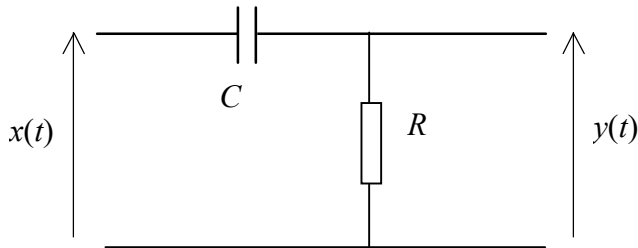
This is by no means inconsistent with the derivation rule of the LT. In fact, if $f(t)$ has a 1st-kind discontinuity $\Delta f = f(0^+) - f(0^-)$ at the origin, for example, the LT of the functions without discontinuity indicates that:

$$f_{md}'(t) \xrightarrow{\text{LT}} sF(s) - f(0^+)$$

However, $f'(t) = f_{md}'(t) + [f(0^+) - f(0^-)]\delta(t) = f_{md}'(t) + f(0^+)\delta(t)$, which gives after Laplace transform:

$$f'(t) \xrightarrow{\text{LT}} sF(s) - f(0^+) + f(0^+) = sF(s)$$

This can be used to solve a circuit equation with the Laplace transform. For example, for a C - R circuit, we can write if $x(t)$ is the input voltage and $y(t)$ the output voltage at the terminals of R : $q = C(x - y)$ for the charge within the capacitor, and by differentiating it yields: $\frac{dy}{dt} + \frac{1}{RC}y = \frac{dx}{dt}$, which gives by taking the LT within the meaning of distributions $sY(s) + Y(s)/RC = sX(s)$.



If $x(t) = V_0\mathbf{U}(t)$, $sX(s) = V_0$, where: $Y(s) = \frac{V_0}{s + \frac{1}{RC}}$ and by identification

$y(t) = V_0 \exp(-t/RC)\mathbf{U}(t)$ for the forced behavior.

A.4. Distribution in principal value p.v. $\left(\frac{1}{x}\right)$ following Cauchy's definition

When integrating a function $\phi(x)$ divided by x , it happens that the integral be only computable as a Cauchy principal value (except if $\phi(x)$ can be divided by x), that is to say by excluding the origin or a discontinuity point:

$$\int \frac{\phi(x)}{x} dx = \lim_{\varepsilon \rightarrow 0^+} \left[\int_a^{-\varepsilon} \frac{\phi(x)}{x} dx + \int_{\varepsilon}^b \frac{\phi(x)}{x} dx \right] = \lim_{\varepsilon \rightarrow 0^+} \left[\int_{|x| > \varepsilon} \frac{\phi(x)}{x} dx \right] \text{ with } a < 0 \text{ and } b > 0.$$

Here, the second-kind discontinuity is located at the origin. The definition domain of the principal value p.v. $\left(\frac{\phi(x)}{x}\right)$ of the function $\frac{\phi(x)}{x}$ is then $]-\infty 0[\cup]0 +\infty[$.

We can then define the distribution T associated with $1/x$ and applied to the function $\phi(x)$: $\langle T_{\frac{1}{x}}, \phi \rangle = \langle \text{p.v.} \left(\frac{1}{x} \right), \phi \rangle = \int \frac{\phi(x)}{x} dx$ and it can be shown that it can be written as $-\int_a^b \phi'(x) \text{Ln}|x| dx$ from integration by parts.

A more general result is $\lim_{\epsilon \rightarrow 0^+} \left[\int_{|x| > \epsilon} \frac{\phi(x)}{x \pm j\epsilon} dx \right] = \mp j\pi \phi(0) + \lim_{\epsilon \rightarrow 0^+} \left[\int_{|x| > \epsilon} \frac{\phi(x)}{x} dx \right]$.

When $\phi(x) = 1 \forall x$, $\phi(0)$ must be replaced by $\delta(0)$.

– Application to the search for the FT of the sign function $\text{sgn}(t)$ and the Heaviside step function $U(t)$:

Let $\text{sgn}(t) = 2U(t) - 1$, which equals -1 for $t < 0$ and $+1$ for $t > 0$, therefore it is an odd function, and $s(t) = \text{FT}^{-1} \left[j \text{p.v.} \left(\frac{1}{f} \right) \right]$, which is therefore also odd, because $j \text{p.v.} \left(\frac{1}{f} \right)$ is purely imaginary.

However, $\text{FT}^{-1} \left[j2\pi f \text{p.v.} \left(\frac{1}{f} \right) \right] = \frac{1}{j} \frac{ds}{dt} \text{FT}^{-1} [j2\pi \times 1] = j2\pi \delta(t)$ because $f \text{p.v.} \left(\frac{1}{f} \right) = \frac{f}{f} = 1$.

Thereby $\frac{ds}{dt} = -2\pi \delta(t)$, which yields that $s(t) = -2\pi U(t) + C$.

Let us determine the constant C by means of the odd symmetry of $s(t)$ and the identity $U(t) + U(-t) = 1$:

$$\begin{aligned} s(t) &= -s(-t) \Rightarrow -2\pi U(t) + C = 2\pi U(-t) - C \Rightarrow C = \pi \Rightarrow s(t) \\ &= -\pi [2U(t) - 1] \end{aligned}$$

Let finally: $s(t) = -\pi \text{sgn}(t)$

Since $\text{FT}^{-1}\left[\text{Vs}\left(\frac{1}{f}\right)\right] = \frac{1}{j}s(t) = j\pi \text{sgn}(t)$ or still $\text{FT}[\text{sgn}(t)] = \frac{1}{j\pi} \text{p.v.}\left(\frac{1}{f}\right)$.

Hence, the FT of $U(t)$: $\text{FT}[U(t)] = \text{FT}\left[\frac{1}{2}(1 + \text{sgn}(t))\right] = \frac{1}{2}\delta(t) + \frac{1}{j2\pi} \text{p.v.}\left(\frac{1}{f}\right)$

We could also demonstrate that $\text{sgn}(f) = -\frac{1}{j\pi} \text{TF}\left[\text{p.v.}\left(\frac{1}{f}\right)\right]$.

A.5. Solving equations with discontinuous functions derivatives

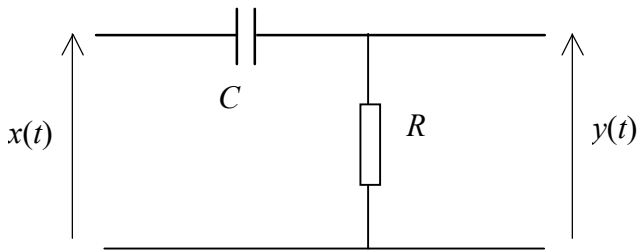
The derivation of distributions can be used to solve equations, especially differential equations, within the meaning of distributions without resorting to the Laplace transform. For a capacitance C , $i(t) = \frac{dq}{dt} = C \frac{dv}{dt} = C \frac{dv_{md}}{dt} + \Delta q \delta(t)$ if a charge impulse Δq is suddenly injected at $t = 0$ and in this case $i(t)$ is a distribution. Otherwise (only physically possible case), it is a function only exhibiting 1st-kind discontinuities.

Similarly, for an inductance L , $e(t) = \frac{d\phi}{dt} = L \frac{di}{dt} = L \frac{di_{md}}{dt} + \Delta\phi \delta(t)$ is a distribution if we impose a sudden variation of the magnetic flux $\Delta\phi$. Otherwise (only physically possible case), it is a function only exhibiting 1st-kind discontinuities.

For a circuit physically implementable C - R , if $x(t)$ is the input voltage and $y(t)$ the output voltage at the terminals of R : $q = C(x - y)$ is the charge stored by the capacitor and we find within the meaning of distributions

$$\frac{dy}{dt} + \frac{1}{RC}y = \frac{dx}{dt}.$$

$$\text{If } x(t) = V_0 U(t): \frac{dy_{md}}{dt} + [y(0^+) - y(0^-)]\delta(t) + \frac{1}{RC}y = [x(0^+) - x(0^-)]\delta(t) = V_0\delta(t).$$



This imposes that there is separate equality between distributions in two members and ordinary functions in two members, that is:

$y(0^+) - y(0^-) = V_0$ for distributions and $\frac{dy_{md}}{dt} + \frac{1}{RC} y_{md} = 0$ for $t > 0$ for ordinary functions. As a result, we automatically have $y(0^+) - y(0^-) = x(0^+) - x(0^-) = V_0$ because there was no sudden charge injection, corresponding to the case where $q = C(x - y) = \int i(t) dt$ remains continuous.

For the function y_{md} , it is deduced that: $y_{md}(t) = K \exp(-t/RC)$ at $t > 0$. Hence finally, $y(t) = V_0 \exp(-t/RC) \mathbf{U}(t) + y(0^-)$ if C was initially charged and with $y(0^-) = 0$ otherwise.

Bibliography

- [AUG 99] AUGER F., *Introduction à la théorie du signal et de l'information*, Technip, Paris, 1999.
- [DED 96] DEDIEU H., DEHOLLAIN C., HASLER M., NEIRYNCK J., *Les filtres électriques*, 3rd ed., Presses Polytechniques et Universitaires Romandes, Lausanne, 1996.
- [FEL 81] FELDMANN M., *Théorie des réseaux et systèmes linéaires*, Eyrolles, Paris, 1981.
- [MAN 89] MANNEVILLE F., ESQUIEU J., *Electronique: Systèmes bouclés linéaires de communication et de filtrage*, Dunod, Paris, 1989.
- [MUR 17] MURET P., *Fundamentals of Electronics 1: Electronic Components and Elementary Functions*, ISTE Ltd, London and John Wiley & Sons, New York, 2017.
- [MUR 18] MURET P., *Fundamentals of Electronics 3: Discrete-time Signals and Systems and Conversion Systems*, ISTE Ltd, London and John Wiley & Sons, New York, 2018.
- [NEI 83] NEIRYNCK J., BOITE R., *Théorie des réseaux de Kirchhoff*, Presses Polytechniques et Universitaires Romandes, Lausanne, 1983.
- [PER 06] PEREZ J.-P., LAGOUTE C., FOURNIOLS J.-Y., BOUHOURS S., *Electronique : Fondements et applications*, Dunod, Paris, 2006.
- [PET 98] PETIT R., *L'outil mathématique pour la physique*, Dunod, Paris, 1998.

[PIC 89] PICINBONO B., *Théorie des signaux et des systèmes*, Bordas, 1989.

[UNS 04] UNSWORTH L., “All-pole equiripple approximations to arbitrary functions of frequency”, *The International Journal for Computation and Mathematics in Electrical and Electronic Engineering*, vol. 23, no. 2, p. 452, 2004.

Index

A

antisymmetric, 214, 216
asymptotic diagram, 17
attenuation, 73, 122–124, 135, 137–
141, 143, 158, 166–68, 170, 172–
193, 195, 211–214, 217, 218
autocorrelation, 7, 8

B

Bayard-Bode, 131–135
Bessel, 69, 70, 140, 143, 144
block diagram, 24, 25, 40, 42, 72, 75,
86, 124–126
Bode, 16, 18, 19, 21, 29, 35–37, 42,
72, 73, 131–133, 135, 137, 138,
143, 156, 159, 177
Butterworth, 69, 70, 140, 144

C

Cauer, 97, 99–101, 141, 154, 157,
158, 162
causality, causal, 12, 131, 132
Chebyshev, 140, 141, 143, 144, 154,
155, 162, 164, 170
Chua, 56, 57, 64, 65, 80
Clapp, 46
Colpitts, 44, 78

complex plane, 2, 3, 10, 13, 17–19,
22, 24, 30, 33, 34, 38, 42, 72–74,
114, 117, 131, 133, 134, 141, 146
continued fraction (expansion), 100,
101, 145, 206
convolution product, 7, 8, 15, 127,
128, 131, 132, 224

D

damping, 13, 16, 20, 24, 42, 49, 60,
69–71, 73, 75, 81, 191, 219, 221
Delyannis-Friend, 148
denormalization, 138, 143, 148, 159,
170, 177
derivation, 6, 13, 14, 23, 27, 129,
130, 226, 227, 230
dipole (or two-port network), 45, 49–
53, 56, 57, 62, 81, 82, 85, 86, 92–
94, 97, 114, 116, 173, 196, 197,
199, 204–206, 214, 220
Dirac, 23, 31–33, 127–132, 224–227
dissipation (or power loss), 49, 150,
151, 156, 204

E, F

electrical, 2, 9, 42, 55, 86, 92, 124,
196, 197

elliptical filter (or Jacobi, Zolotarev, Causer filter), 141, 143, 156, 159, 189–191

feedback, 1, 25–30, 35–37, 46, 48, 66, 71, 75, 76, 89, 90, 111, 117, 146, 148, 149

filters, 41, 47, 86, 95, 102, 104, 122, 165

- analog, 126–130, 146
- all-pass, 135, 196
- band-pass, 21, 101, 120, 128, 130, 137, 142, 143, 150, 154, 155, 165, 187, 188, 189, 192, 211
- band-stop, 100, 128, 137, 143
- high-pass, 128–130, 137, 142, 143, 170, 173
- low-pass, 17–19, 77, 129, 130, 137–139, 142–144, 154, 158, 159, 162, 164, 165, 167, 168, 173–175, 177–179, 204

final value, 13, 73, 75, 76

first degree, 16, 20, 22, 24, 55, 100, 148

forced, free running or regime, 9, 14, 22, 25, 31, 75, 126, 128

Foster, 97, 100, 101, 154

Fourier transform (FT), 5–8, 85, 132, 146

G, H

gain margin, 36

group delay, 135, 136, 140, 143, 144, 194, 221

harmonic, 4, 10, 12, 15, 16, 24, 49, 50, 55, 68, 74–76, 96, 136, 180–183

Hartley, 45

Hurwitz's polynomial, 33, 135

I

image-impedance, 118–124, 193, 214, 216, 217, 218

image-matching, 118–124, 121, 122, 150, 166, 171, 175, 189, 191, 193

impulse response, 31, 126–132, 140, 144, 146

incident, 102–105, 121

instability, 30, 38, 39, 50, 55, 89, 117, 118

integration, 6, 8, 13, 14, 39, 41, 52, 133, 223–226, 229

iterative (impedance), 92, 94, 120, 150

K, L

Kramers-Kronig, 133,

ladder network, 99, 101, 126, 158, 204

Laplace transform (LT), 12–24, 31, 38, 127, 225, 227, 228

lattice filter, 191–194, 214, 215

leapfrog, 125, 126

linear, 1, 6, 8–10, 17, 22, 37–40, 48, 49, 85, 88, 97, 126, 133, 194, 197, 216, 217, 223

loop

- closed, 26, 29, 36, 37, 66, 73, 75
- open, 26–29, 35–37, 66, 67, 72, 73

M, N

minimal phase-shift, 133–135, 137, 194

noise, 8, 43, 48, 55, 56

normalization, 102, 105, 111, 122, 138, 170, 172

Nyquist, 17–21, 33–36, 117

O, P

operational amplifier, 26–29, 44, 66, 69, 70, 72–74, 86, 90, 146–148, 150, 195
 Orchard, 195
 ordinary differential equation (ODE), 8–10, 38, 39
 oscillator, 30, 36, 42–48, 50–57, 62–65, 78, 80, 133
 Padé, 145
 Parseval, 5, 7, 8
 passive, 9, 37, 86, 91, 95, 96, 104, 109, 114, 118, 120–126, 128, 146, 150, 152–154, 166, 183, 195–197, 199, 204, 205, 211
 periodic, 4, 5, 10–13, 56, 136, 225
 phase
 margin, 36, 74
 space, 52, 53, 55, 62, 65
 pole, 16, 24, 31–33, 72, 82, 84, 96, 100, 101, 133, 139, 141, 167, 177, 179–186, 189, 193, 215, 218
 map, 24, 31
 port, 85, 87, 92–94, 100, 103–107, 116, 119, 120, 165–168, 171, 179, 183, 186, 191, 196, 197, 199, 204–207, 210, 214, 220

Q, R

quadripole or two-port network, 85
 quality, 16, 49, 60, 66, 73, 146, 197, 201
 quartz, 44–47, 49, 150, 191, 192, 214, 216, 218
 random (signal), 8, 65
 Rauch, 146
 reciprocal, 27, 91, 104, 122, 137, 153, 157, 164
 regime
 forced, 9, 22
 steady-state, 14, 36

relaxation, 49–52, 56, 57
 resonant, 48, 49, 56, 80, 156, 157, 166
 ripple, 139, 141, 143, 154–158, 162, 174–176, 178, 189–191, 195, 196
 rotating vector, 3

S

Sallen-Key, 146, 147
 second degree, 31, 148
 sinusoidal signals, 2–4, 10, 11
 spectral density, 8
 spectrum, 2–4, 7, 11, 63–65, 136
 stable (or stability), 9, 12, 16, 30, 31, 33, 35–37, 39–42, 47, 48, 52, 55, 58, 61, 67–69, 73, 75, 76, 81, 83, 85, 111, 114, 117, 118, 124–126, 131, 133, 145, 146, 150
 state variables, 37–40, 55, 58, 81, 145
 state-space form, 1, 41, 80
 stationary, 1, 8, 9, 38, 40, 41, 126, 133

T

template, 122, 137–139, 142, 153, 156, 164, 165, 170, 173, 176, 178, 179, 189–191, 194
 terminal, 85, 86, 174, 177
 termination, 92–94, 102, 104, 105, 108, 125, 150, 164–166, 168, 172, 174, 176, 183, 188, 189–191, 194, 195, 211, 212
 transfer function (or transmittance), 10, 12, 15–19, 22, 24–27, 33–36, 38, 41, 42, 48, 67, 70–72, 74–77, 114, 117, 119, 121, 122, 124–126, 128, 130–141, 143, 145, 146, 148–150, 152–156, 158, 159, 161, 166–168, 178, 181, 185, 194, 197, 205, 215, 218, 219, 221

transfer matrix, 102–107, 121, 122
transformer, 102, 165, 195, 197, 198,
201, 202, 204
transistor, 44–48, 78, 80, 197, 203
transmittance, 167

U, V, W

unilateralisation (or neutrodynation),
111
unitarity, 151–154, 158, 162, 165
voltage controlled oscillator (VCO),
48
Wiener-Kinchine, 7, 8

Other titles from

ISTE

in

Electronics Engineering

2017

MURET Pierre

Fundamentals of Electronics 1: Electronic Components and Elementary Functions

BUCCI Davide

Analog Electronics for Measuring Systems

2016

BAUDRAND Henri, TITAOUINE Mohammed, RAVEU Nathalie

The Wave Concept in Electromagnetism and Circuits: Theory and Applications

FANET Hervé

Ultra Low Power Electronics and Adiabatic Solutions

NDJOUNTCHE Tertulien

Digital Electronics 1: Combinational Logic Circuits

Digital Electronics 2: Sequential and Arithmetic Logic Circuits

Digital Electronics 3: Finite-state Machines

2015

DURAFFOURG Laurent, ARCAMONE Julien
Nanoelectromechanical Systems

2014

APPRIOU Alain
Uncertainty Theories and Multisensor Data Fusion

CONSONNI Vincent, FEUILLET Guy
Wide Band Gap Semiconductor Nanowires 1: Low-Dimensionality Effects and Growth

Wide Band Gap Semiconductor Nanowires 2: Heterostructures and Optoelectronic Devices

GAUTIER Jean-Luc
Design of Microwave Active Devices

LACAZE Pierre Camille, LACROIX Jean-Christophe
Non-volatile Memories

TEMPLIER François
OLED Microdisplays: Technology and Applications

THOMAS Jean-Hugh, YAAKOUBI Nourdin
New Sensors and Processing Chain

2013

COSTA François, GAUTIER Cyrille, LABOURE Eric, REVOL Bertrand
Electromagnetic Compatibility in Power Electronics

KORDON Fabrice, HUGUES Jérôme, CANALS Agusti, DOHET Alain
Embedded Systems: Analysis and Modeling with SysML, UML and AADL

LE TIEC Yannick
Chemistry in Microelectronics

2012

BECHERRAWY Tamer
Electromagnetism: Maxwell Equations, Wave Propagation and Emission

LALAUZE René
Chemical Sensors and Biosensors

LE MENN Marc

Instrumentation and Metrology in Oceanography

SAGUET Pierre

Numerical Analysis in Electromagnetics: The TLM Method

2011

ALGANI Catherine, RUMELHARD Christian, BILLABERT Anne-Laure

Microwaves Photonic Links: Components and Circuits

BAUDRANT Annie

Silicon Technologies: Ion Implantation and Thermal Treatment

DEFAY Emmanuel

Integration of Ferroelectric and Piezoelectric Thin Films: Concepts and Applications for Microsystems

DEFAY Emmanuel

Ferroelectric Dielectrics Integrated on Silicon

BESNIER Philippe, DÉMOULIN Bernard

Electromagnetic Reverberation Chambers

LANDIS Stefan

Nano-lithography

2010

LANDIS Stefan

Lithography

PIETTE Bernard

VHF / UHF Filters and Multicouplers

2009

DE SALVO Barbara

Silicon Non-volatile Memories / Paths of Innovation

DECOSTER Didier, HARARI Joseph

Optoelectronic Sensors

FABRY Pierre, FOULETIER Jacques

Chemical and Biological Microsensors / Applications in Fluid Media

GAUTIER Jacques

Physics and Operation of Silicon Devices in Integrated Circuits

MOLITON André

Solid-State Physics for Electronics

PERRET Robert

Power Electronics Semiconductor Devices

SAGUET Pierre

Passive RF Integrated Circuits

2008

CHARRUAU Stéphane

Electromagnetism and Interconnections

2007

RIPKA Pavel, TIPEK Alois

Modern Sensors Handbook